Potassium starvation responses in yeast highlight novel potassium-related functions

Doctoral thesis presented by

DAVID CANADELL i SALA,

graduated in Biotechnology

for the degree of PhD in Biochemistry, Molecular Biology and Biomedicine from the Universitat Autònoma de Barcelona.

Thesis performed at the Departament de Bioquímica i Biologia Molecular of the Universitat Autònoma de Barcelona and at the Institut de Biotecnologia i de Biomedicina.

Thesis supervised by **Dr. Joaquín Ariño Carmona**

David Canadell i Sala Dr. Joaquín Ariño Carmona

Cerdanyola del Vallès, April 2015

Table of contents

Abbreviations

aa	***a***mino ***a***cids
AICAR	5'-phosphoribosyl-5-***a***mino-4-***i***midazole ***car***boxamide
APS	***A***denylyl ***s***ulfate
ATP	***A***denosine ***t***ri***p***hosphate
CDK	***C***yclin ***d***ependent ***k***inase
C-terminal	***C***arboxyl ***terminal***
CoA	***Co***enzyme ***A***
DNA	***D***eoxyribo***n***ucleic ***a***cid
ER	***E***ndoplasmic ***r***eticulum
ESR	***E***nvironmental ***s***tress ***r***esponse
GAAC	***G***eneral ***a***mino ***a***cid ***c***ontrol
GSH	Reduced ***G***lutathione
GSSG	***G***lutathione di***S***ulphide, oxidised glutathione
GTP	***G***uanosine ***t***ri***p***hosphate
HOG	***H***igh ***o***smolarity ***g***lycerol
IP	***I***nositol ***p***hosphate
kDa	***K***ilo ***D***altons
K_m	***M***ichaelis constant
M	**M**olar concentration
MAP	***M***itogen-***a***ctivated ***p***rotein
Mbp	***M***ega ***b***ase ***p***airs
MDR	***M***ulti-***d***rug ***r***esistance
MFS	***M***ajor ***f***acilitator ***s***uperfamily
min	***Min***utes

mM	***m***illi***m***olar
NAD	***N***icotinamide ***a***denine ***d***inucleotide
NAMN	***N***icotinic ***a***cid ***m***ono***n***ucleotide
NCR	***N***itrogen ***c***atabolite ***r***epression
nmol	***n***ano***mol***
NmR	***N***icotina***m***ide ***r***iboside
mg	***m***illi***g***ram
mV	***m***illi***v***olt
N-terminal	Amino ***terminal***
PAPS	***P***hospho***a***denylyl ***p***hospho***s***ulfate
PHO	***Pho***sphate-responsive signalling
P_i	***I***norganic ***p***hosphate
PIC	***P***re***i***nitiation ***c***omplex
PKA	***P***rotein ***k***inase ***A*** (cAMP-dependent protein kinase)
PolyP	***Polyp***hosphates
RAVE	***R***egulator of the ***A***TPase of ***v***acuolar and ***e***ndosomal membranes
RiBi	***Ri***bosome ***Bi***ogenesis
RNA	***R***ibo***n***ucleic ***a***cid
ROS	***R***eactive ***o***xygen ***s***pecies
RTG	***R***e***t***ro***g***rade signalling
S. cerevisiae	***S***accharomyces ***cerevisiae***
SAGA	***S***pt-***A***da-***G***cn5-***A***ctetyltransferasa
SAH	***S***-***a***denosyl-***h***omocysteine
SAM	***S***-***a***denosyl-***m***ethionine

SAP	***S***it4 ***A***ssociated ***P***rotein
SMM	***S*-*m***ethyl***m***ethionine
SPS	***S***sy1-***P***tr3-***S***sy5
SPX	yeast ***S***yg1 and ***P***ho81 and human ***X***PR1
SR	***S***/***R***-rich (Ser/Arg-rich)
TAF	***T***BP-***a***ssociated ***f***actor
TBP	***T***ATA-box ***b***inding ***p***rotein
TOR	***T***arget ***o***f ***r***apamycin
TORC1	***T***arget ***o***f ***r***apamycin ***c***omplex ***1***
UTR	***U***n***t***ranslated ***r***egion
V_{max}	***Max***imum rate in Michaelis–Menten kinetics
µM	***microm***olar
bHLH	***b***asic-***h***elix-***l***oop-***h***elix

Summaries

Mantenir la homeòstasis de cations és essencial per la supervivència dels éssers vius, i en especial pels organismes unicel·lulars. El llevat *Saccharomyces cerevisiae* s'ha utilitzat al llarg dels anys com un organisme model per l'estudi del conjunt de processos que controlen els nivells intracel·lulars de cations. El potassi és el principal catió intracel·lular del llevat i està involucrat en diversos processos de la fisiologia d'aquest organisme. Per aquest motiu la seva homeòstasis està minuciosament controlada per un seguit de transportadors que permeten la seva captació, distribució intracel·lular i eliminació de la cèl·lula i per un conjunt de proteïnes reguladores d'aquests processos. Encara que es té constància de la rellevància del potassi en el llevat, les seves dianes específiques i les bases moleculars d'algunes de les seves funcions són poc conegudes.

En aquest treball, mitjançant aproximacions d'eliminació del potassi del medi de cultiu, s'han pogut determinar els mecanismes d'algunes de les funcions conegudes del potassi i descobrir-ne de noves. S'ha demostrat que la manca de potassi provoca profundes alteracions en el perfil transcripcional del llevat. Entre elles destaquen l'accentuada repressió del gens que codifiquen proteïnes ribosomals i elements necessaris per la síntesi del ribosoma, dotant d'explicació molecular al ja conegut bloqueig en la síntesi de proteïnes provocat per la manca de potassi. L'eliminació del potassi del medi també provoca una caiguda dels nivells dels aminoàcids cisteïna i metionina que condueix a una activació del gens relacionats amb el metabolisme del sulfat i la síntesi d'aminoàcids sulfurats. Igualment, la privació del potassi comporta una acumulació d'espècies reactives de l'oxigen que produeixen un estat d'estrès oxidatiu a la cèl·lula. Aquesta respon amb l'activació transcripcional dels gens necessaris per combatre l'estrès oxidatiu, eliminar els oxidants i retornar la cèl·lula a un correcte estat redox. El llevat creixent en un medi sense potassi i en presència d'amoni acumula grans quantitats d'amoni a l'interior cel·lular a través del transportador de potassi Trk1 aprofitant la similitud química d'ambdós cations. Aquesta acumulació d'amoni activa vies per la seva fixació i eliminació en forma d'aminoàcids com és la via retrograda mitocondrial. L'eliminació del potassi del medi atura la proliferació cel·lular. Els nostres resultats han demostrat que aquesta aturada podria ser deguda a la disminució de les ciclines i d'elements reguladors de la formació dels anells de septines que afecten la progressió del cicle cel·lular.

El potassi també l'hem relacionat amb la homeòstasi d'un nutrient essencial com és el fosfat. L'absència de potassi o la pertorbació de la entrada normal d'aquest catió indueix els gens involucrats en la obtenció i mobilització del fosfat, d'igual manera com ho faria la depleció o limitació del fosfat. En aquetes condicions, la resposta transcripcional d'aquets gens està regulada pels diferents elements que composen la via *PHO*. L'afectació en l'obtenció del potassi impacte en la normal homeòstasis del fosfat provocant la mobilització de les reserves emmagatzemades en forma de polifosfats. La limitació del potassi, però, no modifica els nivells de fosfat lliure intracel·lular però sí que provoca una caiguda del nivells d'ATP i d'ADP, que podrien ser el senyal d'activació de la via *PHO*. A més, la pertorbació de la homeòstasis del potassi afecta el creixement dels llevats en medis amb baixos nivells de fosfat.

El conjunt de dades obtingudes en aquest treball ha permès descobrir nous vincles entre la homeòstasis del potassi i diversos processos cel·lulars, a més de la connexió d'aquest catió amb la homeòstasis de nutrients com el nitrogen, el sulfat i el fosfat.

The maintenance of cation homeostasis is essential for the survival of all living organisms and especially for microorganisms. The yeast *Saccharomyces cerevisiae* has been used over the years as a model organism for study the processes that control intracellular cation levels. Potassium is the major intracellular cation in yeast and it has been associated with various relevant cellular processes. For this reason, potassium homeostasis is tightly controlled by several transporters, that allow the cation uptake, intracellular traffic and efflux, and by a set of proteins regulating these processes. In spite of the importance of potassium for yeast physiology, not all relevant functional potassium-related targets have been identified.

In this work, potassium starvation conditions are used to determine the mechanisms of some of the known potassium functions and to discover new ones. We show that lack of potassium causes major alterations in the transcriptional profile of yeast cells. These transcriptional changes include the marked repression of genes encoding ribosomal proteins and elements necessary for the synthesis and assembly of ribosomes, providing the molecular basis for previously observed halt in protein synthesis caused by potassium deprivation. The elimination of potassium from the medium also causes a drop in cysteine and methionine levels which lead to transcriptional activation of genes related to metabolism of sulfate and biosynthesis of sulfur-contain amino acids. Similarly, cells deprived for potassium accumulate reactive oxygen species which results in oxidative stress. Concomitantly, cells trigger the transcriptional activation of genes necessary to combat oxidative stress, eliminate oxidants and return cells to the proper redox state. Yeast cells growing on ammonium as nitrogen source but lacking potassium accumulate large amounts of intracellular ammonium, which is transported through Trk1 taking advantage of the chemical similarity of both cations. Ammonium accumulation activates the retrograde mitochondrial pathway, resulting in detoxification of ammonium by its integration into amino acids. The complete removal of potassium from the medium leads to growth arrest. Our results show that this arrest could be due to the decrease in cyclins levels and in proteins involved in the assembly of septin rings, elements that are necessary for cell cycle progression.

We also have related potassium to the homeostasis of other essential nutrients such as phosphate. Depletion of potassium from the medium or disturbance of normal potassium uptake induces genes involved in the acquisition and release of phosphate, as it is usually observed in a situation of phosphate starvation. Under these conditions, the transcription of *PHO*-controlled genes is activated by different regulatory elements of the *PHO* pathway. Situations that impact on normal potassium homeostasis also cause mobilization of the phosphate reserves stored in form of polyphosphates. Potassium restrictions, however, does not alter the levels of intracellular free phosphate but it causes a drop in the levels of ATP and ADP, which could be the signal for the activation of the *PHO* pathway. In addition, on media with low levels of phosphate, disruption of normal potassium homeostasis effects yeast growth.

The results obtained in this work have been crucial to uncover new links between potassium homeostasis and many important cellular processes, in particular establishing the link between the homeostasis of this cation with that of other essential nutrients such as nitrogen, sulfate, and phosphate.

Introduction

3.1 The budding yeast *Saccharomyces cerevisiae* and its cell cycle

The yeast *Saccharomyces cerevisiae* is a eukaryotic fungus, belonging to the family of the *Saccharomycetaceae,* which humanity has used for many years in the field of the food industry for the production of bread, wine or beer. Nowadays, in addition to the usage in food business, it is widely used in the field of biotechnology, as a producer of various compounds with commercial interest such as biomass, organoleptic compounds, vaccines, etc., and for protein heterologous expression.

It was not until in the 30s of the 20th century (Roman 1981) that *S. cerevisiae* began to be used as a model in genetic and metabolic studies thanks to its easy cultivation and manipulation. For the past three decades, fundamentally since the achievement of the genome sequence in 1996 (Goffeau et al. 1996), *S. cerevisiae* has been the model system for molecular genetic research because of the conservation of the basic cellular mechanisms (replication, recombination or cell division) and general metabolism between yeast and higher eukaryotes, including mammals (Botstein et al. 1997; Botstein & Fink 2011). Yeast cells can be found as haploid or diploid cells with different size and composition also depending on the growth medium, cells growth phase and strain background. Haploid cells are spheroids of 4 μm of diameter and 70 fL of volume when growing in rich complete medium. In this situation, the composition of haploid yeast cells is 0.017 pg of DNA, 1.2 pg of RNA and 6 pg of proteins (Sherman 2002). The yeast genome is composed by 12.1 Mbp arranged across 16 chromosomes encoding around of 6000 genes of which 85 % have an annotated biological role (Botstein & Fink 2011). The development of genetic engineering techniques has made yeast particularly interesting for the gene characterization and for the study protein functions and interactions. Even more, many high-throughput techniques were developed using *S. cerevisiae,* thus providing large amounts of genome-wide data that has positioned yeast as the best model for eukaryotic Systems Biology (Mustacchi et al. 2006).

All these features make the yeast *S. cerevisiae* an extraordinary research model for understand metabolic complex processes or stress responses at genomic-wide level.

The budding yeast cell cycle

Saccharomyces cerevisiae is a budding yeast that proliferates either as *MAT**a*** or *MATa* haploids or as *MAT**a***/*MATa* diploids created by conjugation of opposite haploid types (Haber 2012). The asexual budding consist in the formation of small bud which will become a separated

daughter cell when reaches a certain size and obtain the mother's duplicated DNA. The cell cycle consists in four different and highly controlled phases (G_1, S, G_2 and M) that involves DNA duplication (S phase) and segregation (M phase or mitosis) and cell division (replication of all cell components and their physical separation to daughter cells) (Tyson et al. 2002). S and M phases are separated in time by two "gap" phases named G_1 and G_2 phases. Proper progression through the cell cycle is guaranteed by several "checkpoints". The G_1 checkpoint controls entry into S phase assuring that cells are large enough, DNA is damage free and there are enough nutrients in the media. The G_2 checkpoint controls entry in mitosis, making sure that DNA is fully replicated, any DNA damage has been repaired and the cell is large enough to divide. The metaphase checkpoint watches the metaphase to anaphase transition checking that chromosomes are properly aligned on the mitotic spindle. In addition to the mentioned checkpoints, the morphogenetic checkpoint monitors the organization of actin and septins and arrests cells in G_2 if a bud fails to form (Tyson et al. 2002).

Progression through the cell cycle is a highly regulated process that is conserved all over eukaryotes. In budding yeast, a single CDK encoded by *CDC28* gene is activated by multiple cyclins to generate the waves of kinase activity necessaries to progress through different stages of the cell cycle (Wittenberg 2005). The G_1 cyclins are Cln1, Cln2, and Cln3 whereas the S and G_2/M are Clb1-6. The G_1 phase cyclins promote bud emergence, spindle pole body duplication, and activation of the Clb1-6 cyclins. The transcription of *CLN3* is only somewhat cell cycle regulated, with a peak in late M or early G_1 (McInerny et al. 1997) whereas the stability of Cln3 protein is precisely controlled (Cross & Blake 1993; Tyers et al. 1992). Another cell cycle function of Cln3 is controlling the transcription activation of the cyclins *CLN1* and *CLN2* to progress from G_1 to S phase (Stuart & Wittenberg 1995). Passage through START is necessary for initiating many events required for the cell division like morphogenic changes leading to the formation of the bud, the nascent daughter cell with its associated septin ring (reviewed in (Bi & Park 2012)). The septins are GTP-binding proteins, localized at the mother-bud neck during the cell cycle forming a ring that act as scaffold for recruiting cell division factors and as barrier to prevent diffusion of specific proteins between mother and daughter cells (McMurray et al. 2011; Gladfelter et al. 2001). Upon bud emergence, the septin ring is converted to "hourglass" shape that is split into two rings during the cytokinesis. The assembly of the septin ring and the changes in the arrangement of septin filaments are controlled by septin modifications, such as phosphorylation, performed by several regulatory protein kinases (Oh & Bi 2011).

The progression through the S phase and the consequence DNA replication requires cyclins Clb5 and Clb6, more abundant in the late G_1 (Schwob & Nasmyth 1993). The Clb1-4 cyclins are necessary to promote the transition from G_2 to M phase and are required for some mitotic events (Fitch et al. 1992). Finally, mitotic cyclin activity is down-regulated to complete cell division because these mitotic-related cyclins also prevent mitotic exit and cytokinesis (Irniger 2002).

3.2 Ionic homeostasis in *Saccharomyces cerevisiae*

Homeostasis is the process that allows a cell or organism to maintain its internal equilibrium even if there are changes in the environment. Maintaining ion homeostasis is essential for the survival of all living organisms and especially microorganisms, such as the yeast *Saccharomyces cerevisiae*, that are usually exposed to highly variable environments that sometimes could be hostile. Many nutrients, especially mineral nutrients, are in solution as charged ions. Charged ions cannot freely diffuse across lipid bilayers, and consequently can be used to establish electrochemical gradients that drive several cellular processes, such as ATP synthesis by oxidative phosphorylation in mitochondria, or secondary transport. The different ions are accumulated into the cell at very different range of concentrations (Eide et al. 2005), and all of them play diverse essential roles. Besides protons, the main monovalent cations in yeast cell biology are potassium and, too much less extents, sodium. The homeostasis of monovalent cations is maintained primarily by systems that import K^+ and extrude H^+ and Na^+ (or other toxic cations like lithium). In *Saccharomyces cerevisiae* many of these ions transporters or related proteins have been identified and characterized (revised in (Ariño et al. 2010)). However, a complete model that assembles all these essential cellular processes and transport systems is still missing because the difficulties to quantify the impact of each transport system to the global ion homeostasis.

One of the most important mechanisms in yeast to maintain cation homeostasis in front of stress is the HOG pathway. This pathway reacts to the hyperosmotic stress that can be generated by high extracellular levels of cations (such as Na^+). After a hyperosmotic shock caused by high Na^+ in the medium, yeast cells shrink within seconds by loss of internal water and react trying to maintain water by accumulating compatible solutes like glycerol and by eliminating the surplus of sodium that enters into the cell (Tamás et al. 1999; Saito & Posas 2012). The osmotic stress activates the HOG signal transduction pathway by phosphorylation

of the MAP kinase Hog1 that in turn stimulates sodium export (Proft & Struhl 2004), arrest of the cell cycle (Escoté et al. 2004), and accumulates glycerol by stimulation of glycolysis and preventing the water efflux from the cell (Dihazi et al. 2004; Tamás et al. 1999). The phosphorylated Hog1 accumulates in the nucleus where it promotes the transcription of several genes necessary for the complete responses to hyperosmotic shock (Posas et al. 2000). All the data generated around the HOG pathway has made possible to generated integrative models of the response to osmotic shock (Klipp et al. 2005; Tomar et al. 2013; Gat-Viks & Shamir 2007).

3.3 The "cationome"

Under a given pH, proteins, organic and inorganic anions give a set of negative charges inside the cell. To maintain the intracellular electroneutrality, the same amount of positive and negative charges is needed, so the cell requires accumulating cations. Besides of neutralizing intercellular negative charges, cations have other important roles in the cell; from controlling intracellular pH and osmotic pressure, to being essential enzyme cofactors or signalling molecules. The life relevant cations are members of alkali (group 1), alkaline earth (group 2), and transition metals.

The family of alkali metals is composed by lithium, sodium, potassium, rubidium, cesium and francium. Only potassium, sodium, lithium and rubidium are found in cells, although it is not known any physiological role for lithium and rubidium. Potassium is the most abundant cation in yeast cells and its functions and its relationship with sodium are explained in detail in the next sections.

3.3.1 Alkaline earth cations

The more relevant alkaline earth cations found in living cells are calcium and magnesium. Ca^{2+} is found in all eukaryotes with several functions; it is used for structural aims (bones or exoskeletons), is an important signalling molecule, and it is necessary for the activity of some enzymes. In yeast, it is found inside of cellular organelles (mainly in the vacuole) (Dunn et al. 1994) at a concentration around 1-2 mM (Halachmi & Eilam 1989). In the cytosol, Ca^{2+} performs its signalling function at very low concentrations (50-200 nM). Among these functions, Ca^{2+} binds and activates protein kinases Cmk1 and Cmk2, and calcineurin (Cyert 2001). Calcineurin is a Ca^{2+}/calmodulin-dependent phosphatase, necessary to respond to

several stresses, including high concentrations of cations in the medium (Mendoza et al. 1994; Nakamura et al. 1993) or alkaline pH (Viladevall et al. 2004; Ruiz et al. 2008; Nakamura et al. 1993). A major role for activated calcineurin is to dephosphorylate the transcription factor Crz1, necessary for the activation of the transcription of genes required to fight against these stresses (Cyert 2003). Ca^{2+} is also necessary to respond to mating factor (Iida, Yagawa, et al. 1990), for glucose uptake and utilization at alkaline pH (Ruiz et al. 2008) and for regulation the cell cycle (Iida, Sakaguchi, et al. 1990). Calcium is transported into the cell by a high affinity system encoded by Mid1, Cch1 and Ecm7 (Cunningham 2011) or a low affinity system related to cell fusion mechanisms (Muller et al. 2003). Calcium is stored into vacuoles, endoplasmic reticulum or Golgi by the action of Pmr1 or Pmc1 Ca^{2+} ATPases (Rudolph et al. 1989; Cronin et al. 2002; Cunningham & Fink 1994) or by the Ca^{2+}/H^{+} antiporter Vcx1 that use the proton motive force generated by V-ATPases to take up calcium (Miseta et al. 1999; Cunningham & Fink 1996). When a Ca^{2+} signal is necessary calcium can be released from the different organelles through Yvc1 Ca^{2+} channel (Denis & Cyert 2002) or can be uptaken from extracellular medium through membrane high affinity calcium transporters (Bonilla et al. 2002; Viladevall et al. 2004) (Figure 1).

Magnesium, found in the low millimolar range inside the cell, is an essential cofactor for over 100 cellular enzymes and is necessary for proliferation and cell growth (Wolf & Trapani 2008). It is stored in vacuoles, mitochondria and cytoplasm mostly bound to negative compounds like phosphate (or polyP), DNA, RNA or ATP. Magnesium is transported into the cell by plasma membrane transporters Alr1 and Alr2 (Lim et al. 2011), into the mitochondria by Mrs2 (Kolisek et al. 2003) and into the vacuole by the Mg^{2+}/H^{+} exchanger Mnr2 (Pisat et al. 2009). Calcium can compete with magnesium when one of them is found in excess respect the other.

3.3.2 Transition metal cations

There are several transition metals involved in essential functions in eukaryotic cells. The main role of these ions is to be the essential cofactor in metalloproteins. Only the metal ions found in metalloproteins are considered nutrient metals (iron, copper, zinc and manganese) in comparison with non-metal nutrients (nickel, cobalt, molybdenum and cadmium) also found in eukaryotic cells in trace amounts performing only a limited number of identified functions (Bleackley & Macgillivray 2011). The concentrations of nutrient metal cations ranges from low mM for Zn to low μM for Mn (Eide et al. 2005). Iron, manganese, and copper are ions with

multiple valence states used to accept or lose electrons in enzymatic redox reactions in biological systems. However, the presence of reduced iron or copper in cells in the presence of oxygen can lead to the formation of ROS and subsequent oxidative damage to cellular components (Herrero et al. 2008). For this reason metal ion homeostasis is tightly regulated according to the availability and cellular necessities for the ion. Iron, zinc, cooper and manganese have a well-stablished and specific network of plasma membrane and organelle transporters, transcription factors and accessory protein to capture, transport and use metal cations (Cyert & Philpott 2013).

3.3.3 Alkali cations

Although the most abundant cation in nature is sodium, found in large quantities in the seas, life mainly use K^+ in the cellular milieu. Potassium is the most abundant intracellular cation in yeast (200-300 mM) and cells tend to maintain potassium at higher intracellular concentrations than it is found in the environment. Yeast cells can growth in media with potassium ranging from very small amount (10 μM K^+) to high concentrations of potassium (under 2.5 M K^+). Potassium cations are required for many physiological functions besides to compensate negative charges of many macromolecules (Rodríguez-Navarro 2000). Potassium has an essential function in the regulation of cell volume (turgor), ionic strength (Merchan et al. 2004; Serrano et al. 1999) and intracellular pH (Madrid et al. 1998). Transport of potassium is necessary for maintenance of stable plasma membrane potential (Madrid et al. 1998). Potassium has been also related with cell cycle (Yenush et al. 2002), protein synthesis (Lubin & Ennis 1964) and found to be required for the activity of some enzymes (Page & Di Cera 2006). However, in many cases the molecular mechanisms behind the K^+ roles are not known.

The yeast cell must maintain a high K^+/Na^+ intracellular ratio, because Na^+ is toxic at high concentrations. The toxicity of sodium combines two mechanisms: first, Na^+ (but not potassium) has the ability to displace essential Mg^{2+} form catalytic sites of some enzymes (Murguía et al. 1995; Albert et al. 2000), and second, high concentrations of external sodium salts causes osmotic stress . The particular cellular targets for sodium (or lithium) toxicity are poorly defined, although several possible candidates explaining toxicity have been proposed (Dichtl et al. 1997; Murguía et al. 1996; Masuda et al. 2001), apart from the water loss caused by osmotic shock (Hohmann 2002). Three different approaches allow yeast cells maintaining low levels of intracellular Na^+ o Li^+ even in the presence of high extracellular amount of these cations. The first it is the ability to differentiate between alkali cations, mainly K^+ from Na^+

and Li^+ (Rodríguez-Navarro 2000). Yeast cells have a very different uptake capability for both K^+ and Na^+ cations, with a K^+/Na^+ K_m ratio of 1:700 when high-affinity potassium uptake is working. At the same extracellular concentrations potassium is taken up much more efficiently than sodium and, therefore, intracellular concentrations are lower (Gómez et al. 1996; Ramos et al. 1985). Regardless of this system, nonspecific cation transporters can mediate influx of both K^+ and Na^+ (Gómez et al. 1996). The second strategy is based in removing the excess of unwanted cations from the cell, using active efflux systems described in the next sections. Finally, the different cations can be sequestered in the vacuole or in the organelles like mitochondria, Golgi apparatus or endosomes. Although Na^+ is not necessary for *S. cerevisiae* growing in plenty of potassium (Camacho et al. 1981), Na^+ can contribute to maintenance of the cell volume, cellular pH and growth when K^+ is limiting (Ramos et al. 1985). In some media with very low concentrations of potassium, the substitution of K^+ by other cations has been proposed to maintain electroneutrality inside the cells. In limiting potassium situations the affinity for potassium of the transport system increases, thus facilitating better discrimination of K^+ over Na^+ (Rodríguez-Navarro 2000). Although high cellular Na^+/K^+ ratios are also damaging, potassium replacement by Na^+ is less toxic than by H^+ (Camacho et al. 1981). The loss of potassium in the absence of Na^+ cations generates cytosol acidification, due to the partial substitution of potassium for H^+ to neutralize negative charges (Ramos et al. 1990).

The selectivity of the cell for K^+ uptake over other monovalent cations is not perfect. For example in yeast and plants, measurement of potassium transport is generally done using the $^{86}Rb^+$ analogue, due to the rather similar transport activity of potassium transporters for both cations (Rodríguez-Navarro 2000). Other cations that can mimic potassium are the ammonium ion (NH_4^+), which actually has an ionic radius (1.43 Å) very similar to K^+ (1.33 Å), and in fact even closer than that Rb^+ (1.47 Å) or Na^+ (0.95 Å) ones. It was described that NH_4^+ could replace potassium in bacteria growing at alkaline pH in potassium-limited chemostat cultures (Buurman et al. 1989). In yeast, Hess and collaborators (Hess et al. 2006) using different potassium-limited chemostat cultures with high concentrations of ammonium ions, observed that ammonium ions can enter into the cell probably via the potassium channels leading to production and excretion of amino acids to reduce internal toxic ammonium levels.

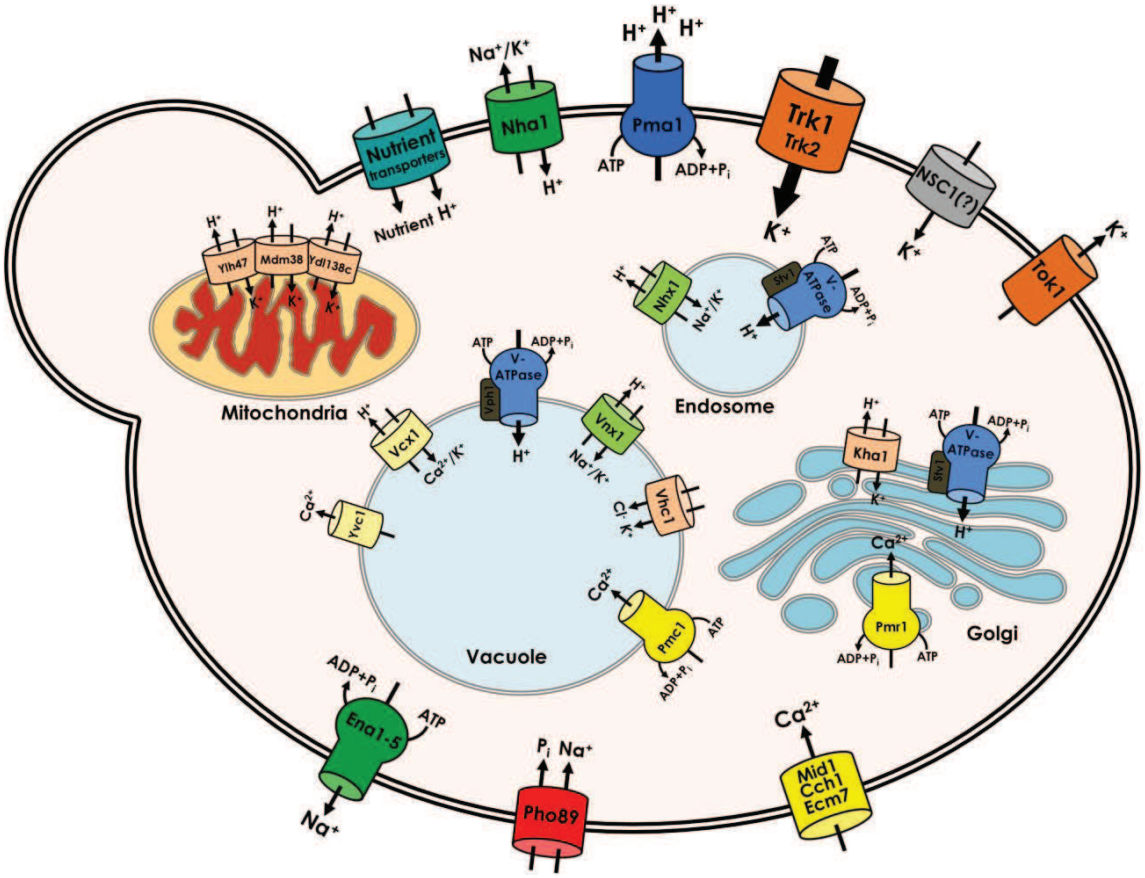

Figure 1. The major plasma membrane and intracellular cation transporters responsible for uptake, efflux and intracellular cation transport in the yeast *S. cerevisiae*. The figure shows transporters related with H^+ (blue), K^+ (orange), Na^+ (green) and Ca^{2+} (yellow) transport. (?) symbol indicates transporter not yet genetically characterized. Adapted from (Ariño et al. 2010; Cyert & Philpott 2013)

3.4 Cation transport

The yeast cells are delimited by a cell wall principally composed by polysaccharides (glucan polymers and a minor proportion of chitin mainly found in bud scars) and other components such as cross-linked glycoproteins (Klis et al. 2006). The cell wall is considered a semi selective porous structure and does not represent an impediment for solutes, therefore only the plasma membrane represents the primary selective barrier for nutrient or cation trafficking into the cell (De Nobel & Barnett 1991). In general, nutrients and ions can move across the membranes by mean of free or facilitated diffusion, and by active transport. Free diffusion is limited to lipid-solute/uncharged small molecules and implicates a favourable gradient. In the same way, facilitated diffusion depends on permeases or channels to transport molecules via the differential solute concentration inside and outside the cell. Some channels are voltage-gated that can be controlled by membrane polarization changes. In yeast cells, active transport is responsible for the uptake of most nutrients. The primary active transport uses ATP as energy source, while secondary active transport use the electrochemical proton gradient generated by ATPases to take up nutrients/cations generally in symport with protons, as well

as cation efflux as an antiport mechanism. Whereas mammalian cells use Na^+/K^+-ATPase to generated a sodium gradient that provides the driving force for several secondary active transporters, which import phosphate, glucose, amino acids, and other nutrients into the cell, the majority of nutrient transport systems necessary for the growth of yeast cells are dependent on the proton gradient. These include some sugar transporters, all amino acids transporters, organic acid transporters, purines, pyrimidines and vitamin transporters, anion transporters, such as phosphate and sulfate, some monovalent or divalent cations, and others transport systems. Only one Na^+/P_i plasma membrane transporter encoded by *PHO89* gene has been described in *S. cerevisiae* (Martinez & Persson 1998; Zvyagilskaya et al. 2008).

Similarly to the plasma membrane, nutrient or cation transport in the vacuole and other acidic intracellular membrane organelles, such as endosomes or the Golgi apparatus, is driven by facilitated diffusion and by active transport. Primary active transport is used to transport calcium or magnesium with specific ATPases, whereas the secondary active transport takes profit of the proton gradient generated by pumping H^+ into the vacuole or organelle for transporting metals, amino acids, cations and polyphosphate across the vacuolar membrane (Li & Kane 2009; Sekito et al. 2008). This proton gradient allows storage of potassium to ensure optimal cytosolic potassium concentrations, diminishing the amounts of toxic sodium or lithium cations in the cytosol, or compensating the negative charges of vacuolar polyphosphates (Klionsky et al. 1990). In addition, transport of cations into the vacuole is used to control cellular turgor and for detoxification the cytosol of diverse toxic compounds. The acidic pH generated inside the vacuole is also essential for many enzymatic processes that take place in the vacuolar lumen.

3.4.1 Proton ATPases, energy source for cation and nutrient transport

Pma1

Although cells tend to charge neutrality, there is a small difference between the number of negative and positive charges inside the cell in favour of negatives charges giving rise to an electric potential between across the plasma membrane with negative value. In the case of yeast, according to the Nernst equation was calculated to be about -300 mV (Rodríguez-Navarro 2000). The electrochemical proton gradient, consisting of the proton concentration gradient (ΔpH) and the electrical potential gradient or membrane potential (ΔΨ), is in part

created by the proton gradient generated by H^+-ATPase at the plasma membrane. This H^+-ATPase belongs to the widely distributed family of P_2-type ATPases and is encoded by the essential *PMA1* gene (Ambesi et al. 2000; Serrano et al. 1986). It is the most abundant protein in the plasma membrane and its activity consumes a significant part of intracellular ATP. Similarly to other members of the P_2 family, the 100 kDa Pma1 protein is folded into 3 cytoplasmic domains that form the catalytic domain anchored in the lipid bilayer by 10 transmembrane helices (Kühlbrandt et al. 2002; Ambesi et al. 2000). A second plasma membrane H^+-ATPase encoded by *PMA2* exist in *S. cerevisiae* (Schlesser et al. 1988). Pma2 has an 89 % of identity with Pma1, but the very low expression levels of Pma2 under normal growth conditions explain the minor impact of this protein in proton export (Supply et al. 1993). Pma1 pumps protons through the plasma membrane out of the cell to create an electrochemical gradient of protons that is indispensable for all mentioned secondary active symporters and antiporters as well as for cytosolic pH regulation. The Pma1 activity also controls the accumulation of K^+ cations, and both processes are crucial to control the plasma membrane potential (Rodríguez-Navarro 2000). For example, the lack of potassium transport produces the hyperpolarization of the membrane (Navarrete et al. 2010; Madrid et al. 1998).

Regulation of Pma1

The activity of Pma1 is strongly regulated by carbon or nitrogen sources such as glucose or amino acid levels and by the metabolic and physiological conditions of cells. Glucose, the most important signal for Pma1 regulation, invokes multiple signalling pathways collaborating to let accurate activation of the ATPase (Figure 2). Pma1 regulation by glucose was described to occur at two different levels: an initial rapid 5- to 10-fold increase in ATPase catalytic activity (Serrano 1983), affecting both K_m and V_{max}, and a second phase involving a slow and moderate increase in the expression of the gene in a process regulated by the transcription factors Rap1 and Gcr1 (Portillo 2000). Pma1 transcription, aside of glucose, is also regulated by nitrogen sources through the transcription factor *GLN3* (Cox et al. 1999). Amino acid uptake is mediated by proton symport, consequently the Gln3-dependent activation of *PMA1* expression may reflect a coordinate regulation of *PMA1* with genes required for uptake and utilization of poor nitrogen sources also regulated by Gln3. *PMA1* transcription and localization is coordinated with the cell cycle because its promoter has a binding site for the cell cycle transcription factor Mcm1 (Kuo & Grayhack 1994). The membrane distribution of Pma1 is controlled by cell cycle, buds and resultant daughters cells have very low levels of Pma1 compared to mother cells (Henderson et al. 2014). The cell aging also influences the

Pma1 levels, older cells accumulate more Pma1 at the membrane that younger cells (Thayer et al. 2014).

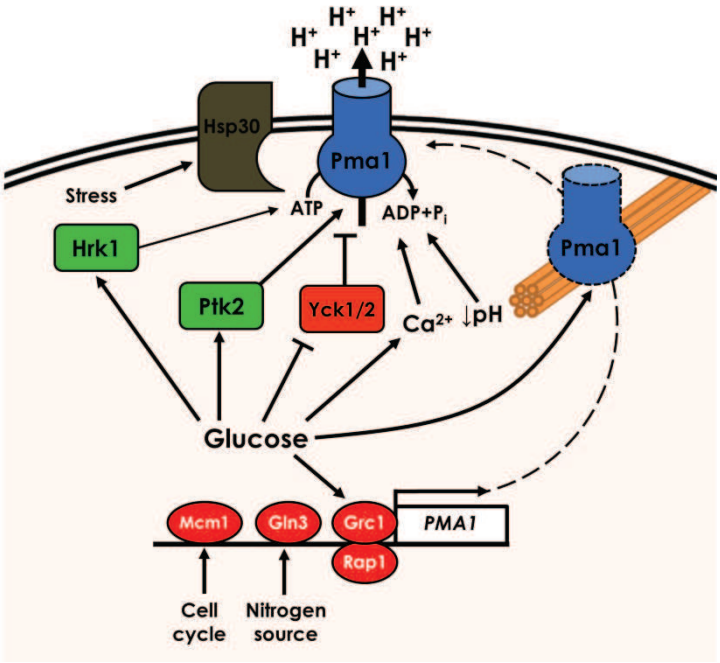

Figure 2. The regulatory network for the plasma membrane H^+-ATPase Pma1. The positive and negative effects on Pma1 levels or activity are indicated. For more details see main text.

The molecular process behind the short-term response to glucose addition has been assigned to glucose-dependent phosphorylation of Pma1. The carboxyl terminus of Pma1 is an autoinhibitory domain (Portillo et al. 1989) where several phosphorylation events have been detected. Pma1 Thr-912 is constitutively phosphorylated (Portillo et al. 1991) but addition of glucose results in further phosphorylation at Ser-911 creating a tandem phosphorylation of Ser-911 and Thr-912 necessary for Pma1 activation by glucose (Lecchi et al. 2007). Other activating phosphorylation in the C-terminal tail of Pma1 in response to glucose is that of Ser-899, mediated by the protein kinase Ptk2 (Goossens et al. 2000; Eraso et al. 2006). On the other hand, the addition of glucose prevents the inhibitory phosphorylation of Pma1 produced by yeast casein kinase I (encoded by the *YCK1* and *YCK2* genes), thus generating an increase in Pma1 activity (Estrada et al. 1996). Other activating effects of glucose on Pma1 are mediated by activation of Ca^{2+}-dependent signalling (Trópia et al. 2006; Bouillet et al. 2012) and by the disruption of the complex of Pma1 with acetylated tubulin occurring after addition of glucose (Campetelli et al. 2005). Therefore, glucose triggers both up- and down-regulation of signalling pathways with the aim of increase the activity of the yeast plasma membrane ATPase. Another protein kinase, Hrk1, also activates Pma1 but with

lesser potency (Goossens et al. 2000) and, consequently, its role in proton extrusion is minor (Barreto et al. 2011). Hsp30 acts as a plasma membrane chaperone of Pma1 to maintain the protein responsive to regulatory events after heat shock or glucose availability (Meena et al. 2011). Pma1 activity is also positively regulated in response to decreased intracellular pH or changes in potassium uptake (Seto-Young & Perlin 1991; Kahm et al. 2012) (Figure2).

V-ATPase

Similar to the plasma membrane, membranes of intracellular organelles also have an ATPase to generate the proton gradient to drive transport of nutrient and cations into and out of the organelles. In this case, besides the generation of the proton gradient, V-ATPases pumping H^+ into the vacuole or organelles, contribute to the maintenance of intracellular pH and the acidification of the vacuole (Martínez-Muñoz & Kane 2008). The V-ATPase is a large, conserved protein complex made up by at least 14 different subunits organized into two subcomplexes: an integral membrane complex V0 and a peripheral ATPase complex V1 (Kane 2006). Two distinct isoform of V-ATPase can be found, one containing Vph1, which targets the V-ATPase to the vacuole, and the other with Stv1, targeting the V-ATPase to the Golgi apparatus/endosome (Kawasaki-Nishi et al. 2001; Manolson et al. 1994).

The V-ATPase activity is controlled at different ways. V-ATPase function can be modulated by regulated assembly/disassembly processes of its two subcomplexes. Similarly to the activation of Pma1, V-ATPase assembly is regulated by glucose and the nutritional status of the cell (Li & Kane 2009; Parra et al. 2014). This regulation seems to be restricted to V-ATPase enzymes residing on vacuoles (Kawasaki-Nishi et al. 2001). Addition of glucose to glucose-deprived cells causes V-ATPase re-assembly, a process that requires some components of the RAVE complex (Smardon et al. 2002), and the activation of PKA pathway (Dechant & Peter 2010; Kane 2012). Simultaneously, intracellular alkalinization triggers the activation of Pma1 at the plasma membrane and, together with the activity of V-ATPase in vacuoles, controls intracellular pH. Otherwise, cells starved for glucose or subjected to less preferred carbon sources tend to V-ATPase disassembling (Parra et al. 2014).

The acidification of vacuoles mediated by proton translocation requires a parallel movement of anions (for example, chloride) to maintain net electroneutrality, for this reason ion transport is necessary to maintain V-ATPase activity (Flis et al. 2002; Gaxiola et al. 1998; Arai et al. 1989). The balance between V-ATPase activity and H^+ gradient consumed by cation transport is essential to control intracellular pH. The regulation of H^+ gradient enables

intracellular nutrient transport between organelles and cytoplasm and endosomal trafficking (Ali et al. 2004; Arai et al. 1989).

3.4.2 Alkali cations uptake

High-affinity potassium transport

In yeast, potassium is the only alkali cation specifically transported; the other alkali cations can enter into the cell non-specifically through potassium transporters or other transporters. The only exception is the Na^+ entrance by the high-affinity Na^+-phosphate cotransported Pho89, who is induced by low phosphate or alkaline pH conditions (Martinez & Persson 1998; Zvyagilskaya et al. 2008).

The first studies of potassium transport in yeast, as well other ion transports, compiled by (Borst-Pauwels 1981) proved that potassium transport is an energy requiring process, but were not able to resolve the kinetic mechanism behind this transport. The handicap of these studies was that they had been performed in non-physiological conditions and used undefined yeast genetic backgrounds. The contemporary studies started with a seminal work unravelling the potassium requirements of *S. cerevisiae* (Camacho et al. 1981) followed by the discovery of the existence of a dual mode of potassium transport, consisting of a high-affinity and a low-affinity transport system (Rodríguez-Navarro & Ramos 1984). High-affinity potassium uptake is mediated by the plasma membrane transporters Trk1 and Trk2 (Gaber et al. 1988; Ko et al. 1990; Ko & Gaber 1991), where Trk1 is the most physiologically relevant. The high-affinity system has a K_m between 25-50 μM and V_{max} of ~30 nmol/mg cells/min (Rodríguez-Navarro & Ramos 1984). The *TRK1* gene encodes a 180 kDa plasma membrane protein with an initially predicted structure of 12 transmembrane domains (Gaber et al. 1988) although nowadays the most plausible structure seems to be a tetra-MPM structure (where M corresponds to a hydrophobic segment and P to an α-helix that connects the M segments) deduced by comparison with the known structure of the KcsA protein of *Streptomyces lividans* (Durell & Guy 1999) (Figure3). This proposed *TRK* structure could be formed by homotetramers of Trk1 or Trk2 (or a mixture of both) and potassium enter into the cell by a central cluster made by four single helices from each monomer (Haro & Rodríguez-Navarro 2002) (Figure 3). The residues necessary for the transport, selectivity, protein folding and targeting to plasma membrane have been identified using experimental approaches, homology modelling and molecular dynamics (Haro & Rodríguez-Navarro 2003; Zayats et al. 2015; Haro & Rodríguez-Navarro 2002). *TRK1* orthologs were identified in other yeast species, fungi and

higher plants (Rodríguez-Navarro 2000; Ramos et al. 2011) and recently, the crystal structures of some of them were solved (Cao et al. 2011; Vieira-Pires et al. 2013). The molecular mechanism of transport is still puzzling. Some proposed mechanisms are based in the presences of 2 binding sites for cations that normally could cotransport two potassium cations, but Na^+/K^+ and H^+/K^+ symport have also been suggested (Haro & Rodríguez-Navarro 2002; Rodríguez-Navarro 2000). Similarly, the driving force utilized by potassium transport systems has not yet been identified and the role of Trk1 as a channel (like other potassium transporters (Cao et al. 2013)) or as a secondary or even primary active transporter is conceivable. Similar to Pma1 (Bagnat et al. 2001), Trk1 is localized to plasma membrane lipid rafts (Yenush et al. 2005). Lipid rafts are sphingolipid-rich microdomains of the plasma membrane important for delivery to and stability of proteins at the cell surface.

TRK2 encodes the second high affinity potassium transporter (Ramos et al. 1994; Michel et al. 2006), although initially was identified as low-affinity potassium transporter (Ko et al. 1990) due to its lower expression levels (Vidal et al. 1995). Trk2 is shorter than Trk1 and presents a 55 % identity with a similar tetrameric structure (Ariño et al. 2010). The principal difference between Trk1 and Trk2 is found in a long loop between the first and second MPM motifs, which is 642 aa-long in Trk1 and only contains 326 aa in Trk2. Cells lacking *trk1 trk2* need 10-fold more potassium than *trk1* cells, where Trk2 is the only high-affinity transporter, indicating the role of Trk2 on potassium transport is not negligible. In addition to the role on K^+ supply, Trk2 is a necessary player to control plasma membrane potential (Petrezsélyová et al. 2011).

Besides potassium, the Trk system is able to transport anions. Although initially inward ion currents, depending on the presence of Trk2 and of extracellular pH and independent on K^+, were reported (Bihler et al. 1999), some years later it was confirmed that the inward currents were in fact caused by exit of Cl^- and that those currents depended equally on Trk1 and Trk2 (Kuroda et al. 2004). These results were confirmed by Rivetta and coworkers (Rivetta et al. 2005), who more recently suggested that Cl^- ions flow through a central pore formed by symmetric aggregation of four *TRK* monomers (Rivetta et al. 2011) (Figure 3). This anion transport, not limited to halides ions, is not coupled to K^+ transport and its physiological role could be to balance charges as a result of H^+ extrusion by Pma1 (Rivetta et al. 2011).

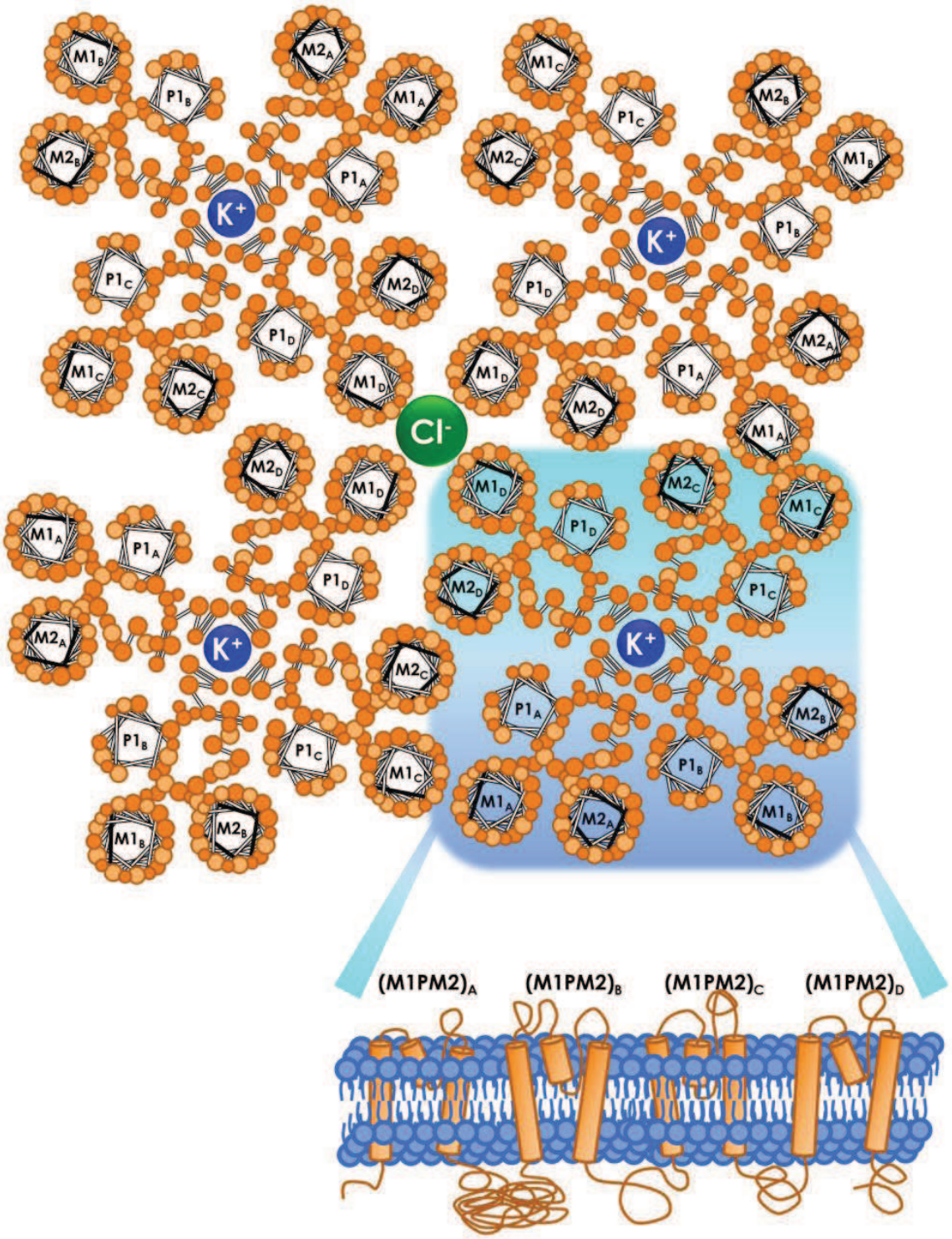

Figure 3. Schematic representation of the putative structure of Trk potassium transport system from *S. cerevisiae*. M corresponds to a hydrophobic segment and P to and α-helix. The formed pores where potassium or chloride ions pass trough are indicated with representative spheres for each anion. The large inset represents the front view of the tetra-MPM structure of one of the four Trk monomers that compose the model. Composition created from (Durell & Guy 1999; Rivetta et al. 2011; Zayats et al. 2015) models.

Regulation of Trk1 and Trk2

The expression of *TRK1* or *TRK2* is not altered by changes in cation levels or under cation stress. *TRK1* seems to be less expressed at stationary phase (Gasch et al. 2000) and *TRK2* expression is repressed by *RPD3* and *SIN3* gene products (members of the histone deacetylase complex) (Vidal et al. 1990; Vidal & Gaber 1991; Vidal et al. 1991) independently of the repression generated by the upstream repressor element (UTR1) located in *TRK2* promoter (Vidal et al. 1995). An increase in *TRK2* expression was detected in genome-wide experiments under some stress situation such as phosphorus limitation (Boer et al. 2003).

Despite these transcriptional changes, the main regulation of *TRK* transporters occurs at the protein level. The activity and/or stability of Trk1,2 are controlled by several protein kinases and phosphatases (Figure 4). The functionally redundant protein kinases Sat4/Hal4 and Hal5 are required to stabilize the Trk transporters at the plasma membrane, especially under low potassium conditions (Pérez-Valle et al. 2007; Mulet et al. 1999), and thus lack of both kinases has a severe impact on high-affinity potassium transport. This role is not restricted to Trk1, and several nutrient transporters are also stabilized by Hal4 and Hal5 (Pérez-Valle et al. 2010). Trk1 is phosphorylated *in vitro* and *in vivo* by protein kinase(s) (Yenush et al. 2005; Swaney et al. 2013; Holt et al. 2009; Helbig et al. 2010) and the phosphorylated Trk1 form has higher potassium transport activity (but no direct phosphorylation of Trks by Hal4 and Hal5 kinases has been reported). In addition, under standard growth conditions, the expression of the *HAL5* gene is under the control of calcineurin and the calcineurin-regulated transcription factor Crz1 (Casado et al. 2010). The role of calcineurin on the regulation of Trk1 activity can be independent of Hal5 and is important under cation stress situations (Pérez-Valle et al. 2007; Casado et al. 2010). Under sodium stress, calcineurin is a necessary element for the transition of the Trk transporter system to the high-affinity potassium state, which helps to discriminate K^+ from Na^+ (Mendoza et al. 1994). Under lithium stress, calcineurin receives the input of Ypi1 (essential regulatory subunit of the Glc7 protein phosphatase) to decrease Trk-mediated Li^+ influx (Marquina et al. 2012).

As mentioned before, the Pma1 capacity to generate the electrochemical H^+ gradient is highly controlled by glucose levels; so it makes sense that the activity of Trks, which is the main consumer of this gradient, is also under glucose control. It has been proposed that the protein kinase Snf1, an essential element for controlling the transcriptional changes associated

with glucose derepression (Sanz 2003), acts as an additional regulator of potassium influx via Trks (Portillo et al. 2005). In the presence of glucoses, Snf1 is found in a non-phosphorylated form, but still displays a weak kinase activity that is able to activate high-affinity K^+ uptake, probably controlling the expression of an unknown gene or genes controlled by the Snf1-regulated transcription factor Sip4 (Portillo et al. 2005).

The trehalose-6-phosphate synthase, encoded by *TPS1* gene, represents an additional link between potassium and carbohydrate metabolism. This gene product activates Trks and decreases the sensitivity of yeast cells to many toxic cations independently of the Trk1 positive regulators Hal4 and Hal5 or of calcineurin (Mulet et al. 2004). Mutants defective in *PGM2* (encoding phosphoglucomutase, the enzyme that catalyses the conversion from glucose-1-phosphate to glucose-6-phosphate) or *HXK2* (encoding hexokinase, which phosphorylates glucose to glucose-6P) exhibited *trk1* related phenotypes similar to those of *tps1* mutants. A positive correlation between the levels of glucose phosphates (Glc-1-P and Glc-6-P) caused by these mutations and Trk activity, lead to propose that these metabolites, directly or indirectly, activate potassium uptake via the Trk system (Mulet et al. 2004). These results correlate with the early observation that potassium uptake in yeast is activated by glucose and other fermentable sugars and that phosphorylation of the sugar was sufficient to trigger the activating pathway (Alijo & Ramos 1993). The observed stimulatory effects of glucose over potassium uptake can be in part attributable to the induction of Pma1 and the resulting increase in electrochemical membrane gradient that is used by Trks for potassium uptake.

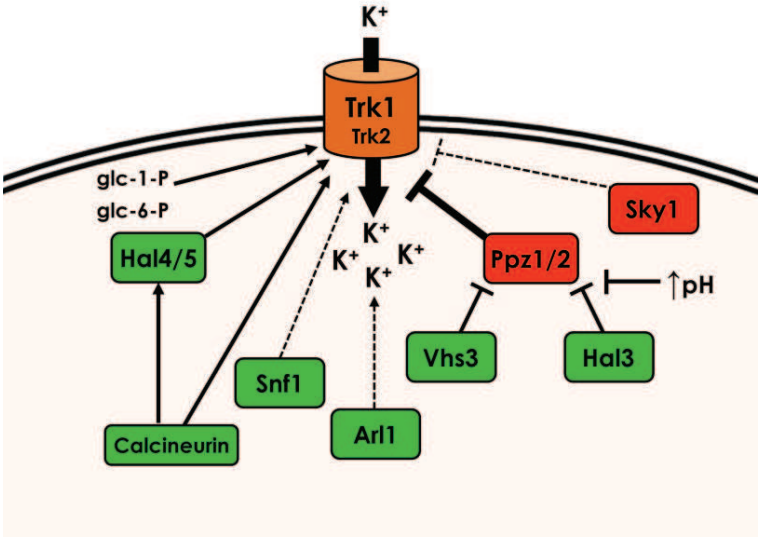

Figure 4. Regulatory pathways of Trk1 and Trk2 plasma membrane potassium transporters. The proteins with green background act as activators and those with red background as repressors of potassium uptake. Discontinuous lines indicate interactions not fully documented. See main text for details.

Finally, the GTPase Arl1, with a role in regulation of membrane traffic, is also a positive regulator of Trk1 (Munson et al. 2004). In spite of its intracellular trafficking function, the loss of *ARL1* had neither effect on Trk1 proper localization to plasma membrane (Munson et al. 2004; Pérez-Valle et al. 2007) nor on the activity of other cation transporters (Marešová et al. 2012). Although Arl1 could control Trk1 activity via regulation of Hal4 and Hal5, its precise role is still poorly defined.

On the other hand, several negative regulators of Trk activity have been described (Figure 4). The best described negative regulators are the protein phosphatases Ppz1 and Ppz2 which was previously related to salt tolerance (Posas et al. 1992; Posas et al. 1995). Ppz1 is more relevant than Ppz2 but some phenotypes are aggravated by deletion of *PPZ2* in *ppz1* mutants (Ariño 2002). Trk1 protein is proposed to be one of the Ppz1 phospho-substrates because Ppz1 physically interacts with Trk1 in plasma membrane rafts, and an increment of phosphorylated Trk1 form was detected in *ppz1 ppz2* mutants (Yenush et al. 2005).

Protein phosphatases are often associated with regulatory subunits that provide substrate specificity, determine subcellular localization, or modulate the activity of the enzyme. Ppz1 is negatively controlled by two regulatory subunits, Sis2/Hal3 and Vhs3 (de Nadal et al. 1998; Ruiz et al. 2004). Hal3 and Vhs3 bind to the C-terminal of Ppz1 and inhibit the phosphatase with a similar potency (Ruiz et al. 2004). However, Vhs3 has a less important role in vivo probably due to lower expression levels. It has been proposed a model in which the activation of Ppz1 would depend on intracellular pH where an increase in intracellular pH would disrupt the interaction between the inhibiting subunit Hal3 and Ppz1 (Yenush et al. 2005). Accordingly with this model, Hal3 would be the link between intracellular pH (and therefore H^+ levels) and cation homeostasis (mainly K^+) by regulating Trk1 through Ppz1 (Yenush et al. 2002). The Ppz1 regulators Hal3 and Vhs3 have moonlighting activities and, in addition to regulating Ppz1, they have essential functions in the CoA biosynthetic pathway together with Cab3 (Ruiz et al. 2009; Abrie et al. 2012). The essential role in CoA biosynthesis explains the lethality of the double *hal3 vhs3* mutation.

A decrease of Ppz activity by deletion of *PPZ1* or overexpression of *HAL3* stimulates potassium influx via Trks (Ferrando et al. 1995; Yenush et al. 2002). Then the elimination of Hal3 or Vhs3 activity should increase Ppz1 function and, consequently, impact negatively on potassium influx. Some phenotypes related with the absence or overproduction of Ppz1 could be due to the changes produced in intracellular potassium concentrations by altered K^+ transport and the consequent deregulation on cell turgor and intracellular pH (Yenush et al.

2002). For example, *PPZ1* and *PPZ2* display functional interactions with mutations in the cell wall integrity pathway because this mutants present a weakened cell wall and this is deleterious in *ppz1* and/or *ppz2* mutants that present high intracellular turgor derivate from K^+ overaccumulation (Posas et al. 1993; Lee et al. 1993; de Nadal et al. 1998; Merchan et al. 2004). In addition to their role in regulating Trk potassium transporters, Ppz phosphatases (essentially Ppz1), positively affect the low affinity potassium transport in *trk1 trk2* mutant strains (Ruiz, del Carmen Ruiz, et al. 2004). Other Ppz1 functions not clearly attributable to intracellular potassium fluctuations are related with cell cycle progression (Clotet et al. 1996; Clotet et al. 1999) or protein translation (de Nadal et al. 2001).

An additional negative regulator of Trk1 activity is the SR protein kinase Sky1 (Forment et al. 2002) Sky1 was defined as a MDR factor (Hillenmeyer et al. 2008) and necessary for the exit of the polyadenylated RNA from the nucleus (Gilbert et al. 2001). There is some controversy on the actual target of the kinase, and Trk-independent roles have been also proposed (Erez & Kahana 2002). The overexpression of Sky1 increases sensitivity to LiCl and this effect depends on the integrity of *PPZ1* but not of *ENA1* (Erez & Kahana 2001). Although it was originally proposed that Sky1 did not significantly affect Pma1 activity (Erez & Kahana 2001), new studies revealed that *sky1* mutants have defects in growth in low-potassium medium with only a slight defect in potassium transport but a pronounced decrease in the proton-pumping activity (Barreto et al. 2011). In the light of these results, the Sky1 target could be Pma1, without discarding direct regulation of Trk1 or the possible role of the kinase in the regulation of mRNA export of some players on cation homeostasis.

Low-affinity potassium transport

In a wild-type strain growing at normal potassium extracellular concentrations, the potassium influx is mediated by Trk1 working as a moderate- low-affinity potassium transporter (Ariño et al. 2010). Trk1, and presumably Trk2, can work as a high-affinity or low-affinity transporter according to the growth conditions and potassium status of the cell (Ariño et al. 2010). Yeast cells switch from low-affinity to high-affinity potassium transport after a period of potassium starvation.

The double mutant *trk1 trk2* is viable but needs extracellular potassium concentrations around 20 mM to grow as a wild-type strain (Navarrete et al. 2010), highlighting the existence an ectopic, Trk-independent low-affinity potassium transport process. This low-affinity potassium transport has a K_m in the mM range (Madrid et al. 1998) and is probably supported

by a putative nonspecific cation "channel" named NSC1 (Bihler et al. 1998; Bihler et al. 2002). This putative transporter mediates K^+ currents that are blocked by Ca^{2+} or other divalent cations (Roberts et al. 1999). The gene(s) encoding NSC1 are still not identified, but recently, the calcium-related transporters Kch1 and Kch2 have been found to sustain growth of *trk1 trk2* mutant cells in low K^+ environments, suggesting they promote K^+ uptake (Stefan & Cunningham 2013).

In addition to these transporters, the ability to transport potassium has been attributed to other nutrient or drug transporters. The drug/H^+ antiporter Qdr2, which acts as MDR factor for several compounds, is capable to transport potassium independently of the Trk system (Vargas et al. 2007). Remarkably, it has been shown that a single amino acid change can transform an amino acid permease such as Bap2 or Hip1 in a likely potassium transporter (Wright et al. 1997). Similarly, some mutations in the hexose transporter genes (*HXT1*, *HXT3* and *GAL2*) are capable to suppress the *trk1 trk2* phenotype at limiting potassium (Ko et al. 1993; Liang et al. 1998). In both types of transporters, potassium transport is not obligatorily coupled to the binding or transport of each nutrient. Finally, Pmp3, a small 55 amino acid hydrophobic polypeptide located at yeast plasma membranes that has high sequence similarity with a family of plant small polypeptides, has been also related to potassium transport (Navarre & Goffeau 2000). The deletion of Pmp3 facilitates nonspecific monovalent cation uptake driven by an increase in the membrane potential independently of Sky and Trk1,2 activities(Erez & Kahana 2002). The fact that the cation uptake caused by Pmp3 deletion is blocked by Ca^{+2} or other divalent cations could indicate that this transport is dependent on NSC1 activity.

3.4.3 Alkali cation efflux systems

The regulation of the activities of both Pma1 and Trk1 is fundamental for the modulation of the electrochemical gradient used by other nutrient symporters. The balance between influx and efflux of K^+, H^+ and other cations sets the level of the plasma-membrane potential (Ke et al. 2013; Mulet et al. 1999; Navarrete et al. 2010). Increase of K^+, Na^+, and H^+ in the medium causes a significant depolarization of *S. cerevisiae* plasma membrane, an effect that is dependent on Trk1,2 transporters only for potassium (Plášek et al. 2013). The coordinated regulation between cation influx and efflux systems is essential for controlling the membrane electrochemical potential in yeast.

Tok1

The voltage-gated K^+-specific channel Tok1 is one of the main participants on potassium efflux in yeast (Ketchum et al. 1995) (Figure1). The structure of Tok1 protein is based in two pore domains in tandem, each of which forms a functional channel permeable to potassium and a carboxyl tail with the function of preventing inner gate closure. The channel is open at positive and less negative than -40 mV membrane voltages (membrane depolarization) (Bertl et al. 1998; Zahrádka & Sychrová 2012). The activity of Tok1 is modulated by external K^+ in yeast (Vergani et al. 1997; Loukin et al. 1997) or even when it is expressed in *Xenopus laevis* oocytes (Ketchum et al. 1995; Reid et al. 1996; Zhou et al. 1995). After an osmotic shock, Tok1 is phosphorylated by Hog1 and, together with the other cation efflux systems, contribute to the short-term relief from NaCl shock (Proft & Struhl 2004). The physiological role of Tok1 consist in mediating intracellular K^+ release when plasma membrane is depolarized in order to regenerate the membrane potential (Bertl et al. 1998). The Tok1 activity serves for fine tuning the plasma-membrane potential together with the other cation importer or exporters (Bertl et al. 2003; Maresova et al. 2006). Tok1 is also able to enter potassium in non-physiological conditions (*trk1 trk2* mutant strain overexpressing *TOK1*) (Fairman et al. 1999). Tok1 is a target of killer K1 toxin, a yeast toxin of viral origin that kills yeast by opening Tok1 channels creating a massive potassium release from the cells (Ahmed et al. 1999).

Nha1

In contrast to Tok1, which is specific for K^+, the other 2 cation efflux systems play a primary role in Na^+ efflux, although are also able to work with K^+ and Li^+ (Figure 1). Nha1 is a proton/Na^+ or K^+ antiporter and Ena1 is a Na^+-ATPase transporter that is also able to transport K^+ when is found at high intracellular concentrations (Bañuelos et al. 1998; Nakayama et al. 2004). Nha1 is a plasma membrane protein localised in lipid rafts rich in the sphingolipids necessary for Nha1 stabilization (Mitsui et al. 2009). Nha1 has similar affinities for extrusion of sodium and potassium at acidic pH (Bañuelos et al. 1998; Prior et al. 1996). Nha1 functions as a dimer with a 12 membrane-spanning segments, structurally similar to other Na^+/H^+ exchangers, and a very long (56 % of the protein) hydrophilic C-terminal cytosolic domain (Pribylová et al. 2006). The conserved amino acids residues located in the transmembrane part of the protein necessaries for the antiport function have been identified (Simón et al. 2001; Simón et al. 2003; Kinclova-Zimmermannova et al. 2006; Kinclova-

Zimmermannova et al. 2005). The long C-terminal domain contains six regions that are conserved in other fungal Na^+/H^+ exchangers, and are required for its targeting to the plasma membrane and cation exchange activity (first 16 residues overlapping with the last transmembrane segment) (K Mitsui et al. 2004; Keiji Mitsui et al. 2004). The C-terminal tail is also necessary for substrate specificity and regulation, for example interacting with 14-3-3 proteins (Kinclova et al. 2001; Simón et al. 2001; K Mitsui et al. 2004; Zahrádka et al. 2012). The Nha1 play an important role in regulation of cell cycle, the overexpression of the transporter suppresses the G_1 arrest in cells with conditional *sit4 hal3* mutations (Simón et al. 2001). The regulation of cell cycle by Nha1 is also attributed to the C-terminal region without relation with cation transport capacity of the Nha1 (Simón et al. 2003).

The principal roles attributed to Nha1 are Na^+ detoxification and K^+ efflux. By mediating K^+ efflux Nha1 contributes to control the membrane potential of yeast cells in coordination with the mechanisms responsible for potassium uptake (Zahrádka & Sychrová 2012; Banuelos et al. 2002). Consequently, the activity of Nha1 affects the uptake of potassium by Trks (Banuelos et al. 2002), and vice versa, the deletion of *trk1 trk2* cause membrane hyperpolarization that blocks the activity of the potassium efflux systems Nha1 and Ena1 (Zahrádka & Sychrová 2012). Therefore, Nha1 activity is also involved in control of intracellular pH or regulation of cell volume. Nha1 also promotes rapid adaptation to alkaline and osmotic stress (Bañuelos et al. 1998; Kinclova et al. 2001; Proft & Struhl 2004). Under alkaline pH the outward gradient of potassium cations can serve as a driving force for proton influx (Kinclova et al. 2001; Bañuelos et al. 1998).

The expression of *NHA1* gene is not affected by any form of stress. However, Nha1 activity is important to respond to sodium stress. After osmotic shock, the Hog1 kinase, activated by the HOG signalling pathway, phosphorylates the C-terminal tail of Nha1 and improve cell growth under sodium osmotic stress (Proft & Struhl 2004). The main role of Nha1 in NaCl stress consists in initiate the active extrusion of the intracellular Na^+ surplus. The activation of Nha1 by Hog1 decrease the Nha1 extrusion of potassium preventing the entrance of sodium by maintaining high intracellular potassium levels (Kinclova-Zimmermannova & Sychrova 2006; Proft & Struhl 2004). Nha1 potassium efflux activity its positive modulated by the Ser/Thr phosphatase Sit4 whose expression is induced by exposure to Li^+, Na^+ or K^+ in cells growing in galactose (Masuda et al. 2000). Sit4 have 4 different regulatory subunits called SAP proteins (Luke et al. 1996), of which two of them, *SAP155* and *SAP185*, are also involved in cation homeostasis. *SAP155* encode a negative modulator of K^+

efflux and *SAP185* encode a positive one (Manlandro et al. 2005). Because these effects are mediated by Sit4 and require Nha1, the more plausible mechanism is that Sap155 and Sap185 would be negative and positive regulators of Sit4, respectively. Finally, Cos3 was identified as a membrane protein that can enhance salinity-resistant cell growth by interacting with the C-terminal of Nha1 and activating this protein cation exporter activity (Keiji Mitsui et al. 2004).

Ena ATPases

The chromosome IV of *S. cerevisiae* contains a cluster of repeated genes, *ENA* genes, each of which encodes a P-type ATPase. The *ENA* genes encode proteins very similar or identical, and the number of copies of *ENA* genes differs from strain to strain (Garciadeblas et al. 1993; Wieland et al. 1995; Haro et al. 1991; Martinez et al. 1991). Most laboratory strains contain between one to five *ENA* genes (Wieland et al. 1995) (CEN.PK strains contains a single atypical *ENA6* gene (Daran-Lapujade et al. 2009)). These ATPase use the energy of ATP hydrolysis to catalyse the extrusion of Na^+, Li^+ or K^+ with different affinity (Benito et al. 1997; Haro et al. 1991) (Figure 1). The putative structure deduced from the amino acid sequence of Ena proteins leads to the prediction of 9-10 transmembrane domains localised in the plasma membrane of *S. cerevisiae* (Wieland et al. 1995). *ENA1* is the most relevant member of the cluster and it is the most studied. It is barely expressed under standard growth conditions, but is rapidly induced by osmotic stress, salt stress or by alkaline pH (see (Ruiz & Ariño 2007) for a review). Deletion of *ENA1* causes strong sensitivity to sodium or lithium (Rodríguez-Navarro et al. 1994; Wieland et al. 1995; Posas et al. 1995; Haro et al. 1991; Garciadeblas et al. 1993) and a growth defect at alkaline pH (Platara et al. 2006; Haro et al. 1991). Ena1 activity is essential upon alkaline pH stress because the other Na^+ or K^+ efflux systems, such as Nha1, cannot function under this condition (Haro et al. 1991; Bañuelos et al. 1998). The combination of Tok1, Nha1 and Ena1 activity contributes significantly to the maintenance of the plasma membrane potential (Maresova et al. 2006). It has been proposed that Ena1 and Nha1 could play an important role controlling the membrane potential, and therefore allowing the maintenance of normal uptake of nutrients through secondary transporters, under stress conditions in which the proton gradient is reduced (Ke et al. 2013).

Cation extrusion by Ena ATPases is regulated at the transcriptional level. The different signals leading to *ENA1* gene expression are integrated at the promotor level as a result of the modulation of different pathways. *ENA1* is regulated by a complex network composed by the HOG osmoresponsive, the calcineurin, the Rim101 pathways, and other pathways related with

nutritional status of the cell. The osmotic stress generated after addition relatively moderate concentrations of NaCl (>0,4 M) activates the HOG pathway that it turns activate the Hog1 kinase (Brewster et al. 1993; Maeda et al. 1994). Under osmotic stress Hog1, besides the previously described activation of Nha1, phosphorylates two different targets acting on the Ena1 promoter and leading to increase *ENA1* expression. The Sko1-Ssn6-Tup1 repressor complex is phosphorylated by Hog1 promoting the disassociation of the repressor transcription factor Sko1 from the general corepressor complex Ssn6-Tup1. This releases the Sko1 repressor from the *ENA1* promoter, allowing the transcription of the gene (Proft et al. 2001). Hog1 also recruits the Rpd3-Sin3 histone deacetylase complex to the *ENA1* promoter, leading to histone deacetylation and the entry of RNA polymerase II to start transcription (De Nadal et al. 2004).

The addition of NaCl or shifting cells to alkaline pH activates *ENA1* expression by the calcineurin-Crz1 system that is activated by the burst of cytosolic calcium produced in cells upon these stresses (Hirata et al. 1995; Márquez & Serrano 1996; Viladevall et al. 2004). The *ENA1* promoter contains two CDRE elements located at positions -813/-821 and -719/-727, where the downstream element is more important for the transcriptional response under saline stress and essential for Crz1-dependent alkaline pH response (Mendizabal et al. 2001; Platara et al. 2006). *ENA1* mRNA levels are higher than normal in a *ppz1 ppz2* mutant strain partially due to the constitutive activation of the calcineurin-Crz1 pathway in this mutant, and partly by the intracellular alkalinisation caused by the deregulation of potassium uptake via Trks (Ruiz et al. 2003).

Another pathway activated by saline stress and alkaline pH that controls *ENA1* expression is mediated by the protein kinase Snf1. The Snf1-mediated effect on *ENA1* depends on Mig2 and Nrg1 repressors (Alepuz et al. 1997; Platara et al. 2006). The Nrg1 repressor is negatively regulated by interaction with Snf1 at alkaline pH (Vyas et al. 2001; Platara et al. 2006). Similarly, the transcription factor Rim101 repress the expression of Nrg1, allowing the transcription of the *ENA1* gene (Platara et al. 2006; Lamb et al. 2001). The high sodium and alkaline stress decrease intracellular levels of cAMP (Márquez & Serrano 1996; Casado et al. 2011) resulting in inhibition of PKA kinase activity. This inhibition has effects on both Crz1 (Kafadar & Cyert 2004) and Sko1 (Proft et al. 2001). Failure to phosphorylate PKA-specific sites of Sko1 limits its repressor activity on the *ENA1* promoter, while decreased PKA-mediated phosphorylation of Crz1 favours its entry to the nucleus. Both mechanisms aim to the same final result: increased *ENA1* expression. The repression of *ENA1* by glucose,

caused by transcriptional repressors Mig1,2, Sko1 and Nrg1 could be useful to avoid a futile cycle in which potassium enters into the cell using the membrane potential generated by the glucose activation of Pma1 and at the same time is excluded from the cell by Ena1 (with the additional energy cost).

ENA1 expression could be regulated by other pathways also related with nutrient availability like TOR. The regulation of *ENA1* by the TOR pathway is controversial since the ATPase gene is induced by rapamycin dependent on the TOR-regulated transcription activators Gln3 and Gat1 (Crespo et al. 2001; Crespo & Hall 2002), but Gln3 localise to the cytoplasm under saline stress (Tate & Cooper 2007).

Mutations or overexpression of a number of other genes has been shown to affect salt tolerance and *ENA1* expression. For example the regulatory subunits of Glc7, Ref2 and Ypi1, regulates *ENA1* expression dependent on Glc7 or calcineurin, respectively (Ferrer-Dalmau et al. 2010; Marquina et al. 2012). Other genes associate with *ENA1* expression with not well-known mechanism are *ISC1* (Betz et al. 2002), *PTC1* (Ruiz et al. 2006), *PRS1* and *PRS2* (Siniossoglou et al. 2000), *HAL9* (Mendizabal et al. 1998), *ATC1* (Hemenway & Heitman 1999), *HAL1* (Gaxiola et al. 1992; Rios et al. 1997), etc.

3.4.4 Intracellular (organelle) alkali cation transport

Yeast cells accumulate alkali cations in the vacuoles and other organelles like Golgi, endosomes or mitochondria. The vast majority of intracellular transporters use the proton gradient generated by V-ATPase to antiport cations into the organelles. Intracellular cation transport is used for regulate the organelle cation composition, control cellular volume and to effective response to cation stress conditions by accumulating the excess of cation or toxic cations into organelles.

Three intracellular K^+ $(Na^+)/H^+$ antiporters with different localizations have been described and characterized in *S. cerevisiae* cells (Figure 1). Vnx1 mediates the majority of cation transport in vacuoles, although it is also found in endoplasmic-reticulum membranes (Cagnac et al. 2007). Vnx1 encodes a 102 kDa protein with 13 predicted transmembrane domains and, like vacuolar calcium transporter Vcx1, is member of the calcium exchanger superfamily. However, whereas Vnx1 cannot transport Ca^{2+}, Vcx1 can transport potassium inside the vacuoles of cells lacking Vnx1 (Cagnac et al. 2010). Recently, a Vhc1 vacuolar membrane cation-chloride cotransporter (CCC) that mediates K^+ and Cl^- cotransport into the

vacuole in a proton-independent manner has been described (Petrezselyova et al. 2013). Another cation/H+ antiporter, Nhx1, is located in late endosomes or prevacuolar membranes (Brett et al. 2005). In addition to cooperate with vacuolar cation transporters in the capture of cations, Nhx1 contributes significantly to the maintenance of stable intracellular pH and it is necessary for proper protein trafficking among endosomes and other organelles (Brett et al. 2005; Bowers et al. 2000). The C-terminal part of Nhx1 is probably N glycosylated (Wells & Rao 2001) and interacts with Gyp6, a necessary event to coordinate the vesicle trafficking between Golgi to late endosomes (Ali et al. 2004; Qiu & Fratti 2010; Kallay et al. 2011; Kojima et al. 2012). Finally, Kha1 is found in the membranes of the Golgi apparatus (Maresova & Sychrova 2005), and its role of K^+/H^+ transport is related to intracellular pH homeostasis (Flis et al. 2005). Like Nhx1, Kha1 is necessary to control intraorganellar pH and alkali cation balance, which influences vesicle trafficking.

A K^+/H^+ exchange activity was detected in the mitochondria and found to be necessary for correct assembly of respiratory chain, mitochondrial morphology and volume homeostasis (Nowikovsky et al. 2012) (Figure 1). The mitochondrial respiratory chain generates a proton gradient in the intermembrane space necessary for oxidative phosphorylation and cation transport. Some proteins necessary for K^+/H^+ exchange have been detected in mitochondria, such as the members of the LETM1 protein family Mdm38 (Nowikovsky et al. 2007) and Ylh47 (alias Mrs7) (Zotova et al. 2010). Another gene, *YDL183C*, encodes a protein that may form an active mitochondrial K^+/H^+ exchange system (Zotova et al. 2010). However these proteins contain a single trans-membrane domain, suggesting that they modulate transport rather than drive it. It is conceivable that these proteins are components of larger protein complex in charge of the essential mitochondrial K^+/H^+ exchange system, (Nowikovsky et al. 2012).

3.5 Stress responses in yeast

Fluctuation in temperature, osmolarity and acidity of the external environment as well as the presence of toxic elements or nutrient/ion starvation can results in perturbation of the internal cell environment. All living cells display a rapid response to adverse environmental conditions and the budding yeast is a good model for its study. Yeast cells react against stress conditions mainly by remodelling the transcriptional expression profile, activating the genes necessaries to adapt to the stress and repressing those not necessaries (Causton et al. 2001). In

yeast exists a general response to stress that protects cells to various stressful stimuli, and a number of specific response pathways for each type of stress. Many general stress-induced genes contain STRE elements in their promoter, which are recognized by the transcription factors Msn2 and Msn4 (Martínez-Pastor et al. 1996). These factors are known as the general stress transcription factors. The use of genome-wide techniques to study different kinds of stress (alkaline pH, heat shock, osmotic, oxidative, etc) has made possible to enlarge the number of genes with a common response to many stressful conditions and classify them as environmental stress response (ESR) genes (Gasch et al. 2000). Approximately 900 genes are defined as ESR, of which ~300 increase their transcript levels and ~600 are repressed in response to the environmental changes (Gasch et al. 2000). Some induced ESR are under the control of Msn2 and Msn4 but other are not (Gasch & Werner-Washburne 2002). The induced genes are enriched in categories related with carbohydrate metabolism and transport, oxidative stress response and many other essential cellular processes, whereas the repressed genes correspond mainly to protein synthesis processes, particularly to those encoding ribosomal proteins and the RiBi regulon, composed by genes necessary for the ribosome biogenesis but also for tRNA and nucleotide metabolism (Bosio et al. 2011).

3.5.1 Oxidative stress response

A shared cellular problem that appears after several stresses, such as heat shock or alkaline pH, is the accumulation of ROS that generates oxidative stress to the cells (Morano et al. 2012; Viladevall et al. 2004). Molecular oxygen is a relatively unreactive molecule but its utilization can produce diverse ROS (superoxide anion, hydrogen peroxide or hydroxyl radical) when oxygen is partial reduced. ROS in yeast are mainly generated by oxidative phosphorylation in mitochondria and other processes like protein folding in ER, or peroxisome-localized reactions, such as like fatty acid degradation or deamination of amino acids (Morano et al. 2012). ROS are continuously produced due to normal cell metabolism, but organisms contain antioxidant defence mechanisms (enzymes or small molecules such as glutathione or ascorbic acid (Amari et al. 2008)) to detoxify ROS and maintain proper intracellular redox status. ROS can damage a wide variety of cellular components by lipid peroxidation, protein oxidation or DNA modifications. *S. cerevisiae* responds to oxidative stress by detoxifying ROS molecules, by reducing their rate of production and by repairing the damage caused. A key feature in this response, like other yeast responses to stress, is the transcriptional reprogramming of gene expression aiming to return to a controlled redox

status. The transcriptional response to oxidative stress requires the transcription factor Yap1, which has a predominant role, but other transcription factors like Skn7 and Msn2/Msn4 are also relevant to responds to oxidative stress (Temple et al. 2005). These transcription factors activate the transcription of genes encoding different ROS detoxifying enzymes such as superoxide dismutase (Sod1 and Sod2) that reduces superoxide anions to hydrogen peroxide that is reduced again by catalases (Ctt1 and Cta1), trough dismutation reactions. Other induced enzymes are the peroxidases that reduce peroxide groups to alcohols or alcohol derivatives by using as electron donors reduced glutathione (glutathione peroxidases) or reduced thioredoxins (peroxiredoxins) (Herrero et al. 2008).

Amino acids are susceptible to oxidation by ROS and especially Cys and Met sulfur amino acids that contain thiol groups which can be easily oxidized by ROS (Stadtman & Levine 2003) (Figure 5). Yeast cells have different systems to prevent protein oxidation and the consequent problems for cellular processes. Thioredoxins reduce the disulfide bonds produced in proteins and are necessary to control the redox state of thiol groups during protein folding, whereas the glutaredoxins have similar functions but using glutathione to break the disulfide bonds or remove glutathione linked to proteins (Herrero et al. 2006; Trotter & Grant 2003) (Figure 5). Glutathione is predominantly present in its reduced form in yeast due to the constitutive action of glutathione reductase but oxidative stress converts glutathione to its oxidized disulfide form (Muller 1996). The main functions of glutathione are to reduce ROS non-enzymatically avoiding the production of peroxides or free radicals and to protect the thiol groups of proteins from oxidation (Penninckx 2002). The system needs the present of glutathione reductases and thioredoxin reductases to recycle oxidized glutathione or oxidized thioredoxins to the reduced form (Morano et al. 2012) (Figure 5). In yeast there are other reductases to protect against oxidative stress, such as methionine sulfoxide reductases that prevent methionine oxidation by catalyzing thiol-dependent reduction of oxidized Met residues (Le et al. 2009).

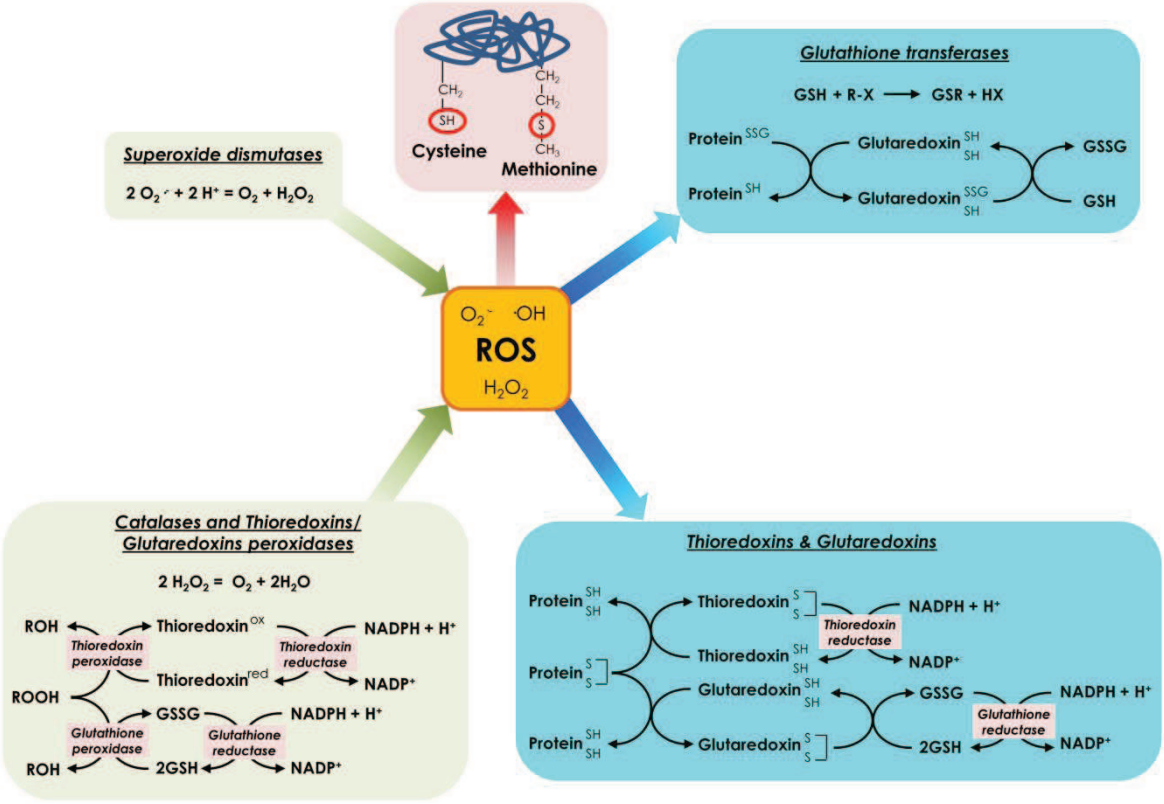

Figure 5. Enzymatic systems involved in ROS detoxification and in control of the redox state of proteins in *S. cerevisiae*. Elements in green background indicate systems mainly involved in ROS detoxification and in blue background systems that control redox state of proteins. For details see the main text. $O_2^{\cdot-}$, superoxide anion; ·OH, hydroxyl radical; H_2O_2, hydrogen peroxide; GSH, reduced glutathione; GSSG, glutathione disulphide. Figure composed using data obtained from (Herrero et al. 2008; Penninckx 2002; Temple et al. 2005)

3.6 Nitrogen homeostasis

Essential nutrients are required for provision of energy and building blocks for growth. The yeast *Saccharomyces cerevisiae* can adjust its growth rate and behaviour in response to the nutrient availability by coordinating progression through the cell cycle with the levels of nutrient. It is known that the depletion for a single essential nutrient cause cell cycle arrest in the G_1 phase and entrance into G_0 (Hartwell 1974). In yeast, cells sense and remodel their metabolism and transcriptional profile in function of the nutrients present in the environment through different nutrient-sensitive pathways. Carbon and nitrogen-containing molecules constitute major nutritional sources and cells not only adapt their growth and metabolism to the quantity and quality of these sources, but also to their relative amounts. Other important nutrient-related pathways are those dealing with phosphate and sulfate (see sections below) or vitamins (Hohmann & Meacock 1998).

Yeast cells obtain energy through fermentation of sugars (preferentially glucose) or, in the absence of this sugar, by oxidation of some non-fermentable products like ethanol or glycerol. The principal pathways involved in adaptation to the carbon source are complex networks interconnected and overlapped with those of other nutrients. Among them are the PKA pathway that controls metabolism, growth capacity, and stress responses depending on carbon source (Thevelein & de Winde 1999), the Snf1 pathway, related to the use of alternative glucose carbon sources (Celenza & Carlson 1984) or Rgt/Snf3, tuning the glucose uptake capacity depending on glucose levels (Ozcan, Dover, et al. 1996; Ozcan, Leong, et al. 1996).

The other essential nutrient highly regulated acquisition and use in yeast is nitrogen. Nitrogen is needed for biosynthesis of amino acids, nucleotides and a variety of nitrogen-containing compounds. *S. cerevisiae* can use a diversity of amino acids or other organic nitrogen compounds as nitrogen sources, but the standard laboratory yeast strains prefer glutamine and ammonium over other nitrogen sources (Zaman et al. 2008). The presence of high-quality nitrogen sources prevents pseudohyphal or invasive growth while the presence of any nitrogen source prevents meiosis and sporulation (Zaman et al. 2008). In standard laboratory synthetic media, ammonium is the main nitrogen source used because it supports growth of yeast cells at an optimal rate. Ammonium is transported into the yeast cells by three ammonium transporters, Mep1, Mep2 and Mep3, but they are not essential for growth on NH_4^+ at high concentrations (>20 mM), suggesting the existence of additional ammonium transport system (Marini et al. 1997). In yeasts grown in glucose, ammonia can be assimilated by two anabolic pathways: the NADPH-dependent reductive amination of 2-ketoglutarate to yield glutamate, catalysed by glutamate dehydrogenases encoded in yeast by the *GDH1* and *GDH3* genes, or by the ATP-dependent synthesis of glutamine from glutamate and ammonia, catalysed by glutamine synthase (*GLN1*). Nitrogen-containing compounds such as amino acids or nucleotides are synthetized from glutamate or glutamine, underlining the importance of these 2 amino acid sin yeast metabolism (Magasanik 2003).

Growth in a preferred nitrogen source leads to repression of genes required for uptake and catabolism of less preferred nitrogen sources trough a pathway named nitrogen catabolite repression or NCR (Hofman-Bang 1999; Magasanik & Kaiser 2002). One example gene subjected to NCR is the general amino acid permease Gap1, that its only found in the plasma membrane under poor nitrogen conditions (Magasanik & Kaiser 2002). The expression of NCR genes results from the interplay of four transcription factors, two activators, Gln3 and Gat1, and two repressors, Gzf3 and Dal80, which bind to GATA sequences in the NCR

promoters (Cooper 2002; Magasanik & Kaiser 2002) (Figure 6). In parallel to NCR, the SPS signalling system senses the external presence of amino acids and during growth on preferred nitrogen sources activates the transcription of several amino acid specific permeases, whereas in poor nitrogen sources or absence of nitrogen these permeases are replaced by Gap1 (Ljungdahl & Daignan-Fornier 2012) (Figure 6).

In the absence of a nitrogen source, cells stop growing and enter to quiescent state even in presences of enough levels of the other nutrients (Klosinska et al. 2011). In the absence of one or more amino acids the pathway involved in the general control of amino acids biosynthesis, the GAAC pathway is activated. Such activation inhibits global translation initiation and activates, through the transcription factor Gcn4, the transcription of genes related with amino acid biosynthesis and nitrogen utilization (Hinnebusch & Natarajan 2002) (Figure 6). In cells exposed to less preferred nitrogen sources or under nitrogen starvation, the TORC1 pathway is inhibited allowing the activation of NCR related genes and other pathways related with nitrogen starvation, such as the mitochondrial retrograde (RTG) pathway necessary for α-ketoglutarate synthesis, that are otherwise partially inhibited by TORC1 pathway in the presence of preferred nitrogen sources (Cooper 2002; Inoki et al. 2005) (Figure 6).

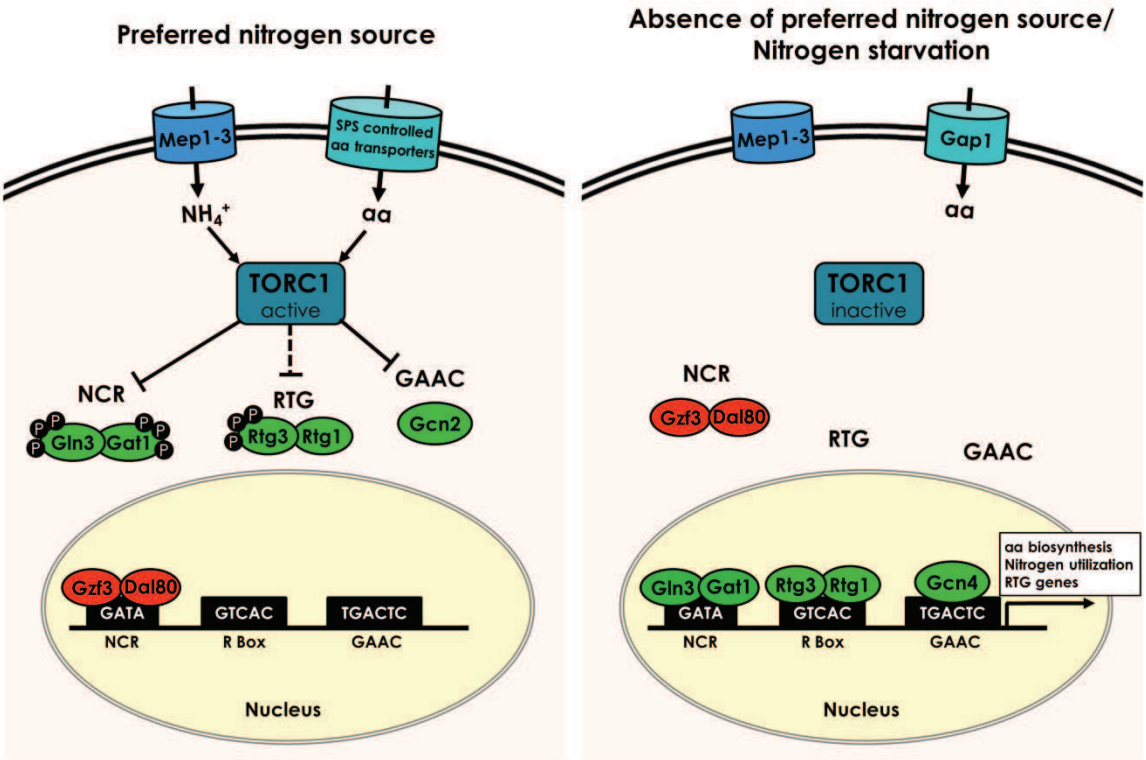

Figure 6. Simplified view of pathways involved in nitrogen metabolism depending on availability/type of nitrogen source. In presence of preferred nitrogen sources, the TORC1 pathway sense levels of preferred amino acids or ammonia and is active, collaborating to repress pathways involved in the metabolism of the less preferred nitrogen sources (NCR), retrograde pathway (RTG) and general synthesis of amino acids (GAAC). In these conditions amino acids subsets are transporter by specific permeases controlled by the SPS amino acid-sensing system. In absence of preferred nitrogen source or under nitrogen starvation, the TORC1 pathway is inactive leading to the activation of the mentioned nitrogen-related pathways mainly by recruiting the specific transcription factors to the promoters of the genes involved in nitrogen utilization of less preferred nitrogen sources (NCR), amino acids biosynthesis (GAAC) and glutamate/glutamine biosynthesis (RTG). Under these conditions the SPS-controlled specific amino acid transporters are replaced by the general amino acid permease Gap1.

3.6.1 Mitochondrial retrograde pathway

The pathways associated with regulation of nitrogen metabolism are regulated by the levels of intracellular pools of glutamate, glutamine, and ammonia, the preferred nitrogen sources and main precursors for amino acid biosynthesis (Butow & Avadhani 2004; Liu & Butow 2006; Chen & Kaiser 2002). The synthesis of glutamate and glutamine by fixation of ammonia needs the activity of TCA enzymes involved in the production of α-ketoglutarate in coordination with glutamate dehydrogenase and glutamine synthetase. Cells repress all the TCA genes during growth on glucose (with some exceptions, see below) and induce them when shift to a respiratory metabolism through the action of the *HAP* activator complex (composed by Hap1, an oxygen-sensing transcriptional activator, and the heteromeric Hap2-5 transcriptional complex (Broach 2012)). However, even when cells normally repress all the TCA genes, the first three genes can still be induced by activation of the RTG pathway (Liu & Butow 1999).

The RTG is a pathway of communication from mitochondria to the nucleus with the aim to transmit mitochondrial signals to modulate cellular responses to changes in the functional state of mitochondria. It is opposite of the normal anterograde pathway that transfers information and material (e.g. proteins necessaries for oxidative phosphorylation) from the nucleus and cytoplasm to mitochondria. The RTG pathway is upregulated in respiratory-deficient cells lacking mtDNA (ρ^0) (Butow & Avadhani 2004). The key function of the retrograde response is to modify the metabolic state of cell in response to the loss of mitochondrial function mainly aiming to maintaining the glutamate supplies to the cell. This is achieved by induction of the enzymes necessaries for the production α-ketoglutarate, a key metabolite for ammonium fixation to glutamate and glutamine (Jazwinski 2013). In cells lacking functional mitochondria the TCA cycle is not able to work as a full cycle (due to the lack of succinate dehydrogenase activity), thus limiting the production of α-ketoglutarate and

acetyl-CoA, required in many anabolic reactions (Butow & Avadhani 2004). The first identified retrograde gene was *CIT2,* which is upregulated as much as 50- to 60- fold in cells with dysfunctional mitochondria (Liao et al. 1991). *CIT2* encode a peroxisomal isoform of citrate synthase (Lewin et al. 1990) and, together with the 3 first enzymes of TCA cycle (*CIT1*, *ACO1* and *IDH1/2*), builds anaplerotic pathways, such as the glyoxylate cycle, that resupply cells with α-ketoglutarate and acetyl-CoA. Thus 3 first activities of TCA cycle are under the control of the RTG pathway instead of HAP complex in conditions that activates the retrograde pathway (Liu & Butow 1999). The RTG-dependent induction of the pyruvate carboxylase gene *PYC1* contributes to the production of oxaloacetate, a precursor for α-ketoglutarate biosynthesis (Menéndez & Gancedo 1998). The RTG pathway also regulates a small set of genes involved in β-oxidation of fatty acids, lysine biosynthetic enzymes (Liu & Butow 2006) and influences life span extension associated with respiratory deficiency (Kirchman et al. 1999). Another prototypic *RTG* gene, with similar expression to *CIT2,* is the D-lactate dehydrogenase gene *DLD3* (Chelstowska et al. 1999). The physiological role for the retrograde expression of *DLD3* in unknown, but should be involved in regenerating NAD^+ in respiration-deficient cells or in production of pyruvate from D-lactate.

The RTG regulatory pathway consists of four positive regulators, Rtg1-3 and Grr1, and four main negative regulators, Mks1, Bmh1, Bmh2, and Lst8 (Figure 7). Rtg1 and Rtg3 form a heterodimeric transcriptional activator that binds to the promoter region at GTCAC consensus sequences, called R box, of the RTG genes (Jia et al. 1997; Liao & Butow 1993). The localization of Rtg1 and Rtg3 is regulated by the other components of the pathway by phosphorylation of the Rtg3 transcription factor. When mitochondria are functional, the transcription factor Rtg3 is hyperphosphorylated and both transcription factors are cytoplasmic localized. A disruption of mitochondrial function results in nuclear localization of the factors due to dephosphorylation of Rtg3 and subsequent transcriptional activation of target genes (Sekito et al. 2000). Regulation of the nuclear/cytoplasmic trafficking of Rtg1/Rtg3 involves complex interactions among Mks1, Rtg2, Grr1, Lst8 and Bmh1/2 (Liu & Butow 2006). Mks1 stimulates the phosphorylated state of Rtg3 and inhibits the nuclear localization of the transcriptions factors Rtg1/3 (Dilova et al. 2004; Sekito et al. 2002). Mks1 function in turn is regulated by Grr1, Bhm1/2 and Rtg2. Grr1 is the adapter necessary to promote ubiquitination and subsequent degradation of Mks1 (Liu et al. 2005). 14-3-3 proteins Bmh1/2 positively regulate Mks1 activity over Rtg3 by two different processes. The first one is preventing Mks1 ubiquitination and degradation by Grr1 (Liu et al. 2005). The second takes

place when Mks1 is phosphorylated, forming then a complex with Bmh1/2 that sequesters Rtg3/Rtg1 in the cytoplasm (van Heusden & Steensma 2001). When the Mks1 phosphorylation decreases, Rtg2 can compete for Bmh1/2 binding with Mks1 and thereby dismiss the activity of Mks1 over Rtg3 and promote transcriptional activation of RTG-genes (Liu et al. 2003). Finally, the integral component of TOR kinase complex Lst8 negatively regulates the RTG pathway at 2 different levels, upstream and downstream of Rtg2 (Chen & Kaiser 2003; Liu et al. 2001). Lst8 is the link between RTG pathway and TORC1. In spite of the TOR inhibitor rapamycin activates the RTG pathway, several evidences suggest that TORC1 does not mediate nutrient regulation of the pathway (Liu & Butow 2006; Dilova et al. 2004; Dilova et al. 2002). Lst8 is also involved in controlling the activity and assembly of the SPS amino acid-sensing system, affecting the ability of the cells to sense external glutamate (Forsberg & Ljungdahl 2001).

The RTG pathway is induced in cells growing on nitrogen sources requiring α-ketoglutarate for its assimilation. The primary signals to initiate RTG activation appears to be the lack of glutamate (Liu & Butow 1999) and mitochondrial dysfunction. Although the point in the regulatory circuitry at which these signals impinge is not precisely known, Rtg2 is the most probable receptor of the signals (Liu & Butow 2006) (Figure 7). Even in respiratory-competent cells, glutamate starvation strongly activates the RTG pathway highlighting the potent repressor role of glutamate on the RTG pathway. Similarly, glutamine has been also proposed to be a signalling molecule for the retrograde response acting in the same way as glutamate (Crespo et al. 2002). The increase in intracellular ammonium is also a signal that produce induction of the retrograde response genes (Tate & Cooper 2003). Additionally, after hyperosmotic shock the transcription factors Rtg1 and Rtg3 are controlled by Hog1. In this situation, Hog1 is required for nuclear accumulation of Rtg1/3 complex and the Hog1 phosphorylation of Rtg3 is needed for the binding to chromatin and initiate transcriptional activity (Ruiz-Roig et al. 2012).

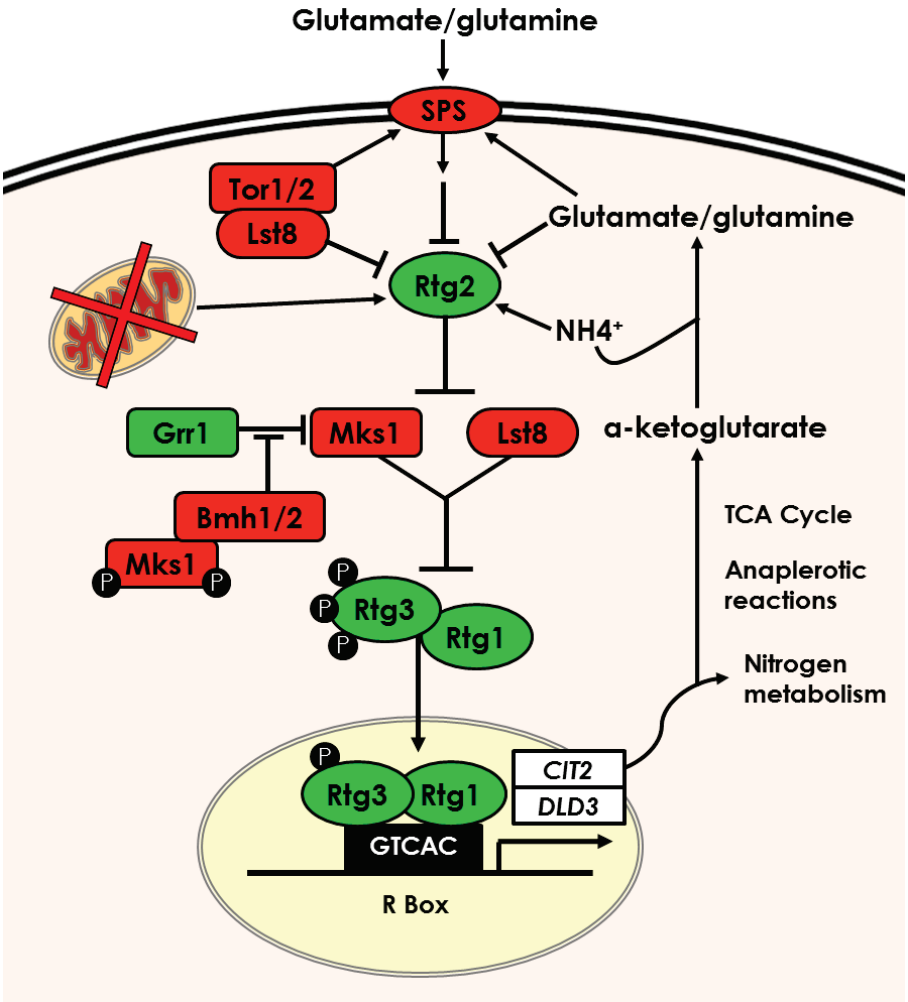

Figure 7. Regulatory model of the RTG pathway. Positive and negative regulators of the RTG pathway are shown in green and red. See main text for details. Adapted from (Liu & Butow 2006).

3.7 Sulfate homeostasis

In yeast, sulfate is used in the biosynthesis of organic sulfur metabolites, cysteine, methionine, and SAM. Normally, *S. cerevisiae* grows in media containing sulfate as sulfur source, but it can grow in the presence of either methionine or cysteine as the sole sulfur source because possess two active trans-sulfuration pathways catalysing the interconversion of homocysteine and cysteine (Thomas & Surdin-Kerjan 1997). In addition, *S. cerevisiae* is also able to grow in SAM or SMM because it has a specific transport systems and enzymes for its utilization as sulfur source (Rouillon et al. 1999).

Sulfate is cotransported into the cells with 3 H^+ by high-affinity sulfate transporters Sul1 and Sul2 (Breton & Surdin-Kerjan 1977; Cherest et al. 1997). For its use, sulfate has to be reduced to sulfide by sequential reactions (Figure 8). The first one consists in transfer the adenosyl-phosphoryl moiety of ATP to sulfate generating APS, which is in turn phosphorylated to PAPS. Then, for cysteine and methionine biosynthesis, activated sulfate is sequentially reduced to sulfite, which is in turn further reduced to sulfide and the reduced sulfur atom can be incorporated into carbon chains generating homocysteine (Thomas & Surdin-Kerjan 1997). The *MET17* gene encodes the O-acetyl homoserine and O-acetyl serine sulfhydrylase enzyme required for the fixation of sulfide to carbon chains derived from the action of Met2 over homoserine (Thomas & Surdin-Kerjan 1997). Some genetic backgrounds like BY4741 are auxotrophic for methionine and cysteine because they have the *MET17* gene mutated. The last steps of cysteine synthesis is achieved by the action of the *CYS3* and *CYS4* gene products using homocysteine and serine as substrates (Thomas & Surdin-Kerjan 1997). The need for serine in the synthesis of cystathionine, a key precursor for cysteine biosynthesis, links the biosynthesis of serine with the metabolism of sulfur amino acids (Cherest et al. 1993). The biosynthesis of cysteine is a trans-sulfuration reaction that could be a reversible process in yeast by the action of genes *STR2* and *STR3* (Hansen & Johannesen 2000). On the other hand, homocysteine is converted to methionine by the gene product of *MET6* and then to SAM by the action of *SAM1* and *SAM2*, reactions that are part of the methyl cycle. SAM is used in some metabolic reactions such as phosphatidylcholine, ubiquinone or biotin biosynthesis resulting in the formation of SAH. The methyl cycle is closed by the transformation of SAH to homocysteine again by the action of Sah1 (Thomas & Surdin-Kerjan 1997).

Sulfur amino acids can be transported into the cell, an essential process when cells cannot use sulfate for sulfur amino acids biosynthesis. This transport is mediated by the general amino acid permease Gap1 (Jauniaux & Grenson 1990) but yeasts also have specific permeases for methionine encoded by the genes Mup1 and Mup3 (Isnard et al. 1996) and for SAM (Sam3) and SMM (Mmp1), that are easily transformed to methionine into the cell (Rouillon et al. 1999; Thomas et al. 2000). Cysteine is transported into the cell by the specific transporter Yct1 (Kaur & Bachhawat 2007).

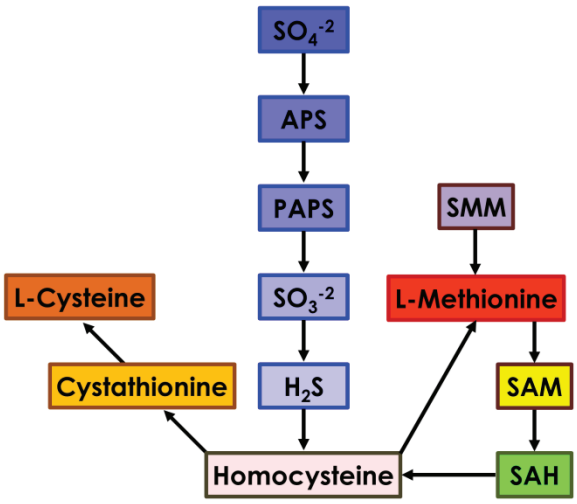

Figure 8. Schematic representation of sulfate assimilation and biosynthesis of cysteine and methionine. Enzymes involved in the reactions are omitted. More detailed information of the pathways can be found in the main text. SAH, S-adenosyl-homocysteine; SAM, S-adenosyl-methionine; SMM, S-methylmethionine.

The regulation of sulfur metabolism

The sulfur amino acid metabolic pathway is regulated by the presence of these amino acids or suflur compatible compounds in the medium. The transcription of genes necessary for the uptake and utilization of sulfate is negatively regulated by the intracellular presence of methionine, cysteine and SAM into the cell (Thomas & Surdin-Kerjan 1997; Hansen & Johannesen 2000). The expression of most genes encoding enzymes of the sulfur amino acid metabolism requires the transcriptional activator Met4 and the transcription factors Met31 and Met32 or Cbf1 (Lee et al. 2010). Met4 lacks DNA-binding activity and therefore needs the transcription factors Met31 and Met32, that binds to CTGTGGC motif, and Cbf1, that binds to CACGTGA site, to activate transcription of *MET* genes (Lee et al. 2010). An additional cofactor, Met28, stabilize DNA-bound Met4 complexes (Kuras et al. 1997; Blaiseau & Thomas 1998) and all these interactions enable Met4 to recruit SAGA and Mediator complexes to sulfur amino acid genes and promote transcription (Leroy et al. 2006; Kuras et

al. 2002). The repressing conditions provoke ubiquitination of Met4 and its cofactors thanks the substrate recognition subunit Met30, targeting all of them to degradation (Ljungdahl & Daignan-Fornier 2012). Finally, the GAAC pathway has a limited role in *MET* gene expression under methionine-limiting conditions, although starvation for other amino acids strong induces some *MET* genes in a Gcn4-dependent manner (Natarajan et al. 2001).

3.8 Phosphate homeostasis

Inorganic phosphate is the most abundant anion in *S. cerevisiae* cells. The total phosphate concentration is in the hundred-millimolar range (Rosenfeld et al. 2010; Eide et al. 2005). It is necessary for the biosynthesis of cellular components such as nucleic acids (DNA and RNA), nucleoproteins, phospholipids, etc. The ATP is the receiver and donor P_i molecule used to transfer P_i to a large number of biomolecules such as nucleotides, sugars, lipids or proteins. P_i is involved in many metabolic and signalling pathways. Phosphate, like carbon, nitrogen or suflur, is required for progression through the cell cycle (Saldanha et al. 2004). Phosphate is necessary for reversible protein phosphorylation, a widespread mechanism of regulation of many biological processes such as metabolism, gene transcription, cell cycle and in response to a plethora of either internal or external stimuli or stresses. Due to the important roles of phosphate, cells needs efficient systems for acquisition, storage, release and metabolic integration of this compound. These systems are composed by numerous enzymes and transporters subjected to fine regulation in response of intracellular phosphate levels or cellular phosphate requirements.

3.8.1 Phosphate transport systems

Similar to potassium transport, yeast cells have dual transport systems (low and high-affinity). The advantage of possessing dual-transport systems could be to enable cells to prepare in advance for nutrient depletion, by using low-affinity transporters to sense a reduction in nutrient level before this reduction becomes limiting for growth, and to improve cell's recovery once nutrients are replenished thanks to high-affinity transporters (Levy et al. 2011). Low-affinity phosphate uptake (K_m ~ 1 mM) is based on a H^+/P_i symport involving Pho87 and Pho90 (Bun-Ya et al. 1991; Ghillebert et al. 2011; Wykoff & O'Shea 2001) The low-affinity system satisfies the cellular need for P_i at normal o high external P_i levels (Roomans et al. 1977). The high-affinity transport, with a K_m ~ 10 μM, is induced under

phosphate-limiting conditions and consist in Pho84 and Pho89 (Bun-Ya et al. 1991; Martinez & Persson 1998; Persson et al. 1999).

Low-affinity P_i transport

The plasma membrane low-affinity phosphate system, responsible for uptake phosphate into the cell, is composed by Pho87 and Pho90, whereas Pho91 is a transporter localised to the vacuolar membrane which export P_i form the vacuole to cytosol (Hürlimann et al. 2007) (Figure 9). Pho87 and Pho90 transport P_i with different capacity, Pho90 being the most important P_i transporter under high P_i conditions in the absence of high-affinity P_i transport (Ghillebert et al. 2011), while Pho87 is involved in P_i transport and sensing (Ghillebert et al. 2011; Pinson et al. 2004; Giots et al. 2003). Mutation of the low affinity P_i transporter genes results in upregulation of phosphate-dependent genes like Pho84 or Pho89 independently of intracellular P_i levels (Auesukaree et al. 2003; Pinson et al. 2004). The basis for extracellular P_i sensing by low-affinity P_i transporters is still unclear although these transporters have an hydrophilic N-terminal extension similar to the C-terminal extension of the glucose sensors Snf3 and Rtg2 (Ozcan, Dover, et al. 1996), and Pho87 is able to induce PKA activity in the absence of Pho84 and Pho4 (Ghillebert et al. 2011). The low affinity transporters Pho87, Pho90 and Pho91 contain the SPX domain, present in many proteins involved in regulating P_i homeostasis in yeast and plants (Secco, Wang, Shou, et al. 2012; Secco, Wang, Arpat, et al. 2012; Hürlimann et al. 2009). Besides P_i, the low affinity P_i transporters also transport selenite (Lazard et al. 2010).

The transcription of *PHO87* and *PHO90* is independent of the phosphate status (Auesukaree et al. 2003). The regulation of Pho87 and Pho90 take place at the protein level by a complex feedback mechanism that enable yeast cells to switch from low to high affinity P_i transporters and vice versa depending on internal P_i availability (Wykoff et al. 2007). The two P_i uptake systems are mutually exclusive, and only one type of P_i transport system can function at a time (Wykoff et al. 2007). One reason may possibly be that Pho87 and Pho90 could mediate P_i efflux under P_i starvation situations (Hürlimann et al. 2009). In phosphate starvation conditions, the low-affinity P_i transporters Pho87 and Pho90 are normally subjected to vacuolar targeting for its degradation. In this condition, whereas the vacuolar targeting of Pho87 is dependent on Spl2, a regulatory factor highly expressed under low phosphate conditions in a Pho4-dependent way, that interact with the SPX domains of low-affinity P_i transporters (Ghillebert et al. 2011; Hürlimann et al. 2009). In contrast, the vacuolar targeting

of the Pho90 is independent on Spl2 and Pho4 but, as for Pho87, requires the SPX domain (Ghillebert et al. 2011). Furthermore, when cells are starved for other essential nutrients or are treated with rapamycin, an inhibitor of the TOR pathway, vacuolar targeting applies to both low-affinity P_i transporters, is independent of Spl2 but still depends on their SPX domain (Ghillebert et al. 2011). Both Pho87 and Pho90 are ubiquitinated in response to P_i starvation by the E3 ubiquitin ligase before being targeted for endocytosis and degraded in vacuole (Estrella et al. 2008).

High-affinity P_i transport

The high-affinity P_i transporters Pho84 cotransports phosphate with H^+, and it is responsible for the vast majority of P_i uptake under low-phosphate conditions at normal acidic growth (Pattison-Granberg & Persson 2000). On the other side, the second high-affinity P_i transporter encoded by *S. cerevisiae*, Pho89, is a phosphate/cation symporter that works most efficiently under alkaline conditions (optimum pH of 9.5) (Zvyagilskaya et al. 2008). When the low-affinity P_i system is missing the high-affinity transporters are overexpressed, even in high phosphate conditions (Auesukaree et al. 2003) (Figure 9).

Pho84

Pho84 is localised in the plasma membrane (Persson et al. 1999). The cotransport of P_i and protons has a K_m for P_i of 1-15 μM and needs 2-3 H^+ per monovalent P_i anion (Cockburn et al. 1975). Consequently, the inward flow of P_i by Pho84 is driven by the proton electrochemical gradient generated by Pma1 (Fristedt, van Der Rest, et al. 1999; Fristedt, Weinander, et al. 1999). Pho84 is a member of the phosphate:H^+ symporter family, belonging to the MFS (Pao et al. 1998). The Pho84 protein is made by 587 amino acid residues and its secondary structure is predicted to consist of 12 transmembrane segments, arranged in two bundles of six helices (Persson et al. 1999). The residues involved in phosphate or proton binding or others necessary for the transport function that might be part of the putative substrate-binding pocket of Pho84 were identified recently (Samyn et al. 2012). Although the kinetic model describing the mechanistic features of Pho84 is still lacking, as member of MFS transporters it possibly works via single binding site accompanied by a rocker-switch movement resulting in three conformational steps (Law et al. 2007). The conformational changes that occur in Pho84 when binds phosphate has been used to create a P_i biosensor based on the Pho84 protein (Basheer et al. 2011). Besides P_i transport, Pho84 is able to transport arsenate (Shen et al. 2012), selenite (Lazard et al. 2010) and it is involved in the low-

affinity uptake of metals such as Mn^{+2}, Cu^{+2}, Co^{+2} and Zn^{+2} (Jensen et al. 2003). Overexpression of Pho84 cause heavy metal accumulation and induces Ire1-dependent unfolded protein response but cells do not develop symptoms of metal toxicity (Ofiteru et al. 2011). Under phosphate starvation *PHO84* is one of the most induced genes but is rapidly degraded when P_i is re-added or the carbon source is exhausted (Martinez et al. 1998). The transport capacity of Pho84 is dependent on intracellular and extracellular pH and it is stimulated by bivalent cations (Borst-Pauwels & Peters 1977; Fristedt, van Der Rest, et al. 1999). Pho84 has been defined as a phosphate transceptor, a concept related to transporters that also act a nutrient sensing proteins. Pho84 transports phosphate and signals to activate the PKA pathway when phosphate is added to starved cells (Giots et al. 2003; Popova et al. 2010). The mutation of some amino acid required for transport does not affect the signalling function of Pho84 indicating that the transport and signalling functions are separated in transceptors (Samyn et al. 2012).

The main regulation of Pho84 takes place at transcriptional level. The expression of *PHO84*, as that of other genes necessaries for acquisition and use of P_i under starvation or low phosphate conditions, is regulated by phosphate levels by the transcription factor Pho4 via the *PHO* pathway (Ogawa et al. 2000) (see next sections for details). *PHO84* mRNA is detected in low amounts under normal phosphate levels. In these conditions the *PHO84* gene region produces 2 antisense RNAs (1.9 kb and 2.3 kb long), both starting at the gene 3' end and the long one extending into the *PHO84* promoter. The *PHO84* antisense RNAs cause transcriptional gene silencing not only in *cis* (Camblong et al. 2007), as occur in other genes, but also in *trans* (Camblong et al. 2009; Castelnuovo et al. 2013). The biological role of antisense *PHO84* production has been recently proved revealing that exist a bimodal *PHO84* expression using sense and antisense transcripts (Castelnuovo et al. 2013). The antisense transcription protects cells from responding to weak activating signals. The constant antisense transcription and the burst of sense transcription after stress modulate the threshold of *PHO84* activation (Castelnuovo et al. 2013).

The use of RNA antisense in *PHO* related genes is not limited to *PHO84*; the acid phosphatase *PHO5*, highly expressed under phosphate starvation, is also controlled by an antisense system. In this case, the transcription of antisense RNA is needed for remodelling the chromatin around the *PHO5* gene allowing transcription when the signal of phosphate starvation arrives (Uhler et al. 2007).

After activation of the expression of *PHO84* the translated protein must be correctly targeted to its final destination on the plasma membrane. Pho84 lacks a signal sequence and its correct sorting is mediated through Pho86 (Lau et al. 2000). Pho86 resides in the endoplasmic reticulum and is required for the specific and correct packaging of Pho84 into COPII vesicles (Lau et al. 2000) (Figure 9). *PHO86* is transcribed in both high and low P_i media, although in low P_i media the levels are slightly more elevated. Another protein probably involved in phosphate homeostasis is Pho88, a membrane protein similar to Pho86 also localized in the ER. Pho88 could participate in N-linked glycosylation of some proteins probably necessary for P_i transport (Yompakdee et al. 1996; Copic et al. 2009).

Pho84 protein is maintained at higher levels in the plasma membrane under low phosphate levels in the medium. When non-repressive amounts of P_i (over 1 mM P_i) are added to phosphate starved cells, Pho84 protein is removed from the plasma membrane and is subjected to vacuolar sorting and degradation (Lagerstedt et al. 2002; Pratt et al. 2004). Phosphate re-addition to phosphate starved cells causes Pho84-mediated activation of the PKA pathway that is responsible for the transporter downregulation by phosphorylation, ubiquination, internalization, and vacuolar breakdown (Lundh et al. 2009). The attachment of ubiquitin to Pho84, necessary for its degradation, is dependent on the ubiquitin conjugating enzymes Ubc2 and Ubc4 (Mouillon & Persson 2005).

Pho89

As mentioned above, uptake of P_i under normal (acidic) growth conditions is mediated by the Pho84 transporter. However, under alkaline conditions the Pho84 activity is still significant even though it is far from its optimum pH (Zvyagilskaya et al. 2008; Serra-Cardona et al. 2014). Therefore, under alkaline conditions P_i is transported by both Pho84 and Pho89. In contrast with mammals, Pho89 seems to be the only membrane monovalent cation/nutrient transporter in *S. cerevisiae*. Phosphate transport through Pho89 requires the existence of an alkali-metal cation gradient, being Na^+ markedly preferred over K^+ or Li^+, with a K_m for P_i of 0.5 μM (Martinez & Persson 1998; Zvyagilskaya et al. 2008) and maximal transport activity is reached at external Na^+ concentrations of 15-25 mM (Martinez & Persson 1998). The maximal activity of Pho89 is at least 100-fold lower than that of Pho84 (Persson et al. 2003). While the sequence identity between Pho89 and Pho84 is as low as 15 %, the structure of both is similar, with 12 transmembrane domains (Persson et al. 2003). Pho89 is

more similar to mammalian type III Na^+-Pi transporters like PiT-2 with which shares a 28 % of identity (Salaün et al. 2001).

PHO89 is induced under P_i limitation by the *PHO* pathway through Pho4, although this response is delayed in comparison with that of *PHO84* (Martinez & Persson 1998; Zvyagilskaya et al. 2008; Serra-Cardona et al. 2014). In addition, as other members of the *PHO* regulon, *PHO89* and *PHO84* are induced by alkalinisation of the medium (Serrano et al. 2002). Under alkaline pH the response of *PHO89* is faster than that of *PHO84* and, in contrast to *PHO84* expression, is in part dependent on calcineurin-Crz1 activation (Serrano et al. 2002; Viladevall et al. 2004; Serra-Cardona et al. 2014). Very recently, Serra-Cardona and coworkers (Serra-Cardona et al. 2014) elegantly demonstrated that *PHO89* expression under alkaline pH is also under the control of both the Snf1 protein kinase, through the Mig2 and Nrg1/2 repressors, and the Rim101 transcription factor, which represses the expression of Nrg1 (Lamb & Mitchell 2003). This regulatory network is very similar to the previously described for Ena1 in response to alkaline pH (Platara et al. 2006) suggesting that both genes products could be functionally coupled. The uptake of P_i through the Pho89 transporter has the forced trade-off of the accumulation of toxic Na^+ cations into the cell. Possibly the role of Ena1 under alkaline pH could be to eliminate the Na^+ introduced by Pho89 as cotransport with Pi to avoid Na^+ toxicity and/or to maintain a Na^+ gradient necessary to support P_i uptake.

Under phosphate deficiency several phosphatases are induced in order to scavenge P_i from macromolecules such as secretable acid phosphatases (Oshima 1997; Toh-e & Kakimoto 1975), vacuolar alkaline phosphatase (Kaneko et al. 1985) or lysophosphatidic acid phosphatase (Reddy et al. 2008). The glycerophosphocholine phosphodiesterase, Gde1, hydrolyses glycerophosphocholine to choline and glycerolphosphate that can be used as a P_i source (Fisher et al. 2005). Gde1 is a cytoplasmic protein, thus for its use as P_i source glycerophosphocholine has to be introduced into the cell by a specific transporter encoded by the *GIT1* gene (Patton-Vogt & Henry 1998) (Figure 9). *GIT1* expression is regulated by multiple factors and the gene is highly expressed under phosphate limitation conditions (Almaguer et al. 2004; Boer et al. 2003). The Gde1 protein, like several P_i-related proteins, also possesses a SPX domain without any specific known function besides the general role in protein interaction (Secco, Wang, Shou, et al. 2012).

3.8.2 The *PHO* pathway

The flexible metabolism of *S. cerevisiae* allows cells to rapid respond to environmental changes, for instance variation in nutrient status. As hinted above, the adaptation to low phosphate levels takes place mainly at transcriptional level. Expression of *PHO84* and *PHO89* transporters genes, as well as that of other genes required for acquisition and utilization of P_i, is increased in response to P_i starvation (Ogawa et al. 2000). Some other genes *PHO*-controlled are the acid phosphatases *PHO5*, *PHO11* and *PHO12*, vacuolar alkaline phosphatase *PHO8*, and proteins involved in polyphosphate metabolism encoded by *VTC1-4* genes and *PPN1*, among others. This response is regulated by the *PHO* signalling pathway, which controls the localization of the transcription factor Pho4 depending on phosphate availability (Auesukaree et al. 2003; Ogawa et al. 1995; Persson et al. 2003) (Figure 9). Unphosphorylated Pho4 accumulates in the nucleus and binds to diverse phosphate-responsive gene promoters triggering their transcription under low phosphate conditions. Under high phosphate conditions Pho4 is hyperphosphorylated by the Pho80–Pho85 cyclin-dependent kinase complex and excluded from the nucleus (Toh-e et al. 1988; Kaffman et al. 1994). Pho85 is a cyclin-dependent kinase able to interact with ten different cyclin partners that modulate its activity regulating different cellular responses to nutrient levels, to environmental conditions, or the progression through the cell cycle (Huang et al. 2007). The multiple targets of Pho85 are dictated by its interaction with specific cyclins, and phosphorylation of these targets results in changes in their localization, stability and enzymatic activity (Carroll & O'Shea 2002). The cyclins that interact with Pho85 can be divided into two subfamilies based on sequence similarity (Measday et al. 1997). A first subfamily, comprised of Pho80, Pcl6, Pcl7, Pcl8, and Pcl10, regulates the response to nutrient levels and environmental conditions. The second subfamily is composed by 5 members, Pcl1, Pcl2, Pcl9, Clg1 involved in regulating cell cycle transcriptional changes and progression through the cell cycle and Pcl5 which regulates the response to amino acid starvation) (Measday et al. 1997; Shemer et al. 2002). The cyclin Pho80 is a member of the first subfamily. The main role of the Pho80-Pho85 complex is to regulate the response to phosphate starvation by phosphorylation of Pho4. Pho80-Pho85 also phosphorylates Rim15 and Cln3, thus linking phosphate levels with the decision to enter G_0 (Wanke et al. 2005; Menoyo et al. 2013). Another role of Pho80-Pho85, not related with phosphate metabolism, is the phosphorylation of Crz1 in the absence of stress, preventing its nuclear localization and the activation of Crz1-controlled genes (Sopko et al. 2006).

Pho4 is a bHLH transcriptional activator that binds with high affinity to CACGTG consensus binding site found in *PHO* controlled genes (Harbison et al. 2004; Oshima 1997; Ogawa et al. 2000). Pho4 has 5 serines with a consensus phosphorylation sequence SPXI/L with distinct roles for each residue (O'Neill et al. 1996; Komeili & O'Shea 1999; Jeffery et al. 2001). The first phosphorylation inactivates the nuclear Pho4 by preventing the interaction with its transcriptional co-activator Pho2, resulting in a lack of induction of the *PHO* regulated genes. The hyperphosphorylated version of Pho4 is transported to the cytoplasm by the complex composed by Msn5 and Gsp1 bound to GTP (Kaffman, Rank, O'Neill, et al. 1998). The phosphorylation of two alternative serine residues is specifically required for the interaction with the exportin Msn5 (Komeili & O'Shea 1999). The fourth phosphorylation residue inhibits the interaction of Pho4 with the importin necessary for Pho4 nuclear import, Pse1 (Komeili & O'Shea 1999; Kaffman, Rank & O'Shea 1998). The function of phosphorylation of the remaining serine site is not determined. The multiplicity of phosphorylation sites provide overlapping and partially redundant layers of regulation that controls the activity of Pho4 (Komeili & O'Shea 1999). The phosphorylation of Pho4 is not enough to fully exclude it from the nucleus because partially phosphorylated Pho4 was found also associated with several promoters under high phosphate conditions (Nishizawa et al. 2008; Springer et al. 2003).

For the transcription of *PHO* regulated genes under low phosphate conditions the transcription factor Pho4, together with Pho2, binds to the specific motif in the promoter of *PHO* genes. For the initiation of transcription, Pho4 interacts with TFIIB (Wu & Hampsey 1999) and binds to the DNA sequence as a homodimer (Shimizu et al. 1997). *PHO2* encodes a homeodomain transcriptional activator that activates transcription in a combinatorial manner with other transcription factors because alone binds DNA with low affinity (Brazas & Stillman 1993). In addition to phosphate utilization, Pho2 is required to express genes in other pathways such as purine nucleotide and histidine biosynthesis (with Swi5 and Bas1) (Bhoite et al. 2002). The Pho2 functions on *PHO* genes are to recruit Pho4 to the DNA and enhancing the activation potential by binding to *PHO* sites in the promoters cooperatively with Pho4 (Barbaric et al. 1998). A phosphorylation on Pho2 by the Cdc28 kinase facilitates the interaction between Pho2 and Pho4 and is required for *PHO* expression under low phosphate conditions (Liu et al. 2000). The binding of Pho4 to the consensus binding sites depends on several factors. The access of Pho4 and Pho2 to specific DNA sites in *PHO* promoter sites is assisted by modifications of the chromatin structure. The expression of some *PHO* genes is

dependent on histone modifications, such as acetylation by SWI/SNF complexes or remodelling factors such asSnf2 and Ino80, whereas other do not need it (Krebs et al. 2000; Sudarsanam et al. 2000; Shen et al. 2012). For instance, very recently the complete set of remodelers involved in *PHO5* promoter chromatin remodelling has been identified and found to have hardly any role in chromatin remodelling at the *PHO8* and *PHO84* promoters (Musladin et al. 2014). In spite of these chromatin modifications, the presence of some nucleosomes blocks the binding of Pho4 to some consensus binding sites found in the genome (Pho4 only binds to ~14 % of this sites) (Zhou & O'Shea 2011). Another factor that influences Pho4 binding to its recognized sites is the competition with the transcription factor Cbf1 that recognizes the same motif as Pho4. Competition with Cbf1 together with the need for cooperation with Pho2, raises the threshold of gene activation and helps to define the specificity of *PHO* gene regulation (Zhou & O'Shea 2011). The recruitment of the TBP in the TAF-independent promoters requires the presence of complexes, such as SAGA, that interacts with transcriptional machinery and can stimulates preinitiation complex (PIC) assembly to initiate transcription (Li et al. 2000; Larschan & Winston 2001) The transcription of several Pho4-controlled genes (Pho84, Pho5, Pho8 and Vtc3) is dependent on the SAGA complex (Nishimura, Yasumura, Igarashi, Harashima, et al. 1999; Bhaumik & Green 2002).. SAGA is a large multiprotein complex and each SAGA-dependent promotor recruits SAGA complex that can be composed by different components. For instance, *PHO84* and *VTC3* requires the same SAGA components except *TAF6* that is not recruited by the *VTC3* promoter (Bhaumik & Green 2002). The expression of Pho4-regulated genes under phosphate starvation needs the presence of the ribosomal protein Rpl12 for a complete induction (Tu et al. 2011). Recently, Pho92 has been identified as a new component of cellular phosphate metabolism via the regulation of *PHO4* mRNA stability by binding to the 3'-UTR in a phosphate-dependent manner (Kang et al. 2014).

A key regulator of the *PHO* pathway is the cyclin-dependent kinase inhibitor Pho81, initially identified as a positive regulator of the *PHO* pathway (Ueda et al. 1975). Pho81 contains a tandem repeat of six ankyrin consensus regions important for protein-protein interactions (Ogawa et al. 1995). Pho81 co-immunoprecipitates with Pho80-Pho85 and inhibits the kinase activity of the complex, thus preventing the phosphorylation of Pho4 (Schneider et al. 1994). In response to phosphate levels, Pho81 coordinates the activity of both the Pho80-Pho85 and Pcl7-Pho85 complexes, linking phosphate levels with cell cycle (Lee et al. 2000). Only a small region of Pho81 containing the ankyrin repeats is sufficient to

inhibit the kinase activity of the Pho80-Pho85 complex (Ogawa et al. 1995; Huang et al. 2001). Pho81 is constitutively associated to Pho80-Pho85 but the kinase activity is only inhibited in conditions of P_i starvation (Schneider et al. 1994). Therefore, in contrast to other cyclin-dependent kinase inhibitors where the protein interaction is sufficient to inactivate the complex (Pavletich 1999), an additional factor is required for P_i starvation-promoted inhibition of the Pho80-Pho85 complex. When phosphate levels decrease, the levels of inositol heptakisphosphate (IP_7) increase and this compound interacts with the Pho81-Pho80-Pho85 complex, reversibly changing Pho81 conformation. This change affects the accessibility of the kinase substrates to the complex, preventing the phosphorylation of Pho4 (Lee et al. 2007; Lee et al. 2008) (Figure 9).

Inositol pyrophosphates (mainly IP_6 and IP_7) are signalling molecules that are important for cellular processes such as membrane trafficking, chemotaxis, ion channel activity, mRNA export, DNA repair and telomere maintenance (York 2006). In yeast, IPs are also critical regulators of cell growth and the general stress response, controlling the histone deacetylase Rpd3L (Worley et al. 2013). It is worth mentioning that IP_3 is a second messenger that controls many cellular processes by generating internal calcium signals (Berridge 1993). In yeast, the biosynthesis of inositol pyrophosphate starts with the hydrolysis of phosphatidylinositol 4,5-biphosphate to IP_3 and diacylglycerol by phospholipase C encode by *PLC1* gene (Yoko-o et al. 1993). Subsequently, IP_3 is converted to IP_4 and IP_5 by the action of the inositol polyphosphate multikinase Arg82 (Zhang et al. 2001), a protein also involved in the regulation of transcription of arginine-responsive genes (Bechet et al. 1970).. The different isomers of IP6 can be generated by Arg82 (Zhang et al. 2001), Kcs1 (Saiardi et al. 2000) (PP-IP_4) or by Ipk1, an inositol 2-kinase (Ives et al. 2000). Only the IP_6 products from Ipk1 can be used as a substrate for generation of IP_7 by the inositol hexakisphophate kinases Kcs1 and Vip1 (Figure 9) and only the Vip1 product (1/3PP-IP_5) is able to inhibit the Pho81-Pho80-Pho85 complex under phosphate starvation (Lee et al. 2007). Finally, the Ddp1 protein phosphatase is able to hydrolyse the different isomers of IP_7 to IP_6 (Safrany et al. 1999).

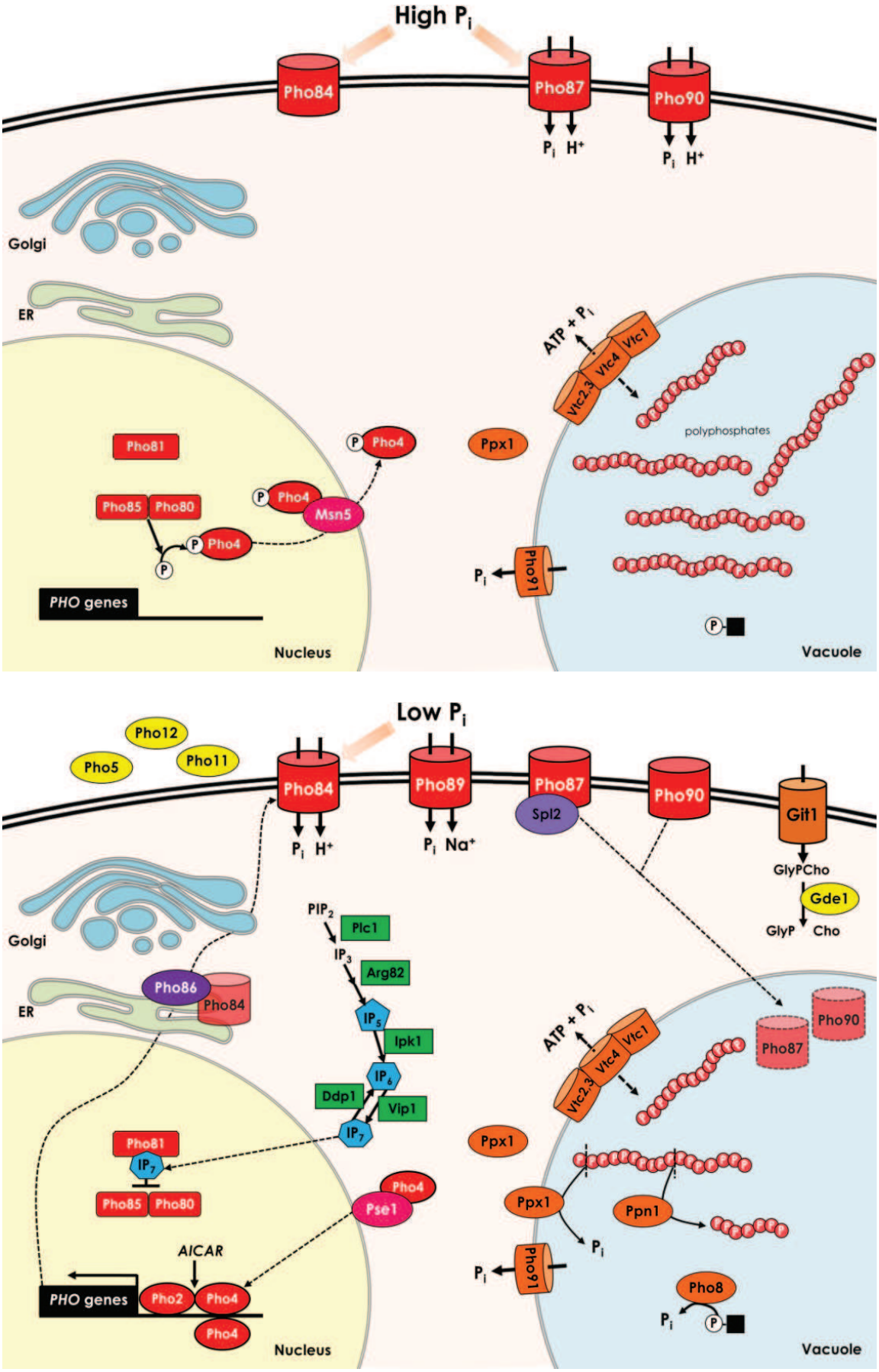
High Pi
Pho84
Pho87
Pho90
Pi H+
Pi H+
Golgi
ER
ATP + Pi
Vtc1
Vtc4
Vtc2,3
polyphosphates
Pho81
Pho85
Pho80
P
Pho4
Msn5
Ppx1
Pi
Pho91
PHO genes
Nucleus
Vacuole
Low Pi
Pho12
Pho5
Pho11
Pho84
Pho89
Pho87
Spl2
Pho90
Git1
Pi H+
Pi Na+
GlyPCho
Gde1
GlyP
Cho
Golgi
PIP2
Plc1
IP3
Arg82
IP5
Ipk1
IP6
Ddp1
Vip1
IP7
Pho86
Pho84
ER
Pho81
IP7
Pho85
Pho80
Pho4
Pse1
AICAR
PHO genes
Pho2
Pho4
Pho4
Nucleus
ATP + Pi
Vtc1
Vtc4
Vtc2,3
Pho90
Pho87
Ppx1
Ppx1
Ppn1
Pi
Pi
Pho91
Pho8
Pi
Vacuole

Figure 9. Schematic model of the *PHO* pathway under low or high phosphate levels. At normal/high P_i extracellular conditions, transport of P_i into cells occurs by the low-affinity system. The Pho81–Pho85–Pho80 complex is active and phosphorylating Pho4, thus preventing itsentrance to the nucleus. Under these conditionsm the *PHO* pathway is inactive. Upon P_i starvation, IP_7 interacts with the tertiary complex of Pho81–Pho85–Pho80, preventing Pho4 phosphorylation by Pho80–Pho85. As a consequence, unphosphorylated Pho4 accumulates in the nucleus leading to the transcription of *PHO*-controlled genes, such as high-affinity P_i transporters and a variety of enzymes involved in the acquisition, storage and release of P_i. Consequently, Pho87 and Pho90 are targeted to the vacuole for degradation. In the vacuole the polyP are synthetized by the Vtc complex and degraded by polyphosphatases. Gde1 is responsible for the hydrolysis of glycerophosphocholine (GlyPCho) into choline (Cho) and glycerophosphate (GlyP), which can be used as a source of P_i for cell growth. Dotted lines indicate intracellular movements of the target element. Composition adapted from (Persson et al. 2003; Secco, Wang, Shou, et al. 2012).

Although the role of inositol phosphates in the regulation *PHO* controlled genes is not completely deciphered, it seems that it is not restricted to IP_7 production and inhibit Pho81-Pho80-Pho85 complex. For example, IP_4 and IP_5 produced by Plc1 and Arg82 has been related to transcriptional induction of some phosphate-responsive genes (like *PHO5*) by affecting the ability of Pho4 or Pho2 to interact with chromatin remodelling complexes (Steger et al. 2003). On the other hand, disruption of *PLC1*, *ARG82* and *KCS1* leads to constitutive expression of several *PHO* controlled genes (El Alami et al. 2003; Auesukaree et al. 2005).

The regulation of IP_7 production under low phosphate conditions is not clear. Increase of *VIP1* mRNA expression was detected after P_i limitation (Ogawa et al. 2000) or in chemostat cultures under low phosphate conditions (Boer et al. 2003). On the other side, in the same chemostat cultures under low phosphate conditions the *KCS1* and *DDP1* genes are also induced (Boer et al. 2003). These transcriptional profiles are contradictories because the expression of *KCS1* and *DDP1* genes leads to diminish the amount of IP_7 (1/3PP-IP_5) synthesized by Vip1 and needed to inhibits Pho81-Pho80-Pho85 complex. Additionally, under P_i starvation Pho4 binds to the coding sequence of *KCS1* to activate transcription of both intragenic and antisense RNAs, resulting in the production of a truncated Kcs1 protein and redirecting the use of IP_6 as a substrate of Vip1 to produce the IP_7 (1/3PP-IP_5) (Nishizawa et al. 2008). However, the rapid kinetics of the transcriptional activation of *PHO*-controlled genes after switching cells to low phosphate medium is difficult to explain by the transcriptional regulation of inositol pyrophosphate kinases. It suggests that the production of IP_7 by phosphate scarcity is not controlled, at least at the first minutes of the responses, by transcriptional changes of the inositol pyrophosphate-related enzymes.

The *PHO* pathway was initially described in *S. cerevisiae* but more recently similar *PHO* pathways have been described in other ascomycetes. In *Schizosaccharomyces pombe* the *PHO* pathway is directly activated by the transcription factor *SpPHO7* under phosphate starvation and the induction is prevented by *SpCsk1* under normal phosphate levels (Henry et al. 2011). The production of IP_7 is not critical during phosphate starvation; it works as an amplifier of the signal (Estill et al. 2014). The *PHO* pathways of *Candida glabrata* and *Neurospora crassa* are more similar to that of *S. cerevisiae* because the regulation of *CgPHO4*/NUC-1 transcription factors is done by a cyclin-dependent kinase complex depending on phosphate levels, as it happens in *S. cerevisiae* (Tomar & Sinha 2014).

3.8.3 Polyphosphates

In rich media, the phosphate transport activity is estimated between $5 \cdot 10^6$ to $8 \cdot 10^7$ P_i molecules/min/cell (Wykoff & O'Shea 2001; Giots et al. 2003; Zvyagilskaya et al. 2008), which corresponds approximately to the amount of phosphate needed to support the main cellular phosphate-consuming processes, RNA and phospholipid biosynthesis. However, in some situations such as DNA replication or under phosphate starvation, the need for phosphate increases.

Inorganic polyphosphates are linear polymers containing tens to hundreds of phosphate residues linked by energy-rich phosphoanhydride bonds (Kulaev 1975). PolyPs are widespread in all living organism and probably were present on Earth at prebiotic time before DNA and RNA (Kornberg et al. 1999; Achbergerová & Nahálka 2011). PolyPs are particularly abundant in *S. cerevisiae*, accounting for the nearly 40 % of the total phosphate content (Kulaev 1975). In yeast, the amount of PolyP depends on the growth phase (Werner et al. 2005) and the culture conditions. For example, in cells deprived of phosphate the intracellular PolyP pool diminishes to almost zero (Martinez et al. 1998). On the other hand, transfer of *S. cerevisiae* cells from a medium without phosphate to a medium with high concentrations of phosphate (a process called "phosphate overplus") leads to hyperaccumulation of polyP (Harold 1966). Yeast cells growing in fermentable energy sources, such as glucose, have higher levels of PolyP as compared to non-fermentable energy sources like ethanol (Schuddemat et al. 1989). In prokaryotes polyP granules are localised in the cytoplasm and around the plasma membrane (Kornberg 1995; Wood & Clark 1988) and in eukaryotes are accumulated in acidocalcisomes (vacuoles, in yeast cells), acidic organelles rich in calcium and other cations also found in bacteria (Docampo et al. 2005). In *S. cerevisiae*, although PolyP has been identified in diverse

subcellular localizations such as nuclei, mitochondria, cytoplasm and plasma membrane, the vacuole appears particularly enriched in this polymer (Kornberg 1995; Saito et al. 2005) and the vacuolar content can represent 95 % of the cellular polyP (Urech et al. 1978). Polyphosphates are involved in many functions and processes in prokaryotes and eukaryotes, as an energy store (Kornberg et al. 1956; Gómez-García & Kornberg 2004), reservoir for phosphate (Harold 1966; Martinez et al. 1998), chelator of metal cations (Archibald & Fridovich 1982), a channel for DNA entry (Castuma et al. 1995), a component in gene or enzyme activity regulation (Tsutsumi et al. 2000; Wang et al. 2003; Kulaev & Kulakovskaya 2000), adaptation to changes in the environment (Crooke et al. 1994; Van Dien & Keasling 1999), and many others. In humans, blood coagulation is accelerated and fibrinolysis is delayed by PolyP (Smith et al. 2006). The main described function of polyP in yeast is phosphate storage to buffer the transient fluctuations in extracellular P_i levels (Martinez et al. 1998; Thomas & O'Shea 2005). Other functions described in yeast are to sequester metal ions (Harold 1966; Dunn et al. 1994; Nishimura, Yasumura, Igarashi & Kakinuma 1999) and regulating stress and survival (Kornberg 1995). Although 255 genes are connected to polyP metabolism (Freimoser et al. 2006) in many cases the basis for these link are unknown.

PolyP can be hydrolysed by two different but related enzymatic activities, exopolyphosphatase and endopolyphosphatase. Yeast exopolyphosphatase activity elicits polyP degradation by a stepwise removal of the terminal P_i residue at a rate of 30,000 P_i residues/min·enzyme molecule at 37 ºC (Wurst & Kornberg 1994). *PPX1* is the only known gene encoding a yeast exopolyphosphatase (Wurst et al. 1995). Ppx1 is a monomer with a molecular mass of 40 kDa that depends on divalent metal ions for optimal activity and does not act on pyrophosphate, ATP, or the cyclic form of tripolyphosphate (Wurst & Kornberg 1994). Although exopolyphosphatase activity is found in cytosol, plasma membrane, vacuoles, mitochondria and nuclei, the product of the *PPX1* gene is only responsible for cytosol, plasma membrane and mitochondrial matrix exopolyphosphatase activity, revealing that other gene(s) could be responsible for the remaining activity (Lichko et al. 2003). Deletion or overexpression of *PPX1* does not increase or decrease polyphosphate content in yeast cells, suggesting a limited role of *PPX1* in polyphosphate metabolism in yeasts under normal growth conditions (Lichko et al. 2014; Wurst et al. 1995).

Endopolyphosphatase activity hydrolyses polyphosphate chains of many hundreds of phosphate residues into shorter lengths up to 3 P_i units (P_3). The *PPN1* gene of *S. cerevisiae* encodes a endopolyphosphatase, and it is a homodimer of 35 kDa subunits that requires

proteolytic activation of a 75 kDa precursor polypeptide (Sethuraman et al. 2001). The enzyme activity is inhibited by the presence of high amounts of P_i or pyrophosphate, likely to prevent wasteful degradation of polyP when phosphate is abundant (Kumble & Kornberg 1996). Whereas inactivation of the *PPX1* gene did not influence the content and chain length of polyPs, *PPN1* inactivation resulted in increased polyP chain length (Lichko et al. 2006). A double *PPN1* and *PPX1* mutant rapidly loses viability in stationary phase (Sethuraman et al. 2001). The double mutant also lacks any exopolyphosphatase activity, suggesting that Ppn1 regulates or might possess exopolyphosphatase activity (Lichko et al. 2006; Shi & Kornberg 2005). Additionally, the *DDP1* gene encoding a diphosphorylated inositol polyphosphatase and diadenosine polyphosphate phosphatase (Safrany et al. 1999) has shown polyP endopolyphosphatase activity in vitro (Lonetti et al. 2011).

Broad-spectrum phosphatases capable to hydrolysing phosphate from a variety of substrates including nucleic acids, phosphosugars, phosphoproteins and phospholipids, could have some role in polyphosphate degradation (Oshima 1997). For example, acid phosphatases located in the extracellular periplasmic space, Pho5, Pho11, Pho12 and Pho3 (Haguenauer-Tsapis et al. 1986), or alkaline phosphatase Pho8, localised in the vacuole (Plankert et al. 1991), could be responsible for the polyphosphatase activity found in their respective cellular localizations.

Few years ago, the enzyme responsible for the polyP kinase activity was described in yeast after several years of search. The polyP polymerase activity takes place within the membrane-integral vacuolar transporter chaperone complex (VTC) (Hothorn et al. 2009). This hetero-complex is composed by Vtc1, Vtc2, Vtc3 and Vtc4 proteins, where Vtc4 generates polyP from ATP. This complex has been implicated in several cellular processes besides polyP biosynthesis, such as vacuolar membrane fusion, V-ATPase stability and trafficking or micro-autophagy (Müller et al. 2003; Cohen et al. 1999; Müller et al. 2002; Uttenweiler et al. 2007). Vtc1 is small transmembrane protein whereas Vtc2, Vtc3 and Vtc4 have a transmembrane domain and additional large cytoplasmic segment with similar sequence between them (Müller et al. 2003). Vtc2, Vtc3 and Vtc4, like other P_i homeostasis-related proteins, harbour N-terminal SPX domains that are not necessary for the catalytic activity of the complex (Secco, Wang, Shou, et al. 2012). The PolyP synthesis is a high ATP-demanding process coupled with polyP transport across the vacuole membrane (Hothorn et al. 2009). The *vtc4* and *vtc1* mutants are unable to accumulate polyP whereas *vtc2* and *vtc3* have significantly reduced amounts (Ogawa et al. 2000). Vtc proteins have genetic and physical interactions with the V-ATPase,

influence vacuolar H^+ uptake and are important factors in vacuolar membrane fusion (Müller et al. 2003). Vtc proteins are mainly localised to the vacuole except Vtc2, that is found around the nucleus under high phosphate and mobilized to vacuoles under low phosphate conditions (Hothorn et al. 2009).

The *VTC* genes and *PPN1* are highly transcribed at low phosphate levels by the *PHO* pathway (Ogawa et al. 2000). In contrast, the expression of the *PPX1* gene does not response to P_i levels or perturbation of the *PHO* regulon. The reserves of polyP are mobilized prior to the sensing of reduced availability of external phosphate by *PHO* pathway, suggesting that polyP degradation is a short-term response to phosphate starvation or it use a different sensing molecule (Pratt et al. 2004) (Figure 9).

3.8.4 Phosphate sensing and its relationship with other pathways

A still-unresolved topic is how cells sense phosphate levels (intracellular or extracellular) and which is the key molecule that activates the *PHO* pathway. External phosphate sensing has been proposed because Pho84 protein is a phosphate transceptor, which means that it is able to both transport phosphate and mediate rapid phosphate activation of the PKA pathway under low phosphate conditions (Popova et al. 2010; Giots et al. 2003). However, *PHO5* is constitutive expressed in the *pho84* mutant due to its low levels of internal phosphate and the absence of polyP (Auesukaree et al. 2004; Wykoff & O'Shea 2001; Pinson et al. 2004). An increase in internal phosphate levels supress *PHO5* overexpression in the *pho84* mutant and in other mutants with low internal phosphate levels, indicating the existence an intracellular phosphate sensing mechanism (Auesukaree et al. 2004). The extracellular phosphate sensing through low-affinity P_i transporters (Pho87) has been also proposed due to the observed increase in *PHO* response when low-affinity P_i transporters are mutated, even if intracellular phosphate levels are normal (Pinson et al. 2004; Ghillebert et al. 2011). For instance, the transition from low-affinity to high-affinity P_i transport is a complex process controlled by extra and intracellular P_i levels. When the concentration of phosphate in the medium decreases approaching the K_m for transport by the low-affinity transport system, phosphate uptake decreases resulting in a drop in intracellular phosphate levels. In response to a decrease in internal phosphate levels, cells activate the *PHO* pathway, triggering several feedback elements (Figure 10): a negative feedback loop consisting in the induction of *PHO84*, which helps to bring phosphate into the cell, and in polyphosphate mobilization to buffer intracellular phosphate fluctuation (Thomas & O'Shea 2005) leading to turn off the *PHO*

pathway. The negative feedback avoids strong activation of the *PHO* pathway at medium phosphate levels where the low induction of Pho84 and partial polyP degradation contribute to ensure intracellular phosphate levels. In coordination with negative feedbacks and exacerbated when phosphates levels decrease further, a positive feedback loop consisting in removing low-affinity Pi transporters form plasma membrane and induction of *VTC* genes becomes relevant. Elimination of low-affinity phosphate transport decreases intracellular free phosphate, whereas induction of *VTC* genes increases phosphate storage in vacuoles in the form of polyP. This generates a positive feedback resulting in the activation of the *PHO* pathway (Wykoff et al. 2007; Ogawa et al. 2000). The coordination of these feedbacks allows an accurate regulation of *PHO* pathway avoiding unnecessary inductions. This process is a bit more complicated, because not all the cells in the population display the same response. When extracellular phosphate levels increase some cells are still activating the *PHO* pathway due to the feedbacks that reduce intracellular levels of phosphate, mainly by the activation of the *SPL2* gene that inhibits the low-affinity plasma membrane transporters. Noise in *SPL2* expression allows stochastic repression of the *PHO* regulon in committed cells growing at high phosphate, as a part of the dual-transporter motif that helps cells to prepare for future nutrient depletion (Vardi et al. 2013).

The *PHO* pathway has been related with other signal molecules different from phosphate (but somehow related). The mutants of *ADO1* and *ADK1,* encoding respectively adenosine and adenylate kinase, which phosphorylates adenosine to AMP and then ADP, have the *PHO* pathway constitutively activated (Gauthier et al. 2008). The effect of these mutations is to lower ATP concentrations that could lead to upregulation of *PHO84* expression (Gauthier et al. 2008). The purine pathway metabolic intermediate AICAR is also a regulator of the *PHO* genes by directly binding to Pho2 and Pho4, which in turn promotes the interaction of these transcription factors (Pinson et al. 2009). AICAR is a major regulator of purine biosynthesis genes, reflecting a possible coregulation of a high phosphate-consumer pathway, such as purine biosynthesis, with the *PHO* pathway. Notably, the effect of *PHO* pathway activation by by *adk1* mutation is independent of the AICAR response, although both elements are members of adenosine phosphate biosynthetic pathway. The activation of the *PHO* pathway, and especially the presence of *PHO8*, is necessary for the control of NAD^+ metabolism. The *PHO* pathway respond to levels of nicotinic acid mononucleotide (NAMN), an intermediary molecule in NAD^+ biosynthesis, to activate expression of the *PHO8* gene necessary for the synthesis of the key regulator nicotinamide riboside (NmR), involved in the maintenance of

the NAD^+ pool (Lu & Lin 2011). Finally, a possible cross-regulation of phosphate and sulfate metabolisms was described based in the facts that the transcription factor Cbf1 recognizes the same DNA sequence that Pho4, and that overexpression of Pho4 suppresses the methionine auxothrophy of the *cbf1* mutant (O'Connell & Baker 1992). The competition between Cbf1 and Pho4 to occupy the same DNA motif increase the threshold for transcriptional activation of *PHO*-regulated genes under normal phosphate conditions (Zhou & O'Shea 2011). However, under phosphate starvation conditions, these competition and the necessity of cooperative interaction of Pho4 with Pho2 for transcriptional gene activation prevent spurious transcriptions of genes outside the *PHO* regulon (Zhou & O'Shea 2011).

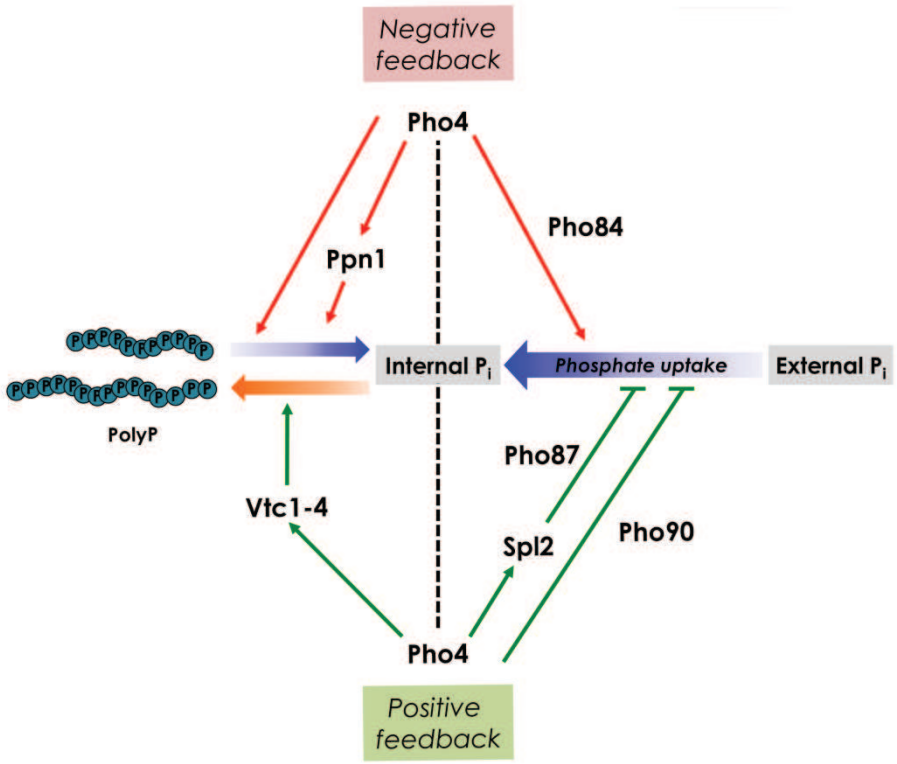

Figure 10. Positive and negative feedback loops that control homeostasis of intracellular phosphate in response to extracellular Pi fluctuations. The positive feedbacks decrease the amount of internal phosphate leading to a strong activation of the *PHO* pathway. On the other hand, negative feedbacks increase intracellular phosphate levels that inhibit *PHO* pathway activation. The coordinated actions of both contradictory feedbacks determine the activation threshold of the *PHO* pathway. For more details see the main text. Grey dotted lines indicate extracellular phosphate sensing. Model adapted from (Wykoff et al. 2007; Vardi et al. 2013).

Objectives

In the context of the importance of potassium in the yeast cell physiology and metabolism and given the scarce knowledge on the functions of the cation at the molecular level, the main aims of this work are:

- To analyse the changes in the transcriptional profile that occur after short-term potassium starvation, as a way to discover and better understand novel roles for potassium in *S. cerevisiae*.
- To characterise the molecular basis that link potassium and phosphate homeostatic mechanisms, studying how alterations of potassium homeostasis affects phosphate metabolism.

Results

5.1 Results publication one

- In *Saccharomyces cerevisiae*, the short-term (up to 120 min) potassium deprivation impacts on the expression levels of almost one third of the genome; 828 genes are induced and 926 are repressed.
- Deletion of potassium transporters genes *TRK1* and *TRK2* under non limiting potassium conditions results in induction of 69 genes and repression of 79 genes. Among the induced genes that stand out are those related to sulfate assimilation.
- The lack of potassium induces the expression of genes involved in sulfur metabolism, including those related to sulfur amino acid biosynthesis. The intracellular levels of the sulfur amino acids methionine and cysteine are rapidly depleted after potassium starvation.
- Potassium starvation triggers a moderate general stress response, which depends on the transcription factors Msn2 Msn4.
- The set of genes repressed after potassium starvation is enriched in ribosomal protein-encoding genes and genes necessary for ribosome biogenesis.
- Potassium starvation leads to accumulation of ROS species. This accumulation is accompanied by a transcriptional activation of genes necessary to fight against oxidative stress and a decrease in the GSH/GSSG ratio.
- The lack of potassium enhances methylglyoxal generation and an induction of genes responsible for methylglyoxal degradation and trehalose metabolism.
- Cells growing under potassium starvation induce the retrograde pathway (RTG) depending on the positive activators of the pathway Rtg1-3, although no mitochondrial morphological or functional alterations are observed.
- Cells growing in a medium with ammonium as nitrogen source but lacking potassium accumulate high levels of ammonium. Ammonium is transported into the cells by the Trk1 transporter, likely by the same mechanism that potassium.
- Potassium starvation causes marked decrease in mRNA and protein levels of most G_1 and G_2-phase cyclins.
- Cells subjected to potassium starvation cannot properly form the septin ring. This is likely not the result of failure to express septin components (as deduced from monitoring Cdc11 levels), but could be influenced by observed down-regulation of genes involved in regulation of the septin ring assembly and bud neck formation.

5.2 Results publication two

- Potassium starvation triggers the induction of genes controlled by the *PHO* regulon, normally induced by phosphate limitation.

- Membrane accumulation of Pho84 transporter is affected by mutations that impact on potassium transport. At limiting potassium conditions, *trk1* and *trk1trl2* mutants, or mutants of positive regulators of Pma1 (necessary for generation the electrochemical membrane gradient) display increased Pho84 levels. On the contrary, mutations that increase the electrochemical gradient results in lesser accumulation of Pho84 at potassium limiting conditions.

- Activation of Ppz1 (a negative regulator of Trk-mediated K^+ transport) by progressive depletion of Hal3 in an conditional *tetO:HAL3 vhs3* mutant results in induction of genes controlled by the *PHO* regulon, including Pho84..

- Deletion of *PPZ1* gene decreases expression of Pho84 in cells grown under low phosphate conditions.

- Potassium deprivation does not modify the total amount of intracellular phosphate but triggers a rapid degradation of polyP reserves and a depletion of ATP and ADP with a concomitant increase in AMP levels. Re-addition of potassium to potassium starved cells allows fast recovering normal polyP levels. Similarly, blockage of potassium transport by manipulation of Ppz1 activity results in a decrease in polyP levels depending on *PPZ1* gene.

- A *trk1 trk2* mutant or a strain with increased Ppz1 activity cannot grow under phosphate-limiting conditions, emphasizing the functional interaction between phosphate and potassium interactions

- The kinetics of the induction of the *PHO* pathway by potassium starvation is similar to phosphate starvation albeit the response is less intense. The expression of Pho84 under potassium starvation requires the classic elements of the *PHO* pathway (Pho81, Pho4 and Pho2) and also the integrity of the IP_7 biosynthesis pathway**.**

General discussion & Conclusions

In the yeast *Saccharomyces cerevisiae,* the requirements of potassium for several cellular processes and growth are known for a long time (Muntz 1947). However, in many cases, the molecular mechanisms behind the roles of potassium are not known. In this study we used an approach based on genome-wide transcriptional analysis to investigate the short-term response of yeast to potassium starvation as a new tool to underscore the relevance of potassium in the yeast cell biology. In yeast, transcriptional analysis has been widely used to discover cellular responses to diverse stressful conditions, such as nutrient starvation or addition of toxic compounds (Gasch et al. 2000; Causton et al. 2001; Boer et al. 2003). Our study provides a comprehensive set of data on the yeast cellular response to the complete lack of potassium in the medium. The short-term response of yeast to potassium starvation has allowed us to detect transcriptional alterations in more than 1700 genes.

The experiments were performed in conditions of complete lack of potassium in the medium during 120 minutes. It is worth noting that under these condition yeast cells still retain substantial amounts of intracellular potassium (Navarrete et al. 2010). In addition, a study of subcellular potassium distribution in *S. cerevisiae* revealed that under normal potassium conditions around 45 % of intracellular potassium is stored in vacuoles, but a few hours of potassium starvation causes a mobilization of vacuolar potassium to the cytoplasm to maintain constant cytoplasmic potassium levels (Herrera et al. 2013). In the cytosol, potassium is important for the regulation of some enzymatic activities (Page & Di Cera 2006). Therefore, it is unlikely that the observed transcriptional changes could occur in response to inactivation of known enzymes acting as potassium targets in the cytosol, because the cytosolic levels of the cation barely change through the studied period of potassium starvation. The same conclusion can be extracted from other potassium-regulated enzymes localised in mitochondria, such as pyruvate kinase (Jurica et al. 1998) or certain aldehyde dehydrogenases (Ald4 and Ald5) (Tessier et al. 1998) because the potassium levels of mitochondria also remain constant during this period of potassium starvation (Herrera et al. 2013). Therefore, it is improbable that the large number of observed transcriptional changes could occur in response to inactivation or malfunction of known potassium functional targets with enzymatic activity.

There is only one previous study at transcriptional level where the effects of limiting potassium to yeast cell were analysed (Hess et al. 2006). As in our study, ammonium was present as nitrogen source but these authors used cells growing in a chemostat under limiting potassium concentrations and they did not completely remove potassium from the medium. Hess and co-workers only found a limited number of transcriptional changes after study yeast

cells growing in a chemostat under different limiting potassium concentrations. Their data derived from the lowest potassium concentrations analysed (1.3 and 0.65 mM K^+) shows transcriptional changes for around only 250 genes, a small number in comparison with our results. The approaches of both studies can be considered complementary: our work is focused on the study of the adaptive and sometimes transient response to severe potassium limitation whereas the chemostat experiments analysed the steady-state conditions of adapted cells at limiting potassium concentrations. Some results and conclusion obtained by both studies are complementary, but our work brings to light more possible potassium roles in the control of cellular metabolism.

A sudden depletion of potassium causes interferences with normal cell growth. A decrease in growth rate could be caused by several reasons but the content of ribosomes is a classic cellular parameter that shows a close correlation with cell growth (Mager & Planta 1991; Kraakman et al. 1993). The absence of ribosomes blocks protein synthesis and consequently the progression of cell growth. Our transcriptional analysis of potassium starvation has shown a strong repression of genes necessaries for biosynthesis of the ribosomes, the so called RiBi regulon and the ribosomal protein-encoding genes. It has been published that the total protein content decrease after few hours of, potassium starvation, an effect that is more drastic in *trk1 trk2* mutant (Gelis et al. 2012). We propose that the absence of ribosome generation could the cause of the observed blockage of cell protein synthesis under long term potassium starvation (Lubin & Ennis 1964), leading to the mentioned decrease in protein levels.

The repression of ribosomal proteins-encoding and RiBi regulon genes is also a characteristic signature of the environmental stress response (ESR), which involves a group of genes with a common response to all stressful conditions (Gasch et al. 2000). The ESR is formed by around 900 genes, 1/3 of them induced and 2/3 repressed (including the ribosomal proteins and RiBi genes). Our results indicate that potassium starvation is a stressful condition that impinges in the transcriptional changes of 70 % of ESR genes. The induced fraction of ESR genes includes genes that respond to general stress conditions and some of them are under the control of the transcriptional factors Msn2 Msn4. Our work has shown that potassium starvation only induces a STRE response of moderate intensity in comparison with other stressful conditions, such as heat-shock. Recently, it has been described that slow growth caused by both environmental and genetic perturbations results in an expression pattern highly similar to the ESR (O'Duibhir et al. 2014). The slow growth caused by

potassium deprivation could contribute to the ESR profile observed in response to limited availability of this cation.

Other genes members of the inductive part of the ESR, also induced by potassium starvation, are involved in oxidative stress responses, trehalose metabolism and glycogen synthesis (Gasch & Werner-Washburne 2002) (Figure 11). A fraction of oxidative stress responsive genes are controlled by the Msn2 Msn4 elements (Martínez-Pastor et al. 1996) but other transcription factors like Yap1 and Skn7 control an important set of these genes under oxidative stress (Temple et al. 2005). It is conceivable that the induction of oxidative stress genes triggered by potassium starvation is not only caused by a general response to stress controlled by Msn2 Msn4 but by a direct signal of cellular oxidative stress caused by ROS accumulation, as it will be discussed later (Figure 11).

The transcriptional profile of the double mutant *trk1 trk2* was analysed in conditions of enough potassium in the medium (50 mM KCl) and compared with the wild type strain at the same conditions. In this situation the WT strain and the *trk1 trk2* mutant are able to proliferate with similar growth rates, the intracellular potassium content in the *trk1 trk2* mutant is only slightly decreased (Navarrete et al. 2010), and they show a comparable intracellular distribution (Gelis et al. 2015). The main differences between the mutant strain and the WT strain in the presence of 50 mM KCl are that *trk1 trk2* has hyperpolarized membrane, slight acidic intracellular pH, and a decrease in proton efflux (Navarrete et al. 2010). Our transcriptomic analysis shows that the *trk1 trk2* mutant only suffers limited changes in the transcriptional profile, resulting in the induction of genes necessary for the synthesis of some amino acid and sulfate assimilation. Study of the proteome of the WT strain versus the *trk1 trk2* mutant at exponential phase using the same non limiting potassium conditions showed small number of differences between the strains (Curto et al. 2010). These changes do not appear to be directly due to strong potassium limitation, but they could be generated by the other collateral effects of elimination of the Trk system. It is known that one of the main functions of Trk1 and, up to some extent of Trk2 (Petrezsélyová et al. 2011), is the regulation of the membrane potential and, consequently, the double mutant presents a strong membrane hyperpolarization (Madrid et al. 1998; Navarrete et al. 2010). Membrane hyperpolarization effects the activity of other transporters, for example cation efflux transporters, resulting in a significant reduction of the potassium efflux in cells starved for potassium (Navarrete et al. 2010; Zahrádka & Sychrová 2012). The Trk1 regulated membrane potential is required for polarity orientation during mating and electric field response of cells

(Haupt et al. 2014). Additional effects of membrane hyperpolarization could be behind of some observed transcriptional changes.

Metabolic effects of potassium starvation

The absence of potassium impacts in the metabolic fluxes of many essential nutrients and in the regulation of nutrient-related pathways. The most induced genes after potassium starvation are members of sulfate assimilation and sulfur amino acids biosynthesis with a similar profile that observed in the response to sulfur-limited chemostat cultures (Boer et al. 2003). These overlapping responses includes genes encoding proteins used for the uptake of sulfate and sulfur-containing molecules (cysteine, methionine, SAM, and others), enzymes necessary for sulfate assimilation, biosynthesis of methionine and cysteine, as well as products that are involved in acquiring and generating intermediates and cofactors for sulfate assimilation and sulfur amino acid biosynthesis and transcriptional regulators of sulfur metabolism (Figure 12). The induction of the complete sulfur-related pathway could response to the observed depletion of cysteine and methionine just after remove potassium from the medium. The notion that the induction of sulfur-related genes is caused by the sulfur amino acid shortage after potassium limitation is reinforced by additional evidences: 1) the addition of increasing amount of methionine in the medium, a known regulator of the sulfur amino acid pathway (Thomas & Surdin-Kerjan 1997; Hansen & Johannesen 2000), specifically attenuates the induction of genes necessary for the biosynthesis of sulfur-containing amino acids under potassium starvation (Figure 11); 2) it is observed a tendency to switch to the expression of isoforms that contains less sulfur-containing amino acids. This is the case for exchange of the isoforms Pdc1 and Pdc5 (with 17 and 18 sulfur amino acids, respectively) for the isoenzyme Pdc6 that contains only 6 sulfur amino acids (Boer et al. 2003). This same effect has been observed upon sulfur starvation (Boer et al. 2003). The effect of lack of potassium seems rather specific for sulfur-containing amino acids, since we do not observe a consistent induction pattern in other amino acid biosynthetic pathways. A relationship between sulfate transport and potassium was observed many years ago, proposing the release of a K^+ cation for every sulfate imported using the proton motive force as energy source (reviewed in (Borst-Pauwels 1981). However this conclusion has to be taken with caution, since it was extracted from measurements performed under non-physiological conditions and under the experimental limitations at that time.

It must be noted that our results were observed in the BY4741 strain, which carries the *met17* mutation and, therefore, it is auxotrophic for methionine since it is unable to incorporate sulfate into homocysteine. This raises the point that the observed effects on sulfur metabolism-related genes could be an artefact derived from the indicated mutation. However, the analyses of the expression of several sulfur-related genes in diverse strains that can assimilate sulfate confirm that they are induced by potassium starvation albeit to a lesser degree. Therefore, the *met17* mutation probably potentiated the impact of K^+ starvation on sulfur-related genes but it is not at the origin of the observed effect.

Remarkably, the increased expression of some genes encoding proteins required for sulfur utilization was also observed in *trk1 trk2* (this work) or in *hal4 hal5* cells growing in the presence of plenty of potassium (Pérez-Valle et al. 2010). The transcriptional expression profile for these genes of both mutant strains is largely overlapping even though the growth media used were different. Hal4 and Hal5 protein kinases regulate the localization of Trks transporters in the plasma membrane, as well as of other nutrient transporters including the high-affinity methionine permeases Mup1 (Pérez-Valle et al. 2007; Pérez-Valle et al. 2010). The *hal4 hal5* double mutant strain requires potassium supplementation for maximal growth and displays a marked defect in rubidium uptake related with the Trk transporters (Mulet et al. 1999). Therefore, the sulfur-containing amino acid related transcriptional profile of the *hal4 hal5* mutant could be caused, at least in part, by a poor potassium uptake of this strain together with the mislocalization of some sulfur amino acids transporters. This suggests that sulfur amino acids metabolism is very sensitive to even minor unbalances in potassium homeostasis. It is worth noting that the sulfur-related response described in *hal4 hal5* mutant was also observed in a W303-1A genetic background. W303-1A is a *MET17* strain and, therefore, able to use sulfate as sulfur source, further supporting the notion that the sulfur-related response it is not solely caused by the incapacity to assimilate sulfate. Additionally, proteomic studies confirmed that some enzymes involved in sulfur amino acid biosynthesis are present in higher amounts in the *trk1 trk2* mutant strain that in WT cells, irrespective of potassium availability (Curto et al. 2010; Gelis et al. 2012).

Our data clearly show that potassium deprivation triggers a transcriptional response congruent with a condition of oxidative stress. ROS formation is detectable after 30 minutes of switching cells to medium lacking potassium, a kinetics that fits well with accumulation of oxidized glutathione (GSSG) and the timing of induction of oxidative stress responsive genes. We do not observe transcriptional changes of oxidative responsive genes in *trk1 trk2* mutant

under non limiting potassium levels, but under potassium starvation conditions increased protein levels of some glutaroredoxins and thioredoxins were detected (Gelis et al. 2012). It was reported that, in a situation of programmed cell death induced by glucose in the absence of additional nutrients, ROS production is concomitant with loss of cellular K^+ (Hoeberichts et al. 2010). It might be possible therefore that the incapacity to uptake potassium renders cells susceptible to development of oxidative stress.

The reasons why potassium starvation would result in oxidative stress are not obvious. One possible link could be found in the observed decrease in sulfur amino acid levels and induction of sulfur-related genes after potassium starvation. The addition of toxic metals and metalloids such as cadmium and arsenic to the medium results in oxidative stress in yeast cells (Brennan & Schiestl 1996; Haugen et al. 2004). In both situations, the addition of the toxic compounds is counteracted by the cells triggering a strong induction of genes involved in oxidative stress response, methionine and cysteine biosynthesis and sulfur metabolism (Haugen et al. 2004; Fauchon et al. 2002; Vido et al. 2001) similarly as it happens in potassium starvation conditions. These authors showed that the detoxification of these toxic compounds requires the use of sulfur-rich molecules and proteins. The sulfur amino acid cysteine is a component of some thiol-metabolites indispensable to fight against oxidative stress. Thus, the synthesis of the antioxidant tripeptide glutathione composed by glycine-cysteine-glutamic is an important consumer of cysteine (Penninckx 2002; Morano et al. 2012) (Figure 12). Glutathione functions as a major redox buffer maintaining the reducing environment of the cytoplasm, and a decrease in GSH levels leads to the appearance of oxidative stress (Penninckx 2002). Furthermore, the catalytic activity of some enzymes necessary for oxidative stress response needs sulfur-containing amino acids. For example, peroxiredoxins use cysteine residues to reduce peroxides (Chae et al. 1994). Thus, it is conceivable that the necessity for the biosynthesis of antioxidant molecules rich in sulfur-containing amino acids increases sulfur amino acid demand and promotes the induction of the expression of genes involved in sulfur metabolism (Fauchon et al. 2002). Under potassium starvation conditions we observed a situation similar to that described above: an immediate decrease in sulfur-amino acid content and induction of sulfur-related genes, followed by appearance of ROS (30 minutes), induction of genes that responses to oxidative stress and a progressive oxidation of GSH to GSSG. We do not observe changes in the total amount of cellular glutathione (the sum of oxidized and reduced glutathione) over the analysed time course. However, the first enzyme involved in glutathione biosynthesis is induced, indicating that cells are switching on the synthesis of

GSH. Our results allow us to suggest two non-exclusive hypotheses linking the decrease of sulfur-containing amino acids with oxidative response under potassium starvation conditions. The sulfur-containing amino acids scarcity could be one of the causes of oxidative stress generation and/or could be an enhancer of the cellular oxidative stress by limiting the production of oxidative stress response molecules composed by sulfur-containing amino acids (Figure 11).

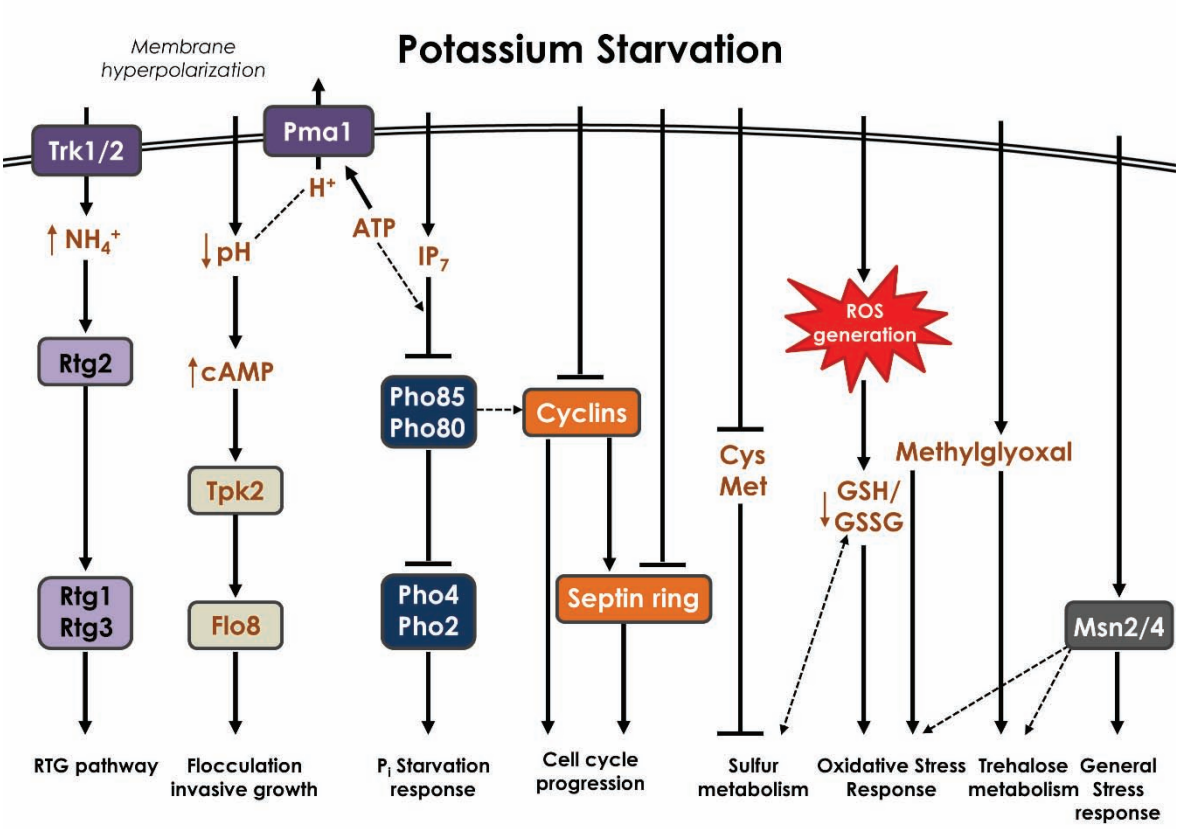

Figure 11. Known signalling pathways affected by potassium starvation. Discontinuous lines denote still uncharacterized links or possible functional relationships. See text for details.

An additional possible cause for the induction of oxidative response genes under potassium starvation conditions is the accumulation of methylglyoxal. Methylglyoxal is a by-product of glycolysis from triose phosphates, and an excess of methylglyoxal causes growth arrest, since it alters some macromolecules diminishing their biological activities (reviewed in (Kalapos 1999)). In yeast and other organisms, the accumulation of methylglyoxal can increase ROS production and activates oxidative stress response genes (Desai et al. 2010; Maeta et al. 2004). We observed a rapid increase of about 3-fold in methylglyoxal levels after potassium starvation followed by induction of genes needed for its degradation, the glyoxalases genes *GLO1* and *GLO2* and the aldose reductase encoded by the *GRE3* gene (Figure 12). These

enzymes are normally induced by an increase of intracellular levels of methylglyoxal (Aguilera & Prieto 2004). Moreover, accumulation of Glo1 and Glo2 proteins were also detected after potassium starvation (Gelis et al. 2012). Under potassium limiting conditions, we also observe an induction of genes necessary for synthesis and degradation of trehalose (*TPS1-3*, *TSL1*, *ATH1* and *NTH1*), the synthesis of glycerol (*GPD1*, *HOR2* and *RHR2*), and the synthesis of glycogen (*PGM2*, *UGP1*, *GLG1*, *GSY1*, *GSY2*, and *GLC3*) (Figure 12). The induction of these genes could be useful for generating a futile cycle based in trehalose synthesis and degradation and accumulation of glycogen, aiming to down-regulate carbon flux through the upper part of the glycolysis and to decrease the generation of methylglyoxal (Figure 12), as it has been suggested by other stresses (Parrou et al. 1997). Remarkably, a functional link between upper part of glycolysis and potassium homeostasis through Trk1 potassium transporter was described (Mulet et al. 2004). Overexpression of genes involved in trehalose biosynthesis activate Trk1-mediated potassium uptake in correlation with increased levels of glucose-1-phosphate and glucose-6-phosphate (Mulet et al. 2004). These findings support the early observation that potassium uptake via the Trk system is activated by phosphorylated sugars (Alijo & Ramos 1993). Therefore, it is conceivable that the increase in expression of trehalose metabolism genes that we observed upon potassium starvation might constitute a physiological response aiming to stimulate high-affinity potassium uptake and the same time that decrease production of methylglyoxal.

One of the main functions of potassium is to neutralize the bulk of intracellular negative charges generated by the different anionic compounds. Our potassium limiting experiments were performed in a YNB-based growth medium whose composition is similar to the standard growth media but containing only traces of potassium (15 μM) and low amounts of sodium (1.3 mM) (Navarrete et al. 2010). It was described long time ago that under situations of potassium starvation, sodium can replace some potassium functions (Rodríguez-Navarro 2000). However, very low amounts of sodium present in the medium were clearly insufficient to allow sodium substitute intracellular potassium functions. Another interchangeable cation present in high amount in our medium is ammonium (~68 mM) that is used as a nitrogen source. The high-affinity potassium transport is able to discriminate potassium from sodium cations very efficiently to avoid Na^+ toxicity (Ramos et al. 1985; Gómez et al. 1996) but is less efficient in discriminating other cations. For example, the measurement of potassium transport is usually done by using the Rb^+ analogue, due to the very similar transport activity of potassium transporters for both cations (Rodríguez-Navarro 2000). Our work has shown

that cells growing in a medium without potassium and in the presence of ammonium the cells partially substitute the lost intracellular potassium by ammonium. Replacement of potassium by ammonium was described in bacteria in potassium-limited chemostat cultures, mainly at alkaline pH (Buurman et al. 1989). In yeast the toxicity of ammonium under low potassium conditions had been reported by several authors (Rodríguez-Navarro & Ramos 1984; Bihler et al. 2002; Barreto et al. 2011). Hess and collaborators (Hess et al. 2006) suggested that if ammonium is present in high concentrations in chemostat potassium-limited cultures, ammonium ions can enter into the cell via Trk potassium channels. Our work has experimentally confirmed the proposed idea by demonstrating that the lack of potassium causes a fast and persistent increase in intracellular ammonium concentration. Even more, we demonstrated that, in this situation, ammonium influx is mediated by the Trk1 transporter, likely following the same transport mechanism that potassium influx does (Figure 11). The potassium mimicking by ammonium ion can be supported by the similitude of the ionic radius of both cations (1.33 Å vs 1.43 Å, respectively). In fact, a *S. cerevisiae* natural strain resistant to high concentration of ammonium (K12) was isolated in sake breweries. This strain has a *TRK1* allele with greater affinity for potassium than the standard allele of *TRK1* found in *Saccharomyces* strains (Reisser et al. 2013), which led the authors to hypothesize that, since greater-affinity transporters are often associated with lower flux rates, this would imply reduced flux of ammonium into the yeast cells under conditions of ammonium toxicity. Ammonium is transported into the yeast cells by three ammonium transporters, Mep1, Mep2 and Mep3, which are under the nitrogen catabolite repression regulation (Marini et al. 1997). A strain lacking all three Mep proteins cannot grow on media containing less than 5 mM NH_4^+, but grows normally on high ammonium, demonstrating the existence of additional low-affinity ammonium transport systems. In the light of our results, it is probably that the Trk system could be in part responsible for the unidentified low affinity ammonium uptake detected in *mep* mutants.

The surplus of intracellular ammonium must be detoxified. Different organisms eliminate the excess of ammonium using various systems; many aquatic animals eliminate directly ammonium to the aqueous media; birds, reptiles, and insects convert ammonium to uric acid and mammals eliminate it in the form of urea. Hess and co-workers (Hess et al. 2006) demonstrated that yeast eliminates ammonium through a rudimentary mechanism consisting in the transformation of ammonium to amino acids, followed by their excretion to the medium probably using SPS-controlled amino acids transporters (Hess et al. 2006). From this

work it is not clear how ammonium surplus remodels yeast metabolism to fix the excess of ammonium to amino acids. Our work tries to clarify this unsolved issue.

We observed, under potassium starvation conditions, a clear induction of genes controlled by the retrograde pathway (*CIT2*, *DLD3*, *ACO1*, and *IDH1/2*) that is dependent on the Rtg1-3 positive regulators (Figure 11). The main role of this pathway is communicate mitochondrial alterations to the nucleus with the aim to modulate cellular responses to changes in the functional state of mitochondria (Butow & Avadhani 2004). A major signal for activation of the retrograde pathway comes from mitochondrial dysfunctions. However, under potassium starvation conditions we do not observe evident alteration of mitochondrial morphology and, although it has been shown that the absence of mitochondrial potassium transport breaks the mitochondrial membrane potential necessary for normal mitochondrial functions, leading to mitophagy and activation of retrograde pathway (Nowikovsky et al. 2009), studies on the subcellular potassium distribution after potassium starvation do not show any changes in mitochondrial potassium content (Herrera et al. 2013). Therefore it is unlikely that activation of the retrograde pathway as a result of potassium starvation would be a consequence of mitochondrial damage or dysfunction.

Some retrograde genes induced by potassium starvation, *CIT2*, *ACO1* and *IDH1/2*, encode early enzymes in the tricarboxylic acid (TCA) cycle necessary for both the glyoxylate cycle and the synthesis of α-ketoglutarate (Figure 12). In cells lacking functional mitochondria, the TCA cycle is not able to work as a full cycle (due to the lack of succinate dehydrogenase activity), thus limiting the production of α-ketoglutarate necessary for ammonium fixation (Jazwinski 2013). Genes activated by the retrograde pathway encode enzymes necessary for the synthesis of α-ketoglutarate and to maintain glutamate levels needed for anabolic reactions as amino acid biosynthesis (Butow & Avadhani 2004; Liu & Butow 2006). Besides mitochondrial dysfunctions, another signal that activates the retrograde pathway is ammonium accumulation (Tate & Cooper 2003). Therefore, we propose that the increase of ammonium observed under potassium starvation could be the signal that activates the retrograde pathway, thus favouring ammonium assimilation and generation of amino acids.

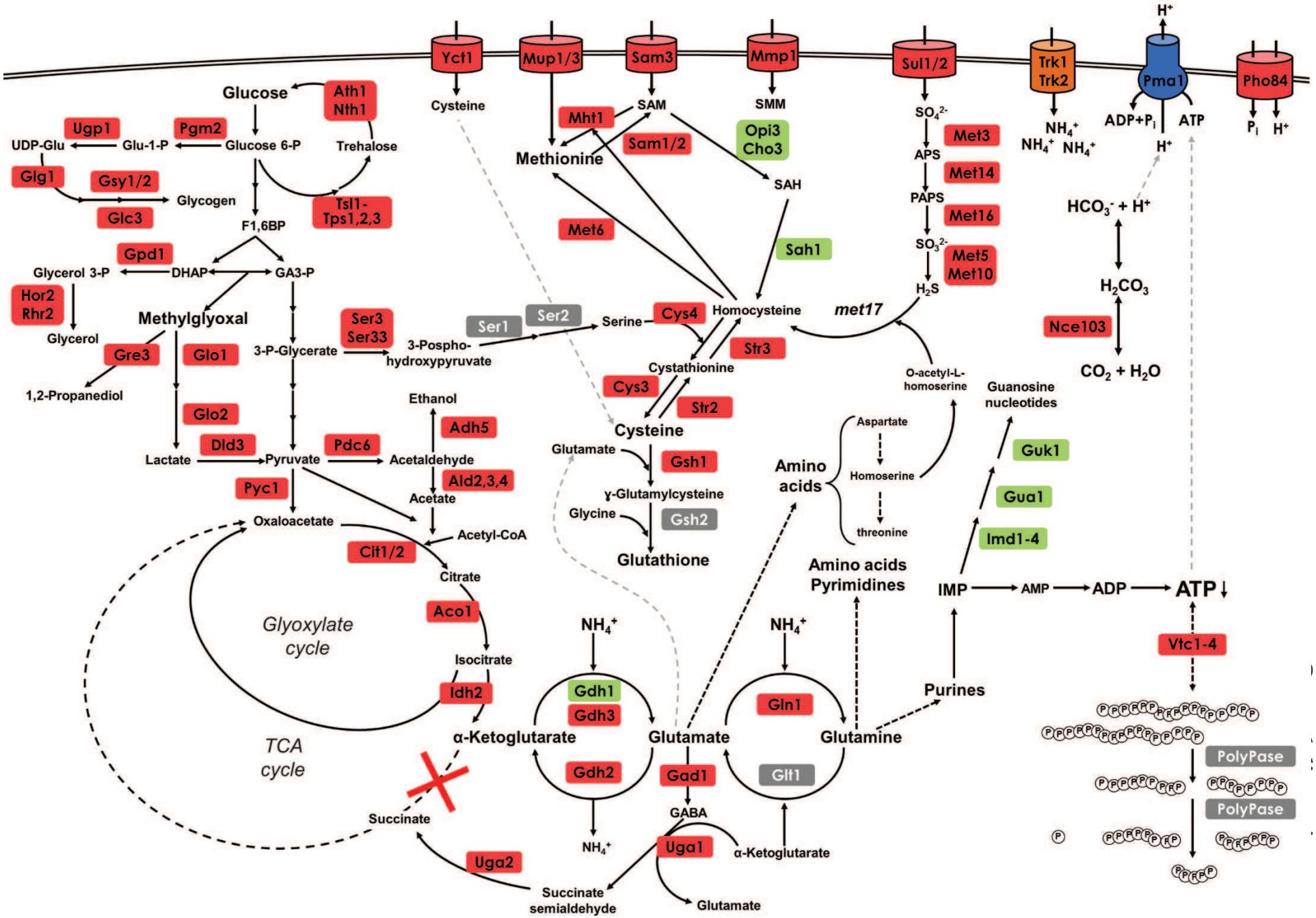
Yct1
Mup1/3
Sam3
Mmp1
Sul1/2
Trk1
Trk2
Pma1
Pho84
H+
Cysteine
SAM
SMM
SO4 2-
NH4+
ADP+Pi
ATP
Pi
Glucose
Ath1
Nth1
Trehalose
Ugp1
Pgm2
UDP-Glu
Glu-1-P
Glucose 6-P
Glg1
Gsy1/2
Glycogen
Glc3
Tsl1-
Tps1,2,3
F1,6BP
Mht1
Sam1/2
Opi3
Cho3
Methionine
SAH
Met3
APS
Met14
PAPS
Met16
Met6
Sah1
Met5
Met10
H2S
HCO3- + H+
H2CO3
Nce103
CO2 + H2O
Gpd1
Glycerol 3-P
DHAP
GA3-P
Hor2
Rhr2
Glycerol
Methylglyoxal
Gre3
Glo1
1,2-Propanediol
3-P-Glycerate
Ser3
Ser33
Ser1
Ser2
Serine
3-Pospho-
hydroxypyruvate
Cys4
Homocysteine
met17
Str3
Cystathionine
Cys3
Str2
Cysteine
O-acetyl-L-
homoserine
Guanosine
nucleotides
Glutamate
Gsh1
γ-Glutamylcysteine
Glycine
Gsh2
Glutathione
Amino
acids
Aspartate
Homoserine
threonine
Guk1
Gua1
Imd1-4
Glo2
Dld3
Pdc6
Lactate
Pyruvate
Acetaldehyde
Ethanol
Adh5
Ald2,3,4
Acetate
Pyc1
Oxaloacetate
Acetyl-CoA
Cit1/2
Citrate
Aco1
Isocitrate
Idh2
Glyoxylate
cycle
TCA
cycle
α-Ketoglutarate
Succinate
Gdh1
Gdh3
Gdh2
Glutamate
Gad1
GABA
Uga1
α-Ketoglutarate
Glutamate
Succinate
semialdehyde
Uga2
Gln1
Glt1
Glutamine
Amino acids
Pyrimidines
Purines
IMP
AMP
ADP
ATP
Vtc1-4
PolyPase
PolyPase

Figure 12. Schematic representation of all described metabolic reactions activated by potassium starvation. Genes induced in response to potassium starvation are in red background, those repressed are in green background and those that not change are in grey background. The reactions controlled by enzymes encoded for more than one gene, only the induced genes are added in the illustration. See text for details. F1-6-P2, fructose-1,6-bisphosphate; Glu-1-P, glucose-1-Phosphate; UDP-Glu, UDP-glucose; GA3-P, glyceraldehyde-3-Phosphate; DHAP, dihydroxyacetone-P; 3P-Glycerate, 3-Phosphoglycerate; G3-P, glycerol-3-Phosphate; SAH, S-adenosyl-homocysteine; SAM, S-adenosyl-methionine; SMM, S-methylmethionine; GABA, gamma-aminobutyric acid.

In addition to *CIT2*, the other prototypic gene of the retrograde pathway, *DLD3*, is also induced by lack of potassium. The specific role of *DLD3* in the retrograde pathway is not solved but could be involved in the production of pyruvate from D-lactate. Detoxification of methylglyoxal generated by potassium starvation leads to accumulation of lactate, which can be transformed to pyruvate by Dld3, thus linking the detoxification of ammonium in potassium starved cells with methylglyoxal degradation (Figure 12). Potassium starvation also induces other genes, as the pyruvate carboxylase *PYC1,* controlled by the RTG pathway (Menéndez & Gancedo 1998).

The metabolic data of amino acid secretion under potassium limitation or excess of ammonia (Hess et al. 2006) was analysed using a metabolic network model (Mo et al. 2009). This model showed that potassium limitation and high ammonium conditions shared a common pattern of accumulation high levels of amino acids and precursors of amino acid biosynthesis such as pyruvate, α-ketoglutarate, glutamine, glutamate, etc. Ammonium can be assimilated by two reactions: the synthesis of glutamate from ammonium and α-ketoglutarate, catalysed by glutamate dehydrogenases encoded in yeast by the *GDH1* and *GDH3* genes, or by the synthesis of glutamine from glutamate and ammonium, catalysed by glutamine synthase (*GLN1*). Under potassium starvation, the profile of induction of genes involved in these reactions and the reverse ones is very similar to the profile obtained under high levels of ammonium: a decrease of *GDH1* and an increase of both *GDH2* and *GLN1* (ter Schure et al. 1995) (Figure 12). The opposite behaviour of *GDH1* and *GDH2*, although apparently surprising, it is not completely unexpected since it has been proposed that both genes are subjected to different transcriptional regulation (ter Schure et al. 2000). High levels of ammonium activate nitrogen catabolite repression which represses nitrogen uptake from the environment (ter Schure et al. 1995). The activation of NCR under potassium starvation conditions is detected, for example, by the strong repression of the general amino acid permease *GAP1,* observed by us and by Hess and co-workers (Hess et al. 2006). Additionally, Mo and co-workers also studied the metabolic pattern of a strain in which the *GDH1* gene was deleted and *GDH2* was overexpressed (simulating the expression profile of these genes

under high ammonium levels). This strain, under standard growth conditions, also shows an altered metabolic profile related to amino acid biosynthesis and, interestingly, displays increased methylglyoxal and lactate accumulation, as it is observed under potassium starvation conditions (Mo et al. 2009). All these results reinforce the proposed model that ammonium poisoning is behind many of metabolic and transcriptional changes observed in cells exposed to lack of potassium.

A remarkable fact is that the *trk1 trk2* mutant shows slight increase in the expression of *CIT2* and *DLD3* and the same happens in the *hal4 hal5* mutant (Pérez-Valle et al. 2010). The other genes targets of retrograde response are not induced in neither of the mutants and the *trk1 trk2* mutant is able to growth on respiratory sources, indicating that the mitochondria are functional. Therefore, it seems that the induction of these two genes in both mutants might not be related with the induction of the retrograde pathway. Whereas the common primary origin for the induction of these genes appears to be related with the Trks transporters, further work is required to clarify this issue.

Functional relationship between potassium and phosphate homeostasis

The transcriptomic analysis presented in the first publication of this Thesis also suggested a functional interaction between potassium and phosphate. We found an induction of some genes related with phosphate uptake and utilization in absence of potassium. This incipient relationship between potassium and phosphate has been extended in the second publication by the combination of biochemical and genetic approaches. We demonstrate that elimination of potassium from the medium or perturbation of the normal influx of the cation in the presence of abundant extracellular potassium triggers a phosphate-related transcriptional response that includes the activation of a set of genes typically induced under phosphate starvation conditions such as *PHO84*, *PHO5*, and *PHO12* (Figure 11).

A possible relationship between potassium availability and normal phosphate uptake in yeast was described many years ago (Schmidt et al. 1949; Goodman & Rothstein 1957). These authors reported that K^+ enhanced phosphate uptake when the medium was adjusted to acidic pH, but decreased it at high pH. However, these experiments were performed with yeast cultures genetically undefined and under non-physiological conditions (transport measurements were made in water or different buffers preceded by long periods of starvation in water), thus making difficult to consider the biological relevance of the finding. Additionally, some observed effects could be related with modifications in the membrane

electrochemical gradient that is necessary for potassium and phosphate normal uptake and with transportable phosphate form. It has not been until a few years ago that the relationship between phosphate and potassium was superficially revisited in a report that studied the effect of phosphate accumulation and metal homeostasis (Rosenfeld et al. 2010). These authors showed that *pho80* mutants, which are unable to down regulate the *PHO* pathway and, consequently, accumulate high levels of intracellular phosphate, also display high levels of diverse metals, including increases in potassium and sodium up to 60 %.

An additional relationship between phosphate transport and cations in yeast is found in the high-affinity sodium-phosphate co-transport (Roomans et al. 1977) mediated by Pho89 transporter (Martinez & Persson 1998). Pho89 prefers Na^+ as a coupling ion with a twofold advantage over K^+ or other alkali cations (Martinez & Persson 1998). We do not observed transcriptional induction of Pho89 under potassium limitation conditions or limiting potassium uptake. This is not surprising because it is known that *PHO89* induction under P_i limitation by the *PHO* pathway is delayed in comparison with other *PHO*-regulated genes, and the strong *PHO89* induction that takes place under alkaline pH is controlled by other elements in addition to Pho4 such as Crz1, Snf1 or Rim101 (Serrano et al. 2002; Viladevall et al. 2004; Serra-Cardona et al. 2014) that are not activated under potassium starvation. In our work we followed the activation of the *PHO* pathway by using Pho84 as readout. Pho84 accumulation is observed in cells harbouring mutations that directly (*trk1*) or indirectly (Pma1 regulators) affect the capacity for potassium uptake. For instance, the WT strain without potassium express the same amounts of Pho84 that *trk1* or *trk1 trk2* mutants growing under limiting amounts of potassium (below K_m values for low-affinity potassium transport). This effect is abolished in *trks* mutants by supplementing the medium with potassium well above the K_m values for the low-affinity potassium transport or by adding normal potassium amounts (over 1 mM KCl) to WT cells. Similar results were obtained by blocking the potassium uptake by decreasing the Pma1 activity and consequently the electrochemical H^+ gradient necessary for K^+ uptake. Decreased Pma1 activity was achieved by the use of *ptk2, brp1*, and *hrk1* mutants. The *ptk2* and *brp1* mutants showed strong induction of Pho84 under potassium limiting conditions, whereas the effect on the *hrk1* mutant was far less evident. The accumulation levels of Pho84 in these mutants strongly correlate with the reported Pma1 activity and growth at potassium limiting conditions; both *ptk2* and *brp1* mutants display a strong defect in Rb^+ uptake, grow poorly on limiting amounts of potassium and express high levels of Pho84, whereas the *hrk1* strain behaves in all parameters similarly to the wild-type strain (Goossens et

al. 2000; Barreto et al. 2011; Porat et al. 2005). These results fit with the previous observations that some Pma1 mutants show constitutive overexpression of another *PHO*-controlled gene, *PHO5* (Lau et al. 1998). In the opposite way, in cells growing under limiting potassium (0.5 mM KCl) conditions, deletion of negative regulators of the H^+ pump that leads to increased Pma1 activity, such as *yck1* or *yck2* (Estrada et al. 1996), results in lower Pho84 expression in comparison with the WT strain. The observation that deletion of *TRK1* in the *ptk2* and *brp1* mutants did not further increase Pho84 levels in cells growing at limiting potassium suggested that the expression of the phosphate transporter as a result of mutation of Pma1 regulatory components was indeed linked to altered potassium transport through *TRK1* and not to limiting phosphate uptake (i.e. caused by changes in the electrochemical potential as a result of altered Pma1 activity). These results suggest that the modulation of potassium uptake regulates the induction of *PHO* pathway.

An additional support to the notion that alterations in phosphate homeostatic mechanisms can occur as a response to regulation of potassium uptake was obtained by increasing the inhibitory activity of Ppz1 over Trks, through mutation of the Ppz1 regulators Hal3 and Vhs3 (Yenush et al. 2002; Ruiz et al. 2004). The double *hal3 vhs3* mutation is lethal due to the fact that these two proteins have moonlighting activities and, in addition to regulating Ppz1, they have essential functions in the CoA biosynthetic pathway (Ruiz et al. 2009; Abrie et al. 2012). For this reason we used a conditional mutant strain with the *VHS3* gene deleted and the promoter of *HAL3* replaced by a *tetO* promoter repressible by doxycycline to increase Ppz1 activity and consequently decrease potassium uptake (Ruiz et al. 2004; González et al. 2013). The conditional mutant *tetO:HAL3 vhs3* in presence of doxycycline manifest strong induction of *PHO*-regulated genes, and this effect is abolished by the mutation of *PPZ1*.

Another parameter involved in membrane transport is the membrane potential. It is known that the removal of potassium from the medium causes hyperpolarization of yeast cells (Navarrete et al. 2010), as detected also in *trk1 trk2* mutant in the presence of 50 mM potassium (Madrid et al. 1998; Maresova et al. 2006; Navarrete et al. 2010). Therefore, it could be thought that membrane hyperpolarization could be at the basis of Pho84 expression. However, membranes in *ptk2* or *brp1* mutants are not hyperpolarized (Barreto et al. 2011) and these strains display a substantial derepression of Pho84 expression under potassium limiting conditions. Furthermore, we measured levels of Pho84 in a number of mutants with hyperpolarized membranes and normal requirements for potassium (Barreto et al. 2011) and no significant differences of Pho84 expression were found in comparison with WT strain.

From these results we can conclude that the induction of genes involved in the phosphate-starvation response does not correlate with membrane potential, but with the ability to successfully transport potassium cations.

We also demonstrate that the induction of these genes under potassium limitation is dependent on the integrity of the *PHO* signalling pathway, including the IP_7 biosynthetic pathway. The deletion of any positive component of the *PHO* pathway or of IP_7 production blocks Pho84 expression under potassium starvation, as it happens under phosphate limitation. Very recently, the dependence on Pho4 for the induction of Pho84 under potassium starvation conditions were confirmed (Anemaet & van Heusden 2014). Additionally, these authors found that induction of Pho84 was also enhanced by a decrease on RNA turnover regulated by antisense transcription of Pho84 (Anemaet & van Heusden 2014). Other stress situations that activate the *PHO* pathway, such as alkaline pH, are also dependent on the transcription factors Pho4 and Pho2 and on CDK Pho81 (Serrano et al. 2002; Ariño 2010).

The most striking effect related with phosphate homeostasis under potassium limitations is the dramatic decrease in polyP levels (Figure 12). This decrease is similar to that observed at phosphate limitation conditions. However, no changes in total amount of phosphate were detected and only a slight, but statistical significant, increase in free phosphate levels was found at long times of potassium deprivation. This increase in free phosphate could be due to the release of phosphate from the degradation of polyP reserves. This would fit with the proposed role of polyP as a buffer filtering transient fluctuations in extracellular Pi levels (Thomas & O'Shea 2005). Although polyP have been identified in diverse subcellular localizations in yeast, vacuole appears to be the major reservoir of these polymers (Urech et al. 1978; Kornberg 1995; Saito et al. 2005). Polyphosphates are linear molecules of phosphoanhydride-linked phosphate residues, therefore carrying a great deal of negative charges which have to be neutralised by positive charges. It has been proposed that some divalent cations like Ca^{2+} or Mg^{+2} could neutralise polyP negative charges (Beeler et al. 1997; Docampo et al. 2005) but in yeast only Mg^{2+} is found in enough intracellular amounts to partially fulfil this role (Eide et al. 2005; Rosenfeld et al. 2010) because Ca^{2+} is found in concentrations around 1-2 mM (Halachmi & Eilam 1989; Dunn et al. 1994). In yeast, potassium is accumulated into vacuoles, with around 45 % of total potassium found in this organelle (Herrera et al. 2013). After potassium starvation, in correlation with polyP degradation, a decrease of 4 to 5-fold in the amount of vacuolar potassium was also observed

(Herrera et al. 2013). In fact, like polyP degradation, potassium vacuolar loss starts as soon as potassium is removed from the medium. This suggests a charge balance effect, in which potassium (the most abundant cation in yeast cells) would participate with other cations in counteracting negatively charges of polyP chains. Interestingly, the addition of potassium to potassium-starved cells is enough to prompt fast recovery of normal polyP levels. Partial polyP recovering is also obtained after adding sodium to the medium. In fact, the addition of 200 mM NaCl is able to regenerate only 74% of the polyP levels reached with 50 mM KCl. The lesser ability of added sodium to mimic the effect of potassium in recovering polyP stores is likely due to the well-known discrimination ability of Trks for the transport of both cations, especially in potassium starved cells (Ramos et al. 1985; Gómez et al. 1996). At the same extracellular concentrations, potassium is taken up much more efficiently than sodium and, therefore, sodium intracellular concentrations are lower. From these results we can speculate that K^+ (or Na^+) cations are necessary to maintain intracellular levels of polyP. Our results also suggest that although ammonium is taken up under potassium starvation conditions, it is not able to promote polyP acumulation. Possibly, this is due to the fact that the intracellular ammonium concentration reached are too low or/and that vacuolar transporters have not been described in *S. cerevisiae*. Therefore, under physiological conditions, task of neutralization polyP charges should be shared by potassium (or sodium when potassium is missing) and other cations such as magnesium that are transported and accumulated into vacuoles.

Under potassium limiting conditions we observed a clear induction of *PHO*-regulated genes, degradation of polyP reserves and no changes on intracellular phosphate levels, indicating that the decrease in intracellular free phosphate is not the cause of the observed induction of the *PHO* pathway. The role of P_i as a signal for the regulation of the *PHO* pathway in *Saccharomyces cerevisiae* was proposed some time ago (Auesukaree et al. 2004), although the authors already suggested the existence of additional signalling molecules. Our results fit with the notion that additional *PHO* signalling elements should exist. Potassium starvation also caused a decline in the levels of ATP and ADP and in the overall level of adenine nucleotides. It has been proposed that the level of adenine nucleotides could function as intracellular signal for phosphate starvation, thus regulating the *PHO* pathway (Gauthier et al. 2008). The role of adenine nucleotides as sensor of phosphate levels seems appropriate because ATP is the key molecule used to incorporate phosphate to any cellular metabolite. Our reported decay in ATP levels under potassium scarcity could be attributed, at least in part, to the increased activity of the Pma1 ATPase, which is immediately activated after removal of

potassium from the medium (Figure 12). Pma1 activation is also observed in *trk1 trk2* mutants even in the presence of 50 mM potassium (Kahm et al. 2012; Hoeberichts et al. 2010). The activation of the *PHO* pathway has been related with the biosynthetic pathways of some phosphate-rich metabolites that need high amounts of phosphate for their synthesis. It has been proposed that the purine biosynthesis pathway regulates the *PHO* pathway by means of two independent metabolites, the mentioned levels of ATP and by the purine pathway metabolic intermediate AICAR (Pinson et al. 2009). The expression of the *IMD1-4*, *GUA1* and *GUK1* genes encoding the branch that derives IMP to the synthesis of GMP is repressed as a result of potassium deprivation. The *IMD1-4* genes are also repressed in *trk1 trk2* mutants even in the presence of plenty of potassium. This transcriptional remodelling of the purine biosynthesis leads to redirect IMP molecules to produce adenosine nucleotides instead of guanosine nucleotides with the aim of increase adenosine nucleotides levels under potassium starvation (Figure 12). All presented data suggest that adenine nucleotides could be a relevant signal to maintain phosphate homeostasis in yeast.

An unsolved issue is how are polyP degraded under potassium deprivation situations. PolyP can be hydrolysed by two different but related enzymatic activities, exopolyphosphatase and endopolyphosphatase activities. We checked that individual or combined mutations of the genes encoding the main polyphosphatases, *PPN1* and *PPX1* genes, did not substantially modify the degradation rate of polyP under potassium starvation. This could indicate that these gene products are not involved in polyP decay under potassium starvation and that additional polyphosphatases are degrading polyP. It has been recently shown that the gene product of *DDP1,* besides its role in inositol phosphate biosynthesis, also possess endopolyphosphatase activity in vitro (Lonetti et al. 2011), so it could be participating in polyP degradation under low potassium conditions. However, it seems unlikely that the polyphosphatase activity remaining in a *ppn1 ppx1* mutant (Lichko et al. 2006) could alone justify the relatively fast and complete polyphosphate degradation observed. As we described above, potassium starvation also decrease ATP levels. The vacuolar VTC complex possesses polyphosphate kinase activity to synthetize polyP using ATP as a substrate. One could hypothesise that if the synthesis of polyP has a turnover rapid enough, the decrease in ATP levels could block new polyP formation. The blocked synthesis of polyP together with the existing polyphosphatase activity could explain the rapid kinetic of polyP degradation observed under potassium starvation (Figure 12). However, additional experiments are needed to verify the proposed hypothesis.

Cytosolic pH determines the relative protonation state of all weak acid compounds of the cytosol and affects many processes in the cell. It is related with redox equilibria, generation of gradients for secondary active transport, signal transduction and together with other cations modulates membrane potential (Orij et al. 2012; Dechant et al. 2010; Orij et al. 2011; Sychrová et al. 1999; Yenush et al. 2002). Therefore, it can be considered that changes in intracellular pH might have some role in the observed metabolic rearrangements caused by potassium starvation. The intracellular potassium accumulation produces cytosol alkalization partially by the stimulation of proton pumping triggered by potassium uptake (Lichtenberg-Fraté et al. 1996; Yenush et al. 2002). On the other hand, blocking potassium uptake produces cytosol acidification (González et al. 2013). However, a short-term potassium deprivation does not significantly affect experimental measured intracellular pH (Navarrete et al. 2010). In these conditions, the resulting pH could be a combination of different opposite events: those that would generate cytosol alkalinisation, such as the activation of H^+ pumping out of the cell, and those processes, such as polyP degradation (Castro et al. 1995) and, potentially, intracellular ammonium accumulation (Plant et al. 1999), that would lead to production of H^+ (Figure 11). We cannot discard that longer exposure to lack of potassium or steady-state adaptations of some mutant strains to low intracellular potassium levels might resuls in a cytosol acidification. Kahm and co-workers (Kahm et al. 2012) proposed a mathematical model to explain the adaptation of yeast cells to potassium starvation. In this model the production of carbonic acid from carbon dioxide participates in H^+ generation, which can be extruded via Pma1, and bicarbonate, that carries negative charges that should be balanced by potassium cations. The accumulation of intracellular negative charges of bicarbonate and pumping H^+ out of the cell generates a membrane hyperpolarization which counteracts the large concentration gradient of potassium and thus limits potassium efflux (Kahm et al. 2012). This model was supported by the strong induction of carbonic anhydrase Nce103 under potassium starvation conditions, even in *trk1 trk2* mutants, observed in our transcriptomic analysis, and by the observed hyperactivation of Pma1 (Kahm et al. 2012) (Figure 12).

Our results clearly indicate that, besides other essential cellular roles, potassium homeostasis impacts on the homeostasis of essential nutrient such as phosphate, nitrogen or sulfate. We observed that the limitation of potassium uptake, by blocking Trk1 potassium transport or by hyperactivation of the Ppz phosphatases, results in growth defects at phosphate-limited media. Nutrient limitation in haploid yeast cells triggers the formation of filaments that results in flocculation, or invasive growth, depending on the type of growth

medium (Gancedo 2001; Broach 2012). The double mutant *trk1 trk2* or the conditional mutant *hal3 vhs3* in presence of doxycycline presents an invasive phenotype (González et al. 2013) (Figure 11). Both phenotypes, limited growth at low phosphate and invasive capacity are abolished by increasing the potassium concentration in the medium. These results further emphasize the functional link between potassium and nutrient homeostasis in yeast cells.

Potassium levels and cell cycle progression

The budding yeast *S. cerevisiae* can grow at very low potassium concentrations in the medium, but removal of the cation drives to a growth arrest (Navarrete et al. 2010; Kahm et al. 2012). The cells can adjust their growth rate in response to their nutritional environmental by altering the length of their cell cycle over at least a 10-fold range (Brauer et al. 2008). The relationship between potassium and cell cycle in yeast is known for a long time but the linking molecular mechanism is still unsolved. The deletion or overexpression of several regulators of cation homeostasis has been related with cell cycle progression (Clotet et al. 1996; Clotet et al. 1999; Di Como et al. 1995). High intracellular potassium levels, achieved for example by deleting Ppz1 and Ppz2 genes or overexpressing *HAL3*, reduce DNA replication efficiency, negatively influencing DNA integrity and produces a cell cycle delay (Merchan et al. 2011). On the other hand, decreased potassium levels have been related with programed cell death (Lauff & Santa-María 2010), at least in part by increase of ROS production (Hoeberichts et al. 2010). *PPZ1* overexpression, which would result in decreased potassium influx, results in a severe slow-growth phenotype (Clotet et al. 1996) and interferes with the normal transition from G_1 to S phase (Clotet et al. 1999) partially dependent on Trk1 Trk2 (Yenush et al. 2002). The presence of Ppz1 is necessary for Hal3 stimulation of cyclin expression and suppression of the growth defect of a *sit4* mutant (Di Como et al. 1995), indicating that altered potassium levels are behind the role of Hal3 in cell cycle (Clotet et al. 1999; de Nadal et al. 1998). Similarly, the overexpression of the Nha1, a cation exporter, suppress the cell cycle blockage of a *sit4 hal3* mutant (Simón et al. 2001). Therefore, it seems evident that modifications of the intracellular levels of potassium can deeply affect cell cycle progression.

Using our potassium starvation approach we observed several changes that could provide, at least in part, the molecular basis on the link between potassium and cell cycle progression. We observed a decline in the mRNA expression or the level of diverse G_1 and G_2-phase cyclins after a potassium starvation stress. The decrease in the amount of RNA of some cyclins was confirmed by monitoring the protein level, which showed even more drastic cyclin depletion profile. Environmental stress conditions and nutrient depletion are situations that

can slow down or even arrest cell cycle progression (Morano et al. 2012; Smets et al. 2010). For example phosphate starvation effects cell cycle progression by promoting Cln3 degradation and also activates Rim15, a factor that promotes cell enter into the quiescent G_0 phase (Jimenez et al. 2015). When phosphate is present, the Pho85/Pho80 complex is active and directly phosphorylates Cln3 preventing its proteasomal degradation. However when phosphate is limiting Cln3 is not phosphorylated by Pho85/Pho80 and, consequently, Cln3 is quickly degraded by the proteasome (Menoyo et al. 2013). Under potassium starvation conditions we observed a similar situation; induction of the *PHO* pathway and degradation of Cln3 protein. It should be noted that upon potassium limitation we observed an induction of *CLN3* mRNA that could counteracts the Cln3 protein degradation causing that the Cln3 decline not be as severe as we could expect. One important cell cycle function of Cln3 is control the transcription activation of the cyclins *CLN1* and *CLN2* to progress from G_1 to S phase (Stuart & Wittenberg 1995). Potassium scarcity affects the amount of both cyclins by decreasing their mRNA and protein levels.

Also related with cell cycle events, we observed that potassium scarcity down-regulates several genes involved in the septin checkpoint, such as protein kinases regulators of the bud neck formation (Figure 11). Septin modifications, such as phosphorylation, performed by several protein kinases are important regulators of septin ring assembly (Oh & Bi 2011; Gladfelter et al. 2005). Our results demonstrate that potassium starved cells are unable to construct proper septin rings, although we did not observed changes at the transcriptional level for septin-encoding genes. We detected that the levels of septin Cdc11 remain stable long after septin rings are disassembled. There are evidences that diverse cyclins, in particular Cln1 and Cln2, are needed to promote proper septin ring assembly (Benton et al. 1993; Cvrcková et al. 1995; Gladfelter et al. 2005), suggesting that the inability to assemble the septin ring under potassium starvation might be caused by altered with cyclin levels. In fact, potassium starvation could block cell cycle progression at two different levels, by down-regulating cyclins and by repressing the expression of several regulators of bud neck formation, thus preventing the assembly of the septin ring necessary for bud formation (Figure 11).

Conclusions

The conclusions of this Thesis are summarised below:

Publication 1: The short-term response of yeast to potassium starvation

From the analysis of short-term transcriptional response to the lack of potassium in *Saccharomyces cerevisiae* it can be concluded that the lack of potassium:

- Is a stressful condition with a strong impact in the yeast transcriptional profile that leads to both gene induction and repression.
- Results in strong decrease in the amount of sulfur-contain amino acids, likely responsible for the induction of genes related with sulfate assimilation and synthesis of sulfur-containing amino acids.
- Prompts the accumulation of the toxic metabolite methylglyoxal and ROS, which generates a state of oxidative stress to the cell. The effects of these accumulations are counteracted by induction of genes involved in the oxidative response and in methylglyoxal detoxification.
- Promotes intracellular ammonium accumulation through the Trk1 transporter. The observed activation of the mitochondrial retrograde pathway is likely a response aiming to the detoxification of ammonium.
- Generates a significant repression of many genes, among them ribosomal protein genes, and the RiBi regulon, providing a molecular explanation for the inhibition of protein synthesis observed in the absence of potassium.
- Blocks the cell cycle progression by down-regulating cell cycle cyclins and several regulators of bud neck formation, and by preventing the assembly of the septin ring.

Publication 2: Functional interactions between potassium and phosphate homeostasis in *Saccharomyces cerevisiae*

- Decreased potassium uptake resulting from 1) inhibition of K^+ transporters activity (*trk1 trk2* and conditional *hal3 vhs3* mutants); 2) disturbing electrochemical proton gradient (Pma1 regulatory mutants); or 3) by potassium starvation, invokes a transcriptional response that mimics phosphate starvation response.

- The induction of the *PHO* pathway depends on the capacity of potassium transport and on the classic components of the *PHO* pathway, including the IP_7 biosynthetic pathway.

- Perturbing potassium homeostasis alters polyP levels similarly as low phosphate conditions does. The relationship between polyP and potassium levels may possibly indicate an important role of K^+ in neutralizing PolyP negative charges in the vacuole.

- The rapid decrease of ATP and ADP levels after potassium starvation and the absence of changes in free phosphate levels supports the previously proposed idea that adenine nucleotides could be a relevant signal to maintain phosphate homeostasis in yeast.

- Our work confirms that the perturbation of phosphate metabolism by changes in potassium homeostasis can affect cell growth under limiting phosphate conditions and highlights the importance of the functional interaction between potassium and other essential nutrients.

References

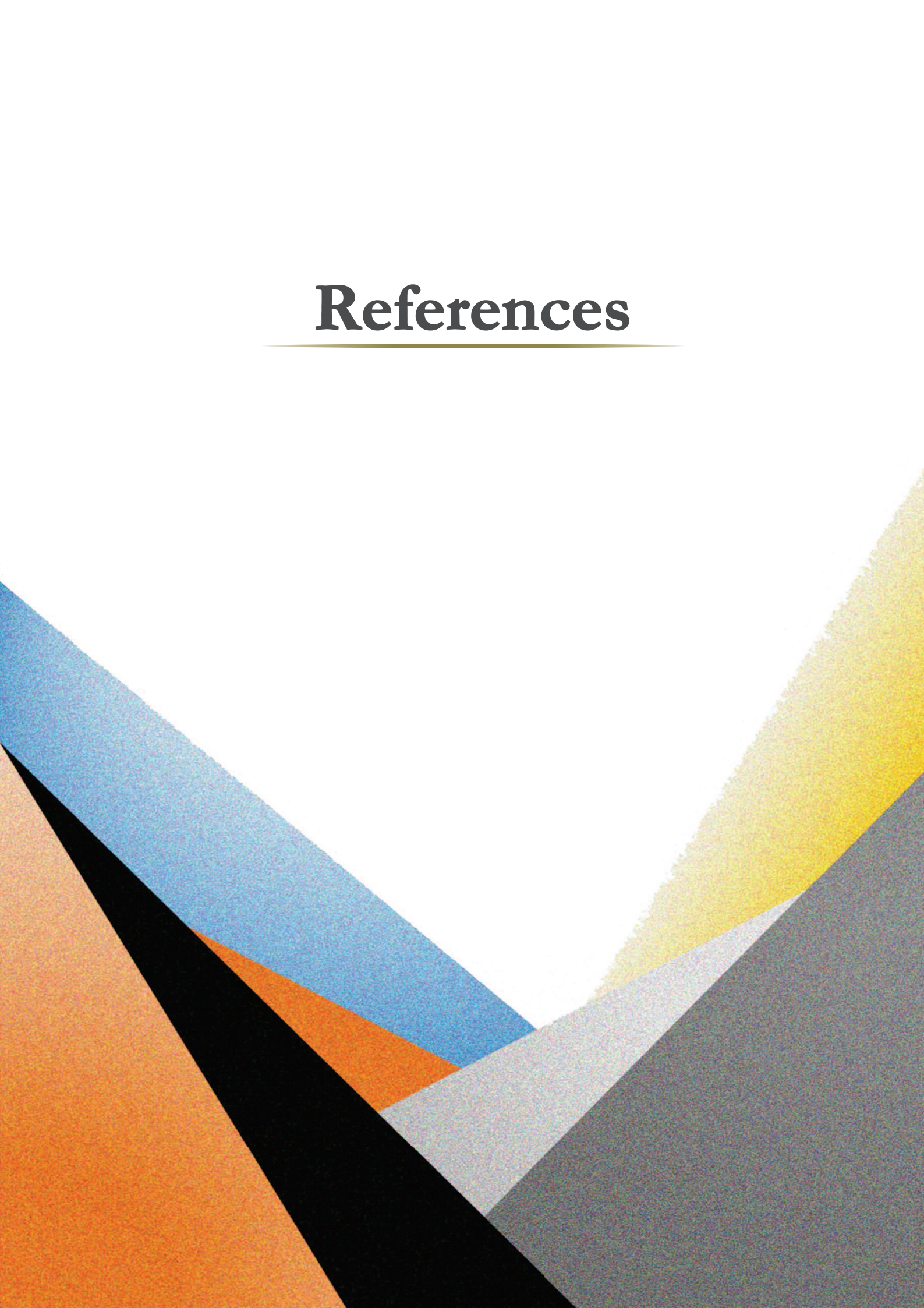

Abrie, J.A. et al., 2012. Functional mapping of the disparate activities of the yeast moonlighting protein Hal3. *The Biochemical journal*, 442(2), pp.357–68.

Achbergerová, L. & Nahálka, J., 2011. Polyphosphate--an ancient energy source and active metabolic regulator. *Microbial cell factories*, 10, p.63.

Aguilera, J. & Prieto, J.A., 2004. Yeast cells display a regulatory mechanism in response to methylglyoxal. *FEMS yeast research*, 4(6), pp.633–41.

Ahmed, A. et al., 1999. A molecular target for viral killer toxin: TOK1 potassium channels. *Cell*, 99(3), pp.283–91.

El Alami, M. et al., 2003. Arg82p is a bifunctional protein whose inositol polyphosphate kinase activity is essential for nitrogen and PHO gene expression but not for Mcm1p chaperoning in yeast. *Molecular Microbiology*, 49(2), pp.457–468.

Albert, A. et al., 2000. X-ray structure of yeast Hal2p, a major target of lithium and sodium toxicity, and identification of framework interactions determining cation sensitivity. *J.Mol.Biol.*, 295(0022-2836; 4), pp.927–938.

Alepuz, P.M., Cunningham, K.W. & Estruch, F., 1997. Glucose repression affects ion homeostasis in yeast through the regulation of the stress-activated ENA1 gene. *Molecular microbiology*, 26(1), pp.91–8.

Ali, R. et al., 2004. Inhibition of sodium/proton exchange by a Rab-GTPase-activating protein regulates endosomal traffic in yeast. *The Journal of biological chemistry*, 279(6), pp.4498–506.

Alijo, R. & Ramos, J., 1993. Several routes of activation of the potassium uptake system of yeast. *Biochimica et biophysica acta*, 1179(2), pp.224–8.

Almaguer, C. et al., 2004. Glycerophosphoinositol, a novel phosphate source whose transport is regulated by multiple factors in Saccharomyces cerevisiae. *The Journal of biological chemistry*, 279(30), pp.31937–42.

Amari, F. et al., 2008. Antioxidant small molecules confer variable protection against oxidative damage in yeast mutants. *Journal of agricultural and food chemistry*, 56(24), pp.11740–11751.

Ambesi, a et al., 2000. Biogenesis and function of the yeast plasma-membrane H(+)-ATPase. *The Journal of experimental biology*, 203(Pt 1), pp.155–60.

Anemaet, I.G. & van Heusden, G.P., 2014. Transcriptional response of Saccharomyces cerevisiae to potassium starvation. *BMC genomics*, 15(1), p.1040.

Arai, H., Pink, S. & Forgac, M., 1989. Interaction of anions and ATP with the coated vesicle proton pump. *Biochemistry*, 28(7), pp.3075–82.

Archibald, F.S. & Fridovich, I., 1982. Investigations of the state of the manganese in Lactobacillus plantarum. *Archives of biochemistry and biophysics*, 215(2), pp.589–96.

Ariño, J., 2010. Integrative responses to high pH stress in S. cerevisiae. *Omics : a journal of integrative biology*, 14(5), pp.517–23.

Ariño, J., 2002. Novel protein phosphatases in yeast. *European journal of biochemistry / FEBS*, 269(4), pp.1072–7.

Ariño, J., Ramos, J. & Sychrová, H., 2010. Alkali metal cation transport and homeostasis in yeasts. *Microbiology and molecular biology reviews : MMBR*, 74(1), pp.95–120.

Auesukaree, C. et al., 2004. Intracellular Phosphate Serves as a Signal for the Regulation of the PHO Pathway in Saccharomyces cerevisiae. *Journal of Biological Chemistry*, 279(17), pp.17289–17294.

Auesukaree, C. et al., 2005. Plc1p, Arg82p, and Kcs1p, enzymes involved in inositol pyrophosphate synthesis, are essential for phosphate regulation and polyphosphate accumulation in Saccharomyces cerevisiae. *The Journal of biological chemistry*, 280(26), pp.25127–33.

Auesukaree, C. et al., 2003. Transcriptional regulation of phosphate-responsive genes in low-affinity phosphate-transporter-defective mutants in Saccharomyces cerevisiae. *Biochemical and Biophysical Research Communications*, 306(4), pp.843–850.

Bagnat, M., Chang, A. & Simons, K., 2001. Plasma membrane proton ATPase Pma1p requires raft association for surface delivery in yeast. *Molecular biology of the cell*, 12(12), pp.4129–38.

Banuelos, M.A. et al., 2002. Role of the Nha1 antiporter in regulating K(+) influx in Saccharomyces cerevisiae. *Yeast (Chichester, West Sussex)*, 19(0749-503; 1), pp.9–15.

Bañuelos, M.A. et al., 1998. The Nha1 antiporter of Saccharomyces cerevisiae mediates sodium and potassium efflux. *Microbiology*, 144 (Pt 1(1350-0872), pp.2749–58.

Barbaric, S. et al., 1998. Cooperative Pho2-Pho4 interactions at the PHO5 promoter are critical for binding of Pho4 to UASp1 and for efficient transactivation by Pho4 at UASp2. *Molecular and cellular biology*, 18(5), pp.2629–2639.

Barreto, L. et al., 2011. A genomewide screen for tolerance to cationic drugs reveals genes important for potassium homeostasis in Saccharomyces cerevisiae. *Eukaryotic cell*, 10(9), pp.1241–50.

Basheer, S. et al., 2011. A membrane protein based biosensor: use of a phosphate--H+ symporter membrane protein (Pho84) in the sensing of phosphate ions. *Biosensors & bioelectronics*, 27(1), pp.58–63.

Bechet, J., Greenson, M. & Wiame, J.M., 1970. Mutations affecting the repressibility of arginine biosynthetic enzymes in Saccharomyces cerevisiae. *European journal of biochemistry / FEBS*, 12(1), pp.31–39.

Beeler, T., Bruce, K. & Dunn, T., 1997. Regulation of cellular Mg2+ by Saccharomyces cerevisiae. *Biochimica et biophysica acta*, 1323(2), pp.310–8.

Benito, B., Quintero, F.J. & Rodríguez-Navarro, A., 1997. Overexpression of the sodium ATPase of Saccharomyces cerevisiae: conditions for phosphorylation from ATP and Pi. *Biochimica et biophysica acta*, 1328(2), pp.214–26.

Benton, B.K. et al., 1993. Genetic analysis of Cln/Cdc28 regulation of cell morphogenesis in budding yeast. *The EMBO journal*, 12(13), pp.5267–75.

Berridge, M.J., 1993. Inositol trisphosphate and calcium signalling. *Nature*, 361(6410), pp.315–325.

Bertl, A. et al., 2003. Characterization of potassium transport in wild-type and isogenic yeast strains carrying all combinations of trk1, trk2 and tok1 null mutations. *Molecular microbiology*, 47(0950-382; 3), pp.767–780.

Bertl, A. et al., 1998. Physiological characterization of the yeast plasma membrane outward rectifying K+ channel, DUK1 (TOK1), in situ. *J.Membr.Biol.*, 162(0022-2631; 1), pp.67–80.

Betz, C. et al., 2002. ISC1-encoded inositol phosphosphingolipid phospholipase C is involved in Na+/Li+ halotolerance of Saccharomyces cerevisiae. *European journal of biochemistry / FEBS*, 269(16), pp.4033–9.

Bhaumik, S.R. & Green, M.R., 2002. Differential requirement of SAGA components for recruitment of TATA-box-binding protein to promoters in vivo. *Molecular and cellular biology*, 22(21), pp.7365–71.

Bhoite, L.T. et al., 2002. Mutations in the Pho2 (Bas2) transcription factor that differentially affect activation with its partner proteins Bas1, Pho4, and Swi5. *Journal of Biological Chemistry*, 277(40), pp.37612–37618.

Bi, E. & Park, H.-O., 2012. Cell polarization and cytokinesis in budding yeast. *Genetics*, 191(2), pp.347–87.

Bihler, H. et al., 1999. The presumed potassium carrier Trk2p in Saccharomyces cerevisiae determines an H+-dependent, K+-independent current. *FEBS letters*, 447(0014-5793; 1), pp.115–120.

Bihler, H., Slayman, C.L. & Bertl, A., 2002. Low-affinity potassium uptake by Saccharomyces cerevisiae is mediated by NSC1, a calcium-blocked non-specific cation channel. *Biochimica et biophysica acta*, 1558(2), pp.109–18.

Bihler, H., Slayman, C.L. & Bertl, A., 1998. NSC1: a novel high-current inward rectifier for cations in the plasma membrane of Saccharomyces cerevisiae. *FEBS letters*, 432(1-2), pp.59–64.

Blaiseau, P.L. & Thomas, D., 1998. Multiple transcriptional activation complexes tether the yeast activator Met4 to DNA. *The EMBO journal*, 17(21), pp.6327–36.

Bleackley, M.R. & Macgillivray, R.T.A., 2011. Transition metal homeostasis: from yeast to human disease. *Biometals : an international journal on the role of metal ions in biology, biochemistry, and medicine*, 24(5), pp.785–809.

Boer, V.M. et al., 2003. The genome-wide transcriptional responses of Saccharomyces cerevisiae grown on glucose in aerobic chemostat cultures limited for carbon, nitrogen, phosphorus, or sulfur. *The Journal of biological chemistry*, 278(5), pp.3265–74.

Bonilla, M., Nastase, K.K. & Cunningham, K.W., 2002. Essential role of calcineurin in response to endoplasmic reticulum stress. *EMBO Journal*, 21(0261-4189; 10), pp.2343–2353.

Borst-Pauwels, G.W., 1981. Ion transport in yeast. *Biochimica et biophysica acta*, 650(2-3), pp.88–127.

Borst-Pauwels, G.W. & Peters, P.H., 1977. Effect of the medium pH and the cell pH upon the kinetical parameters of phosphate uptake by yeast. *Biochimica et biophysica acta*, 466(3), pp.488–95.

Bosio, M.C., Negri, R. & Dieci, G., 2011. Promoter architectures in the yeast ribosomal expression program. *Transcription*, 2(2), pp.71–77.

Botstein, D., Chervitz, S.A. & Cherry, J.M., 1997. Yeast as a model organism. *Science (New York, N.Y.)*, 277(5330), pp.1259–60.

Botstein, D. & Fink, G.R., 2011. Yeast: an experimental organism for 21st Century biology. *Genetics*, 189(3), pp.695–704.

Bouillet, L.E.M. et al., 2012. The involvement of calcium carriers and of the vacuole in the glucose-induced calcium signaling and activation of the plasma membrane H(+)-ATPase in Saccharomyces cerevisiae cells. *Cell calcium*, 51(1), pp.72–81.

Bowers, K. et al., 2000. The sodium/proton exchanger Nhx1p is required for endosomal protein trafficking in the yeast Saccharomyces cerevisiae. *Molecular biology of the cell*, 11(12), pp.4277–94.

Brauer, M.J. et al., 2008. Coordination of growth rate, cell cycle, stress response, and metabolic activity in yeast. *Molecular biology of the cell*, 19(1), pp.352–67.

Brazas, R.M. & Stillman, D.J., 1993. The Swi5 zinc-finger and Grf10 homeodomain proteins bind DNA cooperatively at the yeast HO promoter. *Proceedings of the National Academy of Sciences of the United States of America*, 90(23), pp.11237–11241.

Brennan, R.J. & Schiestl, R.H., 1996. Cadmium is an inducer of oxidative stress in yeast. *Mutation research*, 356(2), pp.171–8.

Breton, A. & Surdin-Kerjan, Y., 1977. Sulfate uptake in Saccharomyces cerevisiae: biochemical and genetic study. *Journal of bacteriology*, 132(1), pp.224–32.

Brett, C.L. et al., 2005. The yeast endosomal Na+K+/H+ exchanger Nhx1 regulates cellular pH to control vesicle trafficking. *Molecular biology of the cell*, 16(3), pp.1396–405.

Brewster, J.L. et al., 1993. An osmosensing signal transduction pathway in yeast. *Science (New York, N.Y.)*, 259(5102), pp.1760–3.

Broach, J.R., 2012. Nutritional Control of Growth and Development in Yeast. *Genetics*, 192(1), pp.73–105.

Bun-Ya, M. et al., 1991. The PHO84 gene of Saccharomyces cerevisiae encodes an inorganic phosphate transporter. *Molecular and cellular biology*, 11(6), pp.3229–38.

Butow, R.A. & Avadhani, N.G., 2004. Mitochondrial signaling: the retrograde response. *Molecular cell*, 14(1), pp.1–15.

Buurman, E.T. et al., 1989. Replacement of potassium ions by ammonium ions in different micro-organisms grown in potassium-limited chemostat culture. *Archives of microbiology*, 152(1), pp.58–63.

Cagnac, O. et al., 2007. Identification and characterization of Vnx1p, a novel type of vacuolar monovalent cation/H+ antiporter of Saccharomyces cerevisiae. *The Journal of biological chemistry*, 282(33), pp.24284–93.

Cagnac, O. et al., 2010. Vacuolar cation/H+ antiporters of Saccharomyces cerevisiae. *The Journal of biological chemistry*, 285(44), pp.33914–22.

Camacho, M., Ramos, J. & Rodríguez-Navarro, A., 1981. Potassium requirements of Saccharomyces cerevisiae. *Current Microbiology*, 6(5), pp.295–299.

Camblong, J. et al., 2007. Antisense RNA stabilization induces transcriptional gene silencing via histone deacetylation in S. cerevisiae. *Cell*, 131(4), pp.706–17.

Camblong, J. et al., 2009. Trans-acting antisense RNAs mediate transcriptional gene cosuppression in S. cerevisiae. *Genes and Development*, 23(13), pp.1534–1545.

Campetelli, A.N. et al., 2005. Activation of the plasma membrane H-ATPase of Saccharomyces cerevisiae by glucose is mediated by dissociation of the H(+)-ATPase-acetylated tubulin complex. *The FEBS journal*, 272(22), pp.5742–52.

Cao, Y. et al., 2011. Crystal structure of a potassium ion transporter, TrkH. *Nature*, 471(7338), pp.336–40.

Cao, Y. et al., 2013. Gating of the TrkH ion channel by its associated RCK protein TrkA. *Nature*, 496(7445), pp.317–22.

Carroll, A.S. & O'Shea, E.K., 2002. Pho85 and signaling environmental conditions. *Trends in biochemical sciences*, 27(2), pp.87–93.

Casado, C. et al., 2010. Regulation of Trk-dependent potassium transport by the calcineurin pathway involves the Hal5 kinase. *FEBS letters*, 584(11), pp.2415–20.

Casado, C. et al., 2011. The role of the protein kinase A pathway in the response to alkaline pH stress in yeast. *The Biochemical journal*, 438(3), pp.523–33.

Castelnuovo, M. et al., 2013. Bimodal expression of PHO84 is modulated by early termination of antisense transcription. *Nature structural & molecular biology*, 20(7), pp.851–8.

Castro, C.D. et al., 1995. In situ 31P nuclear magnetic resonance for observation of polyphosphate and catabolite responses of chemostat-cultivated Saccharomyces cerevisiae after alkalinization. *Applied and environmental microbiology*, 61(12), pp.4448–53.

Castuma, C.E. et al., 1995. Inorganic polyphosphates in the acquisition of competence in Escherichia coli. *The Journal of biological chemistry*, 270(22), pp.12980–3.

Causton, H.C. et al., 2001. Remodeling of yeast genome expression in response to environmental changes. *Molecular biology of the cell*, 12(2), pp.323–37.

Celenza, J.L. & Carlson, M., 1984. Cloning and genetic mapping of SNF1, a gene required for expression of glucose-repressible genes in Saccharomyces cerevisiae. *Molecular and cellular biology*, 4(1), pp.49–53.

Chae, H.Z., Chung, S.J. & Rhee, S.G., 1994. Thioredoxin-dependent peroxide reductase from yeast. *The Journal of biological chemistry*, 269(44), pp.27670–8.

Chelstowska, A. et al., 1999. Signalling between mitochondria and the nucleus regulates the expression of a new D-lactate dehydrogenase activity in yeast. *Yeast (Chichester, England)*, 15(13), pp.1377–91.

Chen, E.J. & Kaiser, C.A., 2002. Amino acids regulate the intracellular trafficking of the general amino acid permease of Saccharomycescerevisiae. *Proceedings of the National Academy of Sciences of the United States of America*, 99(23), pp.14837–42.

Chen, E.J. & Kaiser, C.A., 2003. LST8 negatively regulates amino acid biosynthesis as a component of the TOR pathway. *The Journal of cell biology*, 161(2), pp.333–47.

Cherest, H. et al., 1997. Molecular characterization of two high affinity sulfate transporters in Saccharomyces cerevisiae. *Genetics*, 145(3), pp.627–35.

Cherest, H., Thomas, D. & Surdin-Kerjan, Y., 1993. Cysteine biosynthesis in Saccharomyces cerevisiae occurs through the transsulfuration pathway which has been built up by enzyme recruitment. *Journal of bacteriology*, 175(17), pp.5366–74.

Clotet, J. et al., 1996. The NH2-terminal extension of protein phosphatase PPZ1 has an essential functional role. *The Journal of biological chemistry*, 271(42), pp.26349–55.

Clotet, J. et al., 1999. The yeast ser/thr phosphatases sit4 and ppz1 play opposite roles in regulation of the cell cycle. *Molecular and cellular biology*, 19(0270-7306; 3), pp.2408–2415.

Cockburn, M., Earnshaw, P. & Eddy, A.A., 1975. The stoicheiometry of the absorption of protons with phosphate and L-glutamate by yeasts of the genus Saccharomyces. *The Biochemical journal*, 146(3), pp.705–12.

Cohen, A. et al., 1999. A novel family of yeast chaperons involved in the distribution of V-ATPase and other membrane proteins. *Journal of Biological Chemistry*, 274(0021-9258; 38), pp.26885–26893.

Di Como, C.J., Bose, R. & Arndt, K.T., 1995. Overexpression of SIS2, which contains an extremely acidic region, increases the expression of SWI4, CLN1 and CLN2 in sit4 mutants. *Genetics*, 139(0016-6731; 1), pp.95–107.

Cooper, T.G., 2002. Transmitting the signal of excess nitrogen in Saccharomyces cerevisiae from the Tor proteins to the GATA factors: connecting the dots. *FEMS microbiology reviews*, 26(3), pp.223–38.

Copic, A. et al., 2009. Genomewide analysis reveals novel pathways affecting endoplasmic reticulum homeostasis, protein modification and quality control. *Genetics*, 182(3), pp.757–69.

Cox, K.H., Pinchak, A.B. & Cooper, T.G., 1999. Genome-wide transcriptional analysis in S. cerevisiae by mini-array membrane hybridization. *Yeast (Chichester, England)*, 15(8), pp.703–13.

Crespo, J.L. et al., 2001. The GATA transcription factors GLN3 and GAT1 link TOR to salt stress in Saccharomyces cerevisiae. *The Journal of biological chemistry*, 276(37), pp.34441–4.

Crespo, J.L. et al., 2002. The TOR-controlled transcription activators GLN3, RTG1, and RTG3 are regulated in response to intracellular levels of glutamine. *Proceedings of the National Academy of Sciences of the United States of America*, 99(10), pp.6784–6789.

Crespo, J.L. & Hall, M.N., 2002. Elucidating TOR signaling and rapamycin action: lessons from Saccharomyces cerevisiae. *Microbiology and molecular biology reviews : MMBR*, 66(4), pp.579–91.

Cronin, S.R., Rao, R. & Hampton, R.Y., 2002. Cod1p/Spf1p is a P-type ATPase involved in ER function and Ca2+ homeostasis. *The Journal of cell biology*, 157(6), pp.1017–28.

Crooke, E. et al., 1994. Genetically altered levels of inorganic polyphosphate in Escherichia coli. *The Journal of biological chemistry*, 269(9), pp.6290–5.

Cross, F.R. & Blake, C.M., 1993. The yeast Cln3 protein is an unstable activator of Cdc28. *Molecular and cellular biology*, 13(6), pp.3266–71.

Cunningham, K.W., 2011. Acidic calcium stores of Saccharomyces cerevisiae. *Cell calcium*, 50(2), pp.129–38.

Cunningham, K.W. & Fink, G.R., 1996. Calcineurin inhibits VCX1-dependent H+/Ca2+ exchange and induces Ca2+ ATPases in Saccharomyces cerevisiae. *Molecular and cellular biology*, 16(5), pp.2226–37.

Cunningham, K.W. & Fink, G.R., 1994. Calcineurin-dependent growth control in Saccharomyces cerevisiae mutants lacking PMC1, a homolog of plasma membrane Ca2+ ATPases. *The Journal of cell biology*, 124(3), pp.351–63.

Curto, M. et al., 2010. 2-DE based proteomic analysis of Saccharomyces cerevisiae wild and K+ transport-affected mutant (trk1,2) strains at the growth exponential and stationary phases. *Journal of proteomics*, 73(12), pp.2316–35.

Cvrcková, F. et al., 1995. Ste20-like protein kinases are required for normal localization of cell growth and for cytokinesis in budding yeast. *Genes & development*, 9(15), pp.1817–30.

Cyert, M.S., 2003. Calcineurin signaling in Saccharomyces cerevisiae: how yeast go crazy in response to stress. *Biochemical and biophysical research communications*, 311(0006-291; 4), pp.1143–1150.

Cyert, M.S., 2001. Genetic analysis of calmodulin and its targets in Saccharomyces cerevisiae. *Annual review of genetics*, 35(0066-4197), pp.647–72.

Cyert, M.S. & Philpott, C.C., 2013. Regulation of cation balance in Saccharomyces cerevisiae. *Genetics*, 193(3), pp.677–713.

Daran-Lapujade, P. et al., 2009. An atypical PMR2 locus is responsible for hypersensitivity to sodium and lithium cations in the laboratory strain Saccharomyces cerevisiae CEN.PK113-7D. *FEMS yeast research*, 9(5), pp.789–92.

Dechant, R. et al., 2010. Cytosolic pH is a second messenger for glucose and regulates the PKA pathway through V-ATPase. *The EMBO journal*, 29(15), pp.2515–26.

Dechant, R. & Peter, M., 2010. The N-terminal domain of the V-ATPase subunit "a" is regulated by pH in vitro and in vivo. *Channels (Austin, Tex.)*, 5(1), pp.4–8.

Denis, V. & Cyert, M.S., 2002. Internal Ca(2+) release in yeast is triggered by hypertonic shock and mediated by a TRP channel homologue. *J.Cell Biol.*, 156(0021-9525; 1), pp.29–34.

Desai, K.M. et al., 2010. Oxidative stress and aging: is methylglyoxal the hidden enemy? *Canadian journal of physiology and pharmacology*, 88(3), pp.273–84.

Dichtl, B., Stevens, A. & Tollervey, D., 1997. Lithium toxicity in yeast is due to the inhibition of RNA processing enzymes. *The EMBO journal*, 16(23), pp.7184–95.

Van Dien, S.J. & Keasling, J.D., 1999. Effect of polyphosphate metabolism on the Escherichia coli phosphate-starvation response. *Biotechnology progress*, 15(4), pp.587–93.

Dihazi, H., Kessler, R. & Eschrich, K., 2004. High osmolarity glycerol (HOG) pathway-induced phosphorylation and activation of 6-phosphofructo-2-kinase are essential for glycerol accumulation and yeast cell proliferation under hyperosmotic stress. *The Journal of biological chemistry*, 279(23), pp.23961–8.

Dilova, I. et al., 2004. Tor signaling and nutrient-based signals converge on Mks1p phosphorylation to regulate expression of Rtg1.Rtg3p-dependent target genes. *The Journal of biological chemistry*, 279(45), pp.46527–35.

Dilova, I., Chen, C.-Y. & Powers, T., 2002. Mks1 in concert with TOR signaling negatively regulates RTG target gene expression in S. cerevisiae. *Current biology : CB*, 12(5), pp.389–95.

Docampo, R. et al., 2005. Acidocalcisomes - conserved from bacteria to man. *Nature reviews. Microbiology*, 3(3), pp.251–61.

Dunn, T., Gable, K. & Beeler, T., 1994. Regulation of cellular Ca2+ by yeast vacuoles. *The Journal of biological chemistry*, 269(10), pp.7273–8.

Durell, S.R. & Guy, H.R., 1999. Structural models of the KtrB, TrkH, and Trk1,2 symporters based on the structure of the KcsA K(+) channel. *Biophysical journal*, 77(2), pp.789–807.

Eide, D.J. et al., 2005. Characterization of the yeast ionome: a genome-wide analysis of nutrient mineral and trace element homeostasis in Saccharomyces cerevisiae. *Genome biology*, 6(9), p.R77.

Eraso, P., Mazón, M.J. & Portillo, F., 2006. Yeast protein kinase Ptk2 localizes at the plasma membrane and phosphorylates in vitro the C-terminal peptide of the H+-ATPase. *Biochimica Et Biophysica Acta*, 1758(2), pp.164–170.

Erez, O. & Kahana, C., 2002. Deletions of SKY1 or PTK2 in the Saccharomyces cerevisiae trk1Deltatrk2Delta mutant cells exert dual effect on ion homeostasis. *Biochemical and biophysical research communications*, 295(5), pp.1142–9.

Erez, O. & Kahana, C., 2001. Screening for modulators of spermine tolerance identifies Sky1, the SR protein kinase of Saccharomyces cerevisiae, as a regulator of polyamine transport and ion homeostasis. *Molecular and cellular biology*, 21(0270-7306; 1), pp.175–184.

Escoté, X. et al., 2004. Hog1 mediates cell-cycle arrest in G1 phase by the dual targeting of Sic1. *Nature cell biology*, 6(10), pp.997–1002.

Estill, M., Kerwin-Iosue, C.L. & Wykoff, D.D., 2014. Dissection of the PHO pathway in Schizosaccharomyces pombe using epistasis and the alternate repressor adenine. *Current genetics*, pp.1–9.

Estrada, E. et al., 1996. Phosphorylation of yeast plasma membrane H+-ATPase by casein kinase I. *The Journal of biological chemistry*, 271(50), pp.32064–72.

Estrella, L.A. et al., 2008. The Rsp5 E3 ligase mediates turnover of low affinity phosphate transporters in Saccharomyces cerevisiae. *Journal of Biological Chemistry*, 283(9), pp.5327–5334.

Fairman, C., Zhou, X. & Kung, C., 1999. Potassium uptake through the TOK1 K+ channel in the budding yeast. *The Journal of membrane biology*, 168(2), pp.149–57.

Fauchon, M. et al., 2002. Sulfur sparing in the yeast proteome in response to sulfur demand. *Molecular cell*, 9(4), pp.713–23.

Ferrando, A. et al., 1995. Regulation of cation transport in Saccharomyces cerevisiae by the salt tolerance gene HAL3. *Molecular and cellular biology*, 15(0270-7306; 10), pp.5470–5481.

Ferrer-Dalmau, J. et al., 2010. Ref2, a regulatory subunit of the yeast protein phosphatase 1, is a novel component of cation homoeostasis. *The Biochemical journal*, 426(3), pp.355–64.

Fisher, E. et al., 2005. Glycerophosphocholine-dependent growth requires Gde1p (YPL110c) and Git1p in Saccharomyces cerevisiae. *The Journal of biological chemistry*, 280(43), pp.36110–7.

Fitch, I. et al., 1992. Characterization of four B-type cyclin genes of the budding yeast Saccharomyces cerevisiae. *Molecular biology of the cell*, 3(7), pp.805–18.

Flis, K. et al., 2005. The functioning of mammalian ClC-2 chloride channel in Saccharomyces cerevisiae cells requires an increased level of Kha1p. *The Biochemical journal*, 390(Pt 3), pp.655–64.

Flis, K. et al., 2002. The Gef1 protein of Saccharomyces cerevisiae is associated with chloride channel activity. *Biochemical and biophysical research communications*, 294(5), pp.1144–50.

Forment, J. et al., 2002. The yeast SR protein kinase Sky1p modulates salt tolerance, membrane potential and the Trk1,2 potassium transporter. *Biochim.Biophys.Acta*, 1565(0006-3002; 1), pp.36–40.

Forsberg, H. & Ljungdahl, P.O., 2001. Sensors of extracellular nutrients in Saccharomyces cerevisiae. *Current genetics*, 40(2), pp.91–109.

Freimoser, F.M. et al., 2006. Systematic screening of polyphosphate (poly P) levels in yeast mutant cells reveals strong interdependence with primary metabolism. *Genome biology*, 7(11), p.R109.

Fristedt, U., Weinander, R., et al., 1999. Characterization of purified and unidirectionally reconstituted Pho84 phosphate permease of Saccharomyces cerevisiae. *FEBS letters*, 458(1), pp.1–5.

Fristedt, U., van Der Rest, M., et al., 1999. Studies of cytochrome c oxidase-driven H(+)-coupled phosphate transport catalyzed by the Saccharomyces cerevisiae Pho84 permease in coreconstituted vesicles. *Biochemistry*, 38(48), pp.16010–5.

Gaber, R.F., Styles, C.A. & Fink, G.R., 1988. TRK1 encodes a plasma membrane protein required for high-affinity potassium transport in Saccharomyces cerevisiae. *Molecular and cellular biology*, 8(0270-7306; 7), pp.2848–2859.

Gancedo, J.M., 2001. Control of pseudohyphae formation in Saccharomyces cerevisiae. *FEMS microbiology reviews*, 25(1), pp.107–23.

Garciadeblas, B. et al., 1993. Differential expression of two genes encoding isoforms of the ATPase involved in sodium efflux in Saccharomyces cerevisiae. *Molecular & general genetics : MGG*, 236(2-3), pp.363–8.

Gasch, A.P. et al., 2000. Genomic expression programs in the response of yeast cells to environmental changes. *Molecular biology of the cell*, 11(12), pp.4241–57.

Gasch, A.P. & Werner-Washburne, M., 2002. The genomics of yeast responses to environmental stress and starvation. *Functional & integrative genomics*, 2(4-5), pp.181–92.

Gat-Viks, I. & Shamir, R., 2007. Refinement and expansion of signaling pathways: the osmotic response network in yeast. *Genome research*, 17(3), pp.358–67.

Gauthier, S. et al., 2008. Co-regulation of yeast purine and phosphate pathways in response to adenylic nucleotide variations. *Molecular microbiology*, 68(6), pp.1583–94.

Gaxiola, R. et al., 1992. A novel and conserved salt-induced protein is an important determinant of salt tolerance in yeast. *The EMBO journal*, 11(9), pp.3157–64.

Gaxiola, R.A. et al., 1998. The yeast CLC chloride channel functions in cation homeostasis. *Proceedings of the National Academy of Sciences of the United States of America*, 95(7), pp.4046–50.

Gelis, S. et al., 2015. A physiological, biochemical and proteomic characterization of Saccharomyces cerevisiae trk1,2 transport mutants grown at limiting potassium. *Microbiology (Reading, England)*.

Gelis, S. et al., 2012. Adaptation to potassium starvation of wild-type and K+-transport mutant (trk1,2) of Saccharomyces cerevisiae: 2-dimensional gel electrophoresis-based proteomic approach. *MicrobiologyOpen*, 1(2), pp.182–193.

Ghillebert, R. et al., 2011. Differential roles for the low-affinity phosphate transporters Pho87 and Pho90 in Saccharomyces cerevisiae. *The Biochemical journal*, 434(2), pp.243–251.

Gilbert, W., Siebel, C.W. & Guthrie, C., 2001. Phosphorylation by Sky1p promotes Npl3p shuttling and mRNA dissociation. *RNA (New York, N.Y.)*, 7(2), pp.302–13.

Giots, F., Donaton, M.C. V & Thevelein, J.M., 2003. Inorganic phosphate is sensed by specific phosphate carriers and acts in concert with glucose as a nutrient signal for activation of the protein kinase A pathway in the yeast Saccharomyces cerevisiae. *Molecular microbiology*, 47(4), pp.1163–81.

Gladfelter, A.S. et al., 2005. Interplay between septin organization, cell cycle and cell shape in yeast. *Journal of cell science*, 118(Pt 8), pp.1617–28.

Gladfelter, A.S., Pringle, J.R. & Lew, D.J., 2001. The septin cortex at the yeast mother-bud neck. *Current opinion in microbiology*, 4(6), pp.681–9.

Goffeau, A. et al., 1996. Life with 6000 Genes. *Science*, 274(5287), pp.546–567.

Gómez, M.J., Luyten, K. & Ramos, J., 1996. The capacity to transport potassium influences sodium tolerance in Saccharomyces cerevisiae. *FEMS microbiology letters*, 135(2-3), pp.157–60.

Gómez-García, M.R. & Kornberg, A., 2004. Formation of an actin-like filament concurrent with the enzymatic synthesis of inorganic polyphosphate. *Proceedings of the National Academy of Sciences of the United States of America*, 101(45), pp.15876–80.

González, A. et al., 2013. Molecular analysis of a conditional hal3 vhs3 yeast mutant links potassium homeostasis with flocculation and invasiveness. *Fungal genetics and biology : FG & B*, 53, pp.1–9.

Goodman, J. & Rothstein, A., 1957. The active transport of phosphate into the yeast cell. *The Journal of general physiology*, 40(6), pp.915–23.

Goossens, A. et al., 2000. Regulation of yeast H(+)-ATPase by protein kinases belonging to a family dedicated to activation of plasma membrane transporters. *Molecular and cellular biology*, 20(20), pp.7654–61.

Haber, J.E., 2012. Mating-type genes and MAT switching in Saccharomyces cerevisiae. *Genetics*, 191(1), pp.33–64.

Haguenauer-Tsapis, R., Nagy, M. & Ryter, A., 1986. A deletion that includes the segment coding for the signal peptidase cleavage site delays release of Saccharomyces cerevisiae acid phosphatase from the endoplasmic reticulum. *Molecular and cellular biology*, 6(2), pp.723–9.

Halachmi, D. & Eilam, Y., 1989. Cytosolic and vacuolar Ca2+ concentrations in yeast cells measured with the Ca2+-sensitive fluorescence dye indo-1. *FEBS letters*, 256(1-2), pp.55–61.

Hansen, J. & Johannesen, P.F., 2000. Cysteine is essential for transcriptional regulation of the sulfur assimilation genes in Saccharomyces cerevisiae. *Molecular & general genetics : MGG*, 263(3), pp.535–42.

Harbison, C.T. et al., 2004. Transcriptional regulatory code of a eukaryotic genome. *Nature*, 431(7004), pp.99–104.

Haro, R., Garciadeblas, B. & Rodríguez-Navarro, A., 1991. A novel P-type ATPase from yeast involved in sodium transport. *FEBS letters*, 291(2), pp.189–91.

Haro, R. & Rodríguez-Navarro, A., 2003. Functional analysis of the M2(D) helix of the TRK1 potassium transporter of Saccharomyces cerevisiae. *Biochimica et biophysica acta*, 1613(1-2), pp.1–6.

Haro, R. & Rodríguez-Navarro, A., 2002. Molecular analysis of the mechanism of potassium uptake through the TRK1 transporter of Saccharomyces cerevisiae. *Biochimica et biophysica acta*, 1564(1), pp.114–22.

Harold, F.M., 1966. Inorganic polyphosphates in biology: structure, metabolism, and function. *Bacteriological reviews*, 30(4), pp.772–94.

Hartwell, L.H., 1974. Saccharomyces cerevisiae cell cycle. *Bacteriological reviews*, 38(2), pp.164–98.

Haugen, A.C. et al., 2004. Integrating phenotypic and expression profiles to map arsenic-response networks. *Genome Biology*, 5(12), p.R95.

Haupt, A. et al., 2014. Electrochemical Regulation of Budding Yeast Polarity. *PLoS biology*, 12(12), p.e1002029.

Helbig, A.O. et al., 2010. Perturbation of the yeast N-acetyltransferase NatB induces elevation of protein phosphorylation levels. *BMC genomics*, 11, p.685.

Hemenway, C.S. & Heitman, J., 1999. Lic4, a nuclear phosphoprotein that cooperates with calcineurin to regulate cation homeostasis in Saccharomyces cerevisiae. *Molecular & general genetics : MGG*, 261(2), pp.388–401.

Henderson, K.A., Hughes, A.L. & Gottschling, D.E., 2014. Mother-daughter asymmetry of pH underlies aging and rejuvenation in yeast. *eLife*, 3, p.e03504.

Henry, T.C. et al., 2011. Systematic screen of schizosaccharomyces pombe deletion collection uncovers parallel evolution of the phosphate signal transduction pathway in yeasts. *Eukaryotic Cell*, 10(2), pp.198–206.

Herrera, R. et al., 2013. Subcellular potassium and sodium distribution in Saccharomyces cerevisiae wild-type and vacuolar mutants. *The Biochemical journal*, 454(3), pp.525–32.

Herrero, E. et al., 2006. Glutaredoxins in fungi. *Photosynthesis Research*, 89(2-3), pp.127–140.

Herrero, E. et al., 2008. Redox control and oxidative stress in yeast cells. *Biochimica et biophysica acta*, 1780(11), pp.1217–1235.

Hess, D.C. et al., 2006. Ammonium toxicity and potassium limitation in yeast. *PLoS biology*, 4(11), p.e351.

Van Heusden, G.P. & Steensma, H.Y., 2001. 14-3-3 Proteins are essential for regulation of RTG3-dependent transcription in Saccharomyces cerevisiae. *Yeast (Chichester, England)*, 18(16), pp.1479–91.

Hillenmeyer, M.E. et al., 2008. The chemical genomic portrait of yeast: uncovering a phenotype for all genes. *Science (New York, N.Y.)*, 320(5874), pp.362–5.

Hinnebusch, A.G. & Natarajan, K., 2002. Gcn4p, a master regulator of gene expression, is controlled at multiple levels by diverse signals of starvation and stress. *Eukaryotic cell*, 1(1), pp.22–32.

Hirata, D. et al., 1995. Adaptation to high-salt stress in Saccharomyces cerevisiae is regulated by Ca2+/calmodulin-dependent phosphoprotein phosphatase (calcineurin) and cAMP-dependent protein kinase. *Molecular & general genetics : MGG*, 249(3), pp.257–64.

Hoeberichts, F.A. et al., 2010. The role of K(+) and H(+) transport systems during glucose- and H(2)O(2)-induced cell death in Saccharomyces cerevisiae. *Yeast (Chichester, England)*, 27(9), pp.713–25.

Hofman-Bang, J., 1999. Nitrogen catabolite repression in Saccharomyces cerevisiae. *Molecular biotechnology*, 12(1), pp.35–73.

Hohmann, S., 2002. Osmotic stress signaling and osmoadaptation in yeasts. *Microbiology and molecular biology reviews : MMBR*, 66(2), pp.300–72.

Hohmann, S. & Meacock, P.A., 1998. Thiamin metabolism and thiamin diphosphate-dependent enzymes in the yeast Saccharomyces cerevisiae: genetic regulation. *Biochimica et biophysica acta*, 1385(2), pp.201–19.

Holt, L.J. et al., 2009. Global Analysis of Cdk1 Substrate Phosphorylation Sites Provides Insights into Evolution. *Science*, 325(5948), pp.1682–1686.

Hothorn, M. et al., 2009. Catalytic core of a membrane-associated eukaryotic polyphosphate polymerase. *Science (New York, N.Y.)*, 324(5926), pp.513–6.

Huang, D., Friesen, H. & Andrews, B., 2007. Pho85, a multifunctional cyclin-dependent protein kinase in budding yeast. *Molecular microbiology*, 66(2), pp.303–14.

Huang, S. et al., 2001. Functional analysis of the cyclin-dependent kinase inhibitor Pho81 identifies a novel inhibitory domain. *Molecular and cellular biology*, 21(19), pp.6695–6705.

Hürlimann, H.C. et al., 2007. Pho91 Is a vacuolar phosphate transporter that regulates phosphate and polyphosphate metabolism in Saccharomyces cerevisiae. *Molecular biology of the cell*, 18(11), pp.4438–45.

Hürlimann, H.C. et al., 2009. The SPX domain of the yeast low-affinity phosphate transporter Pho90 regulates transport activity. *EMBO reports*, 10(9), pp.1003–8.

Iida, H., Sakaguchi, S., et al., 1990. Cell cycle control by Ca2+ in Saccharomyces cerevisiae. *The Journal of biological chemistry*, 265(34), pp.21216–22.

Iida, H., Yagawa, Y. & Anraku, Y., 1990. Essential role for induced Ca2+ influx followed by [Ca2+]i rise in maintaining viability of yeast cells late in the mating pheromone response pathway. A study of [Ca2+]i in single Saccharomyces cerevisiae cells with imaging of fura-2. *The Journal of biological chemistry*, 265(22), pp.13391–9.

Inoki, K. et al., 2005. Signaling by target of rapamycin proteins in cell growth control. *Microbiol.Mol.Biol.Rev.*, 69(1092-2172; 1), pp.79–100.

Irniger, S., 2002. Cyclin destruction in mitosis: a crucial task of Cdc20. *FEBS letters*, 532(1-2), pp.7–11.

Isnard, A.D., Thomas, D. & Surdin-Kerjan, Y., 1996. The study of methionine uptake in Saccharomyces cerevisiae reveals a new family of amino acid permeases. *Journal of molecular biology*, 262(4), pp.473–84.

Ives, E.B. et al., 2000. Biochemical and functional characterization of inositol 1,3,4,5, 6-pentakisphosphate 2-kinases. *The Journal of biological chemistry*, 275(47), pp.36575–36583.

Jauniaux, J.C. & Grenson, M., 1990. GAP1, the general amino acid permease gene of Saccharomyces cerevisiae. Nucleotide sequence, protein similarity with the other bakers yeast amino acid permeases, and nitrogen catabolite repression. *European journal of biochemistry / FEBS*, 190(1), pp.39–44.

Jazwinski, S.M., 2013. The retrograde response: when mitochondrial quality control is not enough. *Biochimica et biophysica acta*, 1833(2), pp.400–9.

Jeffery, D.A. et al., 2001. Multi-site phosphorylation of Pho4 by the cyclin-CDK Pho80-Pho85 is semi-processive with site preference. *Journal of molecular biology*, 306(5), pp.997–1010.

Jensen, L.T., Ajua-Alemanji, M. & Culotta, V.C., 2003. The Saccharomyces cerevisiae high affinity phosphate transporter encoded by PHO84 also functions in manganese homeostasis. *The Journal of biological chemistry*, 278(43), pp.42036–40.

Jia, Y. et al., 1997. A basic helix-loop-helix-leucine zipper transcription complex in yeast functions in a signaling pathway from mitochondria to the nucleus. *Molecular and cellular biology*, 17(3), pp.1110–7.

Jimenez, J. et al., 2015. Live fast, die soon: cell cycle progression and lifespan in yeast cells. *Microbial Cell*, 2(3), pp.62–67.

Jurica, M.S. et al., 1998. The allosteric regulation of pyruvate kinase by fructose-1,6-bisphosphate. *Structure (London, England : 1993)*, 6(2), pp.195–210.

Kafadar, K.A. & Cyert, M.S., 2004. Integration of stress responses: modulation of calcineurin signaling in Saccharomyces cerevisiae by protein kinase A. *Eukaryotic cell*, 3(5), pp.1147–53.

Kaffman, A. et al., 1994. Phosphorylation of the transcription factor PHO4 by a cyclin-CDK complex, PHO80-PHO85. *Science (New York, N.Y.)*, 263(5150), pp.1153–6.

Kaffman, A., Rank, N.M., O'Neill, E.M., et al., 1998. The receptor Msn5 exports the phosphorylated transcription factor Pho4 out of the nucleus. *Nature*, 396(6710), pp.482–6.

Kaffman, A., Rank, N.M. & O'Shea, E.K., 1998. Phosphorylation regulates association of the transcription factor Pho4 with its import receptor Pse1/Kap121. *Genes & development*, 12(17), pp.2673–83.

Kahm, M. et al., 2012. Potassium starvation in yeast: mechanisms of homeostasis revealed by mathematical modeling. *PLoS computational biology*, 8(6), p.e1002548.

Kalapos, M.P., 1999. Methylglyoxal in living organisms: chemistry, biochemistry, toxicology and biological implications. *Toxicology letters*, 110(3), pp.145–75.

Kallay, L.M. et al., 2011. Endosomal Na+ (K+)/H+ exchanger Nhx1/Vps44 functions independently and downstream of multivesicular body formation. *The Journal of biological chemistry*, 286(51), pp.44067–77.

Kane, P.M., 2012. Targeting reversible disassembly as a mechanism of controlling V-ATPase activity. *Current protein & peptide science*, 13(2), pp.117–23.

Kane, P.M., 2006. The where, when, and how of organelle acidification by the yeast vacuolar H+-ATPase. *Microbiology and molecular biology reviews : MMBR*, 70(1), pp.177–91.

Kaneko, Y. et al., 1985. Transcriptional and post-transcriptional control of PHO8 expression by PHO regulatory genes in Saccharomyces cerevisiae. *Molecular and cellular biology*, 5(1), pp.248–52.

Kang, H.-J. et al., 2014. A novel protein, Pho92, has a conserved YTH domain and regulates phosphate metabolism by decreasing the mRNA stability of PHO4 in Saccharomyces cerevisiae. *The Biochemical journal*, 457, pp.391–400.

Kaur, J. & Bachhawat, A.K., 2007. Yct1p, a novel, high-affinity, cysteine-specific transporter from the yeast Saccharomyces cerevisiae. *Genetics*, 176(2), pp.877–90.

Kawasaki-Nishi, S. et al., 2001. The amino-terminal domain of the vacuolar proton-translocating ATPase a subunit controls targeting and in vivo dissociation, and the carboxyl-terminal domain affects coupling of proton transport and ATP hydrolysis. *The Journal of biological chemistry*, 276(50), pp.47411–20.

Ke, R., Ingram, P.J. & Haynes, K., 2013. An Integrative Model of Ion Regulation in Yeast N. D. Price, ed. *PLoS Computational Biology*, 9(1), p.e1002879.

Ketchum, K.A. et al., 1995. A new family of outwardly rectifying potassium channel proteins with two pore domains in tandem. *Nature*, 376(6542), pp.690–5.

Kinclova, O. et al., 2001. Functional study of the Saccharomyces cerevisiae Nha1p C-terminus. *Molecular microbiology*, 40(0950-382; 3), pp.656–668.

Kinclova-Zimmermannova, O. & Sychrova, H., 2006. Functional study of the Nha1p C-terminus: involvement in cell response to changes in external osmolarity. *Current genetics*, 49(4), pp.229–36.

Kinclova-Zimmermannova, O., Zavrel, M. & Sychrova, H., 2005. Identification of conserved prolyl residue important for transport activity and the substrate specificity range of yeast plasma membrane Na+/H+ antiporters. *The Journal of biological chemistry*, 280(34), pp.30638–47.

Kinclova-Zimmermannova, O., Zavrel, M. & Sychrova, H., 2006. Importance of the seryl and threonyl residues of the fifth transmembrane domain to the substrate specificity of yeast plasma membrane Na+/H+ antiporters. *Molecular membrane biology*, 23(4), pp.349–61.

Kirchman, P.A. et al., 1999. Interorganelle signaling is a determinant of longevity in Saccharomyces cerevisiae. *Genetics*, 152(1), pp.179–90.

Klionsky, D.J., Herman, P.K. & Emr, S.D., 1990. The fungal vacuole: composition, function, and biogenesis. *Microbiological reviews*, 54(3), pp.266–92.

Klipp, E. et al., 2005. Integrative model of the response of yeast to osmotic shock. *Nature biotechnology*, 23(8), pp.975–82.

Klis, F.M., Boorsma, A. & De Groot, P.W.J., 2006. Cell wall construction in Saccharomyces cerevisiae. *Yeast (Chichester, England)*, 23(3), pp.185–202.

Klosinska, M.M. et al., 2011. Yeast cells can access distinct quiescent states. *Genes & development*, 25(4), pp.336–49.

Ko, C.H., Buckley, A.M. & Gaber, R.F., 1990. TRK2 is required for low affinity K+ transport in Saccharomyces cerevisiae. *Genetics*, 125(2), pp.305–12.

Ko, C.H. & Gaber, R.F., 1991. TRK1 and TRK2 encode structurally related K+ transporters in Saccharomyces cerevisiae. *Molecular and Cellular Biology*, 11(8), pp.4266–4273.

Ko, C.H., Liang, H. & Gaber, R.F., 1993. Roles of multiple glucose transporters in Saccharomyces cerevisiae. *Molecular and cellular biology*, 13(1), pp.638–48.

Kojima, A. et al., 2012. Localization and functional requirement of yeast Na+/H+ exchanger, Nhx1p, in the endocytic and protein recycling pathway. *Biochimica et biophysica acta*, 1823(2), pp.534–43.

Kolisek, M. et al., 2003. Mrs2p is an essential component of the major electrophoretic Mg2+ influx system in mitochondria. *The EMBO journal*, 22(6), pp.1235–44.

Komeili, A. & O'Shea, E.K., 1999. Roles of phosphorylation sites in regulating activity of the transcription factor Pho4. *Science (New York, N.Y.)*, 284(5416), pp.977–980.

Kornberg, A., 1995. Inorganic polyphosphate: toward making a forgotten polymer unforgettable. *Journal of bacteriology*, 177(3), pp.491–6.

Kornberg, A., Kornberg, S.R. & Simms, E.S., 1956. Metaphosphate synthesis by an enzyme from Escherichia coli. *Biochimica et biophysica acta*, 20(1), pp.215–27.

Kornberg, A., Rao, N.N. & Ault-Riché, D., 1999. Inorganic polyphosphate: a molecule of many functions. *Annual review of biochemistry*, 68, pp.89–125.

Kraakman, L.S. et al., 1993. Growth-related expression of ribosomal protein genes in Saccharomyces cerevisiae. *Molecular & general genetics : MGG*, 239(1-2), pp.196–204.

Krebs, J.E. et al., 2000. Global role for chromatin remodeling enzymes in mitotic gene expression. *Cell*, 102(5), pp.587–598.

Kühlbrandt, W., Zeelen, J. & Dietrich, J., 2002. Structure, mechanism, and regulation of the Neurospora plasma membrane H+-ATPase. *Science (New York, N.Y.)*, 297(5587), pp.1692–6.

Kulaev, I. & Kulakovskaya, T., 2000. Polyphosphate and phosphate pump. *Annual review of microbiology*, 54(0066-4227), pp.709–34.

Kulaev, I.S., 1975. Biochemistry of inorganic polyphosphates. *Reviews of physiology, biochemistry and pharmacology*, 73, pp.131–58.

Kumble, K.D. & Kornberg, A., 1996. Endopolyphosphatases for long chain inorganic polyphosphate in yeast and mammals. *The Journal of biological chemistry*, 271(43), pp.27146–51.

Kuo, M.H. & Grayhack, E., 1994. A library of yeast genomic MCM1 binding sites contains genes involved in cell cycle control, cell wall and membrane structure, and metabolism. *Molecular and cellular biology*, 14(1), pp.348–59.

Kuras, L. et al., 2002. Dual regulation of the met4 transcription factor by ubiquitin-dependent degradation and inhibition of promoter recruitment. *Molecular cell*, 10(1), pp.69–80.

Kuras, L., Barbey, R. & Thomas, D., 1997. Assembly of a bZIP-bHLH transcription activation complex: formation of the yeast Cbf1-Met4-Met28 complex is regulated through Met28 stimulation of Cbf1 DNA binding. *The EMBO journal*, 16(9), pp.2441–51.

Kuroda, T. et al., 2004. Chloride channel function in the yeast TRK-potassium transporters. *J.Membr.Biol.*, 198(0022-2631; 3), pp.177–192.

Lagerstedt, J.O. et al., 2002. Mutagenic and functional analysis of the C-terminus of Saccharomyces cerevisiae Pho84 phosphate transporter. *FEBS letters*, 526(1-3), pp.31–7.

Lamb, T.M. et al., 2001. Alkaline response genes of Saccharomyces cerevisiae and their relationship to the RIM101 pathway. *The Journal of biological chemistry*, 276(3), pp.1850–6.

Lamb, T.M. & Mitchell, A.P., 2003. The transcription factor Rim101p governs ion tolerance and cell differentiation by direct repression of the regulatory genes NRG1 and SMP1 in Saccharomyces cerevisiae. *Molecular and cellular biology*, 23(2), pp.677–86.

Larschan, E. & Winston, F., 2001. The S. cerevisiae SAGA complex functions in vivo as a coactivator for transcriptional activation by Gal4. *Genes & development*, 15(15), pp.1946–56.

Lau, W.T. et al., 2000. Pho86p, an endoplasmic reticulum (ER) resident protein in Saccharomyces cerevisiae, is required for ER exit of the high-affinity phosphate transporter Pho84p. *Proceedings of the National Academy of Sciences of the United States of America*, 97(3), pp.1107–12.

Lau, W.W., Schneider, K.R. & O'Shea, E.K., 1998. A genetic study of signaling processes for repression of PHO5 transcription in Saccharomyces cerevisiae. *Genetics*, 150(4), pp.1349–59.

Lauff, D.B. & Santa-María, G.E., 2010. Potassium deprivation is sufficient to induce a cell death program in Saccharomyces cerevisiae. *FEMS Yeast Research*, 10(5), pp.497–507.

Law, C.J. et al., 2007. Kinetic evidence is consistent with the rocker-switch mechanism of membrane transport by GlpT. *Biochemistry*, 46(43), pp.12190–7.

Lazard, M. et al., 2010. Uptake of selenite by Saccharomyces cerevisiae involves the high and low affinity orthophosphate transporters. *The Journal of biological chemistry*, 285(42), pp.32029–37.

Le, D.T. et al., 2009. Functional analysis of free methionine-R-sulfoxide reductase from Saccharomyces cerevisiae. *The Journal of biological chemistry*, 284(7), pp.4354–64.

Lecchi, S. et al., 2007. Tandem phosphorylation of Ser-911 and Thr-912 at the C terminus of yeast plasma membrane H+-ATPase leads to glucose-dependent activation. *The Journal of biological chemistry*, 282(49), pp.35471–81.

Lee, K.S., Hines, L.K. & Levin, D.E., 1993. A pair of functionally redundant yeast genes (PPZ1 and PPZ2) encoding type 1-related protein phosphatases function within the PKC1-mediated pathway. *Molecular and cellular biology*, 13(0270-7306; 9), pp.5843–5853.

Lee, T.A. et al., 2010. Dissection of combinatorial control by the Met4 transcriptional complex. *Molecular biology of the cell*, 21(3), pp.456–69.

Lee, Y.-S. et al., 2008. Molecular basis of cyclin-CDK-CKI regulation by reversible binding of an inositol pyrophosphate. *Nature chemical biology*, 4(1), pp.25–32.

Lee, Y.-S. et al., 2007. Regulation of a cyclin-CDK-CDK inhibitor complex by inositol pyrophosphates. *Science (New York, N.Y.)*, 316(5821), pp.109–12.

Leroy, C., Cormier, L. & Kuras, L., 2006. Independent recruitment of mediator and SAGA by the activator Met4. *Molecular and Cellular Biology*, 26(8), pp.3149–3163.

Levy, S. et al., 2011. The competitive advantage of a dual-transporter system. *Science (New York, N.Y.)*, 334(6061), pp.1408–12.

Lewin, A.S., Hines, V. & Small, G.M., 1990. Citrate synthase encoded by the CIT2 gene of Saccharomyces cerevisiae is peroxisomal. *Molecular and cellular biology*, 10(4), pp.1399–405.

Li, S.C. & Kane, P.M., 2009. The yeast lysosome-like vacuole: endpoint and crossroads. *Biochimica et biophysica acta*, 1793(4), pp.650–63.

Li, X.Y., Bhaumik, S.R. & Green, M.R., 2000. Distinct classes of yeast promoters revealed by differential TAF recruitment. *Science (New York, N.Y.)*, 288(5469), pp.1242–4.

Liang, H. et al., 1998. Trinucleotide insertions, deletions, and point mutations in glucose transporters confer K+ uptake in Saccharomyces cerevisiae. *Molecular and cellular biology*, 18(2), pp.926–35.

Liao, X. & Butow, R.A., 1993. RTG1 and RTG2: two yeast genes required for a novel path of communication from mitochondria to the nucleus. *Cell*, 72(1), pp.61–71.

Liao, X.S. et al., 1991. Intramitochondrial functions regulate nonmitochondrial citrate synthase (CIT2) expression in Saccharomyces cerevisiae. *Molecular and cellular biology*, 11(1), pp.38–46.

Lichko, L. et al., 2006. Inorganic polyphosphates and exopolyphosphatases in cell compartments of the yeast Saccharomyces cerevisiae under inactivation of PPX1 and PPN1 genes. *Bioscience reports*, 26(1), pp.45–54.

Lichko, L.P. et al., 2003. Exopolyphosphatases of the yeast Saccharomyces cerevisiae. *FEMS yeast research*, 3(3), pp.233–8.

Lichko, L.P. et al., 2014. PPX1 Gene Overexpression Has no Influence on Polyphosphates in Saccharomyces cerevisiae. *Biochemistry. Biokhimiia*, 79(11), pp.1211–5.

Lichtenberg-Fraté, H. et al., 1996. The SpTRK gene encodes a potassium-specific transport protein TKHp in Schizosaccharomyces pombe. *The Journal of membrane biology*, 152(2), pp.169–81.

Lim, P.H. et al., 2011. Regulation of Alr1 Mg transporter activity by intracellular magnesium. *PloS one*, 6(6), p.e20896.

Liu, C. et al., 2000. Regulation of the yeast transcriptional factor PHO2 activity by phosphorylation. *The Journal of biological chemistry*, 275(41), pp.31972–8.

Liu, Z. et al., 2005. A novel degron-mediated degradation of the RTG pathway regulator, Mks1p, by SCFGrr1. *Molecular biology of the cell*, 16(10), pp.4893–904.

Liu, Z. et al., 2003. Retrograde signaling is regulated by the dynamic interaction between Rtg2p and Mks1p. *Molecular cell*, 12(2), pp.401–11.

Liu, Z. et al., 2001. RTG-dependent mitochondria to nucleus signaling is negatively regulated by the seven WD-repeat protein Lst8p. *The EMBO journal*, 20(24), pp.7209–19.

Liu, Z. & Butow, R.A., 1999. A transcriptional switch in the expression of yeast tricarboxylic acid cycle genes in response to a reduction or loss of respiratory function. *Molecular and cellular biology*, 19(10), pp.6720–8.

Liu, Z. & Butow, R.A., 2006. Mitochondrial retrograde signaling. *Annual review of genetics*, 40, pp.159–185.

Ljungdahl, P.O. & Daignan-Fornier, B., 2012. Regulation of amino acid, nucleotide, and phosphate metabolism in Saccharomyces cerevisiae. *Genetics*, 190(3), pp.885–929.

Lonetti, A. et al., 2011. Identification of an evolutionarily conserved family of inorganic polyphosphate endopolyphosphatases. *The Journal of biological chemistry*, 286(37), pp.31966–74.

Loukin, S.H. et al., 1997. Random mutagenesis reveals a region important for gating of the yeast K+ channel Ykc1. *The EMBO journal*, 16(16), pp.4817–25.

Lu, S.P. & Lin, S.J., 2011. Phosphate-responsive signaling pathway is a novel component of NAD + metabolism in saccharomyces cerevisiae. *Journal of Biological Chemistry*, 286(16), pp.14271–14281.

Lubin, M. & Ennis, H.L., 1964. ON THE ROLE OF INTRACELLULAR POTASSIUM IN PROTEIN SYNTHESIS. *Biochimica et biophysica acta*, 80, pp.614–631.

Luke, M.M. et al., 1996. The SAP, a new family of proteins, associate and function positively with the SIT4 phosphatase. *Molecular and cellular biology*, 16(6), pp.2744–55.

Lundh, F. et al., 2009. Molecular mechanisms controlling phosphate-induced downregulation of the yeast Pho84 phosphate transporter. *Biochemistry*, 48(21), pp.4497–505.

Madrid, R. et al., 1998. Ectopic potassium uptake in trk1 trk2 mutants of Saccharomyces cerevisiae correlates with a highly hyperpolarized membrane potential. *The Journal of biological chemistry*, 273(24), pp.14838–44.

Maeda, T., Wurgler-Murphy, S.M. & Saito, H., 1994. A two-component system that regulates an osmosensing MAP kinase cascade in yeast. *Nature*, 369(6477), pp.242–5.

Maeta, K. et al., 2004. Activity of the Yap1 transcription factor in Saccharomyces cerevisiae is modulated by methylglyoxal, a metabolite derived from glycolysis. *Molecular and cellular biology*, 24(19), pp.8753–64.

Magasanik, B., 2003. Ammonia assimilation by Saccharomyces cerevisiae. *Eukaryotic cell*, 2(5), pp.827–9.

Magasanik, B. & Kaiser, C.A., 2002. Nitrogen regulation in Saccharomyces cerevisiae. *Gene*, 290(1-2), pp.1–18.

Mager, W.H. & Planta, R.J., 1991. Coordinate expression of ribosomal protein genes in yeast as a function of cellular growth rate. *Molecular and cellular biochemistry*, 104(1-2), pp.181–7.

Manlandro, C.M.A., Haydon, D.H. & Rosenwald, A.G., 2005. Ability of Sit4p to promote K+ efflux via Nha1p is modulated by Sap155p and Sap185p. *Eukaryotic cell*, 4(6), pp.1041–9.

Manolson, M.F. et al., 1994. STV1 gene encodes functional homologue of 95-kDa yeast vacuolar H(+)-ATPase subunit Vph1p. *The Journal of biological chemistry*, 269(19), pp.14064–74.

Maresova, L. et al., 2006. Measurements of plasma membrane potential changes in Saccharomyces cerevisiae cells reveal the importance of the Tok1 channel in membrane potential maintenance. *FEMS yeast research*, 6(7), pp.1039–46.

Maresova, L. & Sychrova, H., 2005. Physiological characterization of Saccharomyces cerevisiae kha1 deletion mutants. *Molecular microbiology*, 55(2), pp.588–600.

Marešová, L., Vydarený, T. & Sychrová, H., 2012. Comparison of the influence of small GTPases Arl1 and Ypt6 on yeast cells' tolerance to various stress factors. *FEMS yeast research*, 12(3), pp.332–40.

Marini, A.M. et al., 1997. A family of ammonium transporters in Saccharomyces cerevisiae. *Molecular and cellular biology*, 17(8), pp.4282–93.

Márquez, J.A. & Serrano, R., 1996. Multiple transduction pathways regulate the sodium-extrusion gene PMR2/ENA1 during salt stress in yeast. *FEBS letters*, 382(1-2), pp.89–92.

Marquina, M. et al., 2012. Modulation of yeast alkaline cation tolerance by Ypi1 requires calcineurin. *Genetics*, 190(4), pp.1355–64.

Martinez, P. et al., 1998. Physiological regulation of the derepressible phosphate transporter in Saccharomyces cerevisiae. *Journal of bacteriology*, 180(8), pp.2253–6.

Martinez, P. & Persson, B.L., 1998. Identification, cloning and characterization of a derepressible Na+-coupled phosphate transporter in Saccharomyces cerevisiae. *Molecular & general genetics : MGG*, 258(6), pp.628–38.

Martinez, R., Latreille, M.T. & Mirande, M., 1991. A PMR2 tandem repeat with a modified C-terminus is located downstream from the KRS1 gene encoding lysyl-tRNA synthetase in Saccharomyces cerevisiae. *Molecular & general genetics : MGG*, 227(1), pp.149–54.

Martínez-Muñoz, G.A. & Kane, P., 2008. Vacuolar and plasma membrane proton pumps collaborate to achieve cytosolic pH homeostasis in yeast. *The Journal of biological chemistry*, 283(29), pp.20309–19.

Martínez-Pastor, M.T. et al., 1996. The Saccharomyces cerevisiae zinc finger proteins Msn2p and Msn4p are required for transcriptional induction through the stress response element (STRE). *The EMBO journal*, 15(9), pp.2227–35.

Masuda, C.A. et al., 2001. Phosphoglucomutase is an in vivo lithium target in yeast. *The Journal of biological chemistry*, 276(41), pp.37794–801.

Masuda, C.A. et al., 2000. Regulation of monovalent ion homeostasis and pH by the Ser-Thr protein phosphatase SIT4 in Saccharomyces cerevisiae. *The Journal of biological chemistry*, 275(40), pp.30957–61.

McInerny, C.J. et al., 1997. A novel Mcm1-dependent element in the SWI4, CLN3, CDC6, and CDC47 promoters activates M/G1-specific transcription. *Genes & development*, 11(10), pp.1277–88.

McMurray, M.A. et al., 2011. Septin filament formation is essential in budding yeast. *Developmental cell*, 20(4), pp.540–9.

Measday, V. et al., 1997. A family of cyclin-like proteins that interact with the Pho85 cyclin-dependent kinase. *Molecular and cellular biology*, 17(3), pp.1212–23.

Meena, R.C., Thakur, S. & Chakrabarti, A., 2011. Regulation of Saccharomyces cerevisiae Plasma membrane H(+)-ATPase (Pma1) by Dextrose and Hsp30 during Exposure to Thermal Stress. *Indian journal of microbiology*, 51(2), pp.153–8.

Mendizabal, I. et al., 2001. Promoter sequences regulated by the calcineurin-activated transcription factor Crz1 in the yeast ENA1 gene. *Mol.Genet.Genomics*, 265(1617-4615; 5), pp.801–811.

Mendizabal, I. et al., 1998. Yeast putative transcription factors involved in salt tolerance. *FEBS letters*, 425(2), pp.323–8.

Mendoza, I. et al., 1994. The protein phosphatase calcineurin is essential for NaCl tolerance of Saccharomyces cerevisiae. *The Journal of biological chemistry*, 269(12), pp.8792–6.

Menéndez, J. & Gancedo, C., 1998. Regulatory regions in the promoters of the Saccharomyces cerevisiae PYC1 and PYC2 genes encoding isoenzymes of pyruvate carboxylase. *FEMS microbiology letters*, 164(2), pp.345–52.

Menoyo, S. et al., 2013. Phosphate-activated cyclin-dependent kinase stabilizes G1 cyclin to trigger cell cycle entry. *Molecular and cellular biology*, 33(7), pp.1273–84.

Merchan, S. et al., 2011. Genetic alterations leading to increases in internal potassium concentrations are detrimental for DNA integrity in Saccharomyces cerevisiae. *Genes to cells : devoted to molecular & cellular mechanisms*, 16(2), pp.152–65.

Merchan, S. et al., 2004. Response of the Saccharomyces cerevisiae Mpk1 mitogen-activated protein kinase pathway to increases in internal turgor pressure caused by loss of Ppz protein phosphatases. *Eukaryotic cell*, 3(1), pp.100–7.

Michel, B. et al., 2006. The yeast potassium transporter TRK2 is able to substitute for TRK1 in its biological function under low K and low pH conditions. *Yeast (Chichester, England)*, 23(8), pp.581–9.

Miseta, A. et al., 1999. The vacuolar Ca2+/H+ exchanger Vcx1p/Hum1p tightly controls cytosolic Ca2+ levels in S. cerevisiae. *FEBS letters*, 451(2), pp.132–6.

Mitsui, K. et al., 2004. A conserved domain in the tail region of the Saccharomyces cerevisiae Na+/H+ antiporter (Nha1p) plays important roles in localization and salinity-resistant cell-growth. *J.Biochem.(Tokyo)*, 135(0021-924; 1), pp.139–148.

Mitsui, K. et al., 2004. A novel membrane protein capable of binding the Na+/H+ antiporter (Nha1p) enhances the salinity-resistant cell growth of Saccharomyces cerevisiae. *The Journal of biological chemistry*, 279(13), pp.12438–47.

Mitsui, K. et al., 2009. Saccharomyces cerevisiae Na+/H+ antiporter Nha1p associates with lipid rafts and requires sphingolipid for stable localization to the plasma membrane. *Journal of biochemistry*, 145(6), pp.709–20.

Mo, M.L., Palsson, B.O. & Herrgård, M.J., 2009. Connecting extracellular metabolomic measurements to intracellular flux states in yeast. *BMC systems biology*, 3, p.37.

Morano, K.A., Grant, C.M. & Moye-Rowley, W.S., 2012. The response to heat shock and oxidative stress in Saccharomyces cerevisiae. *Genetics*, 190(4), pp.1157–95.

Mouillon, J.-M. & Persson, B.L., 2005. Inhibition of the protein kinase A alters the degradation of the high-affinity phosphate transporter Pho84 in Saccharomyces cerevisiae. *Current genetics*, 48(4), pp.226–34.

Mulet, J.M. et al., 1999. A novel mechanism of ion homeostasis and salt tolerance in yeast: the Hal4 and Hal5 protein kinases modulate the Trk1-Trk2 potassium transporter. *Molecular and cellular biology*, 19(5), pp.3328–37.

Mulet, J.M. et al., 2004. The trehalose pathway and intracellular glucose phosphates as modulators of potassium transport and general cation homeostasis in yeast. *Yeast (Chichester, England)*, 21(7), pp.569–82.

Muller, E.G., 1996. A glutathione reductase mutant of yeast accumulates high levels of oxidized glutathione and requires thioredoxin for growth. *Molecular biology of the cell*, 7(11), pp.1805–13.

Muller, E.M. et al., 2003. Fig1p facilitates Ca2+ influx and cell fusion during mating of Saccharomyces cerevisiae. *The Journal of biological chemistry*, 278(40), pp.38461–9.

Müller, O. et al., 2003. Role of the Vtc proteins in V-ATPase stability and membrane trafficking. *Journal of cell science*, 116(Pt 6), pp.1107–1115.

Müller, O. et al., 2002. The Vtc proteins in vacuole fusion: coupling NSF activity to V(0) trans-complex formation. *The EMBO journal*, 21(3), pp.259–69.

Munson, A.M. et al., 2004. Yeast ARL1 encodes a regulator of K+ influx. *Journal of cell science*, 117(Pt 11), pp.2309–20.

Muntz, J.A., 1947. The role of potassium and ammonium ions in alcoholic fermentation. *The Journal of biological chemistry*, 171(2), pp.653–65.

Murguía, J.R., Bellés, J.M. & Serrano, R., 1995. A salt-sensitive 3'(2'),5'-bisphosphate nucleotidase involved in sulfate activation. *Science (New York, N.Y.)*, 267(5195), pp.232–4.

Murguía, J.R., Bellés, J.M. & Serrano, R., 1996. The yeast HAL2 nucleotidase is an in vivo target of salt toxicity. *The Journal of biological chemistry*, 271(46), pp.29029–33.

Musladin, S. et al., 2014. The RSC chromatin remodeling complex has a crucial role in the complete remodeler set for yeast PHO5 promoter opening. *Nucleic acids research*, 42(7), pp.4270–82.

Mustacchi, R., Hohmann, S. & Nielsen, J., 2006. Yeast systems biology to unravel the network of life. *Yeast (Chichester, England)*, 23(3), pp.227–38.

De Nadal, E. et al., 2001. A role for the Ppz Ser/Thr protein phosphatases in the regulation of translation elongation factor 1Balpha. *The Journal of biological chemistry*, 276(18), pp.14829–34.

De Nadal, E. et al., 2004. The MAPK Hog1 recruits Rpd3 histone deacetylase to activate osmoresponsive genes. *Nature*, 427(6972), pp.370–4.

De Nadal, E. et al., 1998. The yeast halotolerance determinant Hal3p is an inhibitory subunit of the Ppz1p Ser/Thr protein phosphatase. *Proceedings of the National Academy of Sciences of the United States of America*, 95(0027-8424; 13), pp.7357–7362.

Nakamura, T. et al., 1993. Protein phosphatase type 2B (calcineurin)-mediated, FK506-sensitive regulation of intracellular ions in yeast is an important determinant for adaptation to high salt stress conditions. *The EMBO journal*, 12(11), pp.4063–4071.

Nakayama, H., Yoshida, K. & Shinmyo, A., 2004. Yeast plasma membrane Ena1p ATPase alters alkali-cation homeostasis and confers increased salt tolerance in tobacco cultured cells. *Biotechnology and bioengineering*, 85(7), pp.776–89.

Natarajan, K. et al., 2001. Transcriptional profiling shows that Gcn4p is a master regulator of gene expression during amino acid starvation in yeast. *Molecular and cellular biology*, 21(13), pp.4347–68.

Navarre, C. & Goffeau, A., 2000. Membrane hyperpolarization and salt sensitivity induced by deletion of PMP3, a highly conserved small protein of yeast plasma membrane. *The EMBO journal*, 19(11), pp.2515–24.

Navarrete, C. et al., 2010. Lack of main K+ uptake systems in Saccharomyces cerevisiae cells affects yeast performance in both potassium-sufficient and potassium-limiting conditions. *FEMS yeast research*, 10(5), pp.508–17.

Nishimura, K., Yasumura, K., Igarashi, K. & Kakinuma, Y., 1999. Involvement of Spt7p in vacuolar polyphosphate level of Saccharomyces cerevisiae. *Biochemical and biophysical research communications*, 257(3), pp.835–8.

Nishimura, K., Yasumura, K., Igarashi, K., Harashima, S., et al., 1999. Transcription of some PHO genes in Saccharomyces cerevisiae is regulated by spt7p. *Yeast (Chichester, England)*, 15(16), pp.1711–7.

Nishizawa, M. et al., 2008. Nutrient-regulated antisense and intragenic RNAs modulate a signal transduction pathway in yeast. *PLoS biology*, 6(12), pp.2817–30.

De Nobel, J.G. & Barnett, J.A., 1991. Passage of molecules through yeast cell walls: a brief essay-review. *Yeast (Chichester, England)*, 7(4), pp.313–23.

Nowikovsky, K. et al., 2007. Mdm38 protein depletion causes loss of mitochondrial K+/H+ exchange activity, osmotic swelling and mitophagy. *Cell death and differentiation*, 14(9), pp.1647–56.

Nowikovsky, K. et al., 2012. Perspectives on: SGP symposium on mitochondrial physiology and medicine: the pathophysiology of LETM1. *The Journal of general physiology*, 139(6), pp.445–54.

Nowikovsky, K., Schweyen, R.J. & Bernardi, P., 2009. Pathophysiology of mitochondrial volume homeostasis: potassium transport and permeability transition. *Biochimica et biophysica acta*, 1787(5), pp.345–50.

O'Connell, K.F. & Baker, R.E., 1992. Possible cross-regulation of phosphate and sulfate metabolism in Saccharomyces cerevisiae. *Genetics*, 132(1), pp.63–73.

O'Duibhir, E. et al., 2014. Cell cycle population effects in perturbation studies. *Molecular systems biology*, 10, p.732.

O'Neill, E.M. et al., 1996. Regulation of PHO4 nuclear localization by the PHO80-PHO85 cyclin-CDK complex. *Science (New York, N.Y.)*, 271(5246), pp.209–12.

Ofiteru, A.M. et al., 2011. Overexpression of the PHO84 gene causes heavy metal accumulation and induces Ire1p-dependent unfolded protein response in Saccharomyces cerevisiae cells. *Applied microbiology and biotechnology*.

Ogawa, N. et al., 1995. Functional domains of Pho81p, an inhibitor of Pho85p protein kinase, in the transduction pathway of Pi signals in Saccharomyces cerevisiae. *Molecular and cellular biology*, 15(2), pp.997–1004.

Ogawa, N., DeRisi, J. & Brown, P.O., 2000. New components of a system for phosphate accumulation and polyphosphate metabolism in Saccharomyces cerevisiae revealed by genomic expression analysis. *Molecular biology of the cell*, 11(12), pp.4309–21.

Oh, Y. & Bi, E., 2011. Septin structure and function in yeast and beyond. *Trends in cell biology*, 21(3), pp.141–8.

Orij, R. et al., 2012. Genome-wide analysis of intracellular pH reveals quantitative control of cell division rate by pH(c) in Saccharomyces cerevisiae. *Genome biology*, 13(9), p.R80.

Orij, R., Brul, S. & Smits, G.J., 2011. Intracellular pH is a tightly controlled signal in yeast. *Biochimica et biophysica acta*, 1810(10), pp.933–44.

Oshima, Y., 1997. The phosphatase system in Saccharomyces cerevisiae. *Genes & genetic systems*, 72(6), pp.323–34.

Ozcan, S., Dover, J., et al., 1996. Two glucose transporters in Saccharomyces cerevisiae are glucose sensors that generate a signal for induction of gene expression. *Proceedings of the National Academy of Sciences of the United States of America*, 93(22), pp.12428–32.

Ozcan, S., Leong, T. & Johnston, M., 1996. Rgt1p of Saccharomyces cerevisiae, a key regulator of glucose-induced genes, is both an activator and a repressor of transcription. *Molecular and cellular biology*, 16(11), pp.6419–26.

Page, M.J. & Di Cera, E., 2006. Role of Na+ and K+ in enzyme function. *Physiological reviews*, 86(4), pp.1049–92.

Pao, S.S., Paulsen, I.T. & Saier, M.H., 1998. Major facilitator superfamily. *Microbiology and molecular biology reviews : MMBR*, 62(1), pp.1–34.

Parra, K.J., Chan, C.-Y. & Chen, J., 2014. Saccharomyces cerevisiae vacuolar H+-ATPase regulation by disassembly and reassembly: one structure and multiple signals. *Eukaryotic cell*, 13(6), pp.706–14.

Parrou, J.L., Teste, M.A. & François, J., 1997. Effects of various types of stress on the metabolism of reserve carbohydrates in Saccharomyces cerevisiae: genetic evidence for a stress-induced recycling of glycogen and trehalose. *Microbiology (Reading, England)*, 143 (Pt 6, pp.1891–900.

Pattison-Granberg, J. & Persson, B.L., 2000. Regulation of cation-coupled high-affinity phosphate uptake in the yeast Saccharomyces cerevisiae. *Journal of bacteriology*, 182(17), pp.5017–9.

Patton-Vogt, J.L. & Henry, S.A., 1998. GIT1, a gene encoding a novel transporter for glycerophosphoinositol in Saccharomyces cerevisiae. *Genetics*, 149(4), pp.1707–15.

Pavletich, N.P., 1999. Mechanisms of cyclin-dependent kinase regulation: structures of Cdks, their cyclin activators, and Cip and INK4 inhibitors. *Journal of molecular biology*, 287(5), pp.821–828.

Penninckx, M.J., 2002. An overview on glutathione in Saccharomyces versus non-conventional yeasts. *FEMS yeast research*, 2(3), pp.295–305.

Pérez-Valle, J. et al., 2010. Hal4 and Hal5 protein kinases are required for general control of carbon and nitrogen uptake and metabolism. *Eukaryotic cell*, 9(12), pp.1881–90.

Pérez-Valle, J. et al., 2007. Key role for intracellular K+ and protein kinases Sat4/Hal4 and Hal5 in the plasma membrane stabilization of yeast nutrient transporters. *Molecular and cellular biology*, 27(16), pp.5725–36.

Persson, B.L. et al., 1999. Phosphate permeases of Saccharomyces cerevisiae: structure, function and regulation. *Biochimica et biophysica acta*, 1422(3), pp.255–72.

Persson, B.L. et al., 2003. Regulation of phosphate acquisition in Saccharomyces cerevisiae. *Current Genetics*, 43(4), pp.225–244.

Petrezselyova, S., Kinclova-Zimmermannova, O. & Sychrova, H., 2013. Vhc1, a novel transporter belonging to the family of electroneutral cation-Cl(-) cotransporters, participates in the regulation of cation content and morphology of Saccharomyces cerevisiae vacuoles. *Biochimica et biophysica acta*, 1828(2), pp.623–31.

Petrezsélyová, S., Ramos, J. & Sychrová, H., 2011. Trk2 transporter is a relevant player in K+ supply and plasma-membrane potential control in Saccharomyces cerevisiae. *Folia microbiologica*, 56(1), pp.23–8.

Pinson, B. et al., 2004. Low affinity orthophosphate carriers regulate PHO gene expression independently of internal orthophosphate concentration in Saccharomyces cerevisiae. *The Journal of biological chemistry*, 279(34), pp.35273–80.

Pinson, B. et al., 2009. Metabolic intermediates selectively stimulate transcription factor interaction and modulate phosphate and purine pathways. *Genes & development*, 23(12), pp.1399–407.

Pisat, N.P., Pandey, A. & Macdiarmid, C.W., 2009. MNR2 regulates intracellular magnesium storage in Saccharomyces cerevisiae. *Genetics*, 183(3), pp.873–84.

Plankert, U., Purwin, C. & Holzer, H., 1991. Yeast fructose-2,6-bisphosphate 6-phosphatase is encoded by PHO8, the gene for nonspecific repressible alkaline phosphatase. *European journal of biochemistry / FEBS*, 196(1), pp.191–6.

Plant, P.J. et al., 1999. Alternative mechanisms of vacuolar acidification in H(+)-ATPase-deficient yeast. *The Journal of biological chemistry*, 274(52), pp.37270–9.

Plášek, J. et al., 2013. Early changes in membrane potential of Saccharomyces cerevisiae induced by varying extracellular K(+), Na (+) or H (+) concentrations. *Journal of bioenergetics and biomembranes*, 45(6), pp.561–8.

Platara, M. et al., 2006. The transcriptional response of the yeast Na(+)-ATPase ENA1 gene to alkaline stress involves three main signaling pathways. *The Journal of biological chemistry*, 281(48), pp.36632–42.

Popova, Y. et al., 2010. Transport and signaling through the phosphate-binding site of the yeast Pho84 phosphate transceptor. *Proceedings of the National Academy of Sciences of the United States of America*, 107(7), pp.2890–5.

Porat, Z. et al., 2005. Mechanism of polyamine tolerance in yeast: novel regulators and insights. *Cellular and molecular life sciences : CMLS*, 62(24), pp.3106–16.

Portillo, F., 2000. Regulation of plasma membrane H(+)-ATPase in fungi and plants. *Biochimica et biophysica acta*, 1469(1), pp.31–42.

Portillo, F., Eraso, P. & Serrano, R., 1991. Analysis of the regulatory domain of yeast plasma membrane H+-ATPase by directed mutagenesis and intragenic suppression. *FEBS letters*, 287(1-2), pp.71–4.

Portillo, F., de Larrinoa, I.F. & Serrano, R., 1989. Deletion analysis of yeast plasma membrane H+-ATPase and identification of a regulatory domain at the carboxyl-terminus. *FEBS letters*, 247(2), pp.381–5.

Portillo, F., Mulet, J.M. & Serrano, R., 2005. A role for the non-phosphorylated form of yeast Snf1: tolerance to toxic cations and activation of potassium transport. *FEBS letters*, 579(2), pp.512–6.

Posas, F. et al., 1992. Molecular cloning and analysis of a yeast protein phosphatase with an unusual amino-terminal region. *The Journal of biological chemistry*, 267(17), pp.11734–40.

Posas, F. et al., 2000. The transcriptional response of yeast to saline stress. *Journal of Biological Chemistry*, 275(0021-9258; 23), pp.17249–17255.

Posas, F., Camps, M. & Arino, J., 1995. The PPZ protein phosphatases are important determinants of salt tolerance in yeast cells. *Journal of Biological Chemistry*, 270(0021-9258; 22), pp.13036–13041.

Posas, F., Casamayor, A. & Arino, J., 1993. The PPZ protein phosphatases are involved in the maintenance of osmotic stability of yeast cells. *FEBS letters*, 318(0014-5793; 3), pp.282–286.

Pratt, J.R. et al., 2004. Effects of methylphosphonate, a phosphate analogue, on the expression and degradation of the high-affinity phosphate transporter Pho84, in Saccharomyces cerevisiae. *Biochemistry*, 43(45), pp.14444–14453.

Pribylová, L. et al., 2006. Exploration of yeast alkali metal cation/H+ antiporters: sequence and structure comparison. *Folia microbiologica*, 51(5), pp.413–24.

Prior, C. et al., 1996. Characterization of the NHA1 gene encoding a Na+/H+-antiporter of the yeast Saccharomyces cerevisiae. *FEBS letters*, 387(0014-5793; 1), pp.89–93.

Proft, M. et al., 2001. Regulation of the Sko1 transcriptional repressor by the Hog1 MAP kinase in response to osmotic stress. *The EMBO journal*, 20(5), pp.1123–33.

Proft, M. & Struhl, K., 2004. MAP kinase-mediated stress relief that precedes and regulates the timing of transcriptional induction. *Cell*, 118(3), pp.351–61.

Qiu, Q.-S. & Fratti, R.A., 2010. The Na+/H+ exchanger Nhx1p regulates the initiation of Saccharomyces cerevisiae vacuole fusion. *Journal of cell science*, 123(Pt 19), pp.3266–75.

Ramos, J. et al., 1994. TRK2 is not a low-affinity potassium transporter in Saccharomyces cerevisiae. *Journal of Bacteriology*, 176(0021-9193; 1), pp.249–252.

Ramos, J., Ariño, J. & Sychrová, H., 2011. Alkali-metal-cation influx and efflux systems in nonconventional yeast species. *FEMS microbiology letters*, 317(1), pp.1–8.

Ramos, J., Contreras, P. & Rodríguez-Navarro, A., 1985. A potassium transport mutant of Saccharomyces cerevisiae. *Archives of Microbiology*, 143(1), pp.88–93.

Ramos, J., Haro, R. & Rodríguez-Navarro, A., 1990. Regulation of potassium fluxes in Saccharomyces cerevisiae. *Biochimica et biophysica acta*, 1029(2), pp.211–7.

Reddy, V.S., Singh, A.K. & Rajasekharan, R., 2008. The Saccharomyces cerevisiae PHM8 gene encodes a soluble magnesium-dependent lysophosphatidic acid phosphatase. *The Journal of biological chemistry*, 283(14), pp.8846–54.

Reid, J.D. et al., 1996. The S. cerevisiae outwardly-rectifying potassium channel (DUK1) identifies a new family of channels with duplicated pore domains. *Receptors & channels*, 4(1), pp.51–62.

Reisser, C. et al., 2013. Genetic Basis of Ammonium Toxicity Resistance in a Sake Strain of Yeast: A Mendelian Case. *G3 (Bethesda, Md.)*.

Rios, G., Ferrando, A. & Serrano, R., 1997. Mechanisms of salt tolerance conferred by overexpression of the HAL1 gene in Saccharomyces cerevisiae. *Yeast (Chichester, England)*, 13(6), pp.515–28.

Rivetta, A., Kuroda, T. & Slayman, C., 2011. Anion currents in yeast K + transporters (TRK) characterize a structural homologue of ligand-gated ion channels. *Pflugers Archiv European Journal of Physiology*, 462(2), pp.315–330.

Rivetta, A., Slayman, C. & Kuroda, T., 2005. Quantitative modeling of chloride conductance in yeast TRK potassium transporters. *Biophysical journal*, 89(4), pp.2412–26.

Roberts, S.K. et al., 1999. Divalent cation block of inward currents and low-affinity K+ uptake in Saccharomyces cerevisiae. *Journal of bacteriology*, 181(1), pp.291–7.

Rodríguez-Navarro, A., 2000. Potassium transport in fungi and plants. *Biochimica et biophysica acta*, 1469(1), pp.1–30.

Rodríguez-Navarro, A., Quintero, F.J. & Garciadeblás, B., 1994. Na(+)-ATPases and Na+/H+ antiporters in fungi. *Biochimica et biophysica acta*, 1187(2), pp.203–5.

Rodríguez-Navarro, A. & Ramos, J., 1984. Dual system for potassium transport in Saccharomyces cerevisiae. *Journal of bacteriology*, 159(3), pp.940–5.

Roman, H., 1981. Development of Yeast as an Experimental Organism. *Cold Spring Harbor Monograph Archive*, 11A(0).

Roomans, G.M., Blasco, F. & Borst-Pauwels, G.W., 1977. Cotransport of phosphate and sodium by yeast. *Biochimica et biophysica acta*, 467(1), pp.65–71.

Rosenfeld, L. et al., 2010. The effect of phosphate accumulation on metal ion homeostasis in Saccharomyces cerevisiae. *Journal of biological inorganic chemistry*, 15(7), pp.1051–62.

Rouillon, A., Surdin-Kerjan, Y. & Thomas, D., 1999. Transport of sulfonium compounds. Characterization of the s-adenosylmethionine and s-methylmethionine permeases from the yeast Saccharomyces cerevisiae. *The Journal of biological chemistry*, 274(40), pp.28096–105.

Rudolph, H.K. et al., 1989. The yeast secretory pathway is perturbed by mutations in PMR1, a member of a Ca2+ ATPase family. *Cell*, 58(1), pp.133–45.

Ruiz, A. et al., 2004. Functional characterization of the Saccharomyces cerevisiae VHS3 gene: A regulatory subunit of the Ppz1 protein phosphatase with novel, phosphatase-unrelated functions. *Journal of Biological Chemistry*, 279(33), pp.34421–34430.

Ruiz, A. et al., 2009. Moonlighting proteins Hal3 and Vhs3 form a heteromeric PPCDC with Ykl088w in yeast CoA biosynthesis. *Nature chemical biology*, 5(12), pp.920–8.

Ruiz, A. et al., 2006. Role of protein phosphatases 2C on tolerance to lithium toxicity in the yeast Saccharomyces cerevisiae. *Molecular microbiology*, 62(0950-382; 1), pp.263–277.

Ruiz, A. & Ariño, J., 2007. Function and regulation of the Saccharomyces cerevisiae ENA sodium ATPase system. *Eukaryotic cell*, 6(12), pp.2175–83.

Ruiz, A., Serrano, R. & Ariño, J., 2008. Direct regulation of genes involved in glucose utilization by the calcium/calcineurin pathway. *The Journal of biological chemistry*, 283(20), pp.13923–33.

Ruiz, A., Yenush, L. & Arino, J., 2003. Regulation of ENA1 Na(+)-ATPase gene expression by the Ppz1 protein phosphatase is mediated by the calcineurin pathway. *Eukaryot.Cell*, 2(1535-9778; 5), pp.937–948.

Ruiz-Roig, C. et al., 2012. The Hog1 SAPK controls the Rtg1/Rtg3 transcriptional complex activity by multiple regulatory mechanisms. *Molecular biology of the cell*, 23(21), pp.4286–96.

Safrany, S.T. et al., 1999. The diadenosine hexaphosphate hydrolases from Schizosaccharomyces pombe and Saccharomyces cerevisiae are homologues of the human diphosphoinositol polyphosphate. Overlapping substrate specificities in a Mutt-type protein phosphohydrolase. *Journal of Biological Chemistry*, 274(31), pp.21735–21740.

Saiardi, A. et al., 2000. The inositol hexakisphosphate kinase family. Catalytic flexibility and function in yeast vacuole biogenesis. *The Journal of biological chemistry*, 275(32), pp.24686–92.

Saito, H. & Posas, F., 2012. Response to hyperosmotic stress. *Genetics*, 192(2), pp.289–318.

Saito, K. et al., 2005. Direct labeling of polyphosphate at the ultrastructural level in Saccharomyces cerevisiae by using the affinity of the polyphosphate binding domain of Escherichia coli exopolyphosphatase. *Applied and environmental microbiology*, 71(10), pp.5692–701.

Salaün, C., Rodrigues, P. & Heard, J.M., 2001. Transmembrane topology of PiT-2, a phosphate transporter-retrovirus receptor. *Journal of virology*, 75(12), pp.5584–92.

Saldanha, A.J., Brauer, M.J. & Botstein, D., 2004. Nutritional homeostasis in batch and steady-state culture of yeast. *Molecular biology of the cell*, 15(9), pp.4089–104.

Samyn, D.R. et al., 2012. Mutational analysis of putative phosphate- and proton-binding sites in the Saccharomyces cerevisiae Pho84 phosphate:H(+) transceptor and its effect on signalling to the PKA and PHO pathways. *The Biochemical journal*, 445(3), pp.413–22.

Sanz, P., 2003. Snf1 protein kinase: a key player in the response to cellular stress in yeast. *Biochemical Society transactions*, 31(Pt 1), pp.178–81.

Schlesser, A. et al., 1988. A second transport ATPase gene in Saccharomyces cerevisiae. *The Journal of biological chemistry*, 263(36), pp.19480–7.

Schmidt, G., Hecht, L. & Thannhauser, S.J., 1949. The effect of potassium ions on the absorption of orthophosphate and the formation of metaphosphate by bakers' yeast. *The Journal of biological chemistry*, 178(2), pp.733–42.

Schneider, K.R., Smith, R.L. & O'Shea, E.K., 1994. Phosphate-regulated inactivation of the kinase PHO80-PHO85 by the CDK inhibitor PHO81. *Science (New York, N.Y.)*, 266(5182), pp.122–6.

Schuddemat, J. et al., 1989. Polyphosphate synthesis in yeast. *Biochimica et biophysica acta*, 1010(2), pp.191–8.

Ter Schure, E.G. et al., 1995. The concentration of ammonia regulates nitrogen metabolism in Saccharomyces cerevisiae. *Journal of bacteriology*, 177(22), pp.6672–5.

Ter Schure, E.G., van Riel, N.A. & Verrips, C.T., 2000. The role of ammonia metabolism in nitrogen catabolite repression in Saccharomyces cerevisiae. *FEMS microbiology reviews*, 24(1), pp.67–83.

Schwob, E. & Nasmyth, K., 1993. CLB5 and CLB6, a new pair of B cyclins involved in DNA replication in Saccharomyces cerevisiae. *Genes & development*, 7(7A), pp.1160–75.

Secco, D., Wang, C., Shou, H., et al., 2012. Phosphate homeostasis in the yeast Saccharomyces cerevisiae, the key role of the SPX domain-containing proteins. *FEBS letters*, 586(4), pp.289–95.

Secco, D., Wang, C., Arpat, B.A., et al., 2012. The emerging importance of the SPX domain-containing proteins in phosphate homeostasis. *The New phytologist*, 193(4), pp.842–51.

Sekito, T. et al., 2008. Novel families of vacuolar amino acid transporters. *IUBMB life*, 60(8), pp.519–25.

Sekito, T. et al., 2002. RTG-dependent mitochondria-to-nucleus signaling is regulated by MKS1 and is linked to formation of yeast prion [URE3]. *Molecular biology of the cell*, 13(3), pp.795–804.

Sekito, T., Thornton, J. & Butow, R.A., 2000. Mitochondria-to-nuclear signaling is regulated by the subcellular localization of the transcription factors Rtg1p and Rtg3p. *Molecular biology of the cell*, 11(6), pp.2103–15.

Serra-Cardona, A. et al., 2014. Co-regulated expression of Na+/phosphate Pho89 transporter and Ena1 Na+-ATPase allows their functional coupling under high pH stress. *Molecular and cellular biology*, 34(24), pp.4420–35.

Serrano, R. et al., 1999. A glimpse of the mechanisms of ion homeostasis during salt stress. *Journal of Experimental Botany*, 50(Special), pp.1023–1036.

Serrano, R., 1983. In vivo glucose activation of the yeast plasma membrane ATPase. *FEBS letters*, 156(1), pp.11–4.

Serrano, R. et al., 2002. The transcriptional response to alkaline pH in Saccharomyces cerevisiae: evidence for calcium-mediated signalling. *Molecular microbiology*, 46(5), pp.1319–33.

Serrano, R., Kielland-Brandt, M.C. & Fink, G.R., 1986. Yeast plasma membrane ATPase is essential for growth and has homology with (Na+ + K+), K+- and Ca2+-ATPases. *Nature*, 319(0028-0836; 6055), pp.689–693.

Sethuraman, A., Rao, N.N. & Kornberg, A., 2001. The endopolyphosphatase gene: essential in Saccharomyces cerevisiae. *Proceedings of the National Academy of Sciences of the United States of America*, 98(15), pp.8542–7.

Seto-Young, D. & Perlin, D.S., 1991. Effect of membrane voltage on the plasma membrane H(+)-ATPase of Saccharomyces cerevisiae. *The Journal of biological chemistry*, 266(3), pp.1383–9.

Shemer, R. et al., 2002. Regulation of the transcription factor Gcn4 by Pho85 cyclin PCL5. *Molecular and cellular biology*, 22(15), pp.5395–404.

Shen, M.W.Y. et al., 2012. Enhanced arsenate uptake in Saccharomyces cerevisiae overexpressing the Pho84 phosphate transporter. *Biotechnology progress*, 28(3), pp.654–61.

Sherman, F., 2002. Getting started with yeast. In *Methods in enzymology*. pp. 3–41.

Shi, X. & Kornberg, A., 2005. Endopolyphosphatase in Saccharomyces cerevisiae undergoes post-translational activations to produce short-chain polyphosphates. *FEBS letters*, 579(9), pp.2014–8.

Shimizu, T. et al., 1997. Crystal structure of PHO4 bHLH domain-DNA complex: Flanking base recognition. *EMBO Journal*, 16(15), pp.4689–4697.

Simón, E. et al., 2001. A screening for high copy suppressors of the sit4 hal3 synthetically lethal phenotype reveals a role for the yeast Nha1 antiporter in cell cycle regulation. *The Journal of biological chemistry*, 276(32), pp.29740–7.

Simón, E., Barceló, A. & Ariño, J., 2003. Mutagenesis analysis of the yeast Nha1 Na+/H+ antiporter carboxy-terminal tail reveals residues required for function in cell cycle. *FEBS letters*, 545(2-3), pp.239–45.

Siniossoglou, S., Hurt, E.C. & Pelham, H.R., 2000. Psr1p/Psr2p, two plasma membrane phosphatases with an essential DXDX(T/V) motif required for sodium stress response in yeast. *The Journal of biological chemistry*, 275(25), pp.19352–60.

Smardon, A.M., Tarsio, M. & Kane, P.M., 2002. The RAVE complex is essential for stable assembly of the yeast V-ATPase. *The Journal of biological chemistry*, 277(16), pp.13831–9.

Smets, B. et al., 2010. Life in the midst of scarcity: adaptations to nutrient availability in Saccharomyces cerevisiae. *Current genetics*, 56(1), pp.1–32.

Smith, S.A. et al., 2006. Polyphosphate modulates blood coagulation and fibrinolysis. *Proceedings of the National Academy of Sciences of the United States of America*, 103(4), pp.903–8.

Sopko, R. et al., 2006. Mapping pathways and phenotypes by systematic gene overexpression. *Molecular cell*, 21(3), pp.319–30.

Springer, M. et al., 2003. Partially phosphorylated Pho4 activates transcription of a subset of phosphate-responsive genes. *PLoS Biology*, 1(2), p.E28.

Stadtman, E.R. & Levine, R.L., 2003. Free radical-mediated oxidation of free amino acids and amino acid residues in proteins. *Amino acids*, 25(3-4), pp.207–18.

Stefan, C.P. & Cunningham, K.W., 2013. Kch1 family proteins mediate essential responses to endoplasmic reticulum stresses in the yeasts Saccharomyces cerevisiae and Candida albicans. *The Journal of biological chemistry*, 288(48), pp.34861–70.

Steger, D.J. et al., 2003. Regulation of chromatin remodeling by inositol polyphosphates. *Science (New York, N.Y.)*, 299(5603), pp.114–6.

Stuart, D. & Wittenberg, C., 1995. CLN3, not positive feedback, determines the timing of CLN2 transcription in cycling cells. *Genes & development*, 9(22), pp.2780–94.

Sudarsanam, P. et al., 2000. Whole-genome expression analysis of snf/swi mutants of Saccharomyces cerevisiae. *Proceedings of the National Academy of Sciences of the United States of America*, 97(7), pp.3364–3369.

Supply, P., Wach, A. & Goffeau, A., 1993. Enzymatic properties of the PMA2 plasma membrane-bound H(+)-ATPase of Saccharomyces cerevisiae. *The Journal of biological chemistry*, 268(26), pp.19753–9.

Swaney, D.L. et al., 2013. Global analysis of phosphorylation and ubiquitylation cross-talk in protein degradation. *Nature Methods*, 10(7), pp.676–682.

Sychrová, H., Ramírez, J. & Peña, A., 1999. Involvement of Nha1 antiporter in regulation of intracellular pH in Saccharomyces cerevisiae. *FEMS microbiology letters*, 171(2), pp.167–72.

Tamás, M.J. et al., 1999. Fps1p controls the accumulation and release of the compatible solute glycerol in yeast osmoregulation. *Molecular microbiology*, 31(4), pp.1087–104.

Tate, J.J. & Cooper, T.G., 2007. Stress-responsive Gln3 localization in Saccharomyces cerevisiae is separable from and can overwhelm nitrogen source regulation. *The Journal of biological chemistry*, 282(25), pp.18467–80.

Tate, J.J. & Cooper, T.G., 2003. Tor1/2 regulation of retrograde gene expression in Saccharomyces cerevisiae derives indirectly as a consequence of alterations in ammonia metabolism. *The Journal of biological chemistry*, 278(38), pp.36924–33.

Temple, M.D., Perrone, G.G. & Dawes, I.W., 2005. Complex cellular responses to reactive oxygen species. *Trends in Cell Biology*, 15(6), pp.319–326.

Tessier, W.D. et al., 1998. Identification and disruption of the gene encoding the K+-activated acetaldehyde dehydrogenase of Saccharomyces cerevisiae. *FEMS Microbiology Letters*, 164(1), pp.29–34.

Thayer, N.H. et al., 2014. Identification of long-lived proteins retained in cells undergoing repeated asymmetric divisions. *Proceedings of the National Academy of Sciences of the United States of America*, 111(39), pp.14019–26.

Thevelein, J.M. & de Winde, J.H., 1999. Novel sensing mechanisms and targets for the cAMP-protein kinase A pathway in the yeast Saccharomyces cerevisiae. *Molecular microbiology*, 33(5), pp.904–18.

Thomas, D., Becker, A. & Surdin-Kerjan, Y., 2000. Reverse methionine biosynthesis from S-adenosylmethionine in eukaryotic cells. *The Journal of biological chemistry*, 275(52), pp.40718–24.

Thomas, D. & Surdin-Kerjan, Y., 1997. Metabolism of sulfur amino acids in Saccharomyces cerevisiae. *Microbiology and Molecular Biology Reviews: MMBR*, 61(4), pp.503–532.

Thomas, M.R. & O'Shea, E.K., 2005. An intracellular phosphate buffer filters transient fluctuations in extracellular phosphate levels. *Proceedings of the National Academy of Sciences of the United States of America*, 102(27), pp.9565–70.

Toh-e, A. et al., 1988. PHO85, a negative regulator of the PHO system, is a homolog of the protein kinase gene, CDC28, of Saccharomyces cerevisiae. *Molecular & general genetics : MGG*, 214(1), pp.162–4.

Toh-e, A. & Kakimoto, S., 1975. Genes coding for the structure of the acid phosphatases in Saccharomyces cerevisiae. *Molecular & general genetics : MGG*, 143(1), pp.65–70.

Tomar, N. et al., 2013. An integrated pathway system modeling of Saccharomyces cerevisiae HOG pathway: a Petri net based approach. *Molecular biology reports*, 40(2), pp.1103–25.

Tomar, P. & Sinha, H., 2014. Conservation of PHO pathway in ascomycetes and the role of Pho84. *Journal of biosciences*, 39(3), pp.525–36.

Trópia, M.J.M. et al., 2006. Calcium signaling and sugar-induced activation of plasma membrane H(+)-ATPase in Saccharomyces cerevisiae cells. *Biochemical and biophysical research communications*, 343(4), pp.1234–43.

Trotter, E.W. & Grant, C.M., 2003. Non-reciprocal regulation of the redox state of the glutathione-glutaredoxin and thioredoxin systems. *EMBO Reports*, 4(2), pp.184–188.

Tsutsumi, K., Munekata, M. & Shiba, T., 2000. Involvement of inorganic polyphosphate in expression of SOS genes. *Biochimica et biophysica acta*, 1493(1-2), pp.73–81.

Tu, W.-Y. et al., 2011. Rpl12p affects the transcription of the PHO pathway high-affinity inorganic phosphate transporters and repressible phosphatases. *Yeast (Chichester, England)*, 28(6), pp.481–93.

Tyers, M. et al., 1992. The Cln3-Cdc28 kinase complex of S. cerevisiae is regulated by proteolysis and phosphorylation. *The EMBO journal*, 11(5), pp.1773–84.

Tyson, J.J., Csikasz-Nagy, A. & Novak, B., 2002. The dynamics of cell cycle regulation. *BioEssays : news and reviews in molecular, cellular and developmental biology*, 24(12), pp.1095–109.

Ueda, Y. et al., 1975. Isolation and characterization of recessive, constitutive mutations for repressible acid phosphatase synthesis in Saccharomyces cerevisiae. *Journal of Bacteriology*, 122(3), pp.911–922.

Uhler, J.P., Hertel, C. & Svejstrup, J.Q., 2007. A role for noncoding transcription in activation of the yeast PHO5 gene. *Proceedings of the National Academy of Sciences of the United States of America*, 104(19), pp.8011–8016.

Urech, K. et al., 1978. Localization of polyphosphate in vacuoles of Saccharomyces cerevisiae. *Archives of microbiology*, 116(3), pp.275–8.

Uttenweiler, A. et al., 2007. The vacuolar transporter chaperone (VTC) complex is required for microautophagy. *Molecular biology of the cell*, 18(1), pp.166–75.

Vardi, N. et al., 2013. Budding yeast escape commitment to the phosphate starvation program using gene expression noise. *Current biology : CB*, 23(20), pp.2051–7.

Vargas, R.C. et al., 2007. Saccharomyces cerevisiae multidrug resistance transporter Qdr2 is implicated in potassium uptake, providing a physiological advantage to quinidine-stressed cells. *Eukaryotic cell*, 6(2), pp.134–42.

Vergani, P. et al., 1997. Extracellular K+ and Ba2+ mediate voltage-dependent inactivation of the outward-rectifying K+ channel encoded by the yeast gene TOK1. *FEBS letters*, 405(3), pp.337–44.

Vidal, M. et al., 1990. Direct selection for mutants with increased K+ transport in Saccharomyces cerevisiae. *Genetics*, 125(2), pp.313–20.

Vidal, M. et al., 1995. Identification of essential nucleotides in an upstream repressing sequence of Saccharomyces cerevisiae by selection for increased expression of TRK2. *Proceedings of the National Academy of Sciences of the United States of America*, 92(6), pp.2370–4.

Vidal, M. et al., 1991. RPD1 (SIN3/UME4) is required for maximal activation and repression of diverse yeast genes. *Molecular and cellular biology*, 11(12), pp.6306–16.

Vidal, M. & Gaber, R.F., 1991. RPD3 encodes a second factor required to achieve maximum positive and negative transcriptional states in Saccharomyces cerevisiae. *Molecular and cellular biology*, 11(12), pp.6317–27.

Vido, K. et al., 2001. A proteome analysis of the cadmium response in Saccharomyces cerevisiae. *The Journal of biological chemistry*, 276(11), pp.8469–74.

Vieira-Pires, R.S., Szollosi, A. & Morais-Cabral, J.H., 2013. The structure of the KtrAB potassium transporter. *Nature*, 496(7445), pp.323–8.

Viladevall, L. et al., 2004. Characterization of the calcium-mediated response to alkaline stress in Saccharomyces cerevisiae. *The Journal of biological chemistry*, 279(42), pp.43614–24.

Vyas, V.K., Kuchin, S. & Carlson, M., 2001. Interaction of the repressors Nrg1 and Nrg2 with the Snf1 protein kinase in Saccharomyces cerevisiae 1. *Genetics*, 158(0016-6731; 2), pp.563–572.

Wang, L. et al., 2003. Inorganic polyphosphate stimulates mammalian TOR, a kinase involved in the proliferation of mammary cancer cells. *Proceedings of the National Academy of Sciences of the United States of America*, 100(20), pp.11249–54.

Wanke, V. et al., 2005. Regulation of G0 entry by the Pho80-Pho85 cyclin-CDK complex. *The EMBO journal*, 24(0261-4189; 24), pp.4271–4278.

Wells, K.M. & Rao, R., 2001. The yeast Na+/H+ exchanger Nhx1 is an N-linked glycoprotein. Topological implications. *The Journal of biological chemistry*, 276(5), pp.3401–7.

Werner, T.P., Amrhein, N. & Freimoser, F.M., 2005. Novel method for the quantification of inorganic polyphosphate (iPoP) in Saccharomyces cerevisiae shows dependence of iPoP content on the growth phase. *Archives of microbiology*, 184(2), pp.129–36.

Wieland, J. et al., 1995. The PMR2 gene cluster encodes functionally distinct isoforms of a putative Na+ pump in the yeast plasma membrane. *The EMBO journal*, 14(16), pp.3870–82.

Wittenberg, C., 2005. Cell cycle: cyclin guides the way. *Nature*, 434(7029), pp.34–5.

Wolf, F.I. & Trapani, V., 2008. Cell (patho)physiology of magnesium. *Clinical science (London, England : 1979)*, 114(1), pp.27–35.

Wood, H.G. & Clark, J.E., 1988. Biological aspects of inorganic polyphosphates. *Annual review of biochemistry*, 57, pp.235–60.

Worley, J., Luo, X. & Capaldi, A.P., 2013. Inositol pyrophosphates regulate cell growth and the environmental stress response by activating the HDAC Rpd3L. *Cell reports*, 3(5), pp.1476–82.

Wright, M.B. et al., 1997. Potassium transport by amino acid permeases in Saccharomyces cerevisiae. *The Journal of biological chemistry*, 272(21), pp.13647–52.

Wu, W.H. & Hampsey, M., 1999. An activation-specific role for transcription factor TFIIB in vivo. *Proceedings of the National Academy of Sciences of the United States of America*, 96(6), pp.2764–2769.

Wurst, H. & Kornberg, A., 1994. A soluble exopolyphosphatase of Saccharomyces cerevisiae. Purification and characterization. *The Journal of biological chemistry*, 269(15), pp.10996–1001.

Wurst, H., Shiba, T. & Kornberg, A., 1995. The gene for a major exopolyphosphatase of Saccharomyces cerevisiae. *Journal of bacteriology*, 177(4), pp.898–906.

Wykoff, D.D. et al., 2007. Positive feedback regulates switching of phosphate transporters in S. cerevisiae. *Molecular cell*, 27(6), pp.1005–13.

Wykoff, D.D. & O'Shea, E.K., 2001. Phosphate transport and sensing in Saccharomyces cerevisiae. *Genetics*, 159(4), pp.1491–9.

Yenush, L. et al., 2005. pH-Responsive, posttranslational regulation of the Trk1 potassium transporter by the type 1-related Ppz1 phosphatase. *Molecular and cellular biology*, 25(19), pp.8683–92.

Yenush, L. et al., 2002. The Ppz protein phosphatases are key regulators of K+ and pH homeostasis: implications for salt tolerance, cell wall integrity and cell cycle progression. *The EMBO journal*, 21(5), pp.920–9.

Yoko-o, T. et al., 1993. The putative phosphoinositide-specific phospholipase C gene, PLC1, of the yeast Saccharomyces cerevisiae is important for cell growth. *Proceedings of the National Academy of Sciences of the United States of America*, 90(5), pp.1804–1808.

Yompakdee, C. et al., 1996. A putative membrane protein, Pho88p, involved in inorganic phosphate transport in Saccharomyces cerevisiae. *Molecular & general genetics : MGG*, 251(5), pp.580–90.

York, J.D., 2006. Regulation of nuclear processes by inositol polyphosphates. *Biochimica et Biophysica Acta - Molecular and Cell Biology of Lipids*, 1761(5-6), pp.552–559.

Zahrádka, J., van Heusden, G.P.H. & Sychrová, H., 2012. Yeast 14-3-3 proteins participate in the regulation of cell cation homeostasis via interaction with Nha1 alkali-metal-cation/proton antiporter. *Biochimica et biophysica acta*, 1820(7), pp.849–58.

Zahrádka, J. & Sychrová, H., 2012. Plasma-membrane hyperpolarization diminishes the cation efflux via Nha1 antiporter and Ena ATPase under potassium-limiting conditions. *FEMS yeast research*, 12(4), pp.439–46.

Zaman, S. et al., 2008. How Saccharomyces responds to nutrients. *Annual review of genetics*, 42(0066-4197), pp.27–81.

Zayats, V. et al., 2015. A refined atomic scale model of the Saccharomyces cerevisiae K+-translocation protein Trk1p combined with experimental evidence confirms the role of selectivity filter glycines and other key residues. *Biochimica et Biophysica Acta (BBA) - Biomembranes*, 1848(5), pp.1183–1195.

Zhang, T., Caffrey, J.J. & Shears, S.B., 2001. The transcriptional regulator, Arg82, is a hybrid kinase with both monophosphoinositol and diphosphoinositol polyphosphate synthase activity. *FEBS Letters*, 494(3), pp.208–212.

Zhou, X. & O'Shea, E.K., 2011. Integrated approaches reveal determinants of genome-wide binding and function of the transcription factor Pho4. *Molecular cell*, 42(6), pp.826–36.

Zhou, X.L. et al., 1995. YKC1 encodes the depolarization-activated K+ channel in the plasma membrane of yeast. *FEBS letters*, 373(2), pp.170–6.

Zotova, L. et al., 2010. Novel components of an active mitochondrial K(+)/H(+) exchange. *The Journal of biological chemistry*, 285(19), pp.14399–414.

Zvyagilskaya, R.A. et al., 2008. Characterization of the Pho89 phosphate transporter by functional hyperexpression in Saccharomyces cerevisiae. *FEMS yeast research*, 8(5), pp.685–96.

Publication one

The short-term response of yeast to potassium starvation

Lina Barreto, **David Canadell,** Daniel Valverde-Saubí, Antonio Casamayor and Joaquín Ariño

Environmental Microbiology (2012) **14**(11), 3026-3042

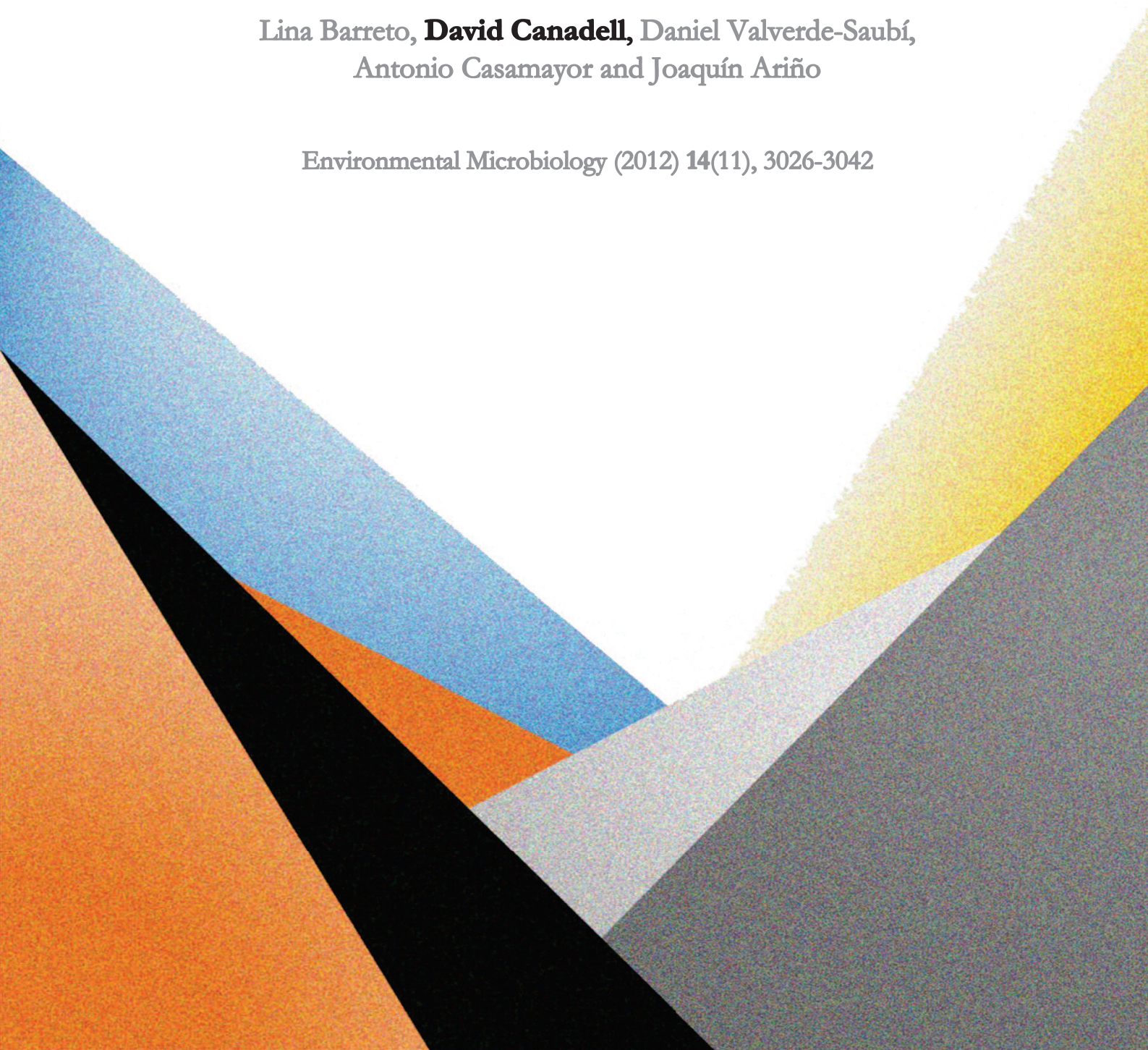

environmental microbiology

Environmental Microbiology (2012) **14**(11), 3026–3042 doi:10.1111/j.1462-2920.2012.02887.x

The short-term response of yeast to potassium starvation

Lina Barreto, David Canadell, Daniel Valverde-Saubí,† Antonio Casamayor and Joaquín Ariño*

Institut de Biotecnologia i Biomedicina and Departament de Bioquímica i Biologia Molecular, Universitat Autónoma de Barcelona, Bellaterra 08193, Barcelona, Spain.

Summary

Potassium is the major intracellular cation in most living cells, including yeasts. Although K^+ has been demonstrated to be necessary for diverse cellular functions, such as enzyme activation, additional, still uncharacterized cellular targets may exist. We show here that in *Saccharomyces cerevisiae* short-term potassium deprivation impacts in the mRNA level of over one thousand genes. Lack of potassium drastically alters sulfur metabolism (mainly Met and Cys metabolism), triggers an oxidative stress response and activates the retrograde pathway, possibly due to the ammonium accumulation that occurs through the Trk1 potassium transporter. We also observe a remarkable halt in the expression of genes required for ribosome biogenesis and translation, a decrease in expression of diverse components (cyclins, protein kinases) required for progression through the cell cycle and a blockage in septins assembly. Only specific subsets of these changes were observed in a strain deleted for the *TRK1* and *TRK2* genes growing in the presence of sufficient potassium (50 mM). Therefore, a shortage of potassium in the environment triggers an acute transcriptional response, which covers different aspects of the cell biology so far unexplored, and whose investigation will likely reveal novel functional roles for this cation.

Introduction

Potassium is an essential component of living cells, which tend to maintain intracellular concentrations of this cation much higher than those normally occurring in their natural habitats. Under standard growth conditions, the intracellular concentration of potassium in the model yeast *Saccharomyces cerevisiae* ranges from 200 to 300 mM. However, *S. cerevisiae* cells are able to grow even in the presence of very low potassium concentrations (< 1 mM). The ability to maintain such steep gradient is based in two key components: (i) the generation of a proton-motive force across membranes by the proton ATPase Pma1, which catalyses the energy-consuming pumping of protons to the environment, and (ii) the existence of plasma-membrane high-affinity potassium transporters, which allow influx of positively charged potassium ions across the membrane driven by the electrochemical gradient generated by Pma1 (see Rodriguez-Navarro, 2000; Arino *et al.*, 2010 for reviews). In *S. cerevisiae*, such high-affinity potassium transport exhibits a K_m of ~ 25–50 μM and a V_{max} of ~ 30 nmol (mg cells)$^{-1}$ min^{-1}, and is mediated by two plasma membrane proteins, Trk1 and Trk2 (Gaber *et al.*, 1988; Ko *et al.*, 1990; Ko and Gaber, 1991). Trk1 is the most physiologically relevant transporter, and mutation of *TRK1* alone substantially impairs high-affinity potassium uptake. Cells lacking both *TRK1* and *TRK2* display a dramatic decrease in affinity for potassium transport (K_m of ~ 20 mM) and lower V_{max} [~ 5 nmol (mg cells)$^{-1}$ min^{-1}] and, consequently, can only grow when the medium contain relatively high amounts of potassium (> 5 mM).

The requirement for high concentrations of intracellular potassium has been attributed to many diverse functions of this cation. For instance, potassium seems pivotal for regulation of cell volume and intracellular pH (Merchan *et al.*, 2004), maintenance of stable potential across the plasma membrane and compensation of negative charges in many macromolecules. In addition, the cation has been reported for many years to be required for protein synthesis (Lubin and Ennis, 1964) and activation of diverse enzymes (see Page and Di Cera, 2006). Although the molecular basis for absolute K^+ requirements have been elucidate in several cases, as for pyruvate kinase, the first enzyme to be identified to require K^+ for optimal catalytic activity (Jurica *et al.*, 1998), there is no evidence that all relevant functional potassium targets have been already identified. For instance, only a few years ago Hess and colleagues (2006) carried out an

Received 2 March, 2012; revised 5 June, 2012; accepted 23 August, 2012. *For correspondence. E-mail Joaquin.Arino@uab.es; Tel. (+34) 93 5812182; Fax (+34) 93 5812011. †Present address: Institute for Research in Biomedicine, Barcelona, Spain.

interesting study of the effects of potassium limitation by means of transcriptomic profiling of yeast steady-state cultures growing under chemostat conditions. Surprisingly, these authors observed only a modest number of genes that changed expression at limiting potassium, although their study revealed that, when external potassium is low, extracellular ammonium becomes toxic and impairs growth. Entry of ammonium was proposed to occur by leakage through the potassium transport systems and to be counteracted by integration of ammonium into amino acids and excretion of such compounds (Hess *et al*., 2006).

To gain further insight into the possible cellular functions requiring potassium, we choose a complementary approach to that used by Hess and co-workers, and investigated the short term effects on gene expression profile derived from the sudden depletion of potassium in the environment. To this end, we used a recently developed YNB-based growth medium (Translucent K^+-free medium), whose composition is similar to the standard growth media, but contains only traces of potassium and ammonium as nitrogen source (Navarrete *et al*., 2010). Our time-course approach has revealed a massive alteration in the expression profile (about one-third of the genome) shortly after potassium is removed from the medium. Analysis of the data indicates that lack of potassium drastically alters sulfur metabolism, triggers an oxidative stress response and activates the mitochondrial retrograde pathway. We also observe a dramatic halt in the expression of genes required for ribosome biogenesis and translation, as well as a decrease in expression of genes required for progression through the cell cycle. Interestingly, the expression of specific subsets of these genes is still altered in *trk1 trk2* cells grown in the presence of sufficient potassium.

Results

The short-term transcriptional response to potassium starvation

Transfer of wild-type *S. cerevisiae* cells to K^+-free medium results in a strong short-term transcriptional response. From 4862 genes with valid data for at least four time points (10–120 min), 828 genes were induced at least at one time point (Table S2). This response was consistent, since among these genes only 13 were repressed at a given time point). While a significant number of genes (80) displayed an early response, being induced at short times (10–20 min, see below), most genes (564) were induced only later after transfer to K^+-free medium (60–120 min, see Fig. 1). The highest number of induced genes was observed after 120 min of shift (see Table 1), although when the peak of the response was calculated, most genes (405 genes) showed a maximum change at 60 min. Similarly, 926 genes were repressed at least at one time point upon depletion of potassium from the medium. Only 59 (6.3%) were repressed already at the early stages (10–20 min), whereas the majority of repressed genes can be considered late genes (60–120 min). In this case, the maximum number of repressed genes was observed at the 60 min time point (Table 1 and Fig. 1).

Gene Ontology analysis of the genes induced by lack of potassium reveals an excess of genes related to metabolism of Methionine and its derivatives ($P < 1.2 \times 10^{-9}$) and, in general, of sulfur metabolism ($P < 1.2 \times 10^{-5}$), suggesting that potassium starvation disturbs metabolism of sulfur-containing amino acids. As it can be observed in Figs 1 and 2, the entire pathway for sulfur assimilation, and Met uptake and biosynthesis is potently induced even at short times. This effect was confirmed by cloning the promoters of several of these genes as translational fusions with the LacZ gene, encoding β-galactosidase, and monitoring the responses of the reporters after shifting cells to K^+-free medium (see Fig. S1A). Investigation of the intracellular levels of Met and Cys showed an almost immediate depletion of these amino acids in cells transferred to K^+-free medium (Fig. 2C). Interestingly, the induction of genes related to sulfur assimilation and Met uptake and biosynthesis after shifting cells to K^+-free medium is specifically attenuated when the amount of Methionine is augmented in the medium (Fig. S1B). We also considered the possibility that the dramatic effect on sulfur metabolism-related genes could be conditioned by the fact that the strain used (BY4741) carries a deletion of the *MET17* gene, which blocks incorporation of sulfate into homocysteine and, hence, results in auxotrophy for Methionine. However, analysis of the indicated reporters in *MET17* strains confirmed that these promoters are still activated, albeit to lesser extent, in response to lack of potassium (Fig. S2). Similarly, genes encoding proteins required for phosphate uptake and utilization, such as *PHO84*, *PHO11*, *PHO12* and *PHO8*, were also induced ($P < 6.4 \times 10^{-5}$). In parallel, we observed increased mRNA levels for a large number of genes related to the general stress response ($P < 1.4 \times 10^{-17}$) and, specifically, to the response to oxidative stress ($P < 1.2 \times 10^{-7}$). However, we have observed that a reporter strain carrying an integrated STRE-driven promoter, which is highly sensitive to the activation of the general stress response (Estruch, 2000), was only very modestly activated upon potassium starvation (Fig. S3). Therefore, potassium starvation does not seem to trigger a general stress response.

Among the genes whose mRNA levels are depleted after transfer of cell to a potassium-free medium, there is an enormous excess of those related to ribosome construction: genes encoding ribosomal proteins ($P < 2.5 \times 10^{-74}$), rRNA processing genes ($P < 2.5 \times 10^{-29}$) and members of the so-called RIBI regulon, including a

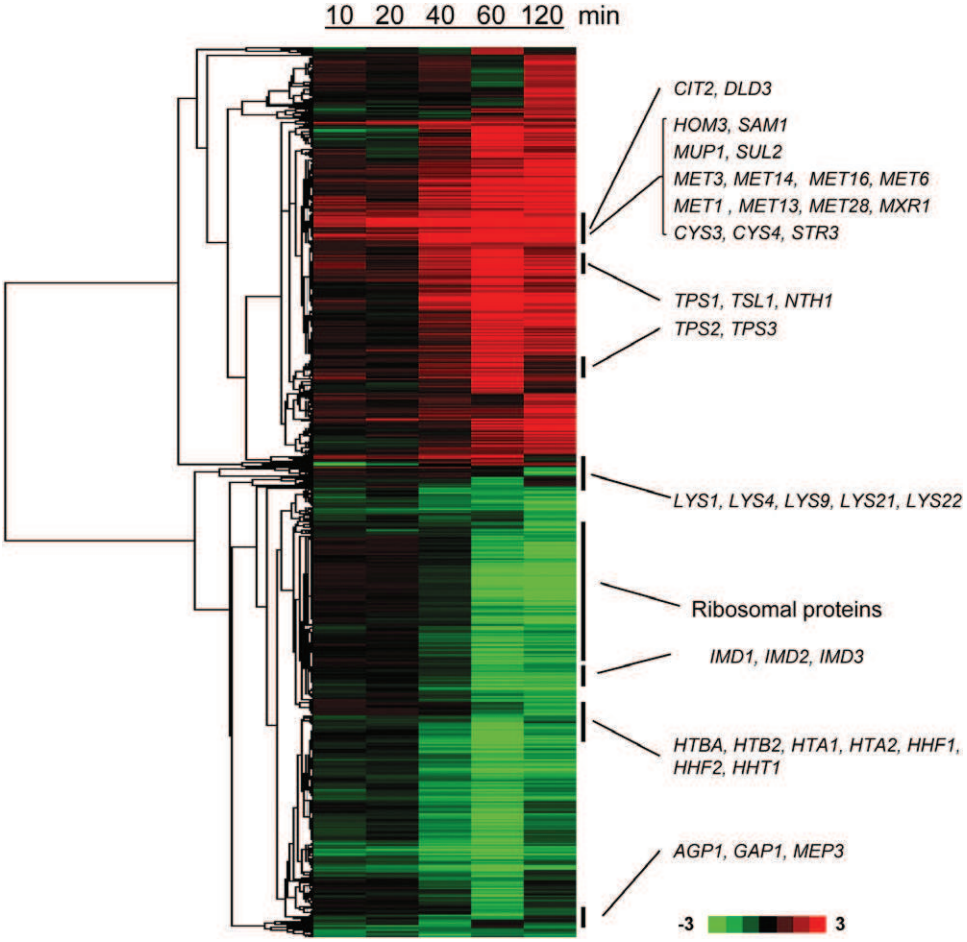

Fig. 1. Clustering of genes induced or repressed after shifting yeast cells to K^+-free medium. Only genes with valid data for at least four time points are represented. Specific group of genes with related functions that cluster closely are highlighted on the right. In several instances, these clusters are further investigated in this work. Scale at the bottom shows changes in log(2) space.

decrease in expression of genes important for biosynthesis of GMP from IMP (see Fig. 1 and Table S3).

We also investigated the effect on the transcriptional profile of the lack of the *TRK1* and *TRK2* genes, encoding the high-affinity potassium transporters. The experiment was performed in the presence of 50 mM potassium, which allows near wild-type growth of this mutant strain. From 4767 genes with valid data, we detected increased expression only for 69 genes (Table S4). Gene Ontology analysis shows an excess of genes related to sulfate assimilation ($P < 4.8 \times 10^{-08}$) (such as *SER3*, *MET10*, *MET28*, *MET3*, *ECM17*, *MET14*, *MET1*, *SUL2*, *MET16* or *MXR1*). Interestingly, genes directly involved in Met or SAM biosynthesis or import that are substantially induced by potassium starvation are not induced at all in *trk1 trk2* cells (denoted with an asterisk in Fig. 2A). Induction of genes encoding enzymes or transporters required for biosynthesis of arginine from Glu or Gln (*ARG7*, *ARG1*, *ARG4*, *ORT1*, *CPA1*) was also observed. Similarly, only 79 genes were repressed in *trk1 trk2* cells when compared with the wild-type strain (Table S4). These included genes related to GMP biosynthesis, transport of amino acids and polyamines, such as *TPO1*, *TPO4*, *GAP1* (general amino acid permease), *AGP2* and *AQR1*, or glycogen biosynthesis.

Table 1. Short-term transcriptional changes associated to potassium starvation.

	Minutes after transfer to K^+-free medium				
Genes	10	20	40	60	120
Induced	53	58	255	568	619
Repressed	45	33	235	733	560

Potassium starvation promotes oxidative stress

Although not evident in the heat map shown in Fig. 1, the time-course response to potassium starvation includes many induced genes that are required to deal with oxida-

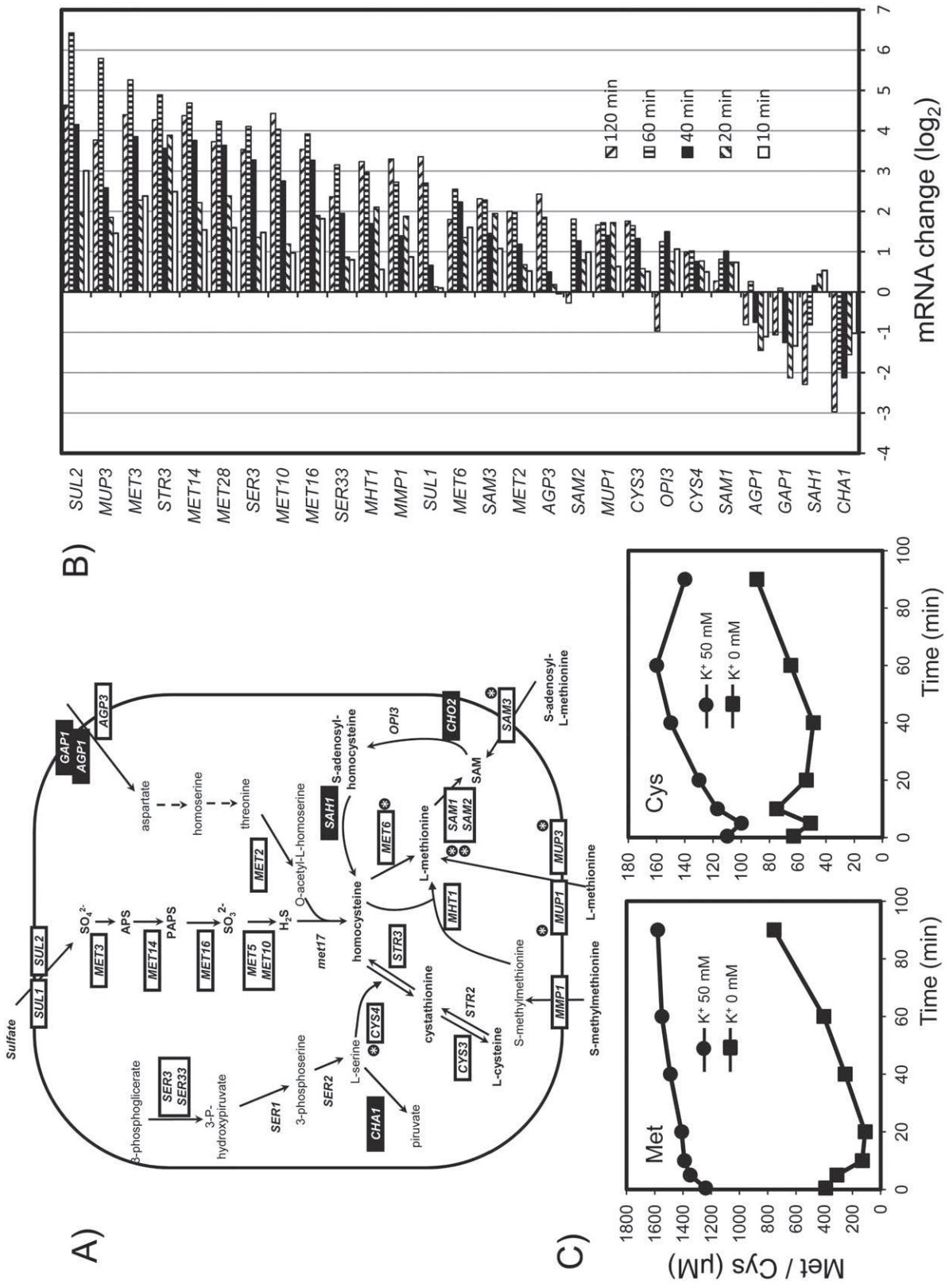

Fig. 2. Effect of potassium deprivation on sulfur amino acid metabolism.
A. A schematic view of sulfur uptake and Met/Cys metabolism. Genes induced or repressed after shift to K^+-free medium are boxed in white or dark background respectively. Unboxed genes do not experience significant changes. The asterisk in dark background indicates genes substantially induced in the absence of potassium but whose expression is not altered in *trk1 trk2* cells. SAM, *S*-adenosyl-L-methionine.
B. mRNA level changes for the indicated genes along the experiment according to microarray data.
C. Intracellular levels of Methionine and Cysteine after transfer cells to K^+-free medium. Data are the mean ± SD from three independent experiments.

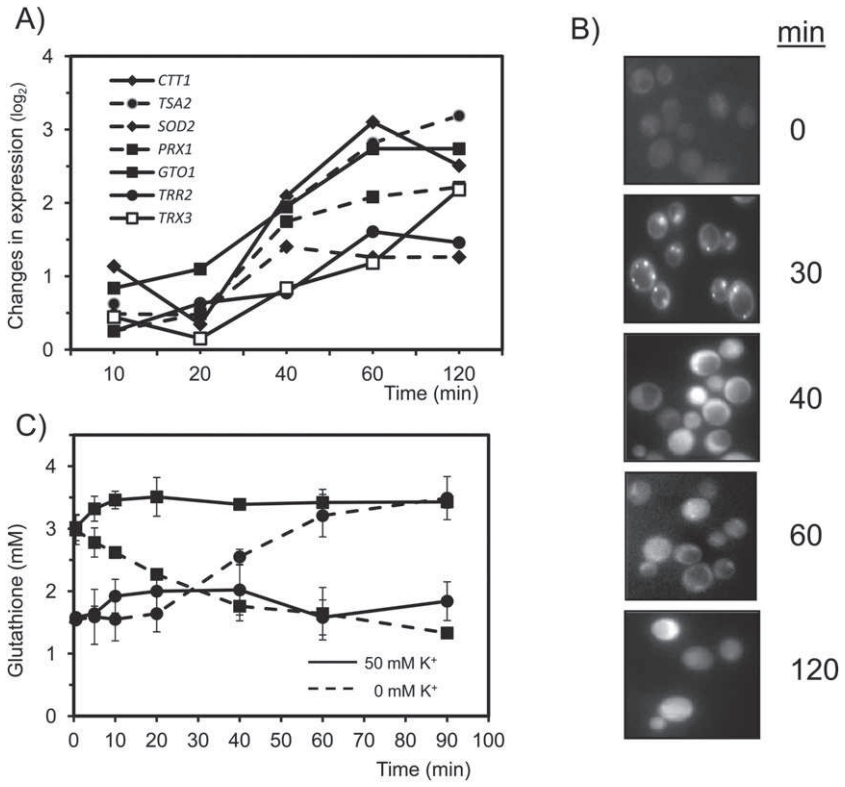

Fig. 3. Potassium starvation triggers an oxidative stress response.
A. Expression levels of several oxidative-stress responsive genes after K^+ starvation. Data are average from at least three microarrays per time point.
B. Exponentially growing BY4741 cells in K^+-free medium supplemented with 50 mM KCl were loaded with dihydrorhodamine 123 for 1 h. Cells were then resuspended in K^+-free medium and incubated for the indicated times. The appearance of ROS oxidizes dihydrorhodamine 123 to the fluorescent derivative rhodamine 123.
C. Oxidized (●) and reduced (■) glutathione levels after K^+ starvation. Data are presented as mean ± SD from three independent experiments.

tive stress and/or known to be induced under this condition, such as *CTT1*, *TSA2* and *SOD2* (Fig. 3A). Most of these genes encode proteins with oxidoreductase activity. This suggested that potassium starvation may trigger a situation of oxidative stress. To test this point, cells were incubated with 1,2,3-dihydrorhodamine, to monitor generation of ROS, and switched to medium lacking potassium. As it can be observed in Fig. 3B, after 30 min cells became fluorescent, indicating oxidation of the dye as a result of ROS formation. Since glutathione is a key molecule in the control of the redox balance, we determined the amounts of both the reduced (GSH) and oxidized (GSSG) forms of this molecule. As shown in Fig. 3C, potassium starvation results in the decline of GSH levels and the accumulation of the GSSG, thus leading to a strong decrease in the GSH/GSSG ratio.

Effect of potassium starvation on methylglyoxal (MG) production and trehalose metabolism

As denoted in Fig. 1, depletion of potassium caused time-dependent changes in the expression of genes required biosynthesis and utilization of trehalose. It also came to our attention an increase in the level of expression of *GLO1, GLO2* and *GRE3*. These genes encode enzymes required for detoxification of methylglyoxal (MG) to lactate (*GLO1* and *GLO2*) or to propanediol (*GRE3*). Whereas trehalose is synthesized from glucose-6P and UDPG, MG is formed as a by-product of glycolysis from triose phosphates through the action of triose-phosphate isomerase (Fig. 4A). Interestingly, production of MG and induction of trehalose metabolism have been linked in the past (Aguilera and Prieto, 2004). As shown in Fig. 4B, shortly after transfer to K^+-free medium (10 min), several genes involved in trehalose biosynthesis (*TPS1*, *TPS2*, *TSL1*) are somewhat induced. After 20 min, mRNA levels return to baseline values but later on (60 min) genes encoding both trehalose-synthesizing and -degrading enzymes are markedly induced. The same profile is also observed for *PGM2*, encoding the phosphoglucomutase activity necessary for generation of UDPG, a substrate for Tps1. The expression kinetics observed for *GLO1, GLO2* and *GRE3* (Fig. 4B), raised the possibility that lack of potassium might enhance methylglyoxal generation. In concordance with this hypothesis, we detected a rather fast increase in MG levels (up to three- to fourfold), which remained steadily higher than normal after 20 min (Fig. 4C). As discussed below, the changes in MG concentrations may be linked to the activation of genes involved in trehalose metabolism.

Potassium starvation may trigger the retrograde response

The retrograde response is a signal transduction pathway from mitochondria to the nucleus that allows cells to

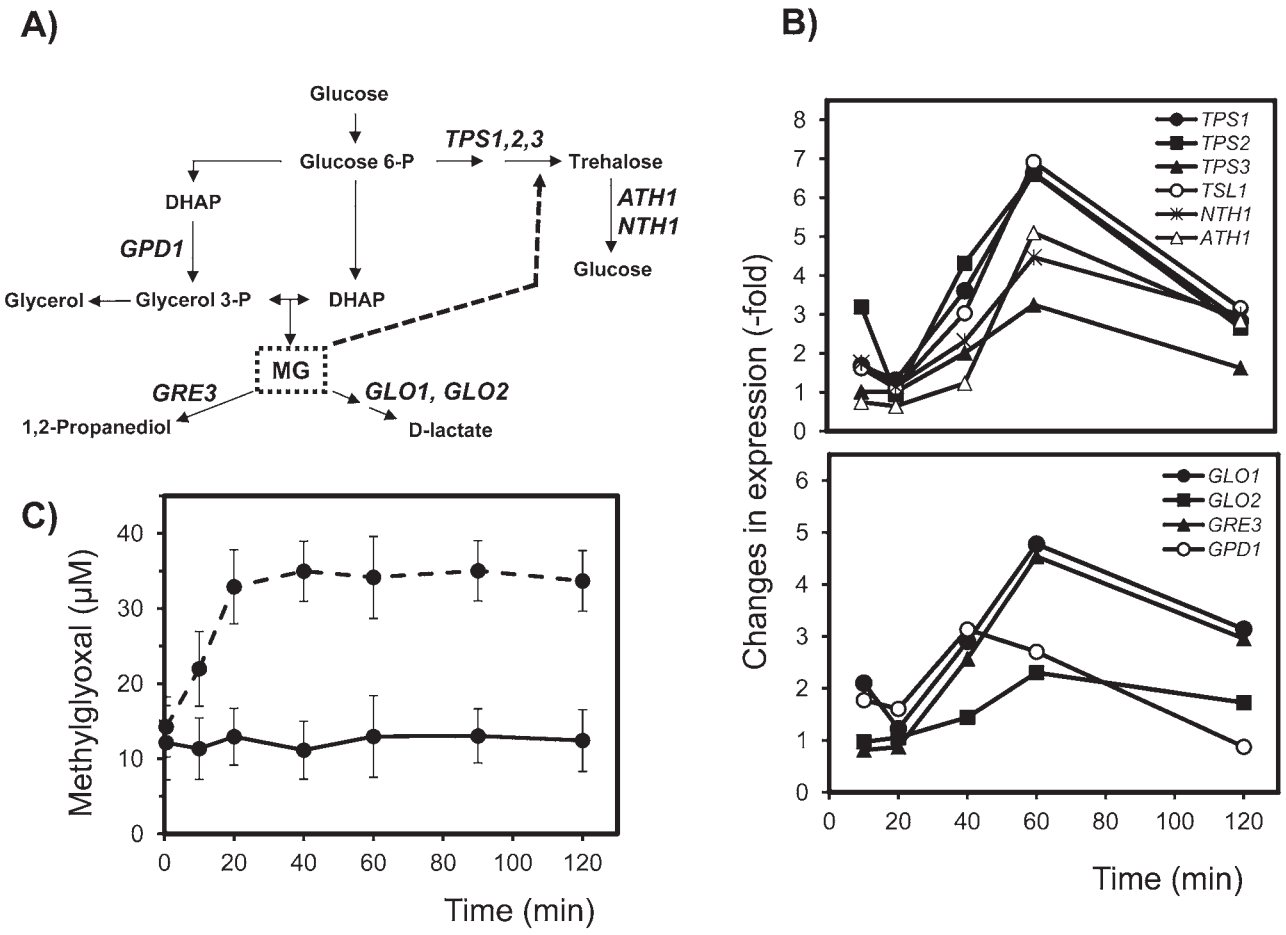

Fig. 4. Methylglyoxal detoxification and threalose metabolism in response to potassium starvation.
A. Schematic depiction of methylglyoxal (MG) generation and degradation and trehalose metabolism (DHAP, dihydroxiacetone phosphate). The discontinuous arrow indicates a proposed positive effect of trehalose biosynthesis (Aguilera and Prieto, 2004).
B. Changes in expression levels of genes involved in trehalose metabolism (upper panel) and MG detoxification, derived from microarray data.
C. Changes in intracellular levels of MG in response to potassium starvation. Cells were resuspended in Translucent medium either without KCl (discontinuous lines) or with 50 mM KCl (continuous lines).
Data were obtained by HPLC-MS and correspond to the mean ± SD from three independent experiments.

respond to changes in the functional state of the organelle via changes in nuclear gene expression. We observed a strong increase in expression of two genes considered prototypic in the retrograde response, *CIT2*, encoding a mitochondrial isoform of citrate synthase, and *DLD3*, encoding a cytoplasmic isoform of D-lactate dehydrogenase (Fig. 5A). Increased expression of *CIT2* and *DLD3* as a consequence of the activation of the retrograde response requires the concerted action of the Rtg3 and Rtg1 transcription factors. As shown in Fig. 5A (lower panel), deletion of *RTG3* results in blockage of the increased expression of *CIT2* and *DLD3* in response to potassium starvation, thus confirming the activation of the retrograde pathway. Consistent with this notion, Rtg1 shows a tendency to accumulate in the nucleus after 20 min of potassium depletion (Fig. S4; note, however, the absence of ammonium in the medium, which might complicate a direct comparison). It is worth noting that we also observe a modest but consistent activation of *CIT1*, *ACO1* and *IDH2*, encoding the first three enzymes of the tricarboxylic acid cycle (Fig. 5A), which represent a second group of target genes for the retrograde pathway. To identify the possible reason for this transcripcional response, we examined the aspect of mitochondria using a GFP version targeted to this organelle. As shown in Fig. 5B, mitochondrial morphology appears normal after 60 min of growth in the absence of potassium. Retrograde gene response has been also associated to increases in the intracellular ammonium content (Tate and Cooper, 2003). Since Hess and colleagues (2006) proposed that long-term potassium limitation could result in intracellular accumulation of ammonium, we considered the possibility

Fig. 5. Analysis of the potassium starvation-triggered retrograde response.
A. Upper panel. Expression levels of genes related to mitochondrial retrograde response during potassium starvation. Data plotted correspond to that of DNA microarray experiments. Lower panel. RT-PCR analysis of *CIT2* and *DLD3* responses. BY4741 wild-type and *rtg3* mutant cells were grown exponentially in 50 mM KCl, resuspended in medium with (+) or without (–) 50 mM KCl and incubated during 60 min. Cells were collected and total RNA was prepared and used for semi-quantitative RT-PCR. The products were analysed by agarose (2%) gel electrophoresis and visualized by ethidium bromide staining. *ACT1*, encoding actin, is shown as a control.
B. Evaluation of mitochondria morphology after short-time potassium starvation. Wild-type cells expressing mitochondria-targeted GFP were grown exponentially with 50 mM (+) KCl and shifted to medium without potassium (–). Cells were collected at the indicated times. The *fzo1* mutant, also expressing mitochondria-targeted GFP, is shown as example of defective mitochondrial morphology. Cells were analysed by fluorescence microscopy (1000×).
C. Changes in intracellular ammonium content after potassium starvation. BY4741 cells were treated as in (A) and samples were taken and processed for ammonium determination at the indicated times. Continuous line denotes the presence of 50 mM KCl in the medium whereas discontinuous line refers to potassium-deprived cultures. Data are expressed as nmol NH_4^+/wet weight and are mean ± SD from three independent experiments.
D. Upper panel. The indicated strains were grown in Translucent medium supplemented with 50 mM potassium up to an OD of 0.5 and then resuspended in the same medium with or without potassium and growth resumed for 60 min. Samples were taken at the indicated times for intracellular ammonium measurement. Lower panel. The BYT1 strain (*trk1*Δ) was transformed with plasmids expressing a wild-type version of Trk1 (pTRK24) or versions of the transporter carrying the indicated mutations. Note that the $Trk1^{M1153R}$ version is virtually unable to transport potassium (Haro and Rodriguez-Navarro, 2003).

that cells subjected to short-term potassium deficiency might actually accumulate this cation, which is present in the medium as nitrogen source. As shown in Fig. 5C intracellular ammonium increases almost immediately after shifting cells to K^+-free medium and becomes three-fold higher after 60 min. We then investigated the possible way of entry of ammonium in the absence of potassium. Interestingly, cells lacking Trk1 or both Trk1 and Trk2 potassium transporters did not show significant ammonium accumulation (Fig. 5D), suggesting that ammonium entry occurred through the Trk1 transporter. To evaluate the link between effective potassium transport and ammonium entry, we expressed in the *trk1* deletion mutant the wild-type Trk1 protein as well as versions carrying the K1147N and M1153R mutations. The former only marginally affects potassium transport, whereas the latter virtually abolishes transport of the cation. As shown in figure 5D, expression of the $Trk1^{M1153R}$ version fails to accumulate ammonium in the absence of potassium in the medium, thus indicating that the Trk1-mediated transport mechanism for potassium and ammonium is likely to be the same.

Transcriptional and post-transcriptional effects of potassium starvation on cyclin levels

Examination of microarray data reveals that lack of potassium causes changes in the levels of diverse cyclins. For instance, a moderate decrease can be observed for the G1 phase cyclins *CLN1* and *CLN2*, whereas *CLN3* mRNA level experiences a slight increase (Fig. 6A). Interestingly, mRNA levels of *CLB1* and *CLB2*, which accumulate during G2 and M phases, decay in a time-dependent manner, reaching a minimum after 120 min of shifting cells to K^+-free medium. In contrast, *CLB3* and *CLB4*, whose transcripts accumulate during S phase and G2, do not experience a significant decrease. Finally, whereas *CLB5* mRNA levels remain almost unaltered, *CLB6* levels declined shortly after removal of potassium. The mRNA abundance of several of these cyclins was also monitored by semi-quantitative RT-PCR after 60 and 120 min of potassium starvation, confirming the changes observed by DNA microarray analysis (Fig. 6B). Since it is known that cyclins are also controlled at the protein level, we monitored the amounts of Cln1, Cln2, Cln3 and Clb2 by immunoblot, using the appropriate strains carrying tagged versions of the proteins. As shown in Fig. 6C, Cln1 levels were almost undetectable even at the shortest time monitored (30 min), Cln2 and Clb2 amounts decreased in a time-dependent manner, being very low or undetectable after 120–180 min. Cln3 levels remained more stable, although with a tendency to decline after 120 min of removal of potassium.

Lack of potassium destabilizes the septin ring

Evaluation of genes that were affected shortly after removal of potassium of the medium highlighted a common pattern for the genes encoding the three similar protein kinases of the bud neck (Gin4, Kcc4, Hsl1) involved in the septin checkpoint. As shown in Fig. 7A (upper panel), all three genes were repressed in a time-dependent fashion, and this effect was noticeable even 10–20 min after transfer to K^+-free medium. In addition, mRNA levels for *BUD4*, encoding a protein involved in bud-site selection that also localizes with septins, were also downregulated (Fig. 7A, upper panel). This suggested that lack of potassium may affect proper septin ring generation, although our microarray data did not indicate relevant changes for any of the genes encoding septins (Fig. 7A, bottom panel). Nevertheless, when septin ring assembly is evaluated in cells expressing a GFP-tagged version of Cdc11, one of the components of

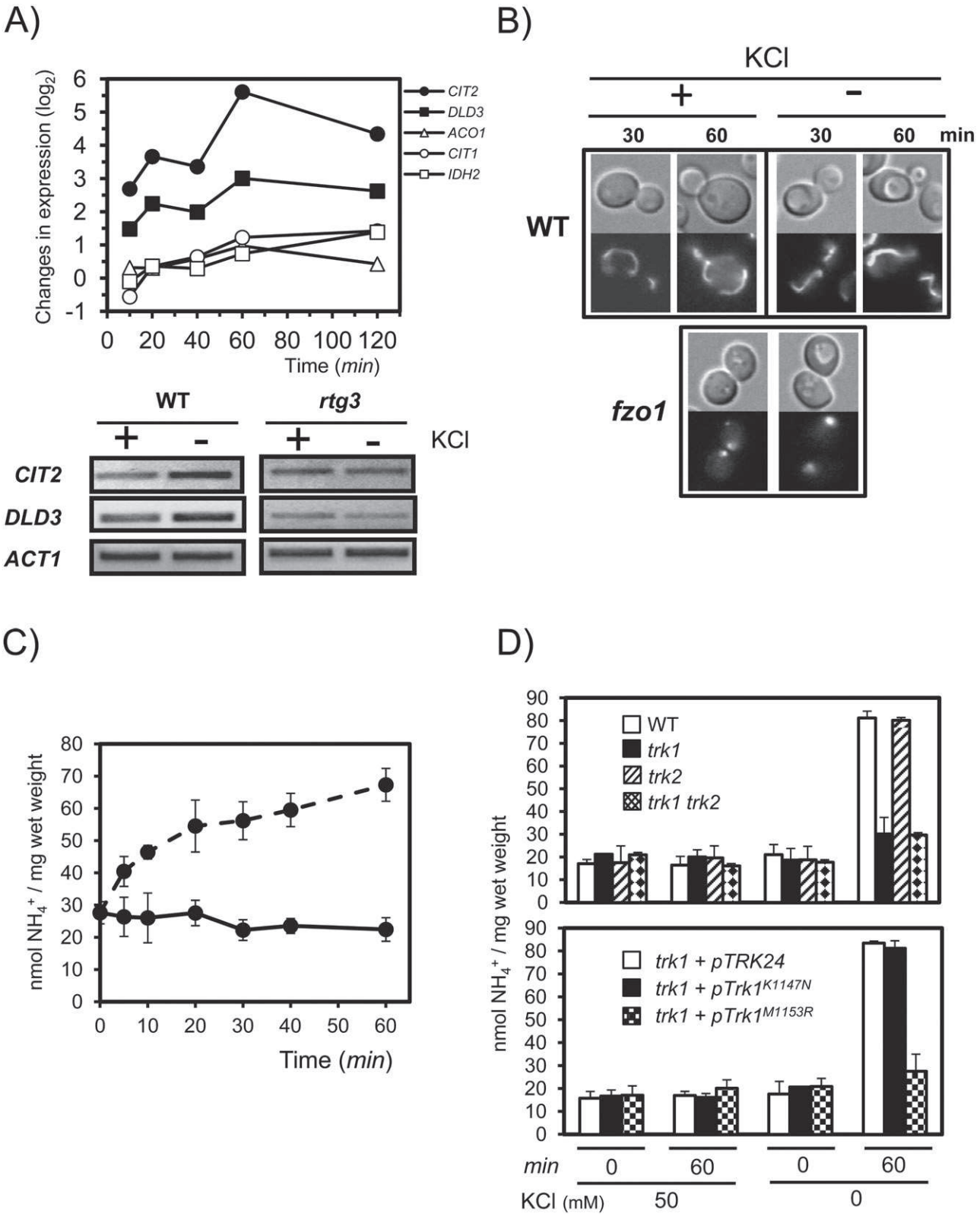
A)
Changes in expression (log2)
6
5
4
3
2
1
0
-1
0 20 40 60 80 100 120
Time (min)
CIT2
DLD3
ACO1
CIT1
IDH2
WT
rtg3
+ - + -
KCl
CIT2
DLD3
ACT1
B)
KCl
+ -
30 60 30 60 min
WT
fzo1
C)
nmol NH4+ / mg wet weight
80
70
60
50
40
30
20
10
0
0 10 20 30 40 50 60
Time (min)
D)
nmol NH4+ / mg wet weight
90
80
70
60
50
40
30
20
10
0
WT
trk1
trk2
trk1 trk2
trk1 + pTRK24
trk1 + pTrk1K1147N
trk1 + pTrk1M1153R
min 0 60 0 60
KCl (mM) 50 0

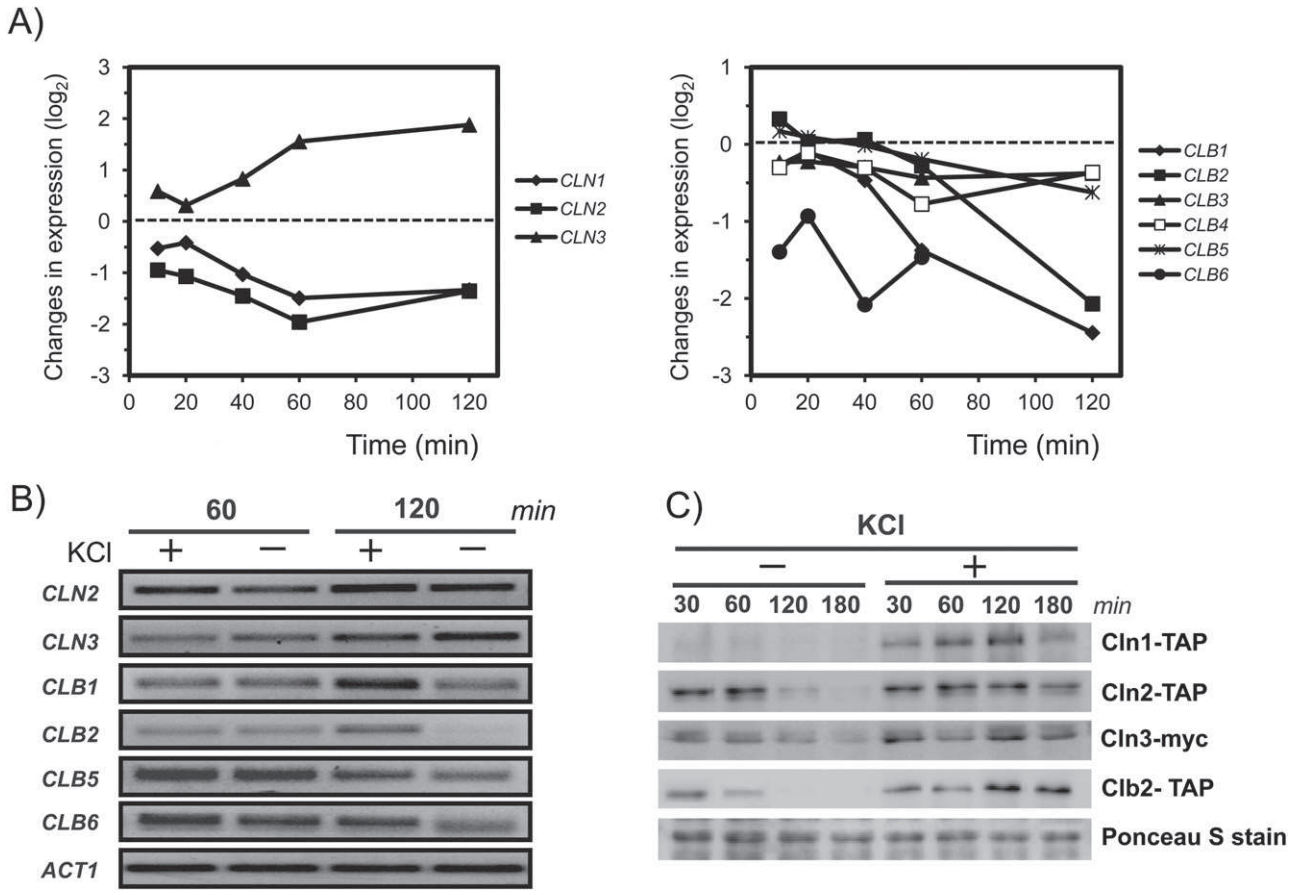

Fig. 6. Effects of K^+ starvation on cyclin levels.
A. Expression levels of the indicated genes during potassium starvation. Data plotted are derived from microarray experiments.
B. Analysis of mRNA abundance of several cyclins by semi-quantitative RT-PCR. BY4741 wild-type cells were grown exponentially in 50 mM KCl and resuspended in medium with 50 mM (+) or without (–) KCl. Cells were collected at the indicated times and total RNA (200 ng) was prepared and used for semi-quantitative RT-PCR. The products were analysed as described in Fig. 5B and *ACT1* is shown as a control.
C. Protein levels of several cyclins during K^+ starvation. BY4741 wild-type cells were grown exponentially in 50 mM KCl and resuspended in Translucent K^+-free medium with 50 mM (+) or without (–) KCl and samples were taken at the indicated times for immunoblot analysis as described in *Experimental procedures*.

the septin ring, it is clearly observed that, after 30 min in the absence of external potassium, the septin ring appears distorted and, after 60 min, it is not longer detectable (Fig. 7B). Since the absence of the septin ring could be caused by destruction of Cdc11, we evaluated the amounts of this septin by immunoblot in extracts of cells grown in the presence or the absence of potassium. As shown in Fig. 7C, the amount of Cdc11 remains nearly constant even after 120 min of culture in potassium-depleted medium in both 15 000 *g* pellet and supernatant fractions. In order to circumvent any possible artefact derived from the use of GFP as marker for Cdc11 localization, we carried out immunolocalization experiment using anti-Cdc11 antibodies. As shown in Fig. 7D, using this technique it can be confirmed that Cdc11 is not properly localized in cells grown for 60 min in a medium lacking potassium. Thus, our data provides evidences that correlate the lack of K^+ with a decrease if the amount of mRNA corresponding to the kinases involved in the septin checkpoint, which is concomitant with a mislocalization of the Cdc11 septin.

Discussion

The genome-wide transcriptional analysis of the short-term response of yeast to potassium starvation presented here underscores the relevance of potassium in the biology of the cell and provides new clues for the investigation of possible functional targets for this cation. We show that lack of potassium causes major alterations in the transcriptional profile, with more than 1700 genes (over 25% of the entire yeast genome) resulting induced or repressed at least at one time point investigated. It is worth noting that a significant part of the observed changes occurs when these cells still retain a substantial amount of potassium (Navarrete *et al*., 2010), well above

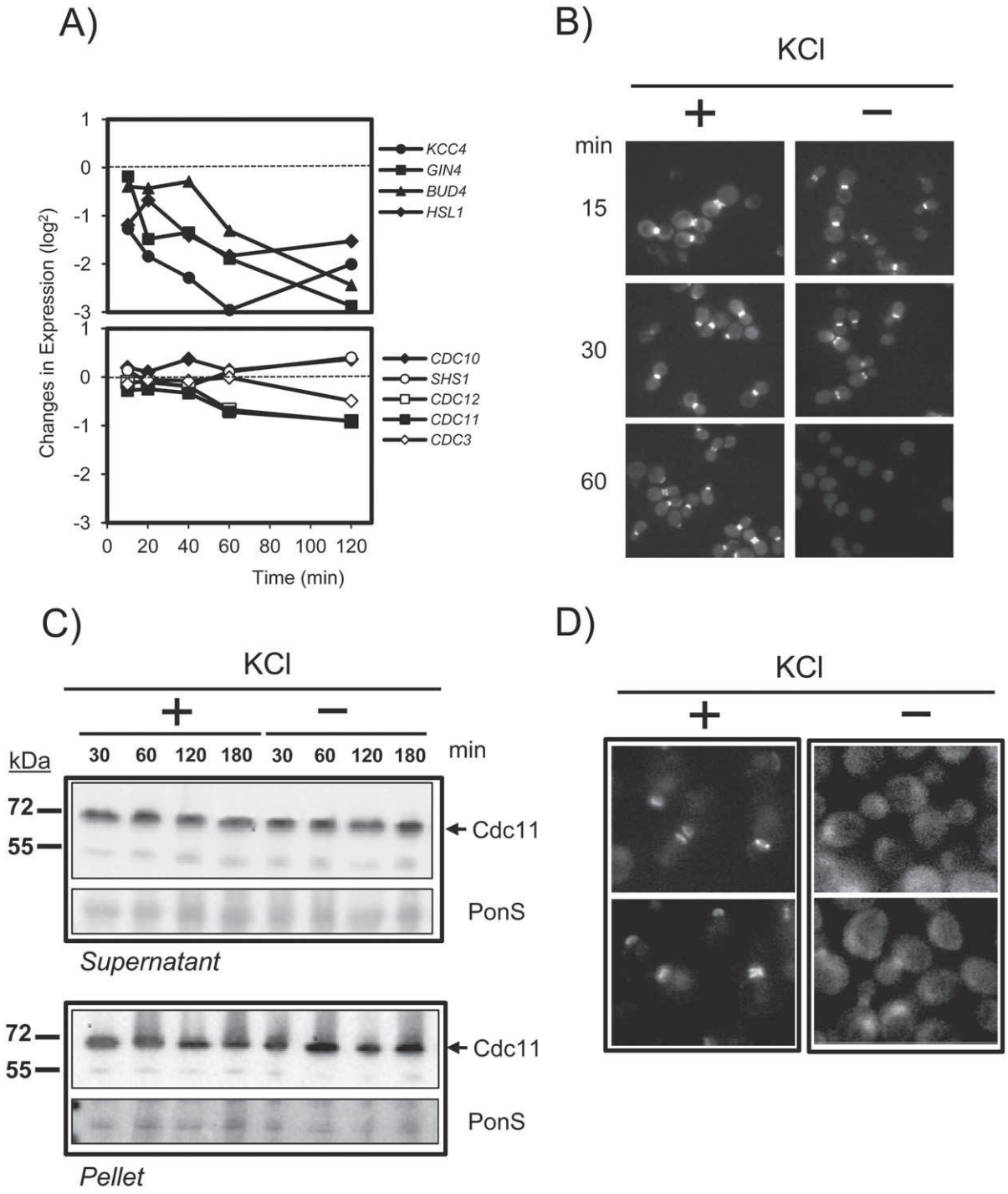

Fig. 7. Lack of potassium disrupts septin ring formation.
A. Expression levels of genes related to bud neck and septin ring formation during potassium starvation. Data from microarray experiment are represented in the graph.
B. Localization of Cdc11-GFP is affected during K^+ starvation. A BY4741 wild-type cells were transformed with centromeric plasmid expressing Cdc11-GFP and grown exponentially in Translucent K^+-free medium containing 50 mM KCl. Cells were resuspended in the same medium with (+) or without (–) KCl and samples were taken at the indicated times for formaldehyde fixation.
C. Levels of Cdc11 protein are constant during potassium starvation. BY4741 wild-type cells were grown exponentially in 50 mM KCl and resuspended in medium with (+) or without (–) KCl. Cells were collected at the indicated times and samples were processed for immunoblot analysis as described in *Experimental procedures*. PonS denotes Ponceau S staining of the membranes.
D. Cultures of wild-type BY4741 cells were treated as in (B). Samples were taken after 60 min and cells processed for immunofluorescence as described in *Experimental procedures* using anti-Cdc11 antibodies.

the known requirement for near full activity of diverse enzymes such as pyruvate kinase (Laughlin and Reed, 1997). Therefore, it is unlikely that the observed transcriptional changes could occur in response to inactivation of known potassium functional targets. This huge transcriptional remodelling event is in contrast with the rather modest number of changes detected by Hess and colleagues (2006) when transcriptomic changes in cells growing in a chemostat under limiting potassium concentrations were examined. In that case, data for the two lowest potassium concentrations used (1.3 and 0.65 mM) shows that only 153 genes were induced and 193 repressed. It must be noted the presence of ammonium in the medium in both experiments. This is an important issue for comparison, since the presence or absence of interchangeable cations (i.e. ammonium or sodium) is known to affect the physiological response to potassium deprivation. It is conceivable that at least part of the acute changes observed in our experiments could represent an adaptive and transient response leading to the steady-state observed in the chemostat experiments. Therefore, our work is likely to highlight changes not identified in the mentioned study and both approaches can be considered complementary.

Our study reveals that a large number of genes involved in sulfur utilization and Met/Cys import and biosynthesis are strongly induced in response to lack of extracellular potassium. The induction profile largely overlaps with that observed in a previous genome-wide transcriptional study in which the response of chemostat cultures limited for sulfur was investigated (Boer *et al*., 2003). This overlapping response includes transcripts encoding proteins for the uptake of sulfate (*SUL2*) and sulfur-containing molecules (*MMP1*, *MUP1*, *MUP3*, *SAM3* and *OPT1*), as well as products that are involved in acquiring and generating intermediates and cofactors for sulfate assimilation (i.e. serine: *AGP3*, *SER33*), structural components of the assimilation pathway (*MET3*, *MET16*, *MET10*, *MET2*, *STR3*, *CYS3*, *MHT1*) and their transcriptional regulators (*MET28* and *MET32*). This profile includes even not so evident sulfur-related genes, such as the pyruvate decarboxylase isozyme *PDC6*, a minor isoform whose transcription is considerably induced under conditions of sulfur limitation (Boer *et al*., 2003) perhaps due to the fact that Pdc6 contains fewer sulfur-containing amino acids than Pdc1 or Pdc5 isoforms. The effect of lack of potassium seems rather specific for sulfur-containing amino acids, since we do not observe an induction pattern in other amino acid biosynthetic pathways. Activation of genes involved in sulfur-related pathways can be confirmed by using translational LacZ fusions of the specific promoters, although in this case the response it is not as dramatic as the one observed from microarray data. This suggests that the drastic changes at the mRNA level could be the combined result of promoter activation and increased mRNA stability. Our results strongly suggest that, in these conditions, yeast cells experience a shortage of Met and Cys. This is confirmed when the intracellular levels of these amino acids are investigated (Fig. 2C) and by the observation that increasing the amount of Met in the medium specifically attenuates the induction of genes relevant for the biosynthesis of sulfur-containing amino acids (Fig. S1B). In addition, the induction is not a direct consequence of the *met17* mutation (although it is probably potentiated by it), since it is also observed in strains that do not contain such mutation. Remarkably, we still observe increased expression of several genes encoding proteins required for sulfur utilization in *trk1 trk2* cells growing in the presence of 50 mM potassium, a concentration well above the K_m of the low-affinity uptake system of the BY4741 strain (~ 20 mM) (Navarrete *et al*., 2010). This suggests that Met/Cys metabolism is very sensitive to even minor unbalances in potassium homeostasis. Hal4 and Hal5 are protein kinases required for normal cation tolerance. Under low potassium conditions, a strain lacking both proteins fails to correctly allocate to the cell membrane the potassium Trk1 transporter, as well as several other nutrient transporters (Perez-Valle *et al*., 2007). Genes belonging to the sulfate assimilation and Met biosynthesis pathways are specifically induced in *hal4 hal5* mutants growing in standard YPD medium (Perez-Valle *et al*., 2010) and this specific transcriptional response was attributed to the observed instability of the Mup1 high-affinity permease. Interestingly, this expression profile is largely overlapping with that observed here for the *trk1 trk2* strain (see Fig. S5), even though the different growth media used. Therefore, it is conceivable that the sulfur-related transcriptional profile of the *hal4 hal5* mutant could be caused, at least in part, by a deficient potassium uptake derived from a defect in proper Trk1 trafficking to the cell membrane. It is worth noting that the sulfur-related response described by Perez-Valle and colleagues (2010) was also observed in a strain prototrophic for Met, further supporting the notion that it is not caused by the *met17* mutation.

Our data clearly show that potassium deprivation triggers a transcriptional response congruent with a condition of oxidative stress. We observe that ROS formation is already detectable after 30 min of switching cells to medium lacking potassium, a kinetics that fits well with the timing of induction of oxidative stress responsive genes (from 40 min onwards) and accumulation of oxidized glutathione. It is not obvious why potassium starvation would result in oxidative stress. It has been recently postulated that, in a situation of programmed cell death induced by glucose in the absence of additional nutrients, ROS production is inhibited by K^+ uptake

(Hoeberichts *et al*., 2010). It may be possible therefore that the incapacity to uptake potassium renders cells susceptible to development of oxidative stress. We also detect a rather rapid increase (around threefold) in MG levels after potassium starvation. MG is a toxic compound that is formed as a by-product of glycolysis from triose phosphates, and its appearance is congruent with the observed induction of several genes needed for its degradation (i.e. *GLO1*, *GLO2* and *GRE3*). It has been postulated that an excess of MG formation can increase ROS production and cause oxidative stress (see Desai *et al*., 2010 for a review), while accumulation of MG has been shown to activate oxidative stress-responsive transcription factors in both budding (Maeta *et al*., 2004) and fission yeast (Zuin *et al*., 2005). Therefore, the early accumulation of this toxic maybe linked, at least in part, to the oxidative stress response observed under potassium limitation. Transcriptional changes caused by MG are postulated to be triggered by the increase in the intracellular levels of this compound, rather than by sensing its extracellular presence (Aguilera and Prieto, 2004). These authors also show that exposure to MG results in increased expression of *GPD1* (encoding the first enzyme in glycerol biosynthesis) and they suggest that this would have the purpose to control the amount of triose phosphates, the precursors of MG. Indeed, under potassium starvation, we observe increased expression not only of *GPD1*, but also of *HOR2* and *RHR2*, encoding the phosphatases catalysing the second step for glycerol generation. Exposure to MG results in upregulation of *TPS1* and *TPS2*, encoding components of the trehalose synthase complex (Aguilera and Prieto, 2004). It is remarkable that we also observe a strong increase in expression of genes related to trehalose metabolism (Fig. 4) involved in both biosynthetic and degradative pathways, and that measurement of trehalose levels reveals that, although a peak of trehalose is observed shortly after potassium removal, the level of the disaccharide rapidly decrease (data not shown). Therefore, our data would support the hypothesis that accumulation of MG would trigger a futile cycle based in trehalose generation and degradation, aiming to downregulate carbon flux through the upper part of the glycolysis, as it has been suggested for other stresses (Parrou *et al*., 1997). Remarkably, a functional link between the upper part of glycolisis and potassium homeostasis was described by Mulet and co-workers a few years ago (Mulet *et al*., 2004). These authors reported that overexpression of *TPS1* resulted in a Trk-dependent increase in cation tolerance, whereas mutation of *TPS1* or *PGM2* (and possibly, *TPS2*) resulted in defective Trk-mediated uptake of potassium. Therefore, it is conceivable that the increase in expression of *PGM2*, *TPS1* and *TPS2* that we observed upon potassium starvation might constitute a physiological response aiming to stimulate high-affinity potassium uptake.

Lack of potassium triggers the induction of several genes involved in the retrograde response, including the prototypic genes *CIT2* and *DLD3* (see Liu and Butow, 2006 for a review). This response is usually elicited by mitochondrial alteration and is mediated by Rtg2 and the Rtg1/Rtg3 transcription factors. We show explicitly here that lack of potassium activates this pathway. However, potassium starvation does not result in evident alterations of mitochondrial morphology, suggesting that it does not drastically affects mitochondria. Several years ago Tate and Cooper demonstrated that an increase in intracellular ammonium could elicit the retrograde response and induce *CIT2* expression (Tate and Cooper, 2003). Here, we demonstrate that lack of potassium actually causes a fast and persistent increase in intracellular ammonium concentration, as it was predicted by Hess and co-workers using chemostat cultures (Hess *et al*., 2006). Therefore, increased intracellular ammonium may contribute to the observed retrograde response in potassium-starved cells. Furthermore, we show here that this ammonium influx is specifically mediated by the Trk1 potassium transporter and that influx is linked to the ability to transport potassium (Fig. 5D). A puzzling observation is that the *trk1 trk2* mutant shows higher-than-normal expression of *CIT2* and *DLD3* (although other secondary targets of the retrograde response, such as *CIT1* or *ACO1*, are not altered), whereas these cells do not accumulate ammonium (Fig. 5D). We have observed that *trk1 trk2* cells are able to grow on respiratory sources (not shown), suggesting again that mitochondria are not likely to be functionally compromised. In any case, the expression profile of the *hal4 hal5* mutant, in which *CIT2* and *DLD3* mRNAs are overexpressed 7.1- and 2.7-fold, respectively, mimics again that of the Trk-deficient strain, suggesting a common primary origin for these changes.

Although wild-type *S. cerevisiae* can grow at appreciable rate even at rather low K^+ concentration in the medium, complete removal of the cation leads to substantial growth arrest (Navarrete *et al*., 2010). We observe here two changes that could provide, at least in part, the molecular basis for this phenomenon. First, the level of diverse G1 and G2-phase cyclins, drastically decline upon K^+ starvation (Fig. 6). Second, K^+-starved cells are unable to construct proper septin rings (Fig. 7). Septins are evolutionarily conserved filament-forming proteins whose localization at the bud neck is required for proper shaping of the bud (Gladfelter *et al*., 2005). It must be noted that, in this case, this defect is likely not due to degradation of septins, since at least Cdc11 levels remains stable long after septin rings are disassembled. There is evidence that diverse cyclins, in

particular Cln1 and Cln2, are needed to promote proper septin ring assembly (see Howell and Lew, 2012 for a recent review). Therefore, the depletion of several cyclins as a result of potassium starvation might be at the basis of the failure to assemble the septin ring.

Potassium is the most abundant cation in all living cells and has been known for many years to be crucial for several basic physiological functions such as protein synthesis and enzyme activation. However, specific targets were poorly recognized and the functions requiring this cation have been only superficially characterized. In this context, our study expands previous work based in chemostat-grown cells and gains insight into the multifaceted interference with normal cell growth caused by sudden depletion of potassium.

Experimental procedures

Escherichia coli *and yeast growth conditions*

Escherichia coli DH5α cells were used as the plasmid DNA host and were grown at 37°C in Luria–Bertani (LB) broth. The LB medium was supplemented with 50 μg ml^{-1} ampicillin when plasmid selection was required. Yeast strains used in this work are described in Table 2 and *Supporting information*. Strains YNR055.1, YPC722 (5), YPC723 and YPC724 were a generous gift from J. Clotet. Yeast cells were grown at 28°C in Translucent K^+-free medium (which carries only ~ 15 μM K^+, ~ 2 mM Na^+ and ~ 70 mM ammonium) containing in each case the specified concentration of KCl. Bacterial and yeast cells were transformed using standard methods (Becker and Lundblad, 1994) and recombinant DNA techniques were performed as described elsewhere (Sambrook and Russell, 2001). When indicated, BYT1 cells (*trk1*Δ) were transformed with plasmid pTRK24 (centromeric plasmid expressing wild-type *TRK1* gene from its own promoter) or plasmids $pTrk1^{K1147N}$ and $pTrk1^{M1153R}$, expressing the corresponding mutant versions of the Trk1 transporter (Haro and Rodriguez-Navarro, 2003).

RNA purification, cDNA synthesis and DNA microarray experiments

For the analysis of the transcriptional response to potassium starvation, Wild-type strain BY4741 cells were grown in Translucent medium supplemented with 50 mM KCl to an optical density of 0.8. Cells were centrifuged and resuspended in fresh Translucent medium either with 50 ml of KCl (non-stressed cells) or without potassium (stressed cells). Samples (20 ml) for microarray analysis were taken at 10, 20, 40, 60 and 120 min by rapid filtration from four biological replicates. For the analysis of the transcriptional response elicited by the lack of Trk1 and Trk2, the expression pattern of exponential BYT12 (*trk1 trk2*) cells growing in by Translucent medium containing 50 mM KCl (OD_{660} = 0.6) was compared with that of wild-type cells in the same conditions. Total RNA was extracted by using the Ribo Pure™-Yeast kit (Ambion) following the manufacturer's instructions. RNA quality was assessed by electrophoresis in denaturing 0.8% agarose gels and quantified by measuring the A_{260} in a BioPhotometer (Eppendorf). Transcriptional analysis was performed using DNA microarrays from our laboratory as described previously (Alberola *et al*., 2004) and dye swapping was performed. The scanner ScanArray 4000 (Packard Instrument) was used to obtain the Cy3 and Cy5 images with a resolution of 10 μm. The fluorescent intensity of the spots was measured and processed using GenePix Pro 6.0 software (Molecular Devices). Spots either with a diameter smaller than 120 μm or whose fluorescence intensity for Cy3 and Cy5 was less than 150 units were not considered for further analysis. A given gene was considered to be induced when the minus/plus potassium signal ratio was equal or higher than 2.0-fold, whereas it was considered to be repressed when this signal was equal or less than 0.50-fold. The GEPAS server (version v3.1) was used to pre-process the data (Herrero *et al*., 2003). Microarray data have been deposited at GEO database with submission numbers GSE24711 (*trk1 trk2* data) and GSE24712 (time-course data).

RT-PCR assays

Wild-type strain BY4741, *rtg3* and *rtg2* mutants were grown in K^+-free medium supplemented with 50 mM KCl at 28°C to

Table 2. Strains used in this work.

Strain	Genotype	Source/reference
BY4741	*MAT**a** his3*Δ1 *leu2*Δ0 *met15*Δ0 *ura3*Δ0	Euroscarf
BYT1	BY4741 *trk1*Δ::loxP	Navarrete *et al*. (2010)
BYT2	BY4741 *trk2*Δ::loxP	Navarrete *et al*. (2010)
BYT12	BY4741 *trk1*Δ::loxP *trk2*Δ::loxP	Navarrete *et al*. (2010)
BY4741 *rtg2*	BY4741 *rtg2::kanMX4*	Euroscarf
BY4741 *rtg3*	BY4741 *rtg3::kanMX4*	Euroscarf
BY4741 *fzo1*	BY4741 *fzo1::kanMX4*	Euroscarf
YNR055.1	BY4741 *CLN3*-13MYC::*KanMX4*	J. Clotet
YPC722 (5)	BY4741 *CLN1*-TAP::*HIS3*	Ghaemmaghami *et al*. (2003)
YPC723	BY4741 *CLN2*-TAP:: *HIS3*	Ghaemmaghami *et al*. (2003)
YPC724	BY4741 *CLB2*-TAP:: *HIS3*	Ghaemmaghami *et al*. (2003)
W303-1A	*MATa ade2 can1 his3 leu2 trp1 ura3*	R. Rothstein
DBY746	*MATα his3-1 leu2-3,112 ura3-52 trp1-289*	D. Botstein

OD_{600} = 0.6. Cells were washed once and either resuspended in fresh K^+-free medium supplemented with 50 mM KCl or 0 mM KCl and incubated for 60 min. Twenty millilitres of cells were collected by filtration and total RNA was prepared as described above. Two hundred nanograms of total RNA (80 ng for *DLD3* determination) was used for semi-quantitative RT-PCR with the Ready-To-Go RT-PCR Beads kit (GE Healthcare) for 27–29 cycles. *CIT2, DLD3, CLN2, CLN3, CLB1, CLB2, CLB5, CLB6* and *ACT1* specific pairs of oligonucleotides were used to determine mRNA levels (see Table S1 for sequences). The products were analysed by agarose (2%) gel electrophoresis and visualized by ethidium bromide staining.

Plasmids construction for β-galactosidase assays

To analyse the expression of *CYS4*, *MET6*, *MET10*, *MUP3*, *SAM3*, *SER3*, *STR3* and *SUL2* promoters, *lacZ* translational fusions were constructed as follows. The regions comprising nucleotides −960 to +71 (pCYS4-LacZ), −437 to +80 (pMET10-LacZ) and −700 to +80 (pSAM3-LacZ) were amplified by PCR with added EcoRI and PstI sites and cloned into the same sites of plasmid YEp357 (Myers *et al*., 1986). Regions comprising −471 to +89 (pMUP3-LacZ) and −528 to +153 (pSTR3-LacZ) were amplified by PCR with artificial EcoRI and BamHI sites and cloned into these sites of plasmid YEp357. The region comprising −923 to +92 (pMET6-LacZ) and −804 to +80 (pSER3-LacZ) were amplified by PCR with artificial EcoRI/HindIII and KpnI/XbaI sites, respectively, and cloned into these sites of plasmid YEp357. The region comprising −481 to +50 (pSUL2-LacZ) was amplified by PCR with artificial EcoRI and SalI sites and cloned into these sites of plasmid YEp357. The oligonucleotides employed are listed in Table S1. Plasmid pPHO84 was described in Serrano and colleagues (2002). To evaluate the promoter activity in response to lack of potassium, yeast cells were grown to saturation in the appropriate dropout medium and then inoculated into 5 ml of YPD and incubated for 4 h to reach an A_{600} of 0.6. Aliquots of 1 ml were centrifuged, washed and resuspended in the same volume of Translucent medium with (50 mM) or without KCl. Growth was resumed for 120 min. Cells were collected and processed for β-galactosidase assay as described (Reynolds *et al*., 1997).

Microscopy techniques

For evaluation of ROS generation, wild-type BY4741 cells were grown exponentially in Translucent medium (OD_{600} of 0.5) and were incubated for 1 h with 2.5 μg ml^{-1} of dihydrorhodamine 123 (D1054, Sigma Aldrich) essentially as described previously (Cabiscol *et al*., 2002). Cells were washed and resuspended in fresh K^+-free medium supplemented either with 50 mM KCl or without added KCl, and 1 ml of samples were taken at the indicated times. Cells were harvested by centrifugation, washed three times with phosphate-buffered saline (PBS) solution and finally resuspended in PBS.

For examination of mitochondria, wild-type BY4741 transformed with plasmid pYX142-mtGFP, expressing mitochondrially targeted green fluorescent protein (GFP) (Westermann and Neupert, 2000), was grown to OD_{600} 0.5–0.6 in Translucent medium with 50 mM KCl. Cells were washed and resuspended in fresh medium supplemented with or without 50 mM KCl and one ml samples were taken at the indicated times. The *fzo1* mutant transformed with pYX142-mtGFP was grown in YPD medium to logarithmic growth phase and used as a control for abnormal mitochondrial morphology. Cells were fixed with 2% formaldehyde, harvested by centrifugation, washed twice with PBS solution and finally resuspended in PBS.

Determination of subcellular localization of Cdc11 was accomplished in two different ways. First, BY4741 cells were transformed with a centromeric plasmid derived from pAC115 (Casamayor and Snyder, 2003) but carrying a *URA3* marker, which expresses a GFP-tagged version of Cdc11. Mid-log-phase cells grown in Translucent K^+-free medium supplemented with 50 mM KCl were harvested by centrifugation and resuspended at the same density in the same media with or without K^+ supplementation (50 mM). Samples (500 μl) were taken at the indicated times and fixed for 10 min with 2% formaldehyde. Fixed cells were washed and resuspended in PBS solution. In addition, indirect immunofluorescence was carried out by preparing cells as in Pringle and colleagues (1991) and incubating samples with anti-Cdc11 (yC-14, Santa Cruz) at 1:250 dilution followed by incubation with anti-rabbit FITC-conjugated IgG (1:100 dilution, Sigma F-9262).

In all cases cells were examined in a Nikon Eclipse E-800 fluorescence microscope with a FITC filter. Images were captured using an ORCA-ER C4742-80-12AG digital camera (Hamamatsu Photonics) and analysed with the Wasabi v. 1.5 software.

Protein extractions and immunoblot analysis

Yeast strains were grown to an A_{600} 0.6 in Translucent medium supplemented with 50 mM KCl. Cells were harvested by centrifugation, and resuspended at the same density in Translucent medium with or without potassium supplementation (50 mM KCl). Samples (5 ml) were taken at the indicated times. For protein extraction, cells from strains YPC722 (5), YPC723 and YPC724 were collected by filtration and resuspended in homogenization buffer (50 mM Tris pH 7.5, 150 mM NaCl, 0.1% Triton X-100) plus 1 mM dithiothreitol (DTT), 10% glycerol (w/v), 2 mM phenylmetylsulfonyl fluoride (PMSF) and protease inhibitor cocktail (Roche) and lysed with one volume of acid-washed glass beads (Sigma) in a Fast Prep cell breaker (30 s, setting 5.5; Bio 101, Vista, CA). After sedimentation at 500 *g* for 10 min at 4°C, the cleared lysate was recovered. Protein concentration was quantified by the Bradford assay and 40 μg of total protein were used for immunoblot analysis.

For detection of Cdc11, BY4741 cells were collected by centrifugation and resuspended in homogenization buffer containing 1 mM EDTA, 1 mM EGTA, 0.2 mM PMSF, 0.1% β-mercaptoethanol plus protease inhibitor cocktail (Roche) and lysed as described above. After sedimentation at 1000 *g* for 1 min at 4°C, the cleared lysate was recovered and centrifuged again for 10 min at 15 000 *g* at 4°C. The supernatant was recovered and used for immunoblot analysis as above. Pellets were resuspended in 20 μl of homogenization buffer containing 1% Triton X-100 and incubated at 95°C for 2 min and the entire sample used for immunoblot analysis.

For strain YNR055.1 (*CLN3*-13MYC::*KanMX4*), cells from 5 ml of culture were harvested, resuspended in one ml of trichloroacetic acid 20% and incubated at 40°C for 30 min. Then, cells were centrifuged at 2300 *g*, washed with 1 ml of 1 M Tris (without pH adjustment), resuspended with 100 µl of sample buffer 2× (125 mM Tris-HCl pH 6.8, 40% glycerol, 8% SDS, 0.2% bromophenol blue, 1 mM DTT) and incubated at 95°C for 2 min. One volume of acid-washed glass beads was added and cells were broken as described above. The cell lysate was recovered and incubated again at 95°C for 2 min. Ten to 20 µl of cell lysate was used for immunoblot analysis.

Proteins were fractionated by SDS-PAGE in 10% polyacrylamide gels and transferred to PVDF membranes (Immobilon-P; Millipore). Membranes were incubated for 1 h with diverse primary antibodies: anti-*c-myc* antibodies (MMS-150P, Covance) at a 1:20 000 dilution, PAP (Peroxidase-Anti-Peroxidase Soluble complex, Sigma) at 1:4000 dilution (for detection of TAP-tagged proteins) or anti-Cdc11 (yC-14, Santa Cruz) at 1:1000 dilution. Membranes were washed and incubated for 30 min with secondary horseradish peroxidase-conjugated anti-mouse or anti-rabbit immunoglobulin G antibodies (Amersham Biosciences) at a 1:20 000 dilution. The immunocomplexes were visualized using an ECL Western blotting detection kit (GE Healthcare). Chemiluminescence was detected using a LAS-3000 equipment (Fuji) and quantified using Multi Gauge software, version 3.0.

Metabolite determinations

Diverse metabolites were determined by both HPLC-mass spectrometry and ^{1}H NMR. Samples were collected as follows. Strain BY4741 was grown at 28°C in Translucent medium supplemented with 50 mM KCl until $OD_{600} = 0.8$. Cells were recovered and resuspended in 250 ml fresh Translucent medium supplemented either with 50 mM KCl or without KCl. Aliquots of 15 ml were taken at 0, 5, 10, 20, 40, 60 and 90 min, quenched in cold methanol and dry pellets obtained. Prior metabolite extraction, samples for HPLC-MS received phosphocreatine at a final concentration of 1 µM as an internal standard for losses correction. ^{1}H NMR samples received 10 µl of 10 mM fumarate. Then, 1.5 ml of glass beads and 2.5 ml of boiling HPLC-quality ethanol (75% v/v) were added to the cell pellet. The mixture was vortexed for 30 s, heated (3 min, 80°C) and vortexed again (30 s). The mixture was centrifuged in a pre-cooled centrifuge (3 min, 2500 *g*, –20°C). The extraction procedure was repeated with 1.5 ml of ethanol (75% v/v). The resulting supernatants were mixed, centrifuged (10 min, 2500 *g* at –20°C) and dried with a speed-vac (Concentrator 5301, Eppendorf). The dried extract was kept at –80°C until analysis.

For HPLC-MS analysis, metabolites were separated by chromatography using a C-18-based HPLC column (Eclipse XDB-C18, 150 × 4.5 mm, 5 µm particle size, Agilent Technologies) and an Agilent HPLC 1200 Series system. The pellets were resuspended in 100 µl of formic acid (0.1% v/v). An injection volume of 20 µl was used. The 5% of the eluted flux was derived to the ESI-Ion Trap Mass Esquire 6000 (Bruker Daltonics) spectrometer. Identification of each metabolite was carried out using the DataAnalysis 3.4 software (Bruker Biospin) and an available metabolite library. Metabolite quantification was made by using calibration curves for each standard compound, correcting for losses.

Dried extracts for NMR analysis were resuspended in 400 µl of D_2O (SDS Cortecnet, France). Ten microlitres of 10 mM trimethylsilyl propionate (TSP) in D_2O was added as a chemical shift reference and for losses correction. pH was adjusted at 6.95–7.05 and D_2O was added to a final volume of 500 µl. 1D pulse and 2D NOESY spectra were acquired using a Bruker AV 500 MHz spectrometer operating at 11T (500 MHz for ^{1}H) with a 5 mm TCI cryoprobe. Spectra were processed using the Bruker BioSpin 2.0 software. Spectra were assigned using the previous knowledge, the BioMagResBank database (http://www.bmrb.wisc.edu/) and the AMIX software (Bruker Biospin).

The intracellular concentration of metabolites was calculated assuming that 1 OD_{600} is equivalent to 2×10^7 cells, and an intracellular volume of approximately 50 fl. Intracellular concentrations were corrected both by the optical density variation with time and by the volume variation with time (Navarrete *et al*., 2010).

For intracellular ammonium determination the indicated strains were grown exponentially in Translucent medium supplemented with 50 mM KCl. Cells were harvested and resuspended at the same density in the same medium with (50 mM) or without KCl supplementation. Samples were processed as described in Van Nuland and colleagues (2006). Briefly, 25–50 mg of cells (wet weight) were collected by rapid filtration at different times after resuspension, washed with cold water and frozen in liquid nitrogen. The frozen cells were resuspended in 500 µl of 0.25 M Na_2CO_3, incubated at 95°C for 20 min in tightly capped vials and centrifuged 1 min at 15000 *g* in a microcentrifuge. Ammonium levels in the supernatant were determined using the Ammonia Assay Kit (Sigma-Aldrich Ref. AA0100).

Acknowledgements

We thank Anna Barceló and Carles Arús for advice, Josep Clotet (UIC, Barcelona) for strains and the anti-myc antibody, Alonso Rodríguez-Navarro (UPM, Madrid) for the pTRK24-derived plasmid series and Benedikt Westermann (University Bayreuth, Germany) for plasmid pYX142. The excellent technical assistance of A. Vilalta and M. Robledo is acknowledged. Thanks are given to the Translucent-1 and -2 project members, particularly to Maik Kschischo and Matthias Kahm, for support.

Work was supported by Grants GEN2006-27748-C2-1-E/SYS (SysMo), EUI2009-04147 (SysMo2) and BFU2011-30197-C3-01 to J.A., and BFU2009-11593 to A.C. (MICINN and FEDER, Spain). J.A. is recipient of 'Ajut de Suport a les Activitats dels Grups de Recerca' (Grants 2009SGR-1091, Generalitat de Catalunya). David Canadell is recipient of a fellowship from the MICINN.

References

Aguilera, J., and Prieto, J.A. (2004) Yeast cells display a regulatory mechanism in response to methylglyoxal. *FEMS Yeast Res* **4:** 633–641.

Alberola, T.M., Garcia-Martinez, J., Antunez, O., Viladevall, L., Barcelo, A., Arino, J., and Perez-Ortin, J.E. (2004) A new set of DNA macrochips for the yeast *Saccharomyces cerevisiae*: features and uses. *Int Microbiol* **7:** 199–206.

Arino, J., Ramos, J., and Sychrova, H. (2010) Alkali metal cation transport and homeostasis in yeasts. *Microbiol Mol Biol Rev* **74:** 95–120.

Becker, D.M., and Lundblad, V. (1994) Manipulation of yeast genes. In *Current Protocols in Molecular Biology*. Ausubel, F.M., Brent, R., Kingston, R.E., Moore, D.D., Seidman, J.G., Smith, J.A., and Struhl, K. (eds). New York, USA: John Wiley & Sons, pp. 13.7.1–13.7.2.

Boer, V.M., de Winde, J.H., Pronk, J.T., and Piper, M.D. (2003) The genome-wide transcriptional responses of *Saccharomyces cerevisiae* grown on glucose in aerobic chemostat cultures limited for carbon, nitrogen, phosphorus, or sulfur. *J Biol Chem* **278:** 3265–3274.

Cabiscol, E., Belli, G., Tamarit, J., Echave, P., Herrero, E., and Ros, J. (2002) Mitochondrial Hsp60, resistance to oxidative stress, and the labile iron pool are closely connected in *Saccharomyces cerevisiae*. *J Biol Chem* **277:** 44531–44538.

Casamayor, A., and Snyder, M. (2003) Molecular dissection of a yeast septin: distinct domains are required for septin interaction, localization, and function. *Mol Cell Biol* **23:** 2762–2777.

Desai, K.M., Chang, T., Wang, H., Banigesh, A., Dhar, A., Liu, J., *et al*. (2010) Oxidative stress and aging: is methylglyoxal the hidden enemy? *Can J Physiol Pharmacol* **88:** 273–284.

Estruch, F. (2000) Stress-controlled transcription factors, stress-induced genes and stress tolerance in budding yeast. *FEMS Microbiol Rev* **24:** 469–486.

Gaber, R.F., Styles, C.A., and Fink, G.R. (1988) TRK1 encodes a plasma membrane protein required for high-affinity potassium transport in *Saccharomyces cerevisiae*. *Mol Cell Biol* **8:** 2848–2859.

Ghaemmaghami, S., Huh, W.K., Bower, K., Howson, R.W., Belle, A., Dephoure, N., *et al*. (2003) Global analysis of protein expression in yeast. *Nature* **425:** 737–741.

Gladfelter, A.S., Kozubowski, L., Zyla, T.R., and Lew, D.J. (2005) Interplay between septin organization, cell cycle and cell shape in yeast. *J Cell Sci* **118:** 1617–1628.

Haro, R., and Rodriguez-Navarro, A. (2003) Functional analysis of the M2(D) helix of the TRK1 potassium transporter of *Saccharomyces cerevisiae*. *Biochim Biophys Acta* **1613:** 1–6.

Herrero, J., Al Shahrour, F., Diaz-Uriarte, R., Mateos, A., Vaquerizas, J.M., Santoyo, J., and Dopazo, J. (2003) GEPAS: A web-based resource for microarray gene expression data analysis. *Nucleic Acids Res* **31:** 3461–3467.

Hess, D.C., Lu, W., Rabinowitz, J.D., and Botstein, D. (2006) Ammonium toxicity and potassium limitation in yeast. *PLoS Biol* **4:** e351.

Hoeberichts, F.A., Perez-Valle, J., Montesinos, C., Mulet, J.M., Planes, M.D., Hueso, G., *et al*. (2010) The role of K(+) and H(+) transport systems during glucose- and H(2)O(2)-induced cell death in *Saccharomyces cerevisiae*. *Yeast* **27:** 713–725.

Howell, A.S., and Lew, D.J. (2012) Morphogenesis and the cell cycle. *Genetics* **190:** 51–77.

Jurica, M.S., Mesecar, A., Heath, P.J., Shi, W., Nowak, T., and Stoddard, B.L. (1998) The allosteric regulation of pyruvate kinase by fructose-1,6-bisphosphate. *Structure* **6:** 195–210.

Ko, C.H., and Gaber, R.F. (1991) TRK1 and TRK2 encode structurally related K+ transporters in *Saccharomyces cerevisiae*. *Mol Cell Biol* **11:** 4266–4273.

Ko, C.H., Buckley, A.M., and Gaber, R.F. (1990) TRK2 is required for low affinity K+ transport in *Saccharomyces cerevisiae*. *Genetics* **125:** 305–312.

Laughlin, L.T., and Reed, G.H. (1997) The monovalent cation requirement of rabbit muscle pyruvate kinase is eliminated by substitution of lysine for glutamate 117. *Arch Biochem Biophys* **348:** 262–267.

Liu, Z., and Butow, R.A. (2006) Mitochondrial retrograde signaling. *Annu Rev Genet* **40:** 159–185.

Lubin, M., and Ennis, H. (1964) On the role of intracellular potassium in protein synthesis. *Biochim Biophys Acta* **80:** 614–631.

Maeta, K., Izawa, S., Okazaki, S., Kuge, S., and Inoue, Y. (2004) Activity of the Yap1 transcription factor in *Saccharomyces cerevisiae* is modulated by methylglyoxal, a metabolite derived from glycolysis. *Mol Cell Biol* **24:** 8753–8764.

Merchan, S., Bernal, D., Serrano, R., and Yenush, L. (2004) Response of the *Saccharomyces cerevisiae* Mpk1 mitogen-activated protein kinase pathway to increases in internal turgor pressure caused by loss of Ppz protein phosphatases. *Eukaryot Cell* **3:** 100–107.

Mulet, J.M., Alejandro, S., Romero, C., and Serrano, R. (2004) The trehalose pathway and intracellular glucose phosphates as modulators of potassium transport and general cation homeostasis in yeast. *Yeast* **21:** 569–582.

Myers, A.M., Tzagoloff, A., Kinney, D.M., and Lusty, C.J. (1986) Yeast shuttle and integrative vectors with multiple cloning sites suitable for construction of *lacZ* fusions. *Gene* **45:** 299–310.

Navarrete, C., Petrezselyova, S., Barreto, L., Martinez, J.L., Zahradka, J., Arino, J., *et al*. (2010) Lack of main K^+ uptake systems in *Saccharomyces cerevisiae* cells affects yeast performance in both potassium-sufficient and potassium-limiting conditions. *FEMS Yeast Res* **10:** 508–517.

Page, M.J., and Di Cera, E. (2006) Role of Na^+ and K^+ in enzyme function. *Physiol Rev* **86:** 1049–1092.

Parrou, J.L., Teste, M.A., and Francois, J. (1997) Effects of various types of stress on the metabolism of reserve carbohydrates in *Saccharomyces cerevisiae*: genetic evidence for a stress-induced recycling of glycogen and trehalose. *Microbiology* **143** (Part 6): 1891–1900.

Perez-Valle, J., Jenkins, H., Merchan, S., Montiel, V., Ramos, J., Sharma, S., *et al*. (2007) Key role for intracellular K^+ and protein kinases Sat4/Hal4 and Hal5 in the plasma membrane stabilization of yeast nutrient transporters. *Mol Cell Biol* **27:** 5725–5736.

Perez-Valle, J., Rothe, J., Primo, C., Martinez, P.M., Arino, J., Pascual-Ahuir, A., *et al*. (2010) Hal4 and Hal5 protein kinases are required for general control of carbon and nitrogen uptake and metabolism. *Eukaryot Cell* **9:** 1881–1890.

Pringle, J.R., Adams, A.E., Drubin, D.G., and Haarer, B.K. (1991) Immunofluorescence methods for yeast. *Methods Enzymol* **194:** 565–602.

Reynolds, A., Lundblad, V., Dorris, D., and Keaveney, M. (1997) Yeast vectors and assays for expression of cloned genes. In C*urrent Protocols in Molecular Biology*. Ausubel, F.M., Brent, R., Kingston, R.E., Moore, D.D., Seidman, J.G., Smith, J.A., and Struhl, K. (eds). New York, USA: John Wiley & Sons, pp. 13.6.1–13.6.6.

Rodriguez-Navarro, A. (2000) Potassium transport in fungi and plants. *Biochim Biophys Acta* **1469:** 1–30.

Sambrook, J., and Russell, D.W. (2001) M*olecular Cloning: A Laboratory Manual*. Cold Spring Harbor, NY, USA: Cold Spring Harbor Laboratory Press.

Serrano, R., Ruiz, A., Bernal, D., Chambers, J.R., and Arino, J. (2002) The transcriptional response to alkaline pH in *Saccharomyces cerevisiae:* evidence for calcium-mediated signalling. *Mol Microbiol* **46:** 1319–1333.

Tate, J.J., and Cooper, T.G. (2003) Tor1/2 regulation of retrograde gene expression in *Saccharomyces cerevisiae* derives indirectly as a consequence of alterations in ammonia metabolism. *J Biol Chem* **278:** 36924–36933.

Van Nuland, A., Vandormael, P., Donaton, M., Alenquer, M., Lourenco, A., Quintino, E., *et al*. (2006) Ammonium permease-based sensing mechanism for rapid ammonium activation of the protein kinase A pathway in yeast. *Mol Microbiol* **59:** 1485–1505.

Westermann, B., and Neupert, W. (2000) Mitochondria-targeted green fluorescent proteins: convenient tools for the study of organelle biogenesis in *Saccharomyces cerevisiae*. *Yeast* **16:** 1421–1427.

Zuin, A., Vivancos, A.P., Sanso, M., Takatsume, Y., Ayte, J., Inoue, Y., and Hidalgo, E. (2005) The glycolytic metabolite methylglyoxal activates Pap1 and Sty1 stress responses in *Schizosaccharomyces pombe*. *J Biol Chem* **280:** 36708–36713.

Supporting information

Additional Supporting Information may be found in the online version of this article:

Fig. S1. Potassium starvation activates the expression of genes related to the metabolism of sulfur-containing amino acids.
A. BY4741 wild-type strain was transformed with reporter YEp357-based plasmids containing the entire promoters of indicated genes, transferred to K^+-free medium for 2 h and processed for measurement of β-galactosidase activity as described in *Experimental procedures*.
B. Methionine supplementation attenuates the induction of sulfur-related genes upon potassium starvation. The BY4741 wild-type strain was transformed with indicated reporters and processed as above except that cells containing the pPHO84 reporter were collected after 90 min of potassium starvation. For this experiment the standard Translucent K^+-free medium, which contains 20 mg l^{-1} Methionine (open bars) was made 40 mg l^{-1} (stripped bars) or 80 mg l^{-1} (closed bars). Data are mean ± SEM from three to five experiments.
Fig. S2. Induction of sulfur-related genes is also observed in *MET17* strains. Wild-type strains BY4741 (BY, *met17*, data from Fig. S1A), W303-1A (W303, *MET17*) and DBY746 (DBY, *MET17*) were transformed with the indicated reporters and processes as in Fig. S1A for β-galactosidase assay. Data are mean ± SEM from three to five experiments.
Fig. S3. STRE-mediated promoter activation response to potassium starvation. Wild-type strain W303-1A and its *msn2 msn4* derivative (MCY5278, a generous gift from M. Carlson, Casado *et al*., 2011) were transformed with plasmid pGM18/17 (Marchler *et al*., 1993) allowing the integration of a (7x)STRE-LacZ element at the *URA3* locus. The strains were transferred for the indicated times to Translucent K^+-free medium either at room temperature or at 37°C (to induce a heat-shock response) and β-galactosidase activity measured. Data are mean SEM from three independent experiments performed by triplicate.
Fig. S4. Strain JC37-1A, which expresses a Rtg1-GFP version (Crespo *et al*., 2002), was grown to exponential phase in K^+-free medium (without ammonium sulfate and containing 5 mM glutamine as nitrogen source) supplemented with 50 mM KCl. Cells were washed and resuspended in fresh medium either with (+) or without (–) 50 mM KCl. One millilitre of samples were taken at different times (only results after 20 min are shown). Cells were fixed with 2% formaldehyde, harvested by centrifugation, washed two times with phosphate-buffered saline (PBS) solution, stained with 0.1 mg ml^{-1} DAPI (4′,6-diamidino-2-phenylindole) and finally resuspended in PBS. Samples were observed by using a Nikon Eclipse E800 fluorescence microscope and a FITC filter.
Fig. S5. Comparison of transcriptional changes in *trk1 trk2* and *hal4 hal5* mutants. The change in mRNA levels (log2 space) for genes related to sulfur metabolism presented in Fig. 2B in the main text, plus *CIT2* and *DLD3*, were plotted. *y*-axis represents data from this work, whereas *x*-axis represents data from Perez-Valle and colleagues (2010). The calculated correlation coefficient was 0.768.
Table S1. Oligonucleotides used in this work.
Table S2. Genes induced after potassium starvation. Log(2) values of the changes are listed for each time point of the experiment.
Table S3. Genes repressed after potassium starvation. Log(2) values of the changes are listed for each time point of the experiment.
Table S4. Genes induced or repressed in the *trk1 trk2* strain growing in 50 mM KCl. Log(2) values of the changes are listed for each time point of the experiment.

Please note: Wiley-Blackwell are not responsible for the content or functionality of any supporting materials supplied by the authors. Any queries (other than missing material) should be directed to the corresponding author for the article.

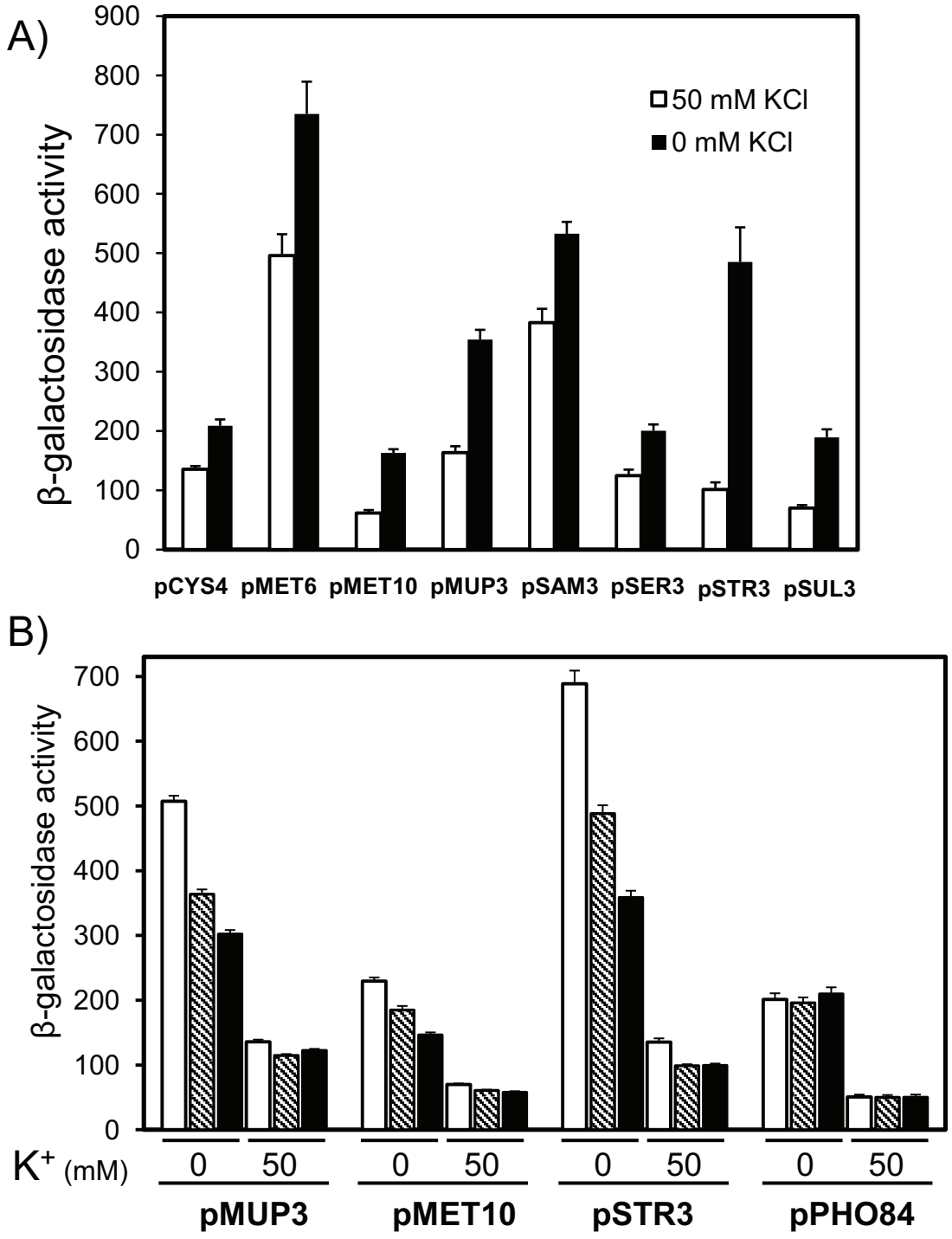

Supplementary Figure 1.- Potassium starvation activates the expression of genes related to the metabolism of sulfur-containing amino acids. (A) BY4741 wild type strain was transformed with reporter YEp357-based plasmids containing the entire promoters of indicated genes, transferred to K^+-free medium for 2 h and processed for measurement of β-galactosidase activity as described in Materials and Methods. (B) Methionine supplementation attenuates the induction of sulfur-related genes upon potassium starvation. The BY4741 wild type strain was transformed with indicated reporters and processed as above except that cells containing the pPHO84 reporter were collected after 90 min of potassium starvation. For this experiment the standard Translucent K^+-free medium, which contains 20 mg/l of Methionine (open bars) was made 40 mg/l (stripped bars) or 80 mg/l (closed bars). Data are mean ± SEM from 3 to 5 experiments.

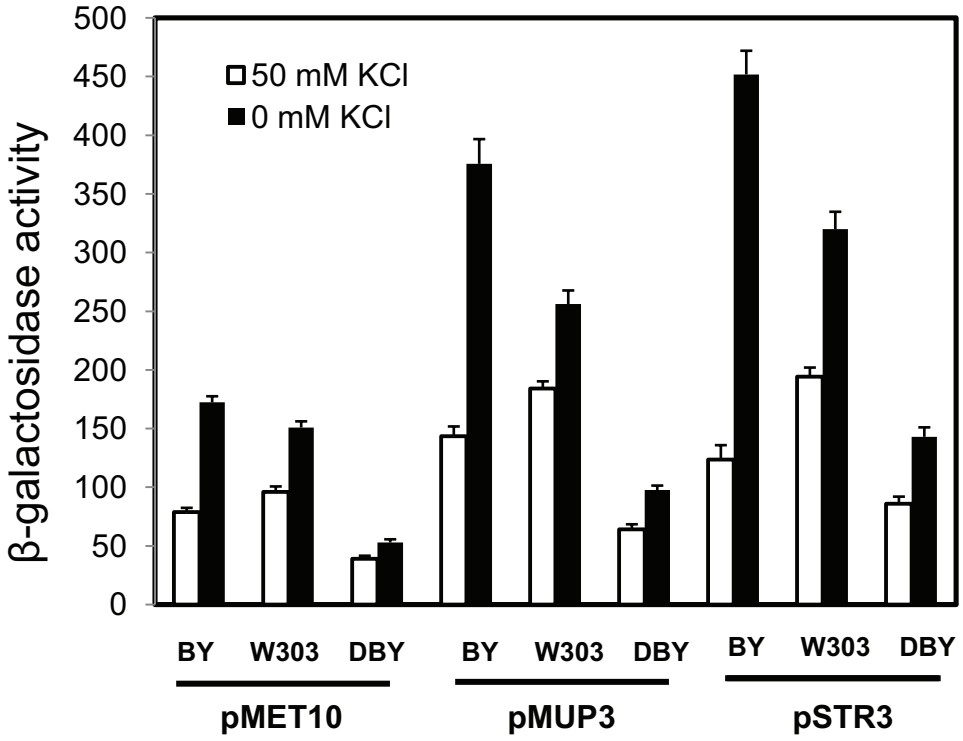

Supplementary Figure 2.- Induction of sulfur-related genes is also observed in *MET17* strains. Wild type strains BY4741 (BY, *met17*, data from Supp. Figure 1A), W303-1A (W303, *MET17*) and DBY746 (DBY, *MET17*) were transformed with the indicated reporters and processes as in Supp. Figure 1A for β-galactosidase assay. Data are mean ± SEM from 3 to 5 experiments.

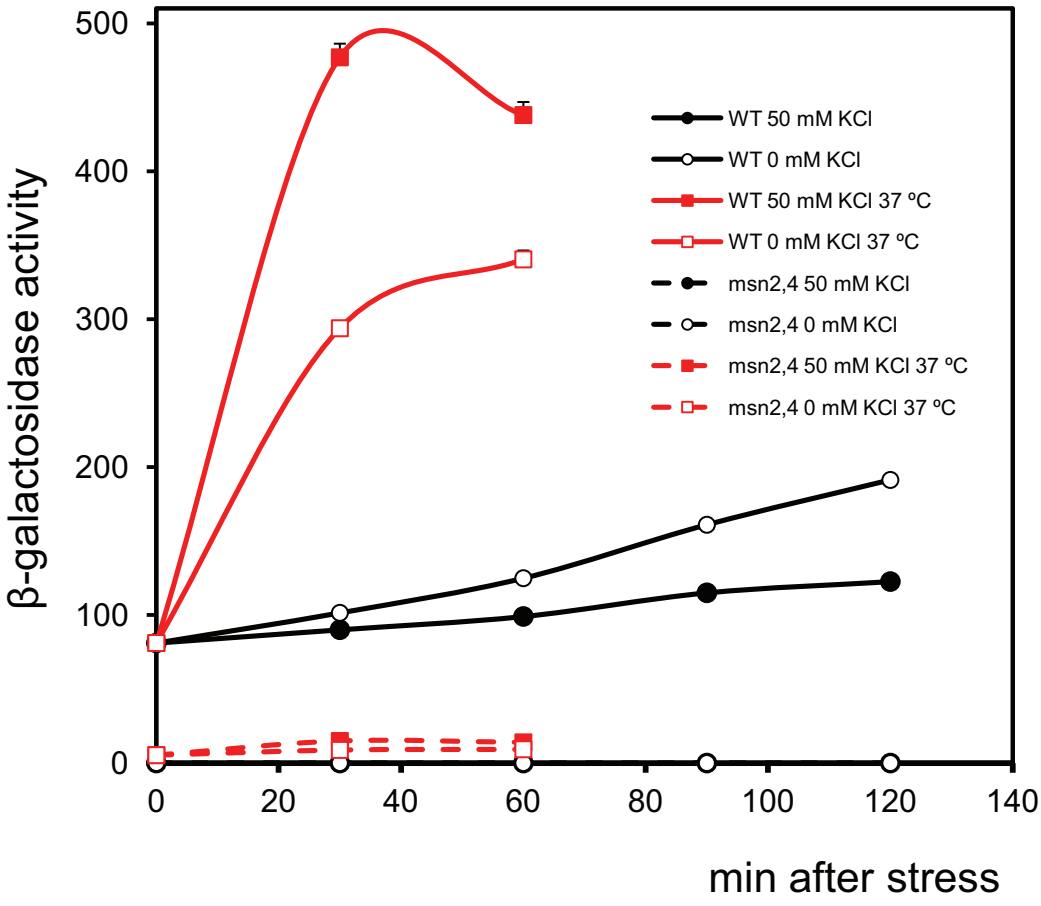

Supplementary Figure 3.- STRE-mediated promoter activation response to potassium starvation. Wild type strain W303-1A and its *msn2 msn4* derivative (MCY5278, a generous gift from M. Carlson, Casado *et al.*, 2011), were transformed with plasmid pGM18/17 (Marchler *et al.*, 1993) allowing the integration of a (7x)STRE-LacZ element at the *URA3* locus. The strains were transferred for the indicated times to Translucent K^+-free medium either at room temperature or at 37ºC (to induce a heat-shock response) and β–galactosidase activity measured. Data are mean SEM from 3 independent experiments performed by triplicate.

Casado,C., Gonzalez,A., Platara,M., Ruiz,A., and Arino,J. (2011). The role of the protein kinase A pathway in the response to alkaline pH stress in yeast. Biochem. J. 438, 523-533.

Marchler,G., Schuller,C., Adam,G., and Ruis,H. (1993). A Saccharomyces cerevisiae UAS element controlled by protein kinase A activates transcription in response to a variety of stress conditions. EMBO J. 12, 1997-2003.

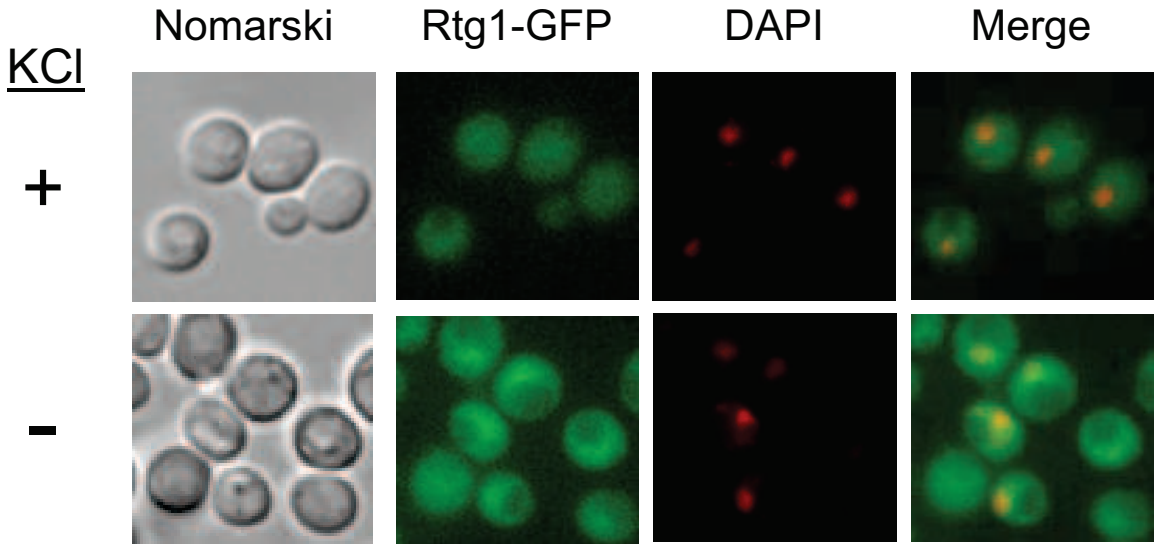

Supplementary Figure 4.- Strain JC37-1A, which expresses a Rtg1-GFP version (Crespo *et al*, 2002), was grown to exponential phase in K^+-free medium (without ammonium sulphate and containing 5 mM glutamine as nitrogen source) supplemented with 50 mM KCl. Cells were washed and resuspended either in fresh medium with (+) or without (-) 50 mM KCl. One ml samples were taken at different times (only results after 20 min are shown). Cells were fixed with 2 % formaldehyde, harvested by centrifugation, washed 2 times with phosphate-buffered saline (PBS) solution, stained with 0.1 mg/ml DAPI (4',6-diamidino-2-phenylindole) and finally resuspended in PBS. Samples were observed by using a Nikon Eclipse E800 fluorescence microscope and a FITC filter.

Crespo,J.L., Powers,T., Fowler,B., and Hall,M.N. (2002). The TOR-controlled transcription activators GLN3, RTG1, and RTG3 are regulated in response to intracellular levels of glutamine. Proc. Natl. Acad. Sci. U. S. A 99, 6784-6789.

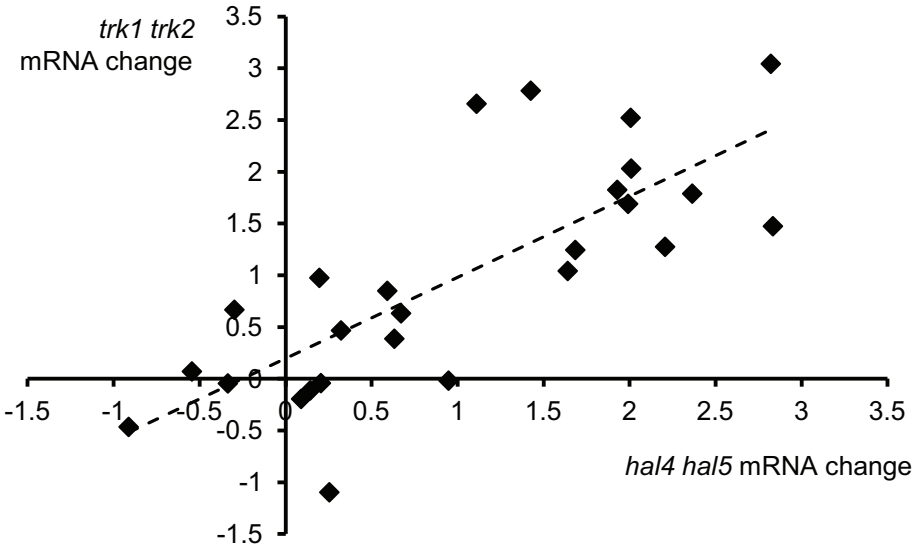

Supplementary Figure 5.- **Comparison of transcriptional changes in *trk1 trk2* and *hal4 hal5* mutants**.The change in mRNA levels (log2 space) for genes related to sulfur metabolism presented in Figure 2B in the main text, plus *CIT2* and *DLD3*, were plotted. Y axis represents data from this work, whereas X axis represents data from Perez-Valle at al, 2010. The calculated correlation coefficient was 0.768.

Perez-Valle,J., Rothe,J., Primo,C., Martinez,P.M., Arino,J., Pascual-Ahuir,A., Mulet,J.M., Serrano,R., and Yenush,L. (2010). Hal4 and Hal5 protein kinases are required for general control of carbon and nitrogen uptake and metabolism. Eukaryot. Cell 9, 1881-1890.

Supplemental Table 1. Oligonucleotides used in this work.

a) Oligonucleotides for LacZ reporter construction

Name	Sequence	Description
5´promCYS4	G**GAATTC**GTCTAATTTAGCTGAAG	5' promoter *CYS4* (-960 pb, added EcoRI)
3´promCYS4	AGA**CTGCAG**CTTAGCATAAATTTGTG	3' promoter *CYS4* (+71 pb added PstI)
5´promMET6	G**GAATTC**GGGTACTTTCTCTAC	5' promoter *MET6* (-923 pb, added EcoRI)
3´promMET6	CAC**AAGCTT**GAATAATTCATCGACAG	3' promoter *MET6* (+ 92 pb, added HindIII)
5´promMET10	G**GAATTC**TCGACAGAAAGGGGA	5' promoter *MET10* (-437 pb, added EcoRI)
3´promMET10	AGA**CTGCAG**CACAGATGAAATGGCA	3' promoter *MET10* +80 pb added PstI)
5´promMUP3	G**GAATTC**ACTCACGTGAGGGC	5' promoter *MUP3* (-471 pb, added EcoRI)
3´promMUP3	CG**GGATCC**AGTATTTGTGGAACCAT	3' promoter *MUP3* (+89 pb, added BamHI)
5´promSAM3	G**GAATTC**AACGAAGTATTGGTG	5' promoter *SAM3* -700 pb, added EcoRI)
3´promSAM3	AGA**CTGCAG**TGAACCAGATCTATCC	3' promoter *SAM3* (+ 80 pb, added PstI)
5´promSER3	AC**GGTACC**TCATTCAACTGTATAG	5' promoter *SER3* (-804 pb, added KpnI)
3´promSER3	GC**TCTAGA**TTGCGTAGGTGAAGTAC	3' promoter *SER3* (+ 80pb, added XbaI)
5´promSTR3	G**GAATTC**ATGCACTATACACGAAA	5' promoter *STR3* (-528 pb, added EcoRI)
3´promSTR3	CG**GGATCC**CGATCTGGAATAATC	3' promoter *STR3* (+ 153 pb, added BamHI)
5´promSUL2	G**GAATTC**TATGACGAGACTGTAGA	5' promoter *SUL2* (-481 pb, added EcoRI)
3´promSUL2	ACA**GTCGAC**GGTGTTGTTAGTTTCC	3' promoter *SUL2* (+50 pb, added SalI)

b) Oligonucleotides for RT-PCR

Name	Sequence	Description
CLN2_Fw	CAAGGAAAACCAAAATCCC	5´ oligo for RT-PCR, *CLN2* gene
CLN2_Rev	TACTTGGGTATTGCCCATAC	3´ oligo for RT-PCR, *CLN2* gene
CLN3_Fw	CTGTGCGTTCAAAAAGATTA	5´ oligo for RT-PCR, *CLN3* gene
CLN3_Rev	AGCGAGTTTTCTTGAGGTTG	3´ oligo for RT-PCR, *CLN3* gene
CLB1_Fw	GGTGGTTACACAAAGGCAAA	5´ oligo for RT-PCR, *CLB1* gene
CLB1_Rev	TCACTCATGCAATGTCATAA	3´ oligo for RT-PCR, *CLB1* gene
CLB2_Fw	CCCGTGTGTCACATGATAAT	5´ oligo for RT-PCR, *CLB2* gene
CLB2_Rev	AAGGTCATTATATCATAGCCG	3´ oligo for RT-PCR, *CLB2* gene
CLB5_Fw	TGGCAGTTACCTCACTTTTCA	5´ oligo for RT-PCR, *CLB5* gene
CLB5_Rev	ATTCTAAGGAAGTGAGCATGAAC	3´ oligo for RT-PCR, *CLB5* gene
CLB6_Fw	TGCCTGTTCATTGCCTGTAAA	5´ oligo for RT-PCR, *CLB6* gene
CLB6_Rev	GGGTTTGGTAGAGATATGTT	3´ oligo for RT-PCR, *CLB6* gene
CIT2_5_RT	TTGCCATGGACCATTTTCCA	5´ oligo for RT-PCR, *CIT2* gene
CIT2_3_RT	GCCCTTGAAACGCCAAATAA	3´ oligo for RT-PCR, *CIT2* gene
5'_DLD3_RT	AAGTCAGAGATTTTGATCCA	5´ oligo for RT-PCR, *DLD3* gene
3'_DLD3_RT	TCTTCCAAACCCAAAACATT	3´ oligo for RT-PCR, *DLD3* gene
RT_ACT1_up2	TGCTGTCTTCCCATCTATCG	5´ oligo for RT-PCR, *ACT1* gene
RT_ACT1_do2	ATTGAGCTTCATCACCAAC	3´ oligo for RT-PCR, *ACT1* gene

Genes induced by potassium starvation (log(2) values)

ID	NAME	10min	20min	40min	60min	120 min
YAL008W	FUN14	0.002	0.041	0.847	1.166	0.645
YAL012W	CYS3	0.509	0.578	1.328	1.643	1.756
YAL017W	PSK1	0.059	0.146	0.757	1.782	0.777
YAL027W	SAW1	0.615	0.003	0.742	0.319	1.783
YAL028W	FRT2	0.568	-0.229	1.047	1.843	2.379
YAL031C	GIP4	0.418	0.006	0.381	0.766	1.168
YAL040C	CLN3	0.587	0.312	0.829	1.554	1.878
YAL051W	OAF1	0.142	0.084	0.161	0.857	1.053
YAL060W	BDH1	0.395	0.401	1.218	1.784	1.637
YAL062W	GDH3	-0.230	0.175	0.104	0.918	1.015
YAL063C	FLO9	-0.138	0.110	-0.254	1.007	0.359
YAR027W	UIP3	-0.338	-0.134	0.729	0.971	1.095
YAR028W		-0.777	-0.509	0.906	1.778	2.824
YAR031W	PRM9	0.112	0.081	0.177		1.161
YAR042W	SWH1	0.441	-0.085	0.321	-0.304	1.119
YAR050W	FLO1	-0.512		-0.581	1.280	0.179
YAR071W	PHO11	1.485	1.572	1.952	1.667	1.667
YBL015W	ACH1	1.892	1.324	2.322	3.618	2.349
YBL016W	FUS3	0.472	0.769	1.012	1.921	1.588
YBL043W	ECM13	0.202	0.169	0.481	-0.247	1.283
YBL045C	COR1	0.491	0.523	0.902	2.208	0.503
YBL062W		0.076	0.670	0.275		1.018
YBL064C	PRX1	0.253	0.491	1.747	2.083	2.215
YBL078C	ATG8	0.152	0.090	1.620	3.802	3.111
YBL086C		0.309	-0.082	0.695	1.117	0.591
YBL095W		0.127	0.168	0.486	-0.318	1.283
YBL101C	ECM21	-0.014	-0.007	0.785	0.763	1.313
YBR001C	NTH2	-0.169	-0.704		1.393	1.032
YBR006W	UGA2	0.394	0.158	1.200	4.064	1.445
YBR012C		-0.017		1.759	2.325	1.910
YBR026C	ETR1	-0.079	0.112	0.606	1.065	0.706
YBR040W	FIG1	0.831	0.254	0.523	0.106	1.749
YBR045C	GIP1	0.113	0.009	-0.081		1.716
YBR052C	RFS1	-0.370	-0.078	0.796	1.031	0.401
YBR053C		0.104	0.155	1.206	1.955	1.244
YBR054W	YRO2	1.835	2.359	3.214	4.183	3.598
YBR056W		0.097	0.031	1.058	1.801	0.917
YBR059C	AKL1	-0.283	-0.108	0.518	1.070	0.525
YBR065C	ECM2	0.028	0.134	0.140	0.577	1.057
YBR066C	NRG2	-0.034	-0.151	0.440	1.578	1.452
YBR067C	TIP1	0.451	0.337	1.053	1.335	2.063
YBR072W	HSP26	-2.915	-1.553	1.164	4.109	4.661
YBR083W	TEC1	0.454	0.614	0.913	1.682	2.466
YBR085W	AAC3	0.387	0.022	0.477	-0.015	1.368
YBR093C	PHO5	1.567	1.638	2.171	2.356	2.463
YBR096W		-0.423	-0.405	0.247	0.798	1.540
YBR098W	MMS4	0.200	-0.759	0.316	-0.662	2.247

YBR105C	VID24	0.012	0.003	0.611	1.279	1.710
YBR108W		0.338	0.114	0.771	1.113	0.671
YBR114W	RAD16		-0.246	-0.387	0.878	1.245
YBR117C	TKL2	1.237		1.770	4.028	3.895
YBR126C	TPS1	0.755	0.399	1.853	2.731	1.501
YBR132C	AGP2	0.592	0.479	0.983	1.640	0.657
YBR139W		0.175	-0.180	0.466	1.112	0.563
YBR145W	ADH5	0.832	1.347	1.800	1.559	1.228
YBR147W		0.150	0.356	0.587	0.617	1.482
YBR161W	CSH1	0.615	0.410	0.788	1.081	1.138
YBR165W	UBS1	0.401	0.130	0.434	-0.171	1.028
YBR166C	TYR1	0.116	-0.055	0.253	-0.123	1.023
YBR169C	SSE2	0.719	0.362	1.645	3.184	1.958
YBR170C	NPL4	-0.070	-0.005	0.498	1.480	0.788
YBR183W	YPC1	0.777	0.307	1.121	1.089	1.369
YBR204C		0.291	0.219	0.618	1.247	1.019
YBR211C	AME1	0.400	0.105	0.536	-0.430	1.388
YBR212W	NGR1	0.108	-0.282	0.421	1.118	0.632
YBR214W	SDS24	0.725	0.186	1.274	1.646	1.067
YBR216C	YBP1	0.110	0.087	0.373	1.082	0.647
YBR222C	PCS60	0.414	0.542	0.967	1.509	1.691
YBR223C	TDP1	0.321	0.196	0.445	1.242	0.391
YBR225W		0.459	0.190	0.694	1.516	1.271
YBR230C	OM14	-0.300	-0.208	1.107	1.532	1.009
YBR237W	PRP5	-0.218	-0.053	-0.060	1.047	0.782
YBR241C		0.047	0.109	0.802	1.337	1.218
YBR256C	RIB5	-0.111	0.222	0.612	0.881	1.165
YBR269C		0.076	0.195	0.742	1.196	1.167
YBR284W		-0.122	-0.726		1.996	1.285
YBR285W		-0.853		0.542	3.395	2.233
YBR287W		0.544	0.353	1.120	1.510	1.265
YBR293W	VBA2	0.236	0.590	0.480	0.861	1.556
YBR294W	SUL1	0.098	0.127	0.664	2.700	3.354
YBR297W	MAL33	0.602	0.633	0.898	2.056	2.329
YCL014W	BUD3	0.361	-0.175	0.368	-0.631	1.115
YCL020W		0.735	0.380	0.849	0.509	1.581
YCL021W-A		-0.483	-0.017	-0.506		0.997
YCL027C-a		-1.174		1.484	3.376	2.629
YCL027W	FUS1	1.026	1.160	1.732	2.458	2.985
YCL030C	HIS4	0.594	1.130	1.642	2.340	1.683
YCL035C	GRX1	-0.007	-0.013	1.118	1.504	1.508
YCL040W	GLK1	0.644	0.293	1.882	2.785	1.310
YCL048W	SPS22		1.216	1.401	2.192	1.375
YCL049C		0.152	-0.057	0.430	0.192	1.089
YCL055W	KAR4	0.362	0.813	1.227	1.764	2.677
YCL059C	KRR1	0.188	0.038	-0.617	-0.722	1.494
YCLX07W		0.467	0.772	0.976		2.104
YCR005C	CIT2	2.689	3.661	3.358	5.610	4.342
YCR009C	RVS161	0.374	0.259	0.862	1.534	1.010
YCR021C	HSP30	1.140	0.666	2.053	3.966	3.192

YCR051W		0.398	0.255	1.007	1.169	1.712
YCR082W	AHC2	-0.054	-0.145	0.337	0.767	1.025
YCR083W	TRX3	0.445	0.153	0.839	1.183	2.182
YCR089W	FIG2	0.653	0.140	0.436	2.100	3.348
YCR091W	KIN82	0.678	-0.334	0.680	2.284	1.618
YDL006W	PTC1	0.035	-0.208	-0.465	1.547	0.749
YDL014W	NOP1	0.541	0.249	1.698	1.990	1.255
YDL022W	GPD1	0.829	0.684	1.648	1.436	-0.189
YDL023C		0.914	0.722	1.715	2.012	-0.007
YDL027C		0.394	0.200	0.593	1.241	0.886
YDL054C	MCH1	-0.823	-0.020	0.080		1.088
YDL059C	RAD59	0.626	0.719	1.570	2.804	2.446
YDL072C	YET3	0.089	-0.028	0.642	1.011	0.837
YDL079C	MRK1	-0.065	-0.274	0.093	1.492	2.528
YDL085W	NDE2	-0.207	0.237	0.489	1.561	2.002
YDL113C	ATG20	0.290	0.293	0.609	1.473	0.935
YDL115C	IWR1	0.156	0.143	0.589	0.931	1.031
YDL124W		0.417	0.339	1.588	2.021	1.268
YDL127W	PCL2	-0.099	0.090	-0.213	0.207	1.161
YDL142C	CRD1	-0.007	0.234	0.305	1.056	1.376
YDL147W	RPN5	0.154	-0.060	0.441	1.145	0.805
YDL149W	ATG9	0.076	-0.082	0.250	1.247	1.376
YDL174C	DLD1	0.152	0.249	0.390	1.172	1.008
YDL181W	INH1	-0.091	0.174	0.706	1.340	
YDL204W	RTN2	0.821	0.104	1.405	2.409	1.784
YDL210W	UGA4	-0.106	-0.069	-0.017		1.017
YDL215C	GDH2	0.388	0.360	0.867	1.460	2.173
YDL220C	CDC13	0.411	-0.105	0.165	-0.859	1.203
YDL222C	FMP45	1.309	-0.288	2.840	3.978	3.365
YDL223C	HBT1	-0.133	-0.223	0.363	2.169	3.127
YDL234C	GYP7	0.497	-0.194	0.245	1.795	1.254
YDL240W	LRG1	0.423	0.119	0.493	0.840	1.296
YDR001C	NTH1	0.817	0.215	1.209	2.161	1.582
YDR003W	RCR2	-0.387	-0.143	0.592	1.228	1.057
YDR022C	CIS1	-1.335		0.206	1.345	0.771
YDR031W	MIC14	0.163	-0.371	-0.084		1.229
YDR033W	MRH1	0.804	0.444	0.726	1.023	0.372
YDR043C	NRG1	0.818	0.470	1.645	2.482	3.121
YDR046C	BAP3	0.261	1.019	0.096	0.191	-0.913
YDR055W	PST1	0.480	-0.227	0.580	2.662	2.220
YDR058C	TGL2	1.023	0.090	0.408	1.331	1.388
YDR059C	UBC5	-0.431	-0.670	0.395	1.076	1.162
YDR067C		-0.086	0.229	0.469	1.051	1.089
YDR074W	TPS2	1.676	-0.074	2.111	2.724	1.410
YDR096W	GIS1	0.869	-0.596	0.925	1.849	0.755
YDR122W	KIN1	-0.173	-0.160	0.516	1.097	0.949
YDR129C	SAC6	0.249	-0.106	0.252	1.053	-0.394
YDR148C	KGD2	0.443	0.287	0.555	1.103	0.247
YDR168W	CDC37	0.292	0.209	0.270	1.140	-0.027
YDR171W	HSP42	0.378	0.084	1.145	1.725	0.943

YDR178W	SDH4	0.387	0.325	1.272	1.597	1.759
YDR216W	ADR1	1.306	1.364	0.664	2.641	2.028
YDR230W		-0.065	-0.407	0.457	0.412	1.104
YDR231C	COX20	-0.099	-0.409	0.481	0.855	1.425
YDR247W	VHS1	1.322	-0.143	1.481	2.873	2.884
YDR248C		0.246	0.455	0.861	1.415	0.295
YDR251W	PAM1	0.166	-0.064	0.430	1.142	0.759
YDR253C	MET32	0.292		1.225	2.530	2.210
YDR254W	CHL4	-0.439	-0.146	-0.008	1.160	0.528
YDR258C	HSP78	0.422	0.272	1.764	2.820	1.253
YDR261C	EXG2	0.199	0.021	0.409	0.952	1.064
YDR262W		0.334	0.332	0.876	1.378	2.117
YDR272W	GLO2	-0.042	0.080	0.530	1.204	0.788
YDR293C	SSD1	0.168	-0.165	0.658	1.645	1.324
YDR330W	UBX5	0.243	0.041	0.442	1.169	0.283
YDR335W	MSN5	-0.134	-0.087	0.502	1.002	0.626
YDR342C	HXT7	0.144	0.541	-0.046	0.849	1.406
YDR343C	HXT6	0.245	0.218	0.380	-0.050	1.147
YDR345C	HXT3	0.533	1.086	-0.308	0.206	0.684
YDR350C	ATP22	0.069	0.037	0.172	1.105	0.973
YDR358W	GGA1	0.688	0.120	1.046	1.938	1.184
YDR368W	YPR1	0.298	0.221	0.698	1.169	0.645
YDR379W	RGA2	0.144	0.091	0.169	1.174	0.902
YDR391C		0.409	0.234	1.266	1.980	1.674
YDR394W	RPT3	-0.036	-0.235	0.288	1.032	0.242
YDR409W	SIZ1	0.434	-0.066	0.539	-0.507	1.055
YDR436W	PPZ2	0.219	-0.134	0.815	1.586	1.007
YDR453C	TSA2	0.625	0.425	1.960	2.818	3.189
YDR474C		0.317	0.401	0.690	1.249	0.736
YDR479C	PEX29	0.217	0.468	0.629	1.106	0.677
YDR481C	PHO8	0.919	1.067	1.402	1.861	1.968
YDR502C	SAM2	0.990	0.799	1.273	1.807	-0.272
YDR516C	EMI2	0.307	0.273	0.742	1.863	0.887
YDR530C	APA2	0.968	0.541	1.115	2.459	2.506
YDR533C	HSP31	0.068	0.135	1.009	1.903	2.432
YEL005C	VAB2	0.161	0.129	0.506	-0.195	1.161
YEL011W	GLC3	0.357	0.000	1.664	3.366	2.546
YEL012W	UBC8	0.047	0.089	0.777	1.498	1.029
YEL020C		0.270	-0.023	0.295	1.242	0.485
YEL024W	RIP1	0.080	0.282	0.712	1.073	0.674
YEL039C	CYC7	0.024	-0.707	0.905	2.004	1.003
YEL044W	IES6	0.210	0.117	0.628	1.008	1.135
YEL045C		-0.258	-0.263	0.052	0.558	1.253
YEL060C	PRB1	0.493	-0.030	1.332	2.366	1.647
YEL071W	DLD3	1.481	2.242	1.989	3.006	2.622
YER020W	GPA2	0.228	0.068	0.715	1.548	1.056
YER035W	EDC2	-0.141	-0.150	1.074	1.275	0.453
YER037W	PHM8	0.706	0.481	1.235	1.214	1.631
YER039C	HVG1	0.166	0.046	0.461	-0.536	1.077
YER042W	MXR1	0.656	1.227	1.887	2.746	2.475

YER045C	ACA1	0.178	0.096	0.345		1.038
YER052C	HOM3	0.748	1.007	1.464	1.589	1.529
YER053C	PIC2	0.848	0.284	1.858	2.934	2.517
YER054C	GIP2	0.299	-0.670	0.815	2.319	1.739
YER062C	HOR2	0.042	0.312	1.026	0.842	0.472
YER067W		1.550	0.498	2.435	4.576	4.058
YER072W	VTC1	0.422	0.603	1.010	0.754	1.695
YER078C		0.071	0.099	0.437	1.094	0.240
YER079W		0.348	0.280	1.310	1.061	0.940
YER081W	SER3	1.475	1.357	3.274	4.103	3.536
YER087W		0.146	0.120	0.541	1.512	0.956
YER088C	DOT6	0.407	0.078	0.465	0.484	1.089
YER091C	MET6	1.600	1.349	2.232	2.547	1.799
YER092W	IES5	0.229	0.783	0.952	1.598	1.389
YER098W	UBP9	0.308	0.110	0.477	2.419	1.305
YER103W	SSA4	-1.982	-0.829	1.721	4.018	2.932
YER115C	SPR6	0.186	0.577	0.511	0.092	1.082
YER116C	SLX8	0.091	0.163	0.512	-0.263	1.033
YER125W	RSP5	1.071	0.773	1.218	1.837	1.276
YER138C		0.223	0.066	0.275	1.598	0.584
YER143W	DDI1	0.046	0.049	0.575	1.022	0.334
YER150W	SPI1	0.023	0.244	2.201	3.257	3.436
YER158C		0.297	-0.456	0.645	1.499	1.176
YER159C	BUR6	0.514	0.422	0.705	1.065	1.139
YER160C		0.223	0.021	0.303	1.698	0.816
YER162C	RAD4	0.081	0.098	0.491	2.208	0.594
YER163C		-0.114	0.087	0.765	1.338	1.044
YER169W	RPH1	-0.220	-0.106	0.254	2.377	0.930
YER175C	TMT1	0.268	0.957	1.721	1.241	1.509
YER182W		0.585	0.181	0.660	0.584	1.060
YFL014W	HSP12	-1.729	-1.385	1.171	1.306	1.639
YFL015C		0.145	0.592	1.687	2.622	2.726
YFL016C	MDJ1	0.224	-0.045	0.718	1.635	0.400
YFL028C	CAF16	0.233	0.218	0.499	0.464	1.063
YFL032W		-0.163	0.152	0.275	0.149	1.667
YFL042C		0.469	0.148	0.590	1.304	0.582
YFL053W	DAK2	0.057	0.184	-0.023	0.181	1.435
YFL054C		0.203	-0.216	0.609	2.032	2.141
YFL055W	AGP3	-0.040	0.185	0.498	1.853	2.426
YFL056C	AAD6		-0.065	-0.645	1.819	2.079
YFL058W	THI5	-1.223	0.159	-0.094		1.558
YFR003C	YPI1	0.186	0.251	1.104	1.792	1.570
YFR014C	CMK1	0.243	0.054	0.595	0.203	1.056
YFR015C	GSY1	0.131	-0.502	0.619	2.051	0.409
YFR016C		-0.195	-0.086	0.202	1.401	0.230
YFR017C		0.307	0.066	0.661	0.807	1.283
YFR020W		0.366	-0.074	0.405	-0.408	1.229
YFR022W	ROG3	-0.205	0.234	0.673	1.854	1.755
YFR030W	MET10	0.970	1.187	2.752	4.036	4.427
YFR033C	QCR6	0.062	0.675	0.740	1.026	0.549

YFR043C	IRC6	0.217	0.145	0.572	-0.330	1.160
YFR047C	BNA6	0.137	0.274	0.622	0.756	1.231
YFR053C	HXK1	1.866	1.499	2.074	3.021	1.950
YFR054C		0.517	0.142	0.788	0.395	1.355
YGL005C	COG7	0.289	0.144	0.537	-0.414	1.034
YGL006W	PMC1	0.222	-0.002	0.549	1.293	0.930
YGL010W		-0.749	-0.528	0.521		1.311
YGL015C		-0.188	-0.276	1.070	1.925	1.590
YGL032C	AGA2	0.531	0.604	1.349	1.263	3.097
YGL036W		0.364	0.110	0.678	1.318	0.851
YGL037C	PNC1	-0.215	-0.069	1.722	2.455	1.090
YGL041C		0.012	-0.053	0.201	0.216	1.331
YGL045W	RIM8	0.083	0.235	0.100	0.692	1.423
YGL046W		0.917	-0.122	0.475	-0.198	1.214
YGL050W	TYW3	0.295	0.122	0.501	-0.596	1.140
YGL053W	PRM8	0.465	0.341	0.896	1.148	1.800
YGL056C	SDS23	0.258	0.497	0.558	0.502	1.040
YGL059W	PKP2	0.629	0.627	1.022	1.487	1.545
YGL062W	PYC1	0.648	1.095	2.013	2.587	1.893
YGL081W		0.284	0.112	0.622	0.233	1.020
YGL085W		0.303	0.189	0.628	-0.479	1.352
YGL088W		0.586	0.072	1.009	-0.265	1.994
YGL095C	VPS45	-0.039	0.106	0.414	1.141	0.639
YGL104C	VPS73	-0.056	0.088	0.941	1.721	1.136
YGL108C		-0.090	0.427	0.368	0.258	1.227
YGL117W		0.606	1.141	1.624	0.671	1.627
YGL121C	GPG1	0.588	0.651	2.971	3.433	3.765
YGL125W	MET13	1.135	1.047	1.768	2.068	1.622
YGL141W	HUL5	0.377	0.288	0.560	1.055	1.112
YGL156W	AMS1	0.347	-0.022	1.304	2.321	2.516
YGL157W		0.374	0.280	1.079	1.284	0.597
YGL164C	YRB30	0.257	0.073	0.539	1.054	0.762
YGL166W	CUP2	0.328		2.293	2.584	3.366
YGL180W	ATG1	0.321	0.032	0.723	2.572	1.802
YGL184C	STR3	2.488	3.887	3.564	4.885	4.269
YGL194C	HOS2	0.504	0.302	0.532	0.860	1.168
YGL208W	SIP2	-0.150	-0.020	0.272	1.118	0.797
YGL215W	CLG1	0.158	0.150	0.437	0.229	1.088
YGL218W		0.107	0.277	0.456	-0.204	1.211
YGL224C	SDT1	0.175	0.181	0.609	-0.304	1.183
YGL227W	VID30	0.839	0.151	1.057	2.041	0.804
YGL240W	DOC1	0.332	0.175	0.518	-0.496	1.304
YGL247W	BRR6	-0.159	-0.238	-0.527	-0.031	1.095
YGL248W	PDE1	0.593	0.856	1.658	2.216	2.266
YGL250W	RMR1	0.081	0.053	0.358	-0.151	1.034
YGL253W	HXK2	0.786	1.078	0.608	0.045	-0.657
YGR008C	STF2	0.730	0.548	1.873	2.904	1.914
YGR019W	UGA1	0.614	0.709	1.392	2.082	1.464
YGR022C		0.297	0.050	0.209	0.397	1.043
YGR023W	MTL1	1.164	0.338	1.274	1.706	2.086

YGR032W	GSC2	-0.293	0.109	0.118	1.738	2.376
YGR042W		0.228	0.039	0.449	-0.094	1.188
YGR043C		0.468	0.141	4.084	4.919	4.859
YGR044C	RME1	0.339	0.129	0.901	1.035	0.643
YGR048W	UFD1	-0.162	-0.166	0.671	1.992	0.595
YGR052W	FMP48	1.542	0.954	2.475	2.697	0.692
YGR053C		0.467	0.204	0.527	-0.001	1.432
YGR055W	MUP1	0.631	1.720	1.406	1.717	1.664
YGR065C	VHT1	0.213	0.830	0.812	1.211	0.645
YGR066C		0.513	0.213	0.713	-0.022	1.705
YGR070W	ROM1	0.458	-0.372	0.712	1.676	1.551
YGR087C	PDC6	0.482	0.629	0.382	2.994	3.962
YGR088W	CTT1	1.138	0.347	2.093	3.103	2.509
YGR092W	DBF2	0.145	0.227	0.449	1.227	0.820
YGR096W	TPC1	0.468	0.304	0.365	0.298	1.204
YGR097W	ASK10	0.625	0.797	0.952	0.915	1.653
YGR100W	MDR1	0.246	-0.473	0.315	1.257	0.608
YGR110W		-0.460	-0.151	0.204	2.083	0.926
YGR120C	COG2	0.160	0.157	0.451	-0.424	1.035
YGR127W		0.576	0.069	1.163	0.991	1.854
YGR136W	LSB1	0.160	0.353	0.920	1.052	0.929
YGR138C	TPO2	0.219	1.119	0.626	1.042	0.835
YGR142W	BTN2	0.877	-0.910	0.956	1.974	0.903
YGR143W	SKN1	0.426	0.283	0.753	1.328	1.033
YGR144W	THI4	0.210	-0.015	0.536	-0.027	1.897
YGR146C		1.628	1.510	1.692	2.573	3.485
YGR147C	NAT2	0.389	0.198	0.631	-0.144	1.079
YGR155W	CYS4	0.497	0.768	0.759	1.017	0.992
YGR161C	RTS3	0.645	0.491	1.253	0.950	1.741
YGR164W		0.371	0.043	0.648	-0.858	1.405
YGR170W	PSD2	0.007	-0.117	0.205	1.100	0.083
YGR174C	CBP4	0.164	0.028	0.261	-0.018	1.427
YGR183C	QCR9	-0.201	0.306	0.639	0.522	1.080
YGR194C	XKS1	0.310	-0.050	1.034	1.771	0.755
YGR200C	ELP2	0.251	0.024	0.739	1.166	0.676
YGR201C		-0.176	0.014	0.461		1.374
YGR204W	ADE3	0.812	0.671	1.282	1.794	1.421
YGR213C	RTA1	0.103	0.162	0.436	-0.340	1.419
YGR226C		0.438	0.244	0.630	-0.635	1.260
YGR230W	BNS1	0.128	-0.124	0.236	-0.521	1.082
YGR233C	PHO81	0.354	0.465	0.710	1.124	1.698
YGR236C	SPG1	0.154	0.087	0.546	-0.593	1.479
YGR237C		0.687	0.125	0.980	1.866	1.137
YGR242W		0.277	-0.060	0.401	-0.214	1.225
YGR243W	FMP43	0.758	0.678	1.038	1.071	0.763
YGR248W	SOL4	-0.679	-0.341	1.893	2.746	1.385
YGR255C	COQ6	-0.035	-0.043	0.621	1.080	0.331
YGR256W	GND2	0.353	0.104	1.029	2.523	2.351
YGR258C	RAD2	0.447	0.187	0.346	1.433	1.134
YGR262C	BUD32	0.276	0.196	0.551	-0.533	1.123

YGR269W		0.666	0.226	0.580	-0.594	2.105
YGR278W	CWC22	0.137	-0.122	-0.374	1.707	
YHL018W		0.479	0.134	0.400	0.302	2.040
YHL021C	AIM17	1.333	0.944	2.681	4.133	2.637
YHL036W	MUP3	1.456	1.850	2.585	5.792	3.769
YHL037C		0.652	0.182	0.467	-0.620	1.611
YHL040C	ARN1	-0.115	0.157	0.094	0.392	1.263
YHL041W		0.923	0.257	0.727	-0.205	2.777
YHL045W		0.604	0.038	0.605	1.369	0.533
YHL047C	ARN2	-0.021	-0.251	-0.071	0.451	1.002
YHR001W-A	QCR10	0.110	-0.334	1.215	0.910	0.869
YHR005C	GPA1	-0.001	0.140	0.392	0.829	1.254
YHR008C	SOD2	0.487	0.473	1.404	1.259	1.262
YHR016C	YSC84	0.083	0.088	0.898	1.683	0.419
YHR018C	ARG4	0.101	0.973	1.463	1.607	0.751
YHR022C		0.630	0.177	0.875	-0.233	1.378
YHR027C	RPN1	-0.134	-0.188	-0.386	1.299	-0.256
YHR030C	SLT2	0.003	0.000	0.436	1.124	0.981
YHR038W	RRF1	0.438	0.154	0.676	-0.431	1.346
YHR046C	INM1	0.522	0.305	0.547	-0.398	1.301
YHR055C	CUP1-2	-0.068	-0.110	0.587	0.225	1.205
YHR062C	RPP1	0.469	0.109	0.386	-0.794	1.401
YHR071W	PCL5	0.486	0.903	1.797	1.417	2.025
YHR080C		-0.010	-0.207	0.494	1.354	0.669
YHR087W		0.717	0.692	3.263	3.669	2.941
YHR090C	YNG2	0.244	0.192	0.555	-0.187	1.119
YHR092C	HXT4	1.011	1.516	0.556	1.479	2.786
YHR095W		0.534	-0.452	0.143	-0.399	2.185
YHR096C	HXT5	0.641		1.023	3.553	2.195
YHR104W	GRE3	-0.299	-0.198	1.363	2.182	1.564
YHR105W	YPT35	0.156	0.113	0.400	-0.531	1.664
YHR106W	TRR2	0.253	0.632	0.774	1.609	1.460
YHR112C		0.556	0.735	1.864	2.771	2.889
YHR113W		0.282	0.005	0.880	1.279	1.001
YHR126C		0.293	0.175	0.544	0.468	1.679
YHR136C	SPL2	0.630	0.280	0.807	-0.350	2.008
YHR138C		0.236	-0.017	0.782	0.631	1.603
YHR140W		-0.276	-0.108	0.510	-0.086	1.212
YHR145C		0.433	0.108	0.622	-0.196	1.626
YHR148W	IMP3	0.085	0.141	0.103	-0.670	1.074
YHR156C	LIN1	0.214	0.055	-0.127	1.296	-0.244
YHR157W	REC104	0.236	0.031	0.514	-0.411	1.426
YHR161C	YAP1801	0.413	0.469	1.073	2.211	1.709
YHR173C		0.431	0.076	0.494	-0.704	1.562
YHR176W	FMO1	0.069		0.969	2.766	2.508
YHR180W		0.522	0.191	0.633	-0.344	1.353
YHR195W	NVJ1	0.419	0.126	0.765	0.522	1.143
YHR198C		0.049	0.001	0.687	0.825	1.043
YHR209W		0.072	-0.179	0.685	1.066	1.311
YHR212C		0.279	0.024	0.302	0.200	1.626

YHR215W	PHO12	1.554	1.622	1.936	1.802	1.640
YIL008W	URM1	0.212	0.067	-0.024	-0.691	1.001
YIL009C-A	EST3	-0.241	0.013	0.627	0.334	1.136
YIL012W		-0.055	-0.066	0.160	-0.632	1.220
YIL015W	BAR1	0.575	0.651	0.872	1.609	1.876
YIL017W		0.634	-0.207	0.642	1.646	0.947
YIL029C		0.263	0.201	0.474	0.092	2.013
YIL033C	BCY1	0.390	0.053	0.384	1.072	0.254
YIL036W	CST6	0.551	0.150	0.755	1.138	1.258
YIL042C	PKP1	0.303	0.156	0.697	0.468	1.046
YIL045W	PIG2	0.384	-0.128	0.815	2.782	1.833
YIL046W	MET30	0.149	0.147	0.654	1.751	2.024
YIL049W	DFG10	-0.080	-0.049	0.488	0.239	1.298
YIL053W	RHR2	0.936	1.342	1.053	-0.214	-0.911
YIL055C		0.180	0.248	1.028	1.730	1.651
YIL056W	VHR1	0.164	0.070	0.419	1.028	0.865
YIL059C		0.301	0.081	0.326	-0.366	1.072
YIL060W		0.183	0.239	0.491	-0.142	1.545
YIL065C	FIS1	0.155	0.044	0.639	0.033	1.097
YIL066C	RNR3	0.372	-0.048	0.406	-0.469	1.100
YIL074C	SER33	0.799	0.865	1.951	3.152	2.360
YIL079C	AIR1	0.000	0.082	-0.017	-0.088	1.495
YIL082W		0.686	0.679	1.145	1.295	2.845
YIL083C		0.835	0.786	0.585		1.927
YIL086C		0.825	0.263	0.084	-0.083	2.361
YIL087C		-0.179	0.282	1.016	1.145	1.409
YIL101C	XBP1	0.695	-0.413	0.773	1.185	0.996
YIL107C	PFK26	-0.065	-0.399	0.454	1.844	1.238
YIL108W		0.241	0.083	0.625	1.080	0.501
YIL112W	HOS4	0.676	1.491	2.060	3.200	3.260
YIL113W	SDP1	-0.606	-1.318		0.498	1.770
YIL116W	HIS5	0.431	0.685	1.285	1.314	1.570
YIL117C	PRM5	0.503	0.523	1.264	1.689	2.236
YIL125W	KGD1	0.172	-0.252	0.482	1.087	0.659
YIL135C	VHS2	0.729	-0.075	0.537	-0.321	1.476
YIL136W	OM45	0.397	0.013	1.190	0.799	1.481
YIL144W	TID3	-0.515	-0.402	0.303	1.187	1.863
YIL152W		0.069	0.301	0.604	1.177	1.022
YIL153W	RRD1	0.095	0.238	0.500	1.238	0.466
YIL154C	IMP2'	0.360	0.307	0.925	1.339	0.224
YIL164C	NIT1	0.135	0.984	1.457	1.797	2.731
YIR002C	MPH1	0.286	-0.270	0.056	1.037	0.735
YIR016W		-0.190	0.140	0.610	1.273	1.096
YIR017C	MET28	1.594	2.383	3.639	4.231	3.726
YIR018W	YAP5	0.475	0.882	1.369		2.252
YIR034C	LYS1	-0.346	0.085	1.183		-0.604
YIR038C	GTT1	-0.302	-0.237	0.407	0.546	1.096
YJL016W		-0.026	-0.338	0.838	2.157	2.288
YJL017W		0.197	0.128	0.804	1.504	2.009
YJL031C	BET4	0.102	0.266	0.544	1.272	0.437

YJL036W	SNX4	0.266	0.049	0.759	1.780	0.396
YJL048C	UBX6	0.720	0.608	1.266	2.351	1.825
YJL053W	PEP8	0.119	0.398	0.698	1.192	0.597
YJL057C	IKS1	0.528	0.104	1.020	2.770	1.839
YJL060W	BNA3	0.839	0.947	1.946	2.604	2.039
YJL066C	MPM1	0.221	0.222	0.948	1.494	1.012
YJL083W	TAX4		0.031	0.381	1.076	0.817
YJL084C	ALY2	0.307	-0.166	0.316	-1.035	1.224
YJL101C	GSH1	0.441	0.482	0.890	1.666	1.241
YJL108C	PRM10	0.281		0.468	1.593	1.198
YJL116C	NCA3	0.899	0.660	1.141	2.062	2.239
YJL141C	YAK1	0.952	0.455	1.439	2.615	2.126
YJL142C	IRC9	0.356	-0.147	1.620	1.886	1.954
YJL144W		0.962		1.429	2.991	1.951
YJL151C	SNA3	0.142	0.158	0.745	0.866	1.098
YJL155C	FBP26	-0.243	-0.551	0.612	2.383	0.660
YJL159W	HSP150	0.693	0.233	1.233	1.786	1.322
YJL161W		-0.110	-0.617	1.167	2.849	2.071
YJL163C		-0.427	-0.666	0.892	1.725	1.063
YJL164C	TPK1	0.678	0.317	1.509	2.538	1.119
YJL165C	HAL5	0.215	0.185	0.378	1.290	0.766
YJL166W	QCR8	0.266	0.328	0.954	1.335	1.290
YJL170C	ASG7	0.893	0.946	2.060	2.823	3.519
YJL185C		-0.066	-0.179	0.380	0.532	1.023
YJL197W	UBP12	-0.210	-0.021	-0.184	1.014	-0.095
YJL212C	OPT1	0.661	0.830	0.691	0.995	1.340
YJL213W		0.735	1.152	1.655	2.370	2.319
YJL217W		0.515	0.721	1.496	1.881	1.750
YJL223C	PAU1	-0.591	0.038	-1.577	1.325	-1.121
YJR008W		0.439	0.323	1.089	1.368	1.014
YJR010W	MET3	2.379	2.278	3.854	5.259	4.395
YJR025C	BNA1	0.437	0.461	1.505	1.610	1.259
YJR029W		0.214	0.110	0.516	1.555	1.050
YJR033C	RAV1	-0.407	-0.199	0.332	1.053	0.662
YJR036C	HUL4	0.466		1.264	2.553	0.459
YJR039W		0.174		-0.037	0.258	1.406
YJR058C	APS2	0.238	0.279	0.479	0.617	1.286
YJR059W	PTK2	0.722	0.323	1.415	1.996	1.317
YJR061W		-0.086	-0.204	-0.012	1.517	0.349
YJR062C	NTA1	0.233	0.279	0.648	1.311	1.385
YJR073C	OPI3	1.065	0.767	1.498	1.249	-0.971
YJR086W	STE18	0.092	0.313	1.068	1.112	1.073
YJR091C	JSN1	0.350	0.154	0.875	1.162	1.503
YJR096W		0.028	-0.068	1.457	2.493	2.295
YJR103W	URA8	0.228	0.020	0.808	1.374	0.602
YJR120W		0.052	0.199	-0.032		2.718
YJR125C	ENT3	-0.003	0.010	0.694	1.191	0.137
YJR135C	MCM22	0.083	0.124	0.471	1.275	0.322
YJR137C	ECM17	1.899	1.572	2.887	4.375	3.696
YJR148W	BAT2	0.064	0.442	1.166	2.350	1.750

YJR149W		-0.444		0.101	2.409	1.606
YJR155W	AAD10	-0.300	1.071	0.611	2.328	2.840
YKL001C	MET14	1.540	2.217	3.759	4.687	4.371
YKL023W		0.493	0.627	0.719	1.213	0.941
YKL026C	GPX1	1.006		1.760	2.975	2.888
YKL035W	UGP1	0.449	-0.140	1.694	2.629	1.945
YKL036C		0.597		1.550	2.901	2.270
YKL043W	PHD1	0.681	0.677	1.058	1.321	1.045
YKL050C		0.024	-0.096	0.074	-0.153	1.002
YKL051W	SFK1	0.191	0.346	0.443	0.735	1.015
YKL066W		0.204	0.200	0.566	1.023	1.198
YKL085W	MDH1	0.748	0.744	1.005	1.617	0.679
YKL091C		-0.038	-0.125	0.706	1.853	1.492
YKL093W	MBR1	0.188	0.041	-0.244		1.425
YKL094W	YJU3	0.089	0.071	0.524	0.899	1.097
YKL100C		0.294	0.239	0.606	1.028	0.863
YKL103C	LAP4	0.112	-0.132	1.571	2.575	1.848
YKL124W	SSH4	0.158	-0.052	0.484	1.352	1.358
YKL133C		-0.132	-0.172	1.038	1.937	1.547
YKL145W	RPT1	0.239	-0.222	0.150	1.069	-0.017
YKL150W	MCR1	0.313	0.255	1.213	1.865	1.854
YKL151C		0.552	0.622	2.189	3.330	3.376
YKL163W	PIR3	0.932	0.151	1.385	3.097	3.469
YKL189W	HYM1	0.635	0.064	1.031	1.894	1.750
YKL195W	MIA40	-0.046	0.218	0.481	1.108	0.161
YKL198C	PTK1	0.463	0.356	0.827	1.251	1.153
YKL199C		0.317	0.430	0.389	1.048	1.308
YKL200C		0.788	0.563	1.233	1.755	2.103
YKL201C	MNN4	0.560	1.056	1.247	2.868	2.529
YKL202W		0.200	0.719	0.997	1.216	1.681
YKL213C	DOA1	0.111	0.185	0.511	1.172	0.539
YKL218C	SRY1	0.115	0.644	0.749	1.416	1.085
YKR011C		0.570	-0.137	1.604	3.349	1.131
YKR016W		0.194	0.268	0.786	1.224	0.593
YKR018C		0.272	0.184	0.418	1.238	0.800
YKR024C	DBP7	-0.522	-0.317	-0.038	0.864	1.157
YKR042W	UTH1	0.781	0.539	1.196	1.313	1.659
YKR049C	FMP46	0.104	0.308	0.822	1.196	1.420
YKR058W	GLG1	0.375	-0.384	0.731	1.967	1.288
YKR069W	MET1	1.670	2.574	2.863	4.390	3.618
YKR075C		0.564	0.843	0.025	0.551	1.883
YKR076W	ECM4	0.011	-0.141	0.821	1.970	2.074
YKR089C	TGL4	0.060	0.173	0.589	1.259	0.878
YKR091W	SRL3	-0.025	0.239	1.036	2.738	1.161
YKR093W	PTR2	0.282	-0.398	0.297	1.456	1.703
YKR096W		0.141	0.117	0.252	1.306	0.703
YKR098C	UBP11	-0.147	-0.390	0.284	1.235	1.188
YLL026W	HSP104	-0.434	-0.429	1.478	3.320	1.040
YLL039C	UBI4	0.096	0.279	1.582	2.400	1.454
YLL040C	VPS13	-0.119	-0.293	-0.067	1.026	0.170

YLL041C	SDH2	0.350	0.283	0.770	1.039	0.102
YLL048C	YBT1	0.265	0.125	0.424	1.452	1.199
YLL055W	YCT1	0.462	0.365	0.837	2.401	3.413
YLL058W		0.185	-0.448	0.651	1.873	1.755
YLL061W	MMP1	0.868	1.878	1.392	2.725	3.296
YLL062C	MHT1	0.559	2.104	1.696	2.969	3.232
YLR001C		-0.195	-0.085	0.465	1.010	0.998
YLR023C	IZH3	0.060	0.225	0.281	0.834	1.286
YLR042C		1.092	1.507	1.745	1.074	1.886
YLR058C	SHM2	0.421	0.055	0.264	0.969	1.390
YLR080W	EMP46	0.302	-0.060	0.774	2.136	1.130
YLR089C	ALT1	0.176	0.325	1.327	2.080	2.592
YLR092W	SUL2	3.006	1.968	4.152	6.425	4.630
YLR094C	GIS3	0.313	0.414	0.492	1.025	1.309
YLR108C		1.309	1.624	1.391	1.607	0.980
YLR120C	YPS1	0.800	0.273	0.890	2.003	1.753
YLR133W	CKI1	0.246	0.009	0.525	1.154	-0.679
YLR136C	TIS11	0.302	0.099	0.703	1.858	2.077
YLR142W	PUT1	-0.217		0.441	2.595	2.478
YLR149C		-0.189	-0.386	0.608	1.604	1.934
YLR151C	PCD1	0.154	-0.208	0.358	1.285	0.439
YLR164W		0.444	-0.088	1.301	1.609	1.386
YLR173W		0.069	0.195	0.193	1.027	0.711
YLR174W	IDP2	-0.184		-0.371	1.329	0.296
YLR177W		0.296	-0.094	0.605	0.992	1.291
YLR178C	TFS1	-0.990	-0.708	2.084	3.167	2.249
YLR180W	SAM1	0.733	0.741	1.012	0.811	0.270
YLR193C	UPS1	0.127	0.284	0.562	0.709	1.109
YLR205C	HMX1	0.471	1.263	1.495	3.674	3.141
YLR225C		0.505	0.475	1.332	2.261	1.429
YLR236C		-0.399	0.356	0.158	-0.484	1.003
YLR240W	VPS34	0.116	-0.069	0.334	1.366	0.766
YLR251W	SYM1	0.247	0.187	1.548	1.868	1.912
YLR252W		-0.050	0.067	0.820	1.192	0.923
YLR257W		0.365	0.209	1.242	1.925	1.455
YLR258W	GSY2	0.510	0.197	1.585	2.304	1.653
YLR267W	BOP2	2.008	2.639	3.329	4.591	3.905
YLR270W	DCS1	0.376	0.112	1.413	2.339	1.778
YLR271W		0.914	0.414	0.936		1.103
YLR272C	YCS4	0.183	-0.193	0.114	1.208	1.986
YLR277C	YSH1	-0.271	-0.171	0.131	0.725	1.078
YLR282C		0.382	0.204	0.242	0.123	1.180
YLR290C		-0.256	-0.075	0.794	0.748	1.016
YLR324W	PEX30	-0.109	-0.175	0.382	1.179	0.548
YLR327C	TMA10	0.287	0.127	0.302	0.472	1.485
YLR331C	JIP3	0.068	0.234	0.151	-0.142	1.078
YLR343W	GAS2	-0.604	-0.424	-0.811	0.232	1.898
YLR345W		0.370	0.443	1.018	2.201	0.992
YLR349W		-0.021	0.434	0.324	1.089	0.670
YLR350W	ORM2	0.694	0.505	1.098	1.521	1.893

YLR356W		-0.175	-0.212	0.894	0.948	1.228
YLR364W	GRX8	0.058	0.250	0.299	0.110	1.541
YLR370C	ARC18	0.130	0.254	0.670	1.003	0.677
YLR382C	NAM2	0.070	-0.160	0.156	0.833	3.777
YLR385C	SWC7	-0.238	0.050	0.154	0.595	1.061
YLR387C	REH1	-0.250	-0.157	0.342	1.107	0.722
YLR414C		0.293	0.260	0.839	1.134	0.660
YLR417W	VPS36	-0.127	-0.206	0.370	1.120	0.489
YLR423C	ATG17	0.049	-0.131	-0.032	1.120	0.403
YLR425W	TUS1	-0.054	-0.040	0.131	0.868	1.093
YLR438W	CAR2	-0.165	0.037	1.105	0.927	1.008
YLR446W		0.236	0.001	0.441	0.732	1.208
YLR454W		-0.249	-0.018	0.154	1.776	0.195
YML004C	GLO1	1.073	0.295	1.538	2.256	1.652
YML035C	AMD1	0.343	0.036	0.329	0.730	1.002
YML054C	CYB2	0.244	0.160	0.681	3.103	2.633
YML057W	CMP2	-0.104	-0.193	0.366	0.725	1.329
YML070W	DAK1	0.301	-0.057	1.255	2.319	1.637
YML091C	RPM2	0.537	0.679	0.907	1.878	1.037
YML100W	TSL1	0.699	0.145	1.601	2.791	1.661
YML112W	CTK3	0.066	0.109	0.665	1.234	0.863
YML117W	NAB6	0.064	0.184	0.514	1.175	0.838
YML117W-a		0.101	0.149	0.775	0.925	1.393
YML118W	NGL3	0.313	0.258	0.821	1.854	0.794
YML120C	NDI1	1.320	0.761	1.656	2.125	1.495
YML123C	PHO84	0.822	1.149	1.442	1.340	3.439
YML128C	MSC1	0.203	-0.289	2.205	3.010	2.519
YML131W		-0.459	-0.086	1.291	2.950	2.526
YMR020W	FMS1	0.200	0.319	0.538	1.147	0.670
YMR030W	RSF1	0.192	-0.159	0.805	1.221	-0.099
YMR035W	IMP2	0.010	0.087	0.340	2.074	-0.124
YMR053C	STB2	0.751		0.808	2.196	0.809
YMR060C	SAM37	-0.406	-0.256	-0.326	1.263	0.070
YMR062C	ECM40	0.236	0.432	1.055	0.870	0.997
YMR065W	KAR5	0.446	0.424	0.467	1.555	1.514
YMR068W	AVO2	0.448	0.367	0.654	0.770	1.808
YMR077C	VPS20	-0.022	0.336	0.474	0.725	1.249
YMR090W		-0.156	-0.082	1.187	1.698	1.896
YMR095C	SNO1	0.484	0.771	1.345	0.752	1.489
YMR096W	SNZ1	0.974	1.223	2.085	2.428	1.734
YMR105C	PGM2	0.732	0.113	2.091	3.631	1.603
YMR110C	HFD1	0.458	0.221	1.316	2.460	1.363
YMR114C		0.129	0.251	0.681	1.427	1.216
YMR115W		-0.073	-0.132	0.299	1.072	0.244
YMR118C		-0.198	-0.265	-0.130	0.175	1.102
YMR120C	ADE17	0.969	0.559	0.372	0.697	1.057
YMR135C	GID8	0.272	-0.048	0.754	1.457	1.478
YMR136W	GAT2	0.508	-0.288	0.989	1.389	1.300
YMR139W	RIM11	0.142	0.089	0.947	1.722	1.147
YMR153W	NUP53	0.484	0.245	0.724	0.761	1.457

YMR160W		0.258	0.203	0.519	1.436	0.348
YMR169C	ALD3	0.611	-0.166	2.811	4.238	3.251
YMR170C	ALD2	0.696	-0.156	2.191	3.785	2.784
YMR171C	EAR1	0.284	0.043	0.232	0.839	1.341
YMR173W	DDR48	0.887	0.337	1.562	2.134	2.198
YMR173W-A		0.403	0.263	1.541	2.190	2.223
YMR181C		0.397	-0.201	0.983	1.871	2.685
YMR195W	ICY1	0.919	1.592	2.310	2.802	2.684
YMR211W	DML1	0.579	0.336	0.666	0.791	1.903
YMR250W	GAD1	0.061	-0.433	1.591	2.428	1.435
YMR251W-A	HOR7	0.366	0.243	1.428	1.693	1.868
YMR253C		-0.097	-0.128	0.392	1.456	0.942
YMR255W	GFD1	0.266	0.529	0.844	1.236	1.264
YMR261C	TPS3	0.020	0.017	1.007	1.700	0.701
YMR262W		-0.263	-0.386	0.515	1.176	1.202
YMR265C		0.483	0.199	0.548	0.557	1.394
YMR271C	URA10	0.133	0.260	0.864	1.280	1.430
YMR284W	YKU70	0.667	0.133	0.826	2.012	0.934
YMR286W	MRPL33	-0.112	-0.049	-0.042		1.002
YMR287C	DSS1	0.456	0.162	0.582	0.438	1.823
YMR288W	HSH155	0.027	-0.161	0.572	-0.778	1.281
YMR291W		1.556	1.063	1.782	2.457	2.634
YMR293C		0.160	0.343	0.004	0.827	1.240
YMR304C-A		-0.085	-0.368	0.011	0.878	1.002
YMR319C	FET4	0.548	0.697	0.316	0.624	1.207
YMR323W	ERR3	-0.020	0.113	-0.140	1.488	2.335
YNL011C		-0.017	0.066	0.750	1.441	1.093
YNL029C	KTR5	0.346	0.256	0.839	1.639	0.904
YNL036W	NCE103	0.739	1.231	2.651	2.924	2.104
YNL045W		0.429	0.051	0.544	1.596	1.361
YNL072W	RNH201	0.615	0.393	0.929	1.400	1.028
YNL077W	APJ1	0.501	-0.006	0.195	1.229	1.325
YNL098C	RAS2	0.431	0.340	0.859	1.353	0.241
YNL107W	YAF9	0.031	0.243	0.002	-0.480	1.455
YNL115C		0.115	-0.030	-0.161	1.412	0.836
YNL117W	MLS1	0.357	0.188	0.548	-0.136	1.361
YNL133C	FYV6	0.023	-0.407	-0.024	-0.214	1.163
YNL134C		0.500	0.513	1.012	1.669	1.387
YNL144C		0.948	0.554	0.526	1.270	1.746
YNL145W	MFA2	0.042	-0.049	0.407	0.709	1.635
YNL157W		0.170	0.124	0.811	0.488	1.276
YNL160W	YGP1	1.270	0.452	2.150	2.861	2.148
YNL191W	DUG3	0.129	0.818	0.630	0.773	1.359
YNL192W	CHS1	-0.007	-0.023	0.319	1.688	1.289
YNL194C			-0.411	1.111	2.234	2.054
YNL195C		-0.727		0.483	1.394	1.564
YNL200C		-0.165	-0.110	1.006	1.899	1.475
YNL208W		-0.053	0.044	0.781	0.979	1.668
YNL220W	ADE12	0.451	0.145	0.516	1.231	0.722
YNL233W	BNI4	0.471	0.073	0.569	0.229	1.401

YNL235C		0.090	-0.053	-0.106	-0.233	1.181
YNL241C	ZWF1	0.559	0.573	1.286	1.895	2.012
YNL259C	ATX1	-0.088	0.262	0.574	0.146	1.093
YNL265C	IST1	-0.032	-0.103	0.655	1.183	1.227
YNL266W		-0.380	0.043	0.533		1.068
YNL274C	GOR1	0.112	0.036	2.145	3.101	2.138
YNL276C		1.012	2.051	2.175	2.450	3.834
YNL277W	MET2	0.521	0.676	1.186	1.970	1.998
YNL279W	PRM1	0.611	0.987	1.037	1.903	3.351
YNL305C		0.132	0.054	1.048	1.663	1.500
YNL325C	FIG4	0.215	-0.275	-0.517	1.539	0.172
YNL331C	AAD14	0.014	0.096	0.053	0.637	1.045
YNL332W	THI12	-1.164		-0.486	1.268	-0.040
YNR001C	CIT1	0.355	0.641	1.226	1.993	1.234
YNR005C		0.021	0.052	0.137		2.049
YNR019W	ARE2	0.536	0.073	0.516	1.753	-0.168
YNR032W	PPG1	0.359	0.025	0.627	0.274	1.163
YNR044W	AGA1	2.149	0.994	1.949	2.745	4.517
YNR062C		0.406	0.037	0.605	-0.328	1.097
YOL016C	CMK2	0.386	-0.297	0.393	1.343	1.579
YOL025W	LAG2	0.378	0.234	0.319	1.077	0.762
YOL032W	OPI10	0.246	-0.074	0.666	1.805	1.286
YOL035C		0.174	0.306	0.646		1.443
YOL036W		0.481	-0.053	0.332	-0.708	1.099
YOL053C-a		0.281	-0.188	3.133	3.125	3.296
YOL053W		-0.127	0.108	-0.204	1.282	0.516
YOL055C	THI20	-0.127	0.293	-0.441	1.136	0.470
YOL058W	ARG1	0.782	0.949	1.069	0.600	-0.436
YOL071W	EMI5	-0.157	0.366	1.020	1.784	1.182
YOL081W	IRA2	-0.276	0.109	0.179	1.114	0.249
YOL082W	ATG19	0.055	-0.095	0.768	1.327	0.718
YOL083W		0.198	-0.026	0.749	1.613	1.073
YOL096C	COQ3	0.171	-0.123	0.247	1.573	0.573
YOL100W	PKH2	0.354	-0.035	0.497	0.994	1.006
YOL110W	SHR5	-0.120	0.260	0.343	0.509	1.114
YOL111C	MDY2	0.796	0.782	1.593	1.955	2.250
YOL119C	MCH4	0.181	0.517	0.896	1.801	1.941
YOL126C	MDH2	0.450	0.279	0.598	1.015	-0.019
YOL133W	HRT1	-0.662	-0.016	0.618	0.570	1.071
YOR003W	YSP3	-0.108	-0.133	-0.916	0.808	2.187
YOR023C	AHC1	0.373	-0.263	0.473	0.815	1.172
YOR027W	STI1	-0.068	-0.444	0.733	1.247	-0.159
YOR028C	CIN5	0.251	0.198	1.794	1.409	
YOR035C	SHE4	0.052	-0.021	0.330	1.393	0.991
YOR036W	PEP12	0.231	0.160	0.968	1.546	1.498
YOR042W	CUE5	0.325	0.000	0.684	1.185	0.326
YOR053W		0.605	0.495	0.340	1.827	0.698
YOR054C	VHS3	1.003	0.404	1.207	2.249	1.521
YOR056C	NOB1	0.237	-0.340	-0.042	-0.378	1.023
YOR077W	RTS2	-0.317	0.043	-0.523	-1.702	1.863

YOR120W	GCY1	1.403	1.646	3.016	4.227	3.373
YOR121C		0.827	1.216	3.212	4.239	3.091
YOR124C	UBP2	-0.121	-0.387	0.517	1.598	0.382
YOR128C	ADE2	0.099	-0.004	0.138	1.076	0.926
YOR130C	ORT1	0.177	0.783	0.986	0.969	1.205
YOR135C	IRC14	0.042	0.559	0.741	1.669	0.975
YOR136W	IDH2	0.362	0.288	0.736	1.480	0.535
YOR152C		-0.748	-0.513	-0.412		1.562
YOR155C	ISN1	0.062	0.117	0.465	1.632	1.009
YOR173W	DCS2	0.286	0.138	1.182	1.809	1.473
YOR178C	GAC1	0.606	0.013	0.232	1.499	1.228
YOR185C	GSP2	-0.308	-0.322	0.478	0.910	1.469
YOR191W	ULS1	-0.051	0.036	-0.051	-0.611	1.430
YOR215C		0.420	0.223	0.970	1.678	1.320
YOR220W		0.496	-0.069	1.316	2.217	1.444
YOR227W		-0.354	-0.423	0.505	1.636	1.184
YOR245C	DGA1	0.213	0.020	0.323	0.858	1.011
YOR259C	RPT4	0.040	-0.095	0.249	1.002	0.167
YOR266W	PNT1	-0.103	0.138	0.091	-0.088	1.029
YOR273C	TPO4	1.227	0.901	1.601	2.048	0.225
YOR285W		-0.115	-0.059	0.520	0.522	1.058
YOR289W		0.508	0.866	2.106	3.197	2.729
YOR292C		0.499	0.588	1.088	1.722	1.855
YOR303W	CPA1	0.375	0.548	0.896	0.824	1.566
YOR347C	PYK2	0.710	0.601	1.399	2.293	0.995
YOR349W	CIN1	0.716	0.185		-0.453	1.277
YOR363C	PIP2	-0.410	-0.335	0.447	0.715	1.063
YOR374W	ALD4	-0.300	-0.240	0.608	1.709	1.195
YOR383C	FIT3	-1.012	-0.840	-0.140	-0.072	1.341
YOR386W	PHR1	0.877	-0.050	1.167	1.668	0.855
YOR393W	ERR1	0.026	0.175	-0.305	0.821	2.053
YPL019C	VTC3	0.503	0.639	0.700	1.079	1.151
YPL024W	RMI1	-0.092	0.002	0.186	-0.855	1.074
YPL033C		0.745		0.648	-0.155	1.826
YPL042C	SSN3	0.257	0.250	0.531	-0.090	1.183
YPL071C		-0.073	0.169	-0.065		1.409
YPL088W		-0.111	0.220	-0.077	0.994	1.182
YPL096W	PNG1	0.230	0.179	0.312	0.374	1.011
YPL111W	CAR1	0.160	0.427	1.165	1.512	1.571
YPL113C		0.362	-0.096	1.238	1.944	1.249
YPL123C	RNY1	0.100	0.138	0.831	1.159	0.951
YPL135W	ISU1	0.270	0.761	1.102	1.596	1.414
YPL144W	POC4	0.417	0.277	0.631	0.149	1.394
YPL150W		-0.037	-0.050	0.049	0.176	1.096
YPL156C	PRM4	0.118	0.502	0.840	1.114	2.109
YPL161C	BEM4	-0.056	-0.208	0.364	1.848	
YPL177C	CUP9	0.036	-0.124	0.227	0.818	1.543
YPL186C	UIP4	0.050	-0.196	0.779	1.824	1.543
YPL188W	POS5	-0.036	0.600	0.308	1.282	1.272
YPL196W	OXR1	0.517	0.249	0.454	1.677	1.423

YPL203W	TPK2	0.225	0.040	0.842	1.379	0.832
YPL205C		0.243	-0.088	0.431		1.179
YPL206C	PGC1	0.498	0.066	0.664	1.269	1.115
YPL222W		-0.081	-0.386	0.187	3.071	1.709
YPL223C	GRE1	2.446		3.291	6.594	6.575
YPL240C	HSP82	-0.323	-0.603	0.275	1.101	-0.907
YPL247C		0.535	-0.155	0.709	1.194	0.628
YPL250C	ICY2	0.315	0.373	1.019	1.181	2.147
YPL260W		0.187	0.015	0.517	1.174	0.800
YPL265W	DIP5	0.204	0.531	0.543	1.846	1.538
YPL271W	ATP15	0.035	0.232	0.738	0.432	1.068
YPL274W	SAM3	1.077	1.943	1.453	2.281	2.310
YPL281C	ERR2	-0.108	0.133	-0.223	1.226	2.181
YPR005C	HAL1	-0.649		0.595	1.557	2.408
YPR026W	ATH1	-0.419		0.301	2.350	1.502
YPR030W	CSR2	0.166	-0.020	0.065		2.266
YPR035W	GLN1	-0.155	0.118	0.273	1.196	0.380
YPR047W	MSF1	0.675	-0.194	0.096		1.013
YPR049C	ATG11	-0.158	0.118	-0.433	0.470	1.377
YPR076W		-0.350	-0.339	-0.687		1.016
YPR081C	GRS2	0.382	0.138	0.503	1.325	0.680
YPR093C	ASR1	0.628	0.600	0.916	1.776	1.426
YPR115W		0.240	-0.046	0.689	1.106	0.799
YPR122W	AXL1	-0.180	0.014	-0.146	0.833	1.128
YPR149W	NCE102	0.233	-0.173	1.113	1.263	0.843
YPR151C	SUE1	-3.551		0.314	2.723	1.520
YPR157W		1.077	0.793	0.791	1.403	
YPR167C	MET16	1.817	1.897	3.267	3.920	3.536
YPR172W		0.116	0.361	0.988	1.331	1.359
YPR178W	PRP4	0.010	0.069	0.569	1.112	0.666
YPR184W	GDB1	-0.230	-0.346	1.489	2.844	2.277

Genes repressed by potassium starvation (log(2) values)

ID	NAME	10min	20min	40min	60min	120 min
YAL003W	EFB1	0.050	0.234	-0.141	-1.045	-0.946
YAL007C	ERP2	-0.071	-0.134	-0.660	-1.348	-1.159
YAL023C	PMT2	-0.316	-0.118	-0.815	-1.437	-1.544
YAL025C	MAK16	0.074	0.032	-0.539	-1.303	-0.267
YAL033W	POP5	-0.119	-0.305	-0.703	-1.370	-0.809
YAL036C	RBG1	0.095	0.077	-0.625	-1.266	-1.089
YAL037C-b		0.223	0.303	0.465	-0.040	-1.182
YAL059W	ECM1	-0.270	-0.496	-1.735	-3.356	-2.202
YAR007C	RFA1	-0.489	-0.853	-0.611	-0.569	-1.195
YAR052C		-0.240	-0.305	-1.001		-0.712
YAR073W	IMD1	-0.092	0.120	-1.191	-2.304	-3.475
YBL002W	HTB2	-0.346	-0.229	-1.557	-3.745	-2.458
YBL003C	HTA2	-0.121	-0.174	-1.469	-3.108	-2.261
YBL004W	UTP20	-0.152	-0.160	-1.498	-2.676	-1.344
YBL008W	HIR1	-1.539	0.114	-1.480		-0.693
YBL018C	POP8	0.039	0.342	-0.138	-2.045	
YBL021C	HAP3	0.105	0.353	-0.523	-1.809	
YBL023C	MCM2	-0.316	-0.805	-0.654	0.338	-1.301
YBL024W	NCL1	-0.194	-0.101	-0.888	-1.415	-1.384
YBL027W	RPL19B	0.488	0.248	-0.182	-1.961	-1.678
YBL028C		0.201	-0.388	-1.349	-2.648	-1.322
YBL032W	HEK2	0.263	0.139	0.103	-0.430	-1.069
YBL035C	POL12	-0.827	-0.961	-1.522	-1.921	-0.984
YBL039C	URA7	-0.578	-0.168	-1.767	-3.243	-2.415
YBL042C	FUI1	-0.873	-0.320	-1.436	-0.955	-1.378
YBL052C	SAS3	-0.464	0.326	-0.466	-0.343	-1.080
YBL055C		-0.052	-0.063	-0.532	-1.144	-0.023
YBL072C	RPS8A	0.126	0.253	-0.070	-1.520	-2.250
YBL081W		-0.320	-0.042	-0.698	-1.517	-1.193
YBL082C	ALG3	-0.048	0.063	-0.638	-1.664	-1.221
YBL083C		0.175	0.331	-0.627	-2.605	
YBL087C	RPL23A	0.264	0.109	-0.283	-1.899	-2.149
YBL092W	RPL32	0.221	0.191	-0.086	-1.678	-2.678
YBL097W	BRN1	-0.189	0.041	-0.156	-1.038	-1.998
YBR009C	HHF1	0.013	-0.060	-1.169	-2.668	-1.742
YBR010W	HHT1	-0.100	-0.019	-0.639	-1.575	-0.957
YBR025C	OLA1	0.096	0.156	-0.208	-0.893	-1.436
YBR029C	CDS1	-0.033	0.016	-0.443		-1.577
YBR030W		-0.371	-0.410	-0.958	-0.618	-1.551
YBR031W	RPL4A	0.164	0.110	-0.256	-1.125	-1.168
YBR034C	HMT1	-0.093	0.046	-1.110	0.147	-0.134
YBR038W	CHS2	-0.148	-0.463	0.218	0.167	-1.686
YBR048W	RPS11B	0.171	0.215	-0.160	-1.847	-2.392
YBR049C	REB1	-0.334	-0.139	-0.579	-0.869	-1.420
YBR061C	TRM7	-0.016	-0.051	-0.183	-1.202	0.513
YBR062C		-0.469	-0.132	-0.552	-1.328	-0.718
YBR064W		-0.227	-0.106	-0.694	-1.679	-0.835

YBR069C	TAT1	-0.810	-0.277	-1.705	-2.771	-1.995
YBR072W	HSP26	-2.915	-1.553	1.164	4.109	4.661
YBR073W	RDH54	-1.205	-1.094	-1.291	-0.708	-1.048
YBR074W		-0.354	-0.475	-0.627	-1.098	-0.452
YBR076W	ECM8	0.393	-0.055	-0.800		-1.231
YBR078W	ECM33	0.039	-0.006	-0.486	-1.478	-1.500
YBR079C	RPG1	0.044	-0.093	-0.421	-1.039	-0.956
YBR084C-A	RPL19A	0.046	0.138	-0.299	-1.604	-2.475
YBR084W	MIS1	0.089	-0.087	-1.142	-2.601	
YBR087W	RFC5	-0.227	-0.390	-0.760	-1.473	-1.119
YBR088C	POL30	-0.718	-1.102	-1.412	-1.242	
YBR089W		-0.930	-1.578	-2.353	-2.345	-2.170
YBR106W	PHO88	0.019	0.064	-0.344	-1.128	-0.790
YBR121C	GRS1	0.173	0.258	-0.174	-0.945	-1.367
YBR135W	CKS1	-0.420	-0.235	-0.682	-1.301	-0.750
YBR141C		-0.414	-0.038	-1.282	-1.426	-0.721
YBR142W	MAK5	-0.215	-0.112	-1.112	-1.352	-0.722
YBR143C	SUP45	0.054	0.054	-0.483	-1.028	-0.835
YBR154C	RPB5	0.105	0.047	-0.393	-1.009	-1.559
YBR155W	CNS1	-0.030	0.312	-0.892	-1.298	-0.552
YBR162C	TOS1	0.151	0.076	-0.276	-1.023	-0.833
YBR181C	RPS6B	0.126	0.227	-0.359	-1.939	-2.563
YBR187W	GDT1	0.111	0.036	-0.319	-1.140	-0.161
YBR189W	RPS9B	0.193	0.219	-0.407	-2.503	-3.051
YBR191W	RPL21A	0.388	0.186	-0.175	-1.988	-2.200
YBR220C		-0.573	-0.233	-0.906	-1.154	-1.382
YBR238C		-0.315	-0.456	-0.647	-1.038	-0.096
YBR242W		-0.119	-0.294	-1.203	-1.914	-0.218
YBR243C	ALG7	-0.289	-0.068	-0.767	-1.707	-1.057
YBR247C	ENP1	-0.247	-0.083	-1.244	-1.852	-0.628
YBR250W	SPO23	-0.381	-0.297	-1.001	-0.025	-0.051
YBR252W	DUT1	-0.222	-0.457	-0.820	-1.746	-1.184
YBR266C	SLM6	-0.091	0.025	-0.388	-1.014	0.308
YBR267W	REI1	-0.103	-0.147	-0.431	-1.404	0.030
YBR271W		-0.511	-0.092	-1.281	-1.748	-0.562
YBR275C	RIF1	-0.655	-0.113	-1.031		-0.897
YBR291C	CTP1	-1.202	-0.427	-0.334	-0.536	-0.624
YBR301W	DAN3	-0.539	0.001	-0.764	-1.191	-1.122
YCL002C		0.323	-0.129	-0.427	-1.321	0.267
YCL003W		-0.016	-0.015	-0.181	-1.064	-0.934
YCL007C		0.119	-0.579	-0.098		-1.017
YCL022C		-0.162	-0.325	-0.202	-1.323	0.309
YCL024W	KCC4	-1.272	-1.840	-2.285	-2.955	-2.004
YCL025C	AGP1	-1.107	-1.450	-0.751	0.259	-0.814
YCL027C-a		-1.174		1.484	3.376	2.629
YCL036W	GFD2	-0.430	-0.023	-2.084	-2.997	-1.899
YCL037C	SRO9	-0.534	-0.139	-0.798	-2.528	-1.571
YCL053C		0.041	-0.004	-0.882	-2.353	-1.136
YCL054W	SPB1	-0.603	-0.280	-1.248	-1.594	-0.842
YCL058C	FYV5	-0.216	0.153	-0.701	-1.337	-0.323

YCL061C	MRC1	-0.508	-0.232	-1.016	-1.249	-0.948
YCL062W		-0.393	-0.436	-0.796	-1.473	-0.269
YCL063W	VAC17	-0.537	-0.407	-0.925	-1.424	-0.731
YCL064C	CHA1	-1.024	-1.553	-2.129	-1.918	-2.974
YCLX02C		-0.015	0.016	-0.789	-1.965	
YCLX04W		-0.033	-0.044	-0.062	-1.176	-0.095
YCR006C		0.048	0.032	-0.295	-1.071	-0.170
YCR016W		0.126	0.247	-0.444	-1.925	-1.490
YCR019W	MAK32	-0.089	0.080	-0.512	-1.718	-1.627
YCR022C		0.006	-0.046	-0.399	-1.504	-1.061
YCR025C		-0.221	-0.119	-0.245	-1.285	-1.378
YCR026C	NPP1	-0.648	-0.282	-1.140		-0.393
YCR029C-a		0.184	0.104	-0.049	-0.813	-1.202
YCR031C	RPS14A	0.042	-0.097	-0.012	-1.227	-1.301
YCR034W	FEN1	-0.216	-0.081	-1.237	-2.321	-2.542
YCR040W	MATALPHA1	-0.189	-0.069	-0.969	-1.927	
YCR043C		-0.452	-0.138	-0.594	-1.454	-1.299
YCR049C		-0.386	0.084	-1.186		-1.006
YCR055C		-0.035	-0.067	-1.151	-2.451	-1.122
YCR058C		-0.262	-0.030	-0.936	-3.586	
YCR065W	HCM1	-0.686	-0.515	-0.755	-1.347	-0.848
YCR072C	RSA4	-0.468	-0.102	-1.138	-2.336	-1.362
YCR084C	TUP1	-0.006	-0.201	-0.289	-1.146	-0.539
YCR087W		0.215	0.033	-0.802	-2.133	-1.325
YCR097Wa		-0.069	-0.072	-0.402	-2.843	-0.152
YCR099C		0.144	0.185		-1.776	-0.187
YCR101C		0.082	-0.051	-0.759	-1.461	0.166
YCR102C		-0.485	0.038	-0.643	-0.366	-1.319
YCR103C		-0.086	-0.141	-0.194	-1.035	-1.169
YCRX04W		0.070	0.019	-0.558	-1.684	-0.595
YCRX05W		0.156	0.056	-0.256	-1.077	-0.360
YCRX06W		-0.202	-0.059	-0.339	-1.129	-0.762
YCRX07W		-0.202	-0.027	-0.696	-1.618	-1.241
YCRX15W		-0.008	-0.098	-0.135	-1.154	-0.694
YCRX16C		0.110	0.013	-0.852	-1.753	-0.856
YCRX20C		-0.424	-0.452	-0.341	-1.696	
YDL003W	MCD1	-1.744	-2.227	-2.531	-2.704	
YDL031W	DBP10	-0.108	-0.157	-0.948	-1.134	-0.299
YDL032W		-0.227	-0.305	-0.077	-1.010	-0.961
YDL036C	PUS9	-0.137	-0.060	-0.842		-1.283
YDL038C		-0.008	-0.078	-0.891	-0.904	-1.004
YDL050C		0.336	0.067	-0.276	-1.578	0.115
YDL051W	LHP1	0.029	0.062	-0.871	-1.875	-1.591
YDL060W	TSR1	-0.448	-0.129	-1.320	-2.021	-0.743
YDL061C	RPS29B	0.388	-0.170	-0.215	-2.001	-1.981
YDL063C		-1.088	-0.218	-1.827	-2.326	
YDL075W	RPL31A	0.299	0.143	-0.207	-1.834	-2.424
YDL076C	RXT3	0.028	-0.014	-0.261	-1.361	-1.388
YDL081C	RPP1A	0.371	-0.083	0.057	-1.075	-1.584
YDL082W	RPL13A	0.207	0.154	-0.308	-1.621	-1.969

YDL083C	RPS16B	0.274	0.178	-0.473	-2.366	-2.859
YDL084W	SUB2	0.153	0.024	-0.261	-0.861	-1.077
YDL101C	DUN1	-0.214	-0.974	-1.437	-0.982	
YDL102W	POL3	-0.332	-0.224	-0.781	-1.063	-0.210
YDL130W	RPP1B	0.100	0.192	0.008	-1.424	-1.447
YDL131W	LYS21	-0.193	0.073	0.169	-0.012	-1.378
YDL136W	RPL35B	0.192	-0.062	-0.332	-1.692	-2.172
YDL148C	NOP14	-0.539	-0.269	-1.301	-2.121	-1.030
YDL153C	SAS10	-0.162	-0.047	-1.167	-2.123	-0.914
YDL156W		-1.336	-0.613	-1.285		-3.486
YDL157C		0.014	-0.165	-0.465	-1.020	-0.672
YDL159W	STE7	-1.005	-0.081	-0.344		0.298
YDL166C	FAP7	-0.264	-0.363	-0.921	-2.399	
YDL167C	NRP1	-0.700	-0.085	-0.738	-1.497	-1.335
YDL170W	UGA3	-2.225	0.642	0.357	0.059	0.659
YDL182W	LYS20	-0.288	0.261	0.322	0.025	-1.371
YDL184C	RPL41A	0.304	-0.004	0.070	-0.974	-1.226
YDL191W	RPL35A	0.154	0.140	-0.350	-1.708	-2.106
YDL192W	ARF1	0.155	0.067	-0.128	-0.870	-1.307
YDL201W	TRM8	0.166	0.082	-0.897	-1.536	-0.614
YDL208W	NHP2	0.088	-0.130	-0.794	-1.899	-1.133
YDL213C	NOP6	0.064	-0.024	-1.041	-1.991	-1.181
YDL219W	DTD1	-0.375	-0.349	-0.654	-0.817	-1.988
YDR012W	RPL4B	0.138	0.161	-0.242	-1.362	-1.277
YDR013W	PSF1	-0.219	-0.426	-0.456	-1.221	0.196
YDR020C		-0.479	0.323	-1.196	-1.091	-0.399
YDR022C	CIS1	-1.335		0.206	1.345	0.771
YDR023W	SES1	0.311	0.221	0.003	-0.591	-1.315
YDR025W	RPS11A	0.038	0.147	-0.354	-2.042	-2.645
YDR037W	KRS1	0.076	0.276	-0.100	-1.055	-1.533
YDR049W		-0.550	-0.152	-0.439	-0.167	-1.223
YDR050C	TPI1	0.224	-0.103	0.296	-0.234	-1.288
YDR060W	MAK21	0.058	-0.247	-1.333	-2.232	-1.450
YDR064W	RPS13	0.086	0.138	-0.346	-1.984	-2.450
YDR083W	RRP8	0.012	0.032	-0.633	-1.086	-1.018
YDR087C	RRP1	-0.087	-0.009	-1.282	-2.292	-0.788
YDR091C	RLI1	-0.326	-0.288	-0.988	-1.363	-0.910
YDR097C	MSH6	-0.422	-0.853	-1.742	-1.917	-1.760
YDR101C	ARX1	-0.509	-0.444	-1.504	-2.539	-1.291
YDR106W	ARP10	-0.597	-0.034	-0.491	-2.103	-1.575
YDR120C	TRM1	-0.502	-0.081	-1.294	-2.046	-0.963
YDR121W	DPB4	-0.499	-0.356	-0.749	-1.071	-0.498
YDR144C	MKC7	-0.581	-0.698	-1.221	-3.571	
YDR181C	SAS4	-0.007	-0.268	-0.335	-1.715	-0.101
YDR184C	ATC1	-0.623	0.051	-1.300	-2.340	-1.041
YDR187C		-0.069	-0.238	-0.726		-1.025
YDR188W	CCT6	-0.256	-0.053	-0.398	-0.338	-1.049
YDR224C	HTB1	-0.199	-0.249	-0.772	-1.820	-1.381
YDR225W	HTA1	-0.168	-0.149	-0.594	-1.493	-1.141
YDR226W	ADK1	0.391	0.098	0.198	-0.519	-1.122

YDR233C	RTN1	-0.058	-0.408	-0.522	-1.159	-0.989
YDR234W	LYS4	-0.598	-0.099	-0.797	-1.275	-1.413
YDR256C	CTA1	-0.249	-0.192	-1.119		-0.051
YDR260C	SWM1	-0.738	-0.374	-0.785		-1.100
YDR300C	PRO1	-0.013	0.268	-0.861	-1.438	-1.199
YDR312W	SSF2	-0.748	-0.223	-1.121	-1.041	-1.265
YDR318W	MCM21	-0.099	-0.038	-0.258	-1.526	-1.460
YDR321W	ASP1	0.109	0.140	-0.259	-0.775	-1.036
YDR324C	UTP4	-0.462	-0.121	-1.337	-1.746	-1.198
YDR341C		-0.009	0.279	-0.344	-0.914	-1.248
YDR361C	BCP1	-0.144	-0.152	-1.076	-2.279	-0.752
YDR367W		-0.175	-0.436	-0.537	-1.970	-1.783
YDR382W	RPP2B	0.449	0.287	-0.123	-1.598	-2.305
YDR384C	ATO3	0.812	0.776	-0.463	-1.074	-0.480
YDR385W	EFT2	0.279	0.306	-0.015	-0.614	-1.457
YDR398W	UTP5	-0.747	-0.306	-1.621	-1.452	
YDR399W	HPT1	-0.217	-0.692	-1.996	-2.359	-0.278
YDR402C	DIT2	-1.019	-0.453	-0.914		-0.573
YDR412W	RRP17	-0.004	-0.025	-0.996	-1.528	-0.779
YDR413C		0.083	0.095		-2.292	-3.002
YDR417C		0.357	0.168	-0.259	-1.790	-2.215
YDR418W	RPL12B	0.154	0.154	-0.297	-1.903	-2.462
YDR425W	SNX41	0.115	0.076	-0.181	-1.651	-1.176
YDR428C	BNA7	0.010	-0.267	-0.588	-1.260	-1.012
YDR429C	TIF35	0.274	-0.084	-0.492	-0.932	-1.059
YDR434W	GPI17	-0.128	0.043	-0.223	-0.756	-1.234
YDR447C	RPS17B	0.262	0.147	-0.342	-1.997	-2.471
YDR449C	UTP6	-0.462	0.189	-1.431	-1.543	-2.094
YDR450W	RPS18A	0.271	-0.430	-0.418	-2.024	-2.669
YDR454C	GUK1	0.094	0.087	-0.145	-1.223	-1.516
YDR465C	RMT2	-0.230	-0.227	-1.157	-2.306	-1.097
YDR471W	RPL27B	0.059	-0.070	-0.618	-2.277	-2.188
YDR492W	IZH1	-0.290	-0.533	-1.172	-1.706	-0.647
YDR496C	PUF6	-0.467	-0.337	-1.517	-2.512	-0.855
YDR500C	RPL37B	0.122	0.158	-0.223	-1.866	-2.060
YDR505C	PSP1	0.004	0.236	-0.035	-0.631	-1.053
YDR507C	GIN4	-1.483	-1.345	-1.889	-2.872	-1.696
YDR508C	GNP1	-0.548	-0.188	-0.750	-0.519	-1.623
YDR528W	HLR1	-0.631	-0.502	-0.561	-1.218	-1.201
YDR538W	PAD1	0.332	0.315	0.253	-0.490	-1.295
YEL003W	GIM4	-0.613	-0.072		-0.902	-1.143
YEL026W	SNU13	0.416	0.183	-0.471	-2.180	-1.457
YEL033W		-0.012	-0.016	-0.301	-1.308	-1.507
YEL034C-a		0.054	-0.123	-0.257	-1.002	-1.334
YEL034W	HYP2	0.040	-0.021	-0.227	-1.163	-1.202
YEL035C	UTR5	-0.119	-0.235	-0.404	-1.141	-1.495
YEL040W	UTR2	-0.575	-0.773	-1.022	-1.847	-2.880
YEL042W	GDA1	-0.191	0.012	-1.044	-1.918	-1.608
YEL046C	GLY1	-0.026	0.205	-0.559	-1.033	-0.926
YEL048C		-0.044	-0.168	-0.509	-1.497	-1.116

YEL053W-a		0.291	-0.300	-0.497	-1.776	-2.247
YEL054C	RPL12A	0.292	0.209	-0.408	-2.154	-2.372
YEL055C	POL5	-0.093	-0.251	-1.025	-1.350	-0.437
YEL061C	CIN8	-0.280	-0.084	-0.528	-1.003	-0.682
YEL065W	SIT1	-1.291	-1.251	-1.796	-2.819	-0.257
YEL066W	HPA3	-0.308	-0.174	-0.582	-1.108	-0.404
YEL068C		-0.069	-0.021	-0.167	-1.243	
YEL073C		0.873	-0.369	0.844	0.130	-1.372
YEL074W		0.004	-0.102	-0.196	-1.036	-1.163
YEL075C		-0.060	-0.078	-0.173	-1.092	-1.150
YER001W	MNN1	-1.345	-0.837	-1.873	-2.471	-1.301
YER003C	PMI40	-0.151	-0.067	-0.665	-1.646	-1.855
YER006W	NUG1	-0.068	0.010	-1.114	-2.581	-1.187
YER009W	NTF2	0.123	0.060	0.011	-0.854	-1.332
YER011W	TIR1	-0.178	-1.815	-0.715	-1.855	-2.776
YER018C	SPC25	-0.556	0.141	-0.622	-1.074	-0.255
YER025W	GCD11	-0.065	0.046	-0.543	-1.284	-1.018
YER026C	CHO1	-0.032	-0.314	-0.406	-0.682	-2.144
YER028C	MIG3	0.223	-0.165	-0.497	-1.313	-0.340
YER031C	YPT31	-0.297	-0.206	-0.271	-0.655	-1.224
YER032W	FIR1	-0.365	-0.496	-0.667	-0.941	-1.037
YER036C	ARB1	-0.173	-0.086	-0.800	-1.468	-1.477
YER043C	SAH1	0.532	0.439	0.159	-0.817	-2.292
YER049W	TPA1	-0.311	-0.100	-0.897	-1.515	-0.704
YER056C	FCY2	-0.501	-0.184	-0.967	-1.043	-0.317
YER056C-A	RPL34A	0.316	0.192	-0.020	-1.501	-1.449
YER064C		-0.523	-0.391	-0.884	-2.093	
YER070W	RNR1	-1.198	-1.942	-2.097	-2.221	-1.555
YER074W	RPS24A	0.204	0.111	-0.164	-1.464	-1.342
YER082C	UTP7	-0.091	0.033	-0.787	-1.342	-1.335
YER086W	ILV1	-0.185	0.382	-0.271	-1.637	-1.048
YER087C-A		-0.037	-0.046	-0.268	-1.301	-0.749
YER102W	RPS8B	0.293	0.225	-0.142	-1.455	-2.305
YER103W	SSA4	-1.982	-0.829	1.721	4.018	2.932
YER110C	KAP123	-0.049	0.010	-0.709	-1.437	-0.384
YER117W	RPL23B	0.275	0.064	-0.159	-1.580	-1.432
YER118C	SHO1	-0.411	-0.283	-0.909	-1.479	-0.964
YER126C	NSA2	0.226	0.284	-0.054	-1.057	0.208
YER127W	LCP5	-0.389	-0.022	-1.254	-1.866	-1.104
YER131W	RPS26B	0.403	0.109	-0.306	-1.776	-2.467
YER142C	MAG1	0.081	0.169	-0.174	-1.466	-1.575
YER145C	FTR1	-1.240	-0.867	-1.727	-2.564	-0.845
YER146W	LSM5	-0.314	-0.257	-0.281	-1.474	-0.849
YER156C		0.116	0.013	-0.720	-1.594	-0.518
YER174C	GRX4	0.368	0.215	0.039	-1.106	0.007
YER183C	FAU1	0.004	0.180	-0.191	-1.211	-1.517
YFL008W	SMC1	-0.717	-0.555	-1.085	-0.280	-0.187
YFL014W	HSP12	-1.729	-1.385	1.171	1.306	1.639
YFL020C	PAU5	-0.457	-0.070	-1.049	0.045	-0.425
YFL025C	BST1	-0.741	-0.257	-0.368	-1.194	-0.937

YFL034C-A	RPL22B	0.068	0.010	-0.751	-1.562	0.099
YFL034W		-0.471	-0.529	-0.396	-1.765	-1.067
YFL058W	THI5	-1.223	0.159	-0.094		1.558
YFL060C	SNO3	0.107	0.113	0.216	-1.009	0.331
YFR001W	LOC1	0.161	-0.132	-0.673	-1.300	-0.232
YFR005C	SAD1	0.252	0.195	0.176	-1.138	-0.896
YFR031C-A	RPL2A	0.292	0.209	-0.243	-2.002	-2.580
YFR032C-A	RPL29	0.066	-0.030	-0.196	-1.452	-2.167
YFR035C		-0.208	-0.177	-0.287	-2.500	-0.638
YFR038W	IRC5	-0.975	-0.412	-0.960	-1.125	-0.826
YGL009C	LEU1	-0.741	0.667	-0.528	-0.780	-1.074
YGL012W	ERG4	-0.441	-0.507	-0.955	-1.377	-0.642
YGL021W	ALK1	-0.261	-0.291	-0.176	-1.234	-1.260
YGL029W	CGR1	0.058	-0.237	-1.031	-1.607	-0.502
YGL030W	RPL30	0.234	0.073	-0.279	-2.042	-2.516
YGL031C	RPL24A	0.268	0.179	-0.188	-1.757	-1.937
YGL055W	OLE1	0.764	0.148	-0.409	-1.396	-0.458
YGL063W	PUS2	-0.330	0.032	-0.438		-1.276
YGL072C		-0.063	0.060	0.091	-1.298	-0.691
YGL076C	RPL7A	0.028	0.204	-0.375	-1.952	-2.765
YGL077C	HNM1	-0.571	-0.518	-1.325	-1.424	-2.299
YGL078C	DBP3	-0.142	0.043	-1.293	-2.012	-1.295
YGL099W	LSG1	-0.279	-0.296	-0.821	-1.356	-0.903
YGL101W		-0.531	-0.536	-1.109	-2.027	-1.740
YGL102C		0.156	0.081	-0.053	-1.600	-2.021
YGL103W	RPL28	0.085	0.153	-0.189	-1.561	-2.003
YGL120C	PRP43	-0.553	-0.099	-1.189	-1.672	-1.673
YGL123W	RPS2	0.350	0.240	-0.372	-2.099	-2.480
YGL135W	RPL1B	0.310	0.097	-0.243	-1.966	-2.310
YGL147C	RPL9A	0.316	0.199	-0.261	-2.387	-3.113
YGL169W	SUA5	-0.164	0.061	-0.705	-1.613	-0.913
YGL171W	ROK1	-0.374	-0.080	-1.070	-1.108	-0.693
YGL189C	RPS26A	0.226	0.144	-0.002	-1.345	-2.118
YGL200C	EMP24	0.031	-0.165	-0.213	-1.014	-0.171
YGL214W		0.086	0.027	-0.208	-1.505	-1.106
YGL225W	VRG4	-0.249	-0.199	-1.118	-2.230	-1.643
YGL245W	GUS1	0.056	0.205	0.034	-0.101	-1.016
YGL255W	ZRT1	0.287	0.366	-1.163	-0.719	-2.380
YGL261C		-0.522	-0.112	-1.368	-0.286	-0.921
YGL263W	COS12	0.511	-0.028		-1.721	-1.586
YGR014W	MSB2	-0.583	-0.309	-0.878	-1.270	-0.423
YGR027C	RPS25A	0.240	0.263	0.005	-1.405	-1.995
YGR034W	RPL26B	0.236	0.109	-0.094	-2.204	-2.354
YGR035C		-0.287	0.287	-0.281	-1.666	-1.066
YGR050C		0.265	0.131	-0.024	-1.390	-1.969
YGR060W	ERG25	-0.566	-0.794	-1.309	-1.966	-0.674
YGR078C	PAC10	0.094	0.179	-0.223	-1.676	-2.105
YGR079W		-1.165	-0.783	-2.142	-2.781	-0.963
YGR081C	SLX9	0.184	0.178	-0.464	-1.000	-0.229
YGR085C	RPL11B	0.262	0.062	-0.133	-1.795	-2.147

YGR094W	VAS1	0.299	0.134	-0.113	-0.639	-1.120
YGR099W	TEL2	-0.390	-0.482	-1.390		-0.775
YGR102C		0.137	0.101	-0.171	-1.662	-1.604
YGR103W	NOP7	-0.437	-0.103	-1.279	-2.662	-1.508
YGR105W	VMA21	-0.062	-0.002	-0.222	-1.178	-1.095
YGR106C		0.063	0.008	-0.137	-1.096	-0.762
YGR108W	CLB1	-0.271	-0.087	-0.467	-1.376	-2.445
YGR118W	RPS23A	0.180	0.092	-0.108	-1.492	-1.754
YGR123C	PPT1	0.087	0.042	-0.754	-2.937	-1.724
YGR124W	ASN2	-0.151	0.102	-0.097	-0.738	-1.270
YGR128C	UTP8	-0.262	-0.204	-1.507	-2.134	-1.716
YGR131W		0.079	-0.186	-1.267	-1.679	-0.989
YGR137W		0.200	0.198	-0.036	-1.218	-1.444
YGR145W	ENP2	-0.126	-0.209	-1.829	-2.823	-1.793
YGR148C	RPL24B	0.235	0.212	-0.007	-1.887	-2.303
YGR152C	RSR1	-0.601	-0.423	-0.567	-1.473	-0.316
YGR159C	NSR1	-0.267	-0.191	-1.931	-3.216	-1.643
YGR160W		0.369	-0.178	-1.755		-0.985
YGR162W	TIF4631	-0.205	-0.002	-0.634	-1.019	-1.181
YGR172C	YIP1	0.085	0.138	-0.148	-1.113	-0.189
YGR173W	RBG2	-0.059	0.121	-0.628	-1.116	-0.726
YGR175C	ERG1	-0.533	-0.221	-0.779	-1.188	-0.756
YGR182C		0.148	0.094	-0.216	-1.521	-1.558
YGR187C	HGH1	-0.159	0.004	-1.068	-1.200	-1.294
YGR189C	CRH1	-0.584	-1.071	-1.096	-1.471	-0.410
YGR211W	ZPR1	0.122	-0.243	-0.688	-1.478	-1.053
YGR214W	RPS0A	0.167	0.294	-0.265	-1.957	-2.752
YGR221C	TOS2	-0.730	-0.649	-1.083	-1.159	-0.757
YGR234W	YHB1	0.259	0.586	-0.179	-1.422	-1.498
YGR245C	SDA1	-0.261	-0.271	-1.448	-2.508	-1.313
YGR272C		-0.234	0.234	-0.418	-1.378	0.298
YGR283C		-0.447	-0.083	-0.994	-2.413	-0.882
YGR295C	COS6	-0.030	0.164	0.033	-1.453	-1.931
YHL001W	RPL14B	0.258	0.056	-0.459	-1.851	-2.069
YHL011C	PRS3	0.183	0.060	-0.586	-1.725	-1.031
YHL020C	OPI1	-0.207	-0.151	-0.396	-0.577	-1.195
YHL022C	SPO11	-0.067	0.341	-0.480		-1.295
YHL028W	WSC4	0.044	-0.642	-0.136	-0.862	-2.444
YHL033C	RPL8A	0.302	0.393	-0.178	-1.744	-2.140
YHL039W		-0.740	-0.352	-1.216	-1.678	-0.826
YHL049C		-0.490	-0.596	-0.775	-0.471	-1.171
YHR010W	RPL27A	0.216	0.110	-0.263	-1.876	-2.088
YHR019C	DED81	0.151	0.296	0.122	-0.758	-1.291
YHR020W		-0.197	0.303	-0.448	-1.330	-0.957
YHR021C	RPS27B	0.379	0.137	-0.041	-1.615	-1.101
YHR045W		-0.244	-0.019	-0.600	-0.216	-1.007
YHR052W	CIC1	-0.137	-0.147	-1.201	-1.682	-1.382
YHR064C	SSZ1	0.133	0.306	0.033	-0.512	-1.148
YHR065C	RRP3	-0.412	-0.303	-0.892	-1.639	-0.813
YHR066W	SSF1	-0.317	-0.135	-1.329	-2.193	-1.314

YHR072W-A	NOP10	0.148	0.114	-0.047	-1.380	
YHR088W	RPF1	0.038	0.021	-0.594	-1.371	-0.050
YHR089C	GAR1	0.313	0.105	-0.655	-2.080	-1.022
YHR109W	CTM1	-0.447	-0.288	-0.586	-2.653	
YHR120W	MSH1	-0.455	-0.168	-1.073	-0.944	-0.881
YHR123W	EPT1	-0.221	-0.187	-0.307	-0.740	-1.345
YHR128W	FUR1	0.060	-0.114	-0.652	-1.322	-0.284
YHR133C	NSG1	-0.224	-0.021	-0.490	-1.290	-0.539
YHR137W	ARO9	-2.745	-1.157	-0.538	-0.340	0.955
YHR141C	RPL42B	0.269	0.060	-0.249	-1.637	-1.455
YHR149C	SKG6	-0.767	-0.721	-1.621	-1.371	-1.942
YHR169W	DBP8	-0.290	-0.204	-1.294	-2.028	-1.297
YHR170W	NMD3	-0.094	0.052	-1.330	-2.534	-1.605
YHR182C-a		0.484	0.459	0.475	-0.059	-1.293
YHR196W	UTP9	-0.560	-0.301	-1.402	-1.895	-1.506
YHR197W	RIX1	-0.311	0.084	-1.348	-2.245	-0.592
YHR203C	RPS4B	0.159	0.328	-0.176	-1.542	-2.610
YHR207C	SET5	-0.095	0.087	-0.628	-1.186	-0.963
YHR216W	IMD2	-0.102	-0.004	-1.271	-2.609	-2.928
YHR218W		-0.649	-0.588	-1.094	0.168	-0.821
YIL011W	TIR3	-0.521	-1.007	-1.886		-1.083
YIL016W	SNL1	-0.042	-0.299	-0.752	-1.363	-0.499
YIL018W	RPL2B	0.252	0.204	-0.216	-1.987	-2.624
YIL051C	MMF1	-0.070	-0.243	-0.503	-1.284	-0.960
YIL052C	RPL34B	0.286	0.223	-0.284	-1.856	-2.030
YIL069C	RPS24B	0.283	0.149	-0.277	-2.095	-2.286
YIL091C		-0.287	-0.068	-1.314	-1.551	-1.155
YIL094C	LYS12	-0.392	0.161	-0.062	-0.905	-1.042
YIL100W		0.072	-0.077	0.015	-1.140	-1.229
YIL104C	SHQ1	-0.388	-0.127	-1.008	-1.644	-0.652
YIL110W		-0.035	-0.017	-0.409	-1.195	-0.676
YIL113W	SDP1	-0.606	-1.318		0.498	1.770
YIL114C	POR2	-0.175	-0.065	-0.105	-1.007	-0.296
YIL123W	SIM1	0.002	-0.027	-0.078	-1.163	-1.008
YIL127C		0.113	-0.019	-0.550	-1.053	-0.111
YIL131C	FKH1	0.356	0.107	-0.495	-2.254	-2.248
YIL133C	RPL16A	0.333	0.018	-0.440	-2.215	-2.028
YIL140W	AXL2	-1.341	-1.126	-1.903	-2.806	-2.074
YIL148W	RPL40A	0.124	0.100	-0.230	-1.905	-2.427
YIL158W		0.190	0.033	-0.286	-2.891	-3.166
YIR022W	SEC11	-0.106	-0.074	-0.190	-1.311	-0.326
YIR026C	YVH1	-0.053	0.014	-1.023	-2.066	-0.783
YJL014W	CCT3	-0.145	-0.074	-0.370	-0.604	-0.999
YJL026W	RNR2	0.012	0.058	-0.043	-0.847	-1.021
YJL034W	KAR2	-0.419	-0.350	-0.275	-0.370	-1.226
YJL050W	MTR4	0.127	-0.173	-1.398	-2.787	-1.423
YJL051W	IRC8	-0.097	-0.578	-0.110		-1.063
YJL069C	UTP18	-0.509	-0.144	-1.292	-1.863	-0.943
YJL073W	JEM1	-0.615	-0.501	-0.961	-1.064	-0.852
YJL074C	SMC3	-0.287	-0.731	-1.808	-1.681	-0.384

YJL080C	SCP160	0.223	0.138	-0.220	-0.545	-1.459
YJL081C	ARP4	-0.381	-0.291	-0.552	-0.867	-1.047
YJL084C	ALY2	0.307	-0.166	0.316	-1.035	1.224
YJL087C	TRL1	-0.133	-0.264	-0.513	-0.475	-1.526
YJL098W	SAP185	-0.089	-0.141	-1.163	-1.002	-0.450
YJL118W		-0.470	-0.062	-0.880	-2.463	-1.927
YJL121C	RPE1	-0.083	0.005	-0.461	-2.028	-1.864
YJL122W	ALB1	-0.135	-0.330	-1.776	-3.655	-2.075
YJL125C	GCD14	-0.570	-0.350	-1.017	-1.703	-0.702
YJL136C	RPS21B	0.104	0.034	-0.259	-1.902	-2.529
YJL137C	GLG2	-0.271	-0.287	0.187	-1.678	-0.568
YJL138C	TIF2	0.307	0.376	0.066	-0.832	-1.334
YJL148W	RPA34	-0.038	-0.325	-1.235	-2.833	-1.579
YJL153C	INO1	0.859	0.141	0.298	0.220	-4.347
YJL158C	CIS3	-0.094	-0.066	-0.540	-1.874	-1.896
YJL167W	ERG20	0.144	-0.012	-0.035	-0.317	-1.166
YJL173C	RFA3	-0.496	-0.393	-1.293	-2.513	-1.332
YJL177W	RPL17B	0.199	0.198	-0.299	-1.971	-2.486
YJL181W		-0.376	-0.753	-1.009	-0.676	-0.609
YJL184W	GON7	0.103	0.182	-0.404	-1.307	-0.474
YJL187C	SWE1	-0.637	-0.784	-0.732	-1.930	-0.251
YJL188C	BUD19	0.210	-0.126	-0.203	-1.821	-2.422
YJL189W	RPL39	0.170	-0.131	-0.181	-1.665	-2.213
YJL190C	RPS22A	0.309	0.071	-0.405	-2.500	-3.208
YJL191W	RPS14B	0.127	0.175	-0.168	-1.673	-1.584
YJL196C	ELO1	-0.262	-0.360	-0.341	-1.261	-1.701
YJL200C	ACO2	-1.059	-0.370	-0.943	-1.455	-2.279
YJL207C	LAA1	-0.426	-0.692	-0.821	-0.417	-1.135
YJL208C	NUC1	-0.493	-0.262	-1.094	-1.515	-1.129
YJL223C	PAU1	-0.591	0.038	-1.577	1.325	-1.121
YJR001W	AVT1	-0.592	-0.752	-0.834	-1.043	-0.279
YJR002W	MPP10	-0.279	0.099	-0.877	-1.224	-0.729
YJR016C	ILV3	-0.265	0.201	-0.443	-1.153	-0.927
YJR024C	MDE1	-0.284	-0.449	-0.850	-1.763	-1.445
YJR041C	URB2	-0.017	-0.211	-0.704	-1.510	-0.332
YJR063W	RPA12	-0.413	-0.278	-0.964	-2.629	-0.655
YJR064W	CCT5	-0.237	-0.229	-0.664	-0.655	-1.162
YJR069C	HAM1	-0.173	-0.008	-0.431	-1.310	-0.976
YJR071W		0.051	-0.116	-1.496	-2.815	-1.995
YJR092W	BUD4	-0.394	-0.430	-0.289	-1.309	-2.439
YJR105W	ADO1	0.257	0.242	0.059	-0.912	-1.482
YJR112W	NNF1	-0.469	-0.115	-0.743		-1.386
YJR118C	ILM1	-0.184	-0.398	-0.737	-1.374	
YJR123W	RPS5	0.223	0.315	-0.111		-2.051
YJR124C		-0.358	-0.078	-0.696	-1.305	-1.373
YJR129C		-0.221	-0.049	-0.798	-0.498	-1.559
YJR136C		-0.249	-0.132	-0.179	-1.045	0.085
YJR143C	PMT4	-0.093	-0.058	-0.425	-1.178	-1.031
YJR145C	RPS4A	0.091	0.267	-0.206	-1.560	-2.585
YJR147W	HMS2	-0.282	0.262	-0.382	-1.164	-0.150

YJR156C	THI11	0.264	-0.025	-0.060	0.274	-1.322
YJR159W	SOR1	-0.305	0.252	-0.500	-0.430	-1.759
YKL004W	AUR1	-0.309	0.070	-0.678	-1.459	-0.596
YKL006W	RPL14A	0.202	0.109	-0.355	-2.166	-2.526
YKL009C		-0.128	-0.271	-0.993	-2.090	-1.131
YKL009W	MRT4	-0.033	-0.186	-0.733	-2.949	-2.023
YKL014C	URB1	-0.098	-0.389	-0.669	-2.008	-0.069
YKL021C	MAK11	-0.058	0.044	-0.733	-1.031	-0.531
YKL045W	PRI2	-0.255	-1.201	-1.110	-0.928	-0.881
YKL056C	TMA19	0.263	0.273	0.181	-1.024	-1.458
YKL078W	DHR2	-0.167	-0.213	-0.366	-1.000	-0.443
YKL081W	TEF4	0.282	0.421	-0.154	-1.388	-2.018
YKL082C	RRP14	-0.245	0.092	-0.762	-1.401	-0.538
YKL084W	HOT13	0.128	0.290	-0.019	-1.537	-0.161
YKL101W	HSL1	-1.190	-0.677	-1.407	-1.833	-1.526
YKL113C	RAD27	-0.693	-1.229	-1.853	-2.200	-1.867
YKL143W	LTV1	-0.097	-0.094	-1.867	-2.898	-1.089
YKL144C	RPC25	-0.253	-0.240	-1.257	-2.306	-0.923
YKL156W	RPS27A	-0.063	-0.193	-0.790	-1.613	-1.387
YKL164C	PIR1	-0.416	0.031	-0.576	-2.169	-0.701
YKL172W	EBP2	-0.069	-0.135	-1.091	-2.268	-1.217
YKL180W	RPL17A	0.049	0.214	-0.019	-1.318	-1.993
YKL181W	PRS1	0.153	0.069	-0.769	-1.692	-1.074
YKL182W	FAS1	0.207	-0.025	-0.108	-0.500	-1.785
YKL191W	DPH2	-0.360	-0.174	-1.306	-2.256	-1.776
YKL205W	LOS1	-0.393	-0.555	-0.656	-1.097	-0.524
YKL216W	URA1	0.242	-0.015	-0.637	-1.067	-1.565
YKR013W	PRY2	-0.699	-0.339	-0.989	-2.439	-0.765
YKR036C	CAF4	-0.003	0.046	-0.081	-0.917	-1.299
YKR037C	SPC34	-0.351	-0.226	-0.466	-1.034	-0.259
YKR039W	GAP1	-1.336	-2.128	-1.253	0.096	-1.062
YKR043C		-0.186	0.207	-0.200	-0.830	-1.080
YKR044W	UIP5	-0.181	0.290	-0.558	-1.104	-0.724
YKR057W	RPS21A	0.220	0.099	-0.342	-2.046	-2.289
YKR059W	TIF1	0.222	0.334	0.067	-0.817	-1.318
YKR081C	RPF2	0.025	-0.159	-1.469	-2.485	-1.568
YKR092C	SRP40	-0.465	-0.340	-1.400	-2.775	-0.976
YKR094C	RPL40B	0.048	0.093	-0.025	-1.412	
YKR099W	BAS1	-0.674	-0.352	-1.259	-0.561	-0.630
YKR104W		-0.121	-0.375	-1.040	-0.194	-0.033
YLL002W	RTT109	-1.105	-0.541	-1.019	-1.666	-1.309
YLL008W	DRS1	-0.022	0.004	-0.279	-1.057	-0.835
YLL011W	SOF1	-0.328	-0.169	-1.226	-1.458	-1.127
YLL014W		0.055	-0.004	-0.193	-1.396	-1.308
YLL017W		-0.012	0.089	-0.401	-1.428	-1.450
YLL021W	SPA2	-0.437	-0.434	-1.111	-1.390	-0.970
YLL022C	HIF1	-0.694	-0.676	-1.468	-1.931	-1.056
YLL028W	TPO1	-0.814	-1.185	-0.790	-0.894	-1.797
YLL030C		-0.373	0.083	-0.651	-0.452	-1.093
YLL034C	RIX7	-0.444	-0.265	-1.661	-1.313	-1.866

YLL044W		0.434	0.299	-0.164	-1.724	-2.551
YLL045C	RPL8B	0.141	0.359	-0.236	-2.147	-1.898
YLL064C		-0.448	0.145	-1.027	-0.391	-1.134
YLL065W		-0.129	-0.043	-0.896		-2.159
YLR003C		-0.225	-0.074	-1.011	-1.775	-0.409
YLR007W	NSE1	-0.639	-0.597	-1.136	-0.639	0.289
YLR008C	PAM18	-0.249	-0.014	-0.526	-1.253	-1.285
YLR009W	RLP24	-0.057	-0.116	-1.233	-1.937	-1.026
YLR017W	MEU1	-0.279	-0.216	-1.131	-2.325	-1.460
YLR029C	RPL15A	0.191	0.197	-0.305	-1.734	-2.259
YLR031W		0.178	0.061	0.029	-0.935	-1.478
YLR037C	DAN2	-0.104	0.117	-0.312	-1.235	-1.147
YLR043C	TRX1	0.140	0.057	0.113	-1.046	-1.771
YLR045C	STU2	-0.255	-0.231	-0.599	-0.727	-1.276
YLR048W	RPS0B	0.189	0.268	-0.294	-1.969	-2.702
YLR049C		-0.961	-0.854	-1.379	-0.724	-0.980
YLR050C		-0.262	-0.383	-0.697	-1.411	-0.366
YLR051C	FCF2	0.083	0.112	-0.540	-1.101	-0.239
YLR056W	ERG3	-1.007	-1.088	-1.530	-2.539	-0.407
YLR061W	RPL22A	0.126	0.091	-0.220	-2.043	-1.883
YLR062C	BUD28	0.260	-0.049	-0.182	-1.901	-2.350
YLR073C		-0.381	-0.153	-1.078	-2.300	-0.766
YLR075W	RPL10	0.223	0.273	-0.073	-1.247	-1.924
YLR076C		0.287	0.187	-0.150	-1.441	-2.264
YLR083C	EMP70	-0.030	0.017	-0.505	-1.156	-0.973
YLR106C	MDN1	-0.460	0.010	-0.432	-1.048	-1.191
YLR111W		0.111	-0.063	-0.191	-1.756	-1.872
YLR112W		-1.241		-0.616	-0.930	-0.748
YLR124W		0.065	0.035	-0.378	-1.962	-1.508
YLR129W	DIP2	-0.541	-0.356	-1.177	-1.545	-1.331
YLR132C		-0.543	-0.739	-0.143		-1.256
YLR137W		-0.255	0.159	-0.467	-2.248	-2.009
YLR140W		0.046	0.040	-0.412	-1.708	-1.417
YLR143W		-0.039	-0.106	-0.149	-0.818	-0.996
YLR146C	SPE4	-0.292	-0.369	-0.993	-1.866	-0.758
YLR147C	SMD3	-0.170	-0.004	-0.308	-1.196	-0.880
YLR150W	STM1	0.295	0.413	0.031	-1.171	-2.246
YLR153C	ACS2	0.026	0.001	-0.192	-0.222	-1.000
YLR154C	RNH203	-0.186	-0.123	-0.362	-1.821	-1.807
YLR156W		-0.228	-0.028	-0.464	-1.628	-1.532
YLR159W		-0.045	-0.004	-0.390	-1.816	-1.762
YLR167W	RPS31	0.223	0.164	-0.176	-1.729	-2.700
YLR172C	DPH5	0.142	0.083	-0.384	-1.564	-0.983
YLR175W	CBF5	0.059	0.196	-0.914	-2.032	-1.630
YLR183C	TOS4	-1.260	-1.449	-2.154	-3.800	-2.194
YLR185W	RPL37A	0.175	0.222	-0.133	-1.790	-2.115
YLR186W	EMG1	-0.267	-0.380	-1.033	-2.104	-1.162
YLR196W	PWP1	-0.305	0.055	-1.210	-2.152	-1.359
YLR197W	SIK1	-0.086	0.067	-0.884	-2.034	-1.809
YLR198C		0.395	0.015	-0.568	-1.904	-1.215

YLR200W	YKE2	-0.135	0.136	-0.246	-0.942	-1.344
YLR202C		-0.059	-0.072	0.075	-1.067	-0.605
YLR212C	TUB4	-0.851	-0.577	-1.332		-1.182
YLR217W		-0.349	-0.049	-0.451	-1.403	-1.431
YLR221C	RSA3	0.044	0.008	-0.765	-1.668	-0.089
YLR222C	UTP13	-0.261	0.125	-1.100	-1.799	-1.806
YLR230W		-0.163	0.103	-0.425	-1.466	-1.746
YLR232W		-0.060	0.094	-0.087	-1.477	-1.214
YLR249W	YEF3	0.241	0.245	-0.326	-1.803	-2.189
YLR254C	NDL1	0.383	0.271	0.615	0.201	-1.864
YLR264W	RPS28B	0.050	0.017	-0.322	-1.884	-1.838
YLR269C		-0.154	-0.016	-0.530	-1.911	-1.699
YLR276C	DBP9	-0.252	-0.100	-1.253	-2.318	-0.992
YLR292C	SEC72	-0.014	0.162	-0.154	-0.981	-1.141
YLR293C	GSP1	0.298	0.037	0.094	-0.742	-1.136
YLR302C		-0.138	0.147	-0.343	-1.225	-0.218
YLR311C		-0.270	0.048	-0.445	-1.840	-1.204
YLR332W	MID2	-1.029	-0.596	-1.129	-1.666	-0.672
YLR333C	RPS25B	0.103	0.174	-0.076	-1.450	-1.945
YLR334C		-0.061	-0.021	-0.079	-1.355	
YLR336C	SGD1	-0.541	-0.180	-1.085		-0.917
YLR339C		0.422	0.328	-0.126	-1.255	-2.144
YLR340W	RPP0	0.189	0.332	-0.053	-1.356	-2.278
YLR346C		-0.201	-0.106	-0.106	-1.286	-0.773
YLR354C	TAL1	0.179	0.201	0.179	-0.574	-1.361
YLR355C	ILV5	-1.032	-0.641	-1.300	-1.750	-0.865
YLR358C		0.218	0.230	-0.070	-1.091	-0.380
YLR365W		0.064	-0.003	-0.230	-1.814	-1.474
YLR372W	SUR4	-0.060	0.036	-0.904	-2.173	-2.026
YLR374C		0.050	0.169	-0.104	-1.222	-1.298
YLR377C	FBP1	-0.476	0.009	-0.587	-1.052	-0.844
YLR378C	SEC61	-0.298	-0.195	-0.504	-1.193	-0.980
YLR388W	RPS29A	0.221	0.020	-0.202	-1.289	-0.259
YLR401C	DUS3	-0.214	0.145	-0.997	-0.610	-0.337
YLR405W	DUS4	-0.348	-0.139	-0.934	-1.423	-1.332
YLR406C	RPL31B	-0.178	-0.547	-0.353	-1.542	-0.898
YLR407W		-0.370	-0.083	-0.504	-1.007	0.186
YLR408C		-0.060	0.018	-0.153	-1.016	-0.587
YLR413W		-0.507	-1.047	-1.248	-2.714	-1.528
YLR415C		-0.024	0.079	-0.255	-1.126	-0.706
YLR428C		0.064	-0.027	-0.242	-1.354	
YLR432W	IMD3	-0.196	-0.054	-1.346	-2.851	-3.054
YLR433C	CNA1	0.103	0.057	-0.134	-1.031	-0.443
YLR441C	RPS1A	0.204	0.271	-0.244	-1.667	-2.252
YLR448W	RPL6B	-0.006	0.210	-0.354	-1.978	-2.501
YLR449W	FPR4	0.185	0.167	-0.674	-1.855	-1.435
YLR451W	LEU3	-0.314	-0.103	-1.269	-1.999	-2.297
YLR453C	RIF2	-0.690	-0.299	-0.739	-1.062	0.262
YLR459W	GAB1	-0.323	-0.324	-0.573	-1.076	-0.696
YLR461W	PAU4	-0.112	0.006	-0.296	-1.165	-0.870

YML008C	ERG6	-0.188	-0.263	-0.585	-0.875	-1.104
YML022W	APT1	0.073	-0.020	-0.626	-1.862	-1.273
YML024W	RPS17A	0.140	0.069	-0.208	-1.901	-2.503
YML027W	YOX1	-1.336	-1.333	-2.058	-4.362	-2.173
YML037C			-0.243	-0.882	-1.091	-0.860
YML043C	RRN11	-0.466	-0.196	-0.929	-1.084	-1.303
YML052W	SUR7	-0.191	-0.493	-0.270	-1.067	-0.997
YML056C	IMD4	-0.349	-0.311	-1.689	-3.092	-2.461
YML060W	OGG1	-0.725	-0.643	-2.024	-2.766	-2.372
YML061C	PIF1	-0.665	-0.792	-0.765		-1.176
YML063W	RPS1B	-0.052	0.260	-0.257	-1.732	-2.753
YML065W	ORC1	-0.341	-0.119	-0.830	-1.194	-1.120
YML073C	RPL6A	0.291	0.160	-0.241	-1.681	-2.477
YML080W	DUS1	-0.538	-0.124	-1.381	-2.590	-1.795
YML082W		-0.178	0.055	-0.229	-1.003	-0.956
YML087C		-0.283	0.150	-0.495	-0.769	-1.159
YML094W	GIM5	-0.039	-0.266	-0.473	-1.763	-0.655
YML096W		-0.426	-0.164	-1.263	-2.011	-0.950
YML102W	CAC2	-0.600	-0.650	-1.318	-2.272	-1.443
YML106W	URA5	0.266	0.249	-0.153	-1.105	-0.857
YML108W		0.027	0.147	-0.427	-1.529	
YML125C	PGA3	-0.014	-0.122	-0.766	-1.442	-0.983
YML126C	ERG13	-0.116	-0.192	-0.463	-0.758	-1.061
YML129C	COX14	0.091	0.072	-0.136	-1.135	-0.772
YMR003W		-0.383	-0.177	-0.938	-2.248	-1.261
YMR006C	PLB2	-0.115	-0.079	-1.033	-1.262	-0.869
YMR007W		-0.058	-0.116	-0.058	-1.048	-0.588
YMR011W	HXT2	0.337	0.469	-1.179	-2.569	-0.377
YMR014W	BUD22	-0.331	-0.014	-1.043	-1.483	-1.042
YMR048W	CSM3	-0.856	-0.661	-0.973	-0.416	-1.220
YMR049C	ERB1	-0.378	-0.232	-1.406	-2.281	-1.751
YMR058W	FET3	-0.906	-0.583	-0.875	-1.909	-0.683
YMR075C-a		-0.052	0.134	-0.417	-1.710	-1.181
YMR086C-a		-0.078	-0.104	-0.026	-1.271	0.225
YMR093W	UTP15	-0.302	-0.035	-0.844	-2.370	-0.331
YMR116C	ASC1	0.323	0.249	-0.147	-1.585	-2.763
YMR117C	SPC24	-0.046	-0.069	-0.473	-1.842	-2.339
YMR121C	RPL15B	0.029	0.327	-0.361	-1.419	-1.980
YMR123W	PKR1	-0.098	0.006	-0.432	-1.340	-0.867
YMR127C	SAS2	-0.303	-0.017	-0.769	-1.184	-0.347
YMR128W	ECM16	0.017	0.030	-0.991	-2.635	
YMR131C	RRB1	-0.079	0.092	-1.171	-3.394	-2.374
YMR137C	PSO2	-0.014	0.063	-0.178	-0.742	-1.047
YMR142C	RPL13B	0.136	0.196	-0.251	-1.915	-2.634
YMR144W		-0.776	-0.616	-1.347	-3.107	-2.117
YMR177W	MMT1	-0.507	-0.165	-0.965	-1.203	-0.618
YMR194W	RPL36A	0.042	-0.024	-0.474	-1.784	-1.878
YMR199W	CLN1	-0.525	-0.415	-1.031	-1.493	-1.335
YMR202W	ERG2	-0.099	0.001	-0.507	-1.221	-0.738
YMR215W	GAS3	-0.389	-0.062	-1.183	-2.051	-2.011

YMR217W	GUA1	0.037	0.271	-0.619	-2.251	-1.625
YMR221C		-0.408	-0.059	-0.764	-1.224	-0.438
YMR231W	PEP5	0.065	0.166	-0.265	-1.091	-1.252
YMR233W	TRI1	0.194	0.090	-0.105	-1.430	-1.583
YMR236W	TAF9	0.121	0.224	-0.236	-1.707	-1.432
YMR239C	RNT1	-0.191	0.078	-1.264	-1.877	-0.487
YMR242C	RPL20A	0.175	0.188	-0.375	-2.203	-2.435
YMR243C	ZRC1	-0.182	-0.123	-0.661	-1.147	-0.557
YMR252C		-0.073	0.120	-0.358	-1.461	-0.932
YMR260C	TIF11	0.093	0.028	-0.074	-0.842	-1.032
YMR269W	TMA23	-0.128	-0.049	-0.835	-1.097	0.334
YMR292W	GOT1	-0.187	-0.251	-0.923	-2.071	-0.794
YMR294W	JNM1	0.214	0.162	0.235	0.071	-1.265
YMR305C	SCW10	-0.313	-0.303	-1.072	-1.993	-0.619
YMR307W	GAS1	-0.338	-0.146	-1.189	-2.267	-2.213
YMR308C	PSE1	-0.101	-0.353	-0.834	-1.001	-0.659
YMR309C	NIP1	0.006	-0.049	-0.367	-1.253	-1.355
YMR310C		0.005	-0.006	-0.527	-1.176	-0.134
YMR321C		0.318	0.267	-0.015	-1.654	-1.257
YNL002C	RLP7	0.134	0.128	-0.807	-1.841	-1.501
YNL010W		0.253	0.152	-0.045	-0.879	-1.071
YNL019C		-0.088	-0.021	-0.231	-1.339	-0.831
YNL030W	HHF2	0.000	0.037	-1.129	-2.170	-1.102
YNL031C	HHT2	0.000	0.141	-0.487	-1.331	-0.883
YNL033W		-0.133	0.065	-0.568	-1.246	-0.312
YNL041C	COG6	0.361	0.240	0.330	-1.873	0.363
YNL042W	BOP3	0.065	-0.037	-0.375	-1.247	-0.505
YNL043C		0.157	-0.169	-0.089	-1.517	-0.695
YNL044W	YIP3	-0.003	-0.262	-0.308	-1.265	-1.000
YNL050C		0.076	0.090	-0.188	-1.016	-0.751
YNL061W	NOP2	-0.471	-0.246	-1.113	-1.914	-1.626
YNL065W	AQR1	-1.590	-1.331	-2.481	-1.679	-2.149
YNL067W	RPL9B	0.286	0.130	-0.411	-1.920	-2.165
YNL069C	RPL16B	0.315	0.239	-0.160	-1.686	-1.775
YNL075W	IMP4	0.092	0.028	-0.219	-1.253	-0.274
YNL087W	TCB2	-0.092	-0.214	-0.893	-1.941	-0.531
YNL088W	TOP2	-0.747	-0.582	-1.025	-0.965	-0.683
YNL089C		-0.274	-0.250	-0.502	-1.467	-0.503
YNL090W	RHO2	-0.426	-0.209	-0.530	-1.596	-0.770
YNL096C	RPS7B	0.159	0.007	-0.753	-2.118	-2.012
YNL110C	NOP15	0.061	0.022	-0.869	-1.828	-1.165
YNL111C	CYB5	-0.364	-0.242	-0.925	-1.950	-0.028
YNL112W	DBP2	-0.713	-0.902	-2.259	-3.255	-1.867
YNL113W	RPC19	0.092	-0.095	-0.651	-2.166	0.087
YNL114C		0.146	-0.107	-0.905	-1.849	-0.127
YNL121C	TOM70	0.023	-0.332	-0.123	-0.433	-1.043
YNL126W	SPC98	-0.843	-0.305	-1.132	-0.446	
YNL132W	KRE33	0.076	-0.210	-1.289	-1.924	-1.380
YNL141W	AAH1	-0.301	-0.436	-1.958	-2.554	-1.905
YNL151C	RPC31	0.084	0.217	-0.462	-1.273	-0.684

YNL162W	RPL42A	0.180	0.143	-0.394	-1.990	-2.121
YNL175C	NOP13	0.013	-0.229	-0.682	-1.033	-0.892
YNL178W	RPS3	0.315	0.222	-0.294	-1.873	-2.259
YNL182C	IPI3	-0.782	-0.294	-1.765	-1.684	-0.754
YNL209W	SSB2	0.300	0.299	-0.277	-1.573	-2.273
YNL216W	RAP1	-0.679	-0.520	-1.163	-1.844	-1.888
YNL228W		-0.237	0.188	-0.345	-1.098	0.438
YNL230C	ELA1	-0.363	0.156	-0.319	-1.132	-0.991
YNL231C	PDR16	-0.405	-0.340	-0.655	-1.165	-1.151
YNL244C	SUI1	0.012	-0.256	-0.352	-1.022	-0.274
YNL247W		-0.096	0.112	-0.360	-1.074	-1.129
YNL251C	NRD1	0.152	0.156	-0.333	-1.738	-2.471
YNL262W	POL2	-0.541	-0.788	-1.622	0.495	-1.119
YNL289W	PCL1	-1.602	-1.136	-2.170	-3.558	-2.519
YNL290W	RFC3	-0.298	-0.112	-0.455	-1.311	-1.395
YNL292W	PUS4	-0.444	-0.159	-0.972	-1.330	-0.947
YNL300W		-0.811	-1.445	-2.153	-4.131	-2.092
YNL301C	RPL18B	0.204	0.109	-0.363	-2.108	-2.439
YNL302C	RPS19B	0.321	0.113	-0.334	-1.851	-2.248
YNL308C	KRI1	-0.057	-0.379	-0.718	-1.198	-0.727
YNL313C		-0.302	-0.284	-0.896	-1.006	-0.487
YNL332W	THI12	-1.164		-0.486	1.268	-0.040
YNL333W	SNZ2	-0.149	0.336	-0.151		-1.105
YNL339C	YRF1-6	0.073	-0.211	-0.122	-0.894	-2.392
YNR009W	NRM1	-0.854	-0.287	-1.267	-6.015	
YNR010W	CSE2	-0.286	0.179	-0.095	-1.057	0.152
YNR015W	SMM1	-0.194	-0.341	-0.361	-0.996	-0.266
YNR016C	ACC1	0.353	0.180	0.059	0.005	-1.913
YNR018W		-0.263	-0.186	-0.552	-1.297	-0.519
YNR024W		0.110	0.168	0.125	-1.072	
YNR025C		-0.250	0.203	-0.116	-1.359	
YNR038W	DBP6	-0.335	0.114	-0.821	-1.658	-0.391
YNR046W	TRM112	0.172	0.150	-0.302	-1.670	-0.051
YNR050C	LYS9	-0.421	-0.224	-0.337	0.100	-1.225
YNR053C	NOG2	-0.826	-0.090	-1.540	-1.903	
YNR054C	ESF2	0.070	-0.088	-0.372	-1.051	-0.145
YNR056C	BIO5	-0.188	0.280	-1.106		0.635
YNR061C		0.075	0.051	-0.501	-1.635	-0.331
YNR076W	PAU6	-0.519	0.171	-1.369	0.094	-0.933
YOL020W	TAT2	-0.458	0.040	-0.728	-1.104	-1.323
YOL026C	MIM1	-1.121	-0.205	0.007	-0.695	0.245
YOL034W	SMC5	-0.489	-0.109	-1.192		-0.500
YOL039W	RPP2A	0.276	0.240	0.083	-1.374	-1.783
YOL040C	RPS15	0.211	0.170	-0.081	-1.536	-2.245
YOL061W	PRS5	-0.241	-0.156	-0.659	-1.034	-0.207
YOL077C	BRX1	0.042	-0.150	-1.503	-3.079	-1.914
YOL080C	REX4	-0.357	-0.012	-1.768	-2.784	-1.922
YOL090W	MSH2	-0.537	-0.701	-0.466	-0.449	-1.111
YOL092W		-0.198	0.002	-0.664	-1.423	-0.581
YOL093W	TRM10	-0.191	0.031	-0.878	-1.443	-0.987

YOL097C	WRS1	-0.063	0.104	-0.365	-1.009	-1.296
YOL102C	TPT1	-0.340	-0.200	-0.561	-1.175	-0.060
YOL109W	ZEO1	0.013	-0.352	-0.510	-1.081	-0.646
YOL120C	RPL18A	0.112	-0.080	-0.150	-1.354	-1.893
YOL124C	TRM11	-0.545	-0.200	-1.852	-2.308	-3.677
YOL125W	TRM13	0.297	0.262	-0.744	-1.554	-0.282
YOL127W	RPL25	0.239	0.157	-0.142	-1.904	-2.659
YOL139C	CDC33	0.230	-0.058	-0.273	-1.017	-1.072
YOL141W	PPM2	-0.187	0.179	-0.753	-1.330	-0.669
YOL146W	PSF3	-0.424	-0.289	-0.963	-1.792	-1.172
YOL154W	ZPS1	-0.045	0.013	-0.558	-2.429	-1.597
YOL157C		-0.329	0.013	-0.798	-0.174	-1.071
YOR004W	UTP23	-0.548	-0.521	-1.956	-2.612	-1.434
YOR016C	ERP4	-0.325	-0.408	-0.805	-1.390	-0.535
YOR021C		0.259	-0.291	-0.674	-1.072	-0.552
YOR025W	HST3	-0.217	-0.363	-0.239	-0.833	-1.050
YOR040W	GLO4	0.085	-0.063	-0.101	-1.340	-1.488
YOR046C	DBP5	-0.114	-0.049	-0.378	-0.368	-1.080
YOR063W	RPL3	0.108	0.237	-0.308	-1.441	-1.942
YOR073W	SGO1	-0.332	-0.357	-1.232	-1.982	-2.283
YOR074C	CDC21	-0.806	-0.675	-1.585	-2.140	-1.842
YOR077W	RTS2	-0.317	0.043	-0.523	-1.702	1.863
YOR078W	BUD21	-0.095	-0.082	-0.954	-1.371	-0.983
YOR083W	WHI5	-0.476	0.045	-0.385	-0.612	-1.226
YOR091W	TMA46	-0.242	-0.105	-0.691	-1.511	-1.182
YOR095C	RKI1	-0.172	0.029	-1.285	-2.642	-1.393
YOR096W	RPS7A	0.230	0.165	-0.310	-1.973	-2.703
YOR101W	RAS1	-0.456	-0.524	-1.484	-2.248	-1.925
YOR108W	LEU9	-0.413	-0.031	-0.788	-1.334	-0.771
YOR133W	EFT1	0.081	0.350	-0.094	-0.674	-1.564
YOR143C	THI80	-0.005	-0.157	-0.682	-0.794	-1.033
YOR144C	ELG1	-0.580	-0.758	-1.158	-2.155	
YOR145C	PNO1	-0.182	-0.242	-1.218	-2.070	-0.499
YOR149C	SMP3	0.070	0.090	-0.278	-1.450	-1.712
YOR153W	PDR5	-0.189	-0.736	-0.468	-1.505	0.012
YOR182C	RPS30B	0.314	0.030	-0.278	-1.788	-1.716
YOR188W	MSB1	-0.405	-0.079	-0.695	-1.227	-0.436
YOR195W	SLK19	-0.091	0.245	-0.291	-0.768	-1.268
YOR204W	DED1	-0.523	-0.517	-1.135	-1.431	-1.797
YOR206W	NOC2	-0.288	0.157		-2.271	-1.391
YOR234C	RPL33B	0.152	0.072	-0.415	-1.900	-2.327
YOR236W	DFR1	-0.009	-0.171	-1.202	-2.560	-0.908
YOR253W	NAT5	-0.202	-0.204	-0.524	-1.469	-0.918
YOR271C	FSF1	0.121	0.089	-0.036	-0.520	-1.108
YOR272W	YTM1	-0.494	-0.197	-1.615	-3.445	-1.479
YOR276W	CAF20	0.242	0.316	-0.133	-1.213	-1.419
YOR277C		0.156	0.032	-0.361	-1.412	-1.170
YOR287C		-0.163	-0.062	-1.348	-1.302	-1.525
YOR294W	RRS1	0.047	-0.063	-0.975	-2.037	-0.744
YOR309C		0.496	0.020	-1.083	-2.495	-2.034

YOR310C	NOP58	-0.228	-0.078	-1.146	-2.445	-1.536
YOR312C	RPL20B	0.213	0.132	-0.525	-2.298	-2.507
YOR324C	FRT1	-0.794	-0.416	-0.577	0.064	-1.020
YOR335C	ALA1	-0.174	0.072	-0.697	-1.272	-1.762
YOR340C	RPA43	-0.124	-0.143	-1.525	-2.448	-1.889
YOR342C		-0.290	-0.414	-1.207	-1.500	0.160
YOR351C	MEK1	-0.192	0.194	-0.217	-1.203	-1.504
YOR361C	PRT1	-0.071	-0.180	-0.691	-1.189	-1.187
YOR369C	RPS12	0.356	0.069	-0.181	-1.490	-2.149
YOR375C	GDH1	-0.333	-0.328	-0.959	-1.347	-1.943
YOR383C	FIT3	-1.012	-0.840	-0.140	-0.072	1.341
YPL007C	TFC8	-0.004	-0.075	-0.427	-1.207	-1.188
YPL012W	RRP12	0.289	0.002	-1.058	-2.077	-0.703
YPL016W	SWI1	-1.244	-1.087	-0.865		-0.385
YPL018W	CTF19	0.008	0.098	-0.069	-1.350	-0.727
YPL037C	EGD1	0.300	0.086	0.134	-0.726	-1.065
YPL043W	NOP4	-0.526	-0.198	-1.139	-1.861	-0.968
YPL044C		-0.341	0.160	-0.623	-2.167	-0.185
YPL051W	ARL3	0.086	0.178	-0.211	-1.418	-1.020
YPL068C		-0.811	-0.123	-0.824	-1.445	-0.307
YPL079W	RPL21B	0.118	-0.399	-0.363	-1.973	-2.516
YPL080C		0.034	0.170		-2.767	-1.026
YPL081W	RPS9A	-0.191	0.130	-0.435	-1.942	-2.298
YPL086C	ELP3	-0.270	-0.038	-1.147	-1.522	
YPL090C	RPS6A	0.244	0.141	-0.396	-1.924	-2.661
YPL093W	NOG1	-0.792	-0.937	-1.795	-2.840	-2.230
YPL094C	SEC62	0.059	0.046	-0.331	-1.303	-0.612
YPL116W	HOS3	-0.023	0.133	-0.110	-1.334	-1.496
YPL126W	NAN1	-0.772	-0.186	-1.291	-2.225	-0.802
YPL127C	HHO1	-0.180	-0.169	-0.409	-1.636	-1.358
YPL131W	RPL5	0.283	0.262	-0.209	-1.799	-2.508
YPL142C		0.202	0.109	-0.170	-1.903	-2.394
YPL143W	RPL33A	0.024	0.081	-0.343	-1.887	-2.329
YPL146C	NOP53	-0.354	-0.237	-1.076	-1.740	-0.591
YPL153C	RAD53	-0.840	-0.573	-1.713	-0.780	-1.142
YPL155C	KIP2	-0.069	-0.097	-0.905	-1.386	-0.888
YPL157W	TGS1	-0.452	0.134	-1.069	-0.828	-0.500
YPL163C	SVS1	-0.832	-1.144	-1.962	-3.420	-2.002
YPL183C	RTT10	0.052	-0.091	-0.891	-1.349	-0.447
YPL198W	RPL7B	0.168	0.068	-0.514	-1.621	-2.320
YPL207W	TYW1	-0.297	-0.013	-0.868	-1.408	-0.476
YPL211W	NIP7	0.109	-0.091	-1.488	-2.275	-1.350
YPL217C	BMS1	-0.020	-0.015	-0.808	-1.051	-0.279
YPL220W	RPL1A	0.134	0.153	-0.419	-2.089	-2.333
YPL226W	NEW1	0.015	-0.423	-1.017	-1.418	-1.145
YPL227C	ALG5	0.212	0.256	-0.002	-0.448	-1.008
YPL233W	NSL1	-0.452	0.068	-0.638	-1.195	-0.203
YPL237W	SUI3	0.226	-0.027	-0.467	-1.222	-0.854
YPL251W		-0.481	0.208	-0.531	-2.169	0.376
YPL255W	BBP1	0.030	0.239	0.174	-0.232	-1.019

YPL256C	CLN2	-0.948	-1.069	-1.450	-1.961	-1.356
YPL267W	ACM1	-0.318	-0.843	-1.094	-1.917	-1.828
YPL272C		0.324	0.083	0.192	-0.261	-1.051
YPL273W	SAM4	-0.096	0.045	-0.371	-1.459	-1.387
YPL275W	FDH2	-0.267	-0.557	-1.013	-0.969	-0.681
YPR009W	SUT2	-1.004	-0.422	-1.149	-1.063	-0.784
YPR010C	RPA135	0.069	-0.199	-1.270	-2.372	-1.330
YPR037C	ERV2	-0.561	-0.404	-1.225	-1.209	-0.516
YPR043W	RPL43A	0.241	-0.260	-0.140	-1.783	-2.483
YPR044C	OPI11	0.243	-0.138	-0.106	-1.835	-2.382
YPR060C	ARO7	-0.004	-0.410	-0.341	-1.179	-1.487
YPR069C	SPE3	-0.109	0.135	-0.004	-0.569	-1.291
YPR074C	TKL1	0.423	0.475	0.261	-0.132	-1.162
YPR080W	TEF1	0.223	0.118	0.181	-0.360	-1.039
YPR095C	SYT1	-0.221	-0.045	-1.286		-0.138
YPR102C	RPL11A	0.133	-0.235	-0.170	-1.751	-2.267
YPR118W	MRI1	-0.157	-0.174	-0.827	-1.320	-1.084
YPR119W	CLB2	0.329	0.034	0.061	-0.278	-2.069
YPR132W	RPS23B	-0.039	0.082	-0.247	-1.590	-1.851
YPR133C	SPN1	-0.076	-0.223	-0.390	-0.096	-1.073
YPR137W	RRP9	-0.325	-0.025	-0.728	-1.181	-0.604
YPR138C	MEP3	-0.869	-1.162	-0.930	-0.866	-0.278
YPR144C	NOC4	-0.213	0.061	-0.903	-1.308	-0.602
YPR145W	ASN1	-0.569	-0.502	-0.332	-0.638	-1.208
YPR151C	SUE1	-3.551		0.314	2.723	1.520
YPR163C	TIF3	0.181	0.215	-0.258	-1.065	-1.242
YPR170C		-0.027	-0.092	-0.147	-1.191	-0.662
YPR174C		-1.292	-0.395	-1.041	-0.766	-0.713
YPR187W	RPO26	-0.292	-0.508	-0.903	-1.664	-1.235

Genes induced in trk1,2 strain

ID	NAME	trk1,2 vs wt
YBL049W	MOH1	2.218
YBL078C	ATG8	1.045
YBR012C		2.441
YBR040W	FIG1	1.056
YBR054W	YRO2	1.867
YBR067C	TIP1	2.236
YBR104W	YMC2	1.224
YBR158W	AMN1	1.198
YBR249C	ARO4	0.998
YCL027W	FUS1	1.135
YCL055W	KAR4	1.149
YCR005C	CIT2	3.043
YDL037C	BSC1	1.912
YDR441C	APT2	1.030
YEL009C	GCN4	1.015
YEL071W	DLD3	2.783
YER042W	MXR1	1.260
YER081W	SER3	2.657
YER159C	BUR6	1.331
YFL058W	THI5	1.069
YFR030W	MET10	1.825
YGL032C	AGA2	1.535
YGL062W	PYC1	1.028
YGL121C	GPG1	1.760
YGL166W	CUP2	1.669
YGL184C	STR3	1.042
YGL255W	ZRT1	2.211
YGL256W	ADH4	1.480
YGR096W	TPC1	2.105
YHR053C	CUP1-1	1.902
YHR055C	CUP1-2	1.966
YHR071W	PCL5	2.516
YHR112C		1.368
YIL116W	HIS5	1.066
YIL117C	PRM5	1.162
YIR017C	MET28	1.275
YJL170C	ASG7	1.910
YJL217W		2.081
YJR010W	MET3	1.690
YJR029W		1.292
YJR078W	BNA2	1.681
YJR137C	ECM17	1.789
YKL001C	MET14	2.522
YKL043W	PHD1	1.573
YKR069W	MET1	1.245
YKR093W	PTR2	1.100
YLL061W	MMP1	0.998
YLR042C		2.454

Genes repressed in trk1,2 strain

ID	NAME	trk1,2 vs wt
YAR028W		-1.259
YAR073W	IMD1	-2.320
YBL042C	FUI1	-1.047
YBR072W	HSP26	-2.707
YBR132C	AGP2	-1.097
YBR149W	ARA1	-1.102
YBR169C	SSE2	-1.077
YBR286W	APE3	-1.122
YCL064C	CHA1	-2.547
YCR004C	YCP4	-1.126
YDR231C	COX20	-1.087
YDR342C	HXT7	-1.141
YEL011W	GLC3	-1.188
YEL039C	CYC7	-1.311
YEL065W	SIT1	-3.599
YEL073C		-1.361
YER001W	MNN1	-1.019
YER145C	FTR1	-2.318
YFL014W	HSP12	-4.315
YFR015C	GSY1	-1.714
YGL055W	OLE1	-1.435
YGL077C	HNM1	-1.951
YGR086C	PIL1	-1.138
YGR108W	CLB1	-1.307
YGR218W	CRM1	-1.038
YGR238C	KEL2	-1.017
YGR248W	SOL4	-1.611
YGR259C		-1.081
YGR260W	TNA1	-1.266
YGR281W	YOR1	-1.650
YHL028W	WSC4	-1.298
YHR096C	HXT5	-1.190
YHR216W	IMD2	-2.003
YIL051C	MMF1	-1.301
YIL087C		-1.338
YIL111W	COX5B	-1.303
YIL121W	QDR2	-1.649
YIL128W	MET18	-1.028
YJL035C	TAD2	-1.266
YJL078C	PRY3	-1.022
YJL153C	INO1	-1.824
YJL210W	PEX2	-1.036
YJR073C	OPI3	-1.141
YJR115W		-1.677
YKL035W	UGP1	-1.193
YKL182W	FAS1	-1.377
YKL216W	URA1	-1.389
YKR039W	GAP1	-2.138

YLR092W	SUL2	1.474
YLR460C		1.012
YML047C	PRM6	1.916
YML131W		2.204
YMR062C	ECM40	1.130
YMR096W	SNZ1	1.618
YMR164C	MSS11	1.102
YNL036W	NCE103	2.161
YNL160W	YGP1	1.109
YNL332W	THI12	1.166
YNR044W	AGA1	1.655
YOL058W	ARG1	1.116
YOL150C		1.309
YOR130C	ORT1	1.072
YOR202W	HIS3	1.127
YOR247W	SRL1	1.610
YOR248W		1.567
YOR292C		1.076
YOR303W	CPA1	1.465
YPL156C	PRM4	1.193
YPR167C	MET16	2.031

YLL028W	TPO1	-1.031
YLR112W		-1.102
YLR132C		-1.092
YLR178C	TFS1	-1.862
YLR231C	BNA5	-1.347
YLR354C	TAL1	-1.132
YLR432W	IMD3	-1.844
YML100W	TSL1	-1.925
YML118W	NGL3	-1.235
YML123C	PHO84	-5.348
YML128C	MSC1	-1.587
YMR058W	FET3	-2.253
YMR102C		-1.393
YMR105C	PGM2	-1.905
YMR250W	GAD1	-1.867
YMR316W	DIA1	-1.038
YNL065W	AQR1	-1.561
YNL112W	DBP2	-1.583
YNL141W	AAH1	-1.301
YNL170W		-1.139
YNL262W	POL2	-1.096
YOL126C	MDH2	-1.596
YOL143C	RIB4	-1.005
YOR153W	PDR5	-1.917
YOR178C	GAC1	-1.382
YOR185C	GSP2	-1.523
YOR273C	TPO4	-1.137
YPL004C	LSP1	-1.160
YPL019C	VTC3	-1.810
YPR149W	NCE102	-1.128

Publication two

Functional interactions between potassium and phosphate homeostasis in *Saccharomyces cerevisiae*

David Canadell, Asier González, Carlos Casado and Joaquín Ariño

Molecular Microbiology (2015) **95**(3), 555-572

Molecular Microbiology (2015) 95(3), 555–572 ■
doi:10.1111/mmi.12886
First published online 22 December 2014

Functional interactions between potassium and phosphate homeostasis in *Saccharomyces cerevisiae*

David Canadell, Asier González,† Carlos Casado‡ and Joaquín Ariño*
Institut de Biotecnologia i Biomedicina and Departament de Bioquímica i Biologia Molecular, Universitat Autònoma de Barcelona, Bellaterra, Barcelona 08193, Spain.

Summary

Maintenance of ion homeostatic mechanisms is essential for living cells, including the budding yeast *Saccharomyces cerevisiae*. Whereas the impact of changes in phosphate metabolism on metal ion homeostasis has been recently examined, the inverse effect is still largely unexplored. We show here that depletion of potassium from the medium or alteration of diverse regulatory pathways controlling potassium uptake, such as the Trk potassium transporters or the Pma1 H^+-ATPase, triggers a response that mimics that of phosphate (Pi) deprivation, exemplified by accumulation of the high-affinity Pi transporter Pho84. This response is mediated by and requires the integrity of the *PHO* signaling pathway. Removal of potassium from the medium does not alter the amount of total or free intracellular Pi, but is accompanied by decreased ATP and ADP levels and rapid depletion of cellular polyphosphates. Therefore, our data do not support the notion of Pi being the major signaling molecule triggering phosphate-starvation responses. We also observe that cells with compromised potassium uptake cannot grow under limiting Pi conditions. The link between potassium and phosphate homeostasis reported here could explain the invasive phenotype, characteristic of nutrient deprivation, observed in potassium-deficient yeast cells.

Introduction

Potassium is the major intracellular cation in most living cells and it is an absolute requirement in yeasts (Aiking and Tempest, 1976). The intracellular concentration of this cation in the budding yeast *Saccharomyces cerevisiae* ranges from 200 to 300 mM. Remarkably, this organism still proliferates in the presence of very low external potassium concentrations (below 1 mM). This steep gradient can be maintained by the activity of plasma-membrane high-affinity potassium transporters, which allow influx of positively charged potassium ions across the membrane driven by the electrochemical gradient generated by the H^+-ATPase Pma1 (see Rodriguez-Navarro, 2000; Arino *et al.*, 2010 for reviews). *S. cerevisiae* contains two of such transporters, Trk1 and Trk2 (Gaber *et al.*, 1988; Ko *et al.*, 1990; Ko and Gaber, 1991), of which Trk1 is the most physiologically relevant. Cells lacking both *TRK1* and *TRK2* display a dramatic decrease in affinity for potassium transport and require relatively high amounts of potassium in the medium (> 10 mM) for growth.

The regulation of potassium transport through Trk1 and Trk2 is still a poorly understood process. Whereas early reports suggested that these transporters might be regulated by phosphorylation involving the Hal4 and Hal5 protein kinases (Mulet *et al.*, 1999), subsequent work demonstrated that these kinases are not required for direct regulation of Trk1 activity, but to stabilize these transporters at the plasma membrane under low-K^+ conditions, preventing their degradation (Perez-Valle *et al.*, 2007). A role for the SR (Ser/Arg-rich) protein kinase Sky1 in the regulation of Trk1 and Trk2 has been proposed (Forment *et al.*, 2002), although there is some controversy on the actual target of the kinase, and Trk-independent roles have been also proposed (Erez and Kahana, 2002). A strong candidate for Trk1 and Trk2 activity regulation is the protein phosphatase Ppz1 (see Fig. 1), which was previously related to salt tolerance (Posas *et al.*, 1992; 1995). Ppz1 is negatively controlled by two regulatory subunits, Hal3 and Vhs3 (de Nadal *et al.*, 1998; Ruiz *et al.*, 2004). Deletion of *PPZ1* or overexpression of *HAL3* is known to increase potassium influx via Trks (Ferrando *et al.*, 1995; Yenush *et al.*, 2002). Trk1 is phosphorylated *in vivo*, and it has been shown that Trk1 interacts with Ppz1 in plasma-membrane 'rafts' and that the level of phosphorylation of Trk1 increases in *ppz1 ppz2* mutants (Yenush *et al.*, 2005).

The requirement for high concentrations of intracellular potassium has been attributed to many diverse functions of this cation. Thus, potassium has been reported for many years to be required for protein synthesis (Lubin and Ennis,

Accepted 21 November, 2014. *For correspondence. E-mail joaquin.arino@uab.es; Tel. (+34) 93 5812182; Fax (+34) 93 5812011. Present addresses: †Department of Biochemistry, Biozentrum, University of Basel, Switzerland. ‡Evolva A/S, Copenhagen, Denmark.

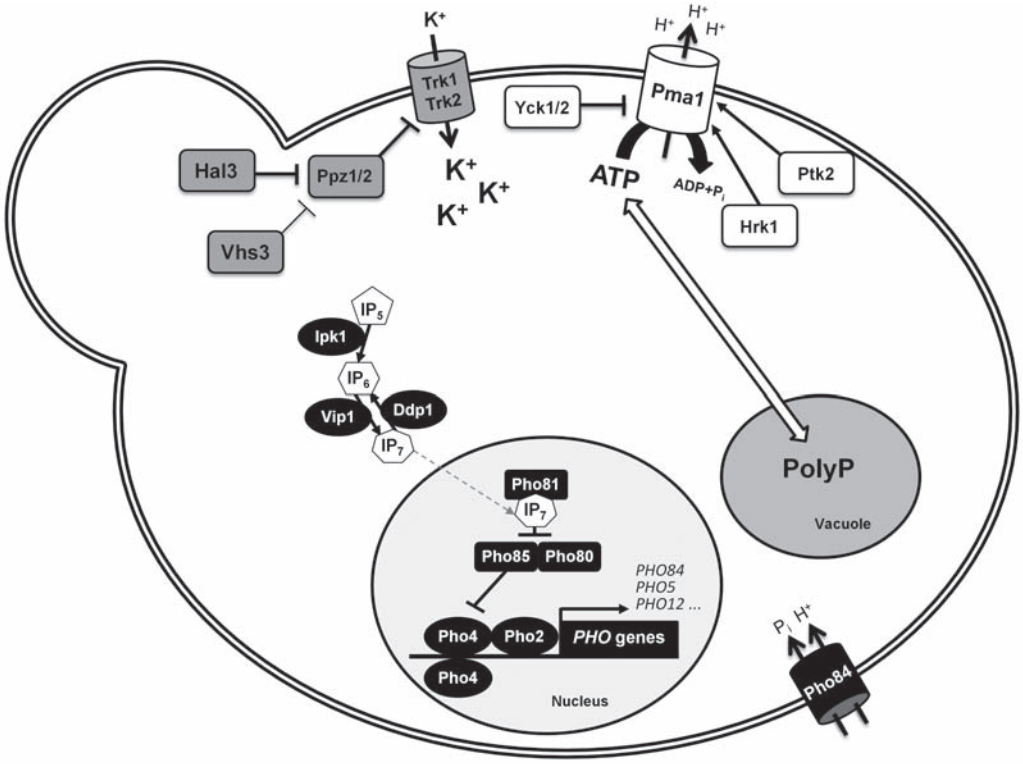

Fig. 1. Schematic cartoon describing plasma-membrane high-affinity potassium influx and proton efflux systems, and the main elements of the *PHO* signaling pathway in *S. cerevisiae*. Known mechanisms for regulation of the transporter activities are also depicted. See the Introduction section for details.

1964) and activation of diverse enzymes (see Page and Di Cera, 2006 and references therein), and the cation seems essential for regulation of cell volume and intracellular pH (Merchan *et al.*, 2004), maintenance of stable potential across the plasma membrane and for compensation of negative charges in many macromolecules. More recent work (Barreto *et al.*, 2012) has shown that shortage of potassium alters many other key cellular functions, including redox homeostasis and cell cycle progression.

Inorganic phosphate (Pi) is one of the most abundant anions in the cell. It is necessary for the biosynthesis of cellular components such as nucleic acids, nucleoproteins and phospholipids, and is involved in many metabolic and signaling pathways. Transport of Pi across the cell membrane is mediated by several transporters differing in their affinity for Pi. Pho87 and Pho90 H^+/Pi symporters constitute the low-affinity transport system ($K_m \sim 1$ mM), sufficient for growth at normal external Pi (Bun-ya *et al.*, 1996; Wykoff and O'Shea, 2001; Ghillebert *et al.*, 2011). High-affinity Pi uptake ($K_m \sim 10$ μM) is mediated by the plasma-membrane Pho84 and Pho89 transporters (Bun-ya *et al.*, 1991; Martinez and Persson, 1998; Persson *et al.*, 1999). Pho84 cotransports phosphate with H^+, it is mostly active at acidic pH and is responsible for most of the high-affinity Pi uptake under normal growth conditions (Pattison-Granberg and Persson, 2000). Pho89 is a phosphate/Na^+ symporter and works most efficiently under alkaline conditions (Martinez and Persson, 1998; Zvyagilskaya *et al.*, 2008). When Pi in the external medium is abundant, the expression levels of both *PHO84* and *PHO89* transporter-encoding genes are low. Expression of these genes, as well as that of other genes required for the use of Pi, such as the acid phosphatases *PHO5* and *PHO12*, is increased in response to Pi starvation and this transcriptional response is triggered by the activation of the *PHO* signaling pathway (Ogawa *et al.*, 1995; Auesukaree *et al.*, 2003; Persson *et al.*, 2003). This pathway (see Fig. 1) involves activation of the cyclin-dependent kinase inhibitor Pho81, which leads to inhibition of the Pho85–Pho80 cyclin-dependent kinase complex. The increase in the levels of IP_7, synthesized from IP_6 by the inositol hexakisphosphate kinase encoded by the *VIP1* gene, has been described as one of the signals that lead to the inhibition of the Pho81–Pho85–Pho80 complex (Lee *et al.*, 2007; 2008). Unphosphorylated transcription factor Pho4 then accumulates in the nucleus and binds to diverse phosphate-responsive gene promoters, including *PHO84*, stimulating their transcription. When extracellular Pi is not limiting, Pho81 is

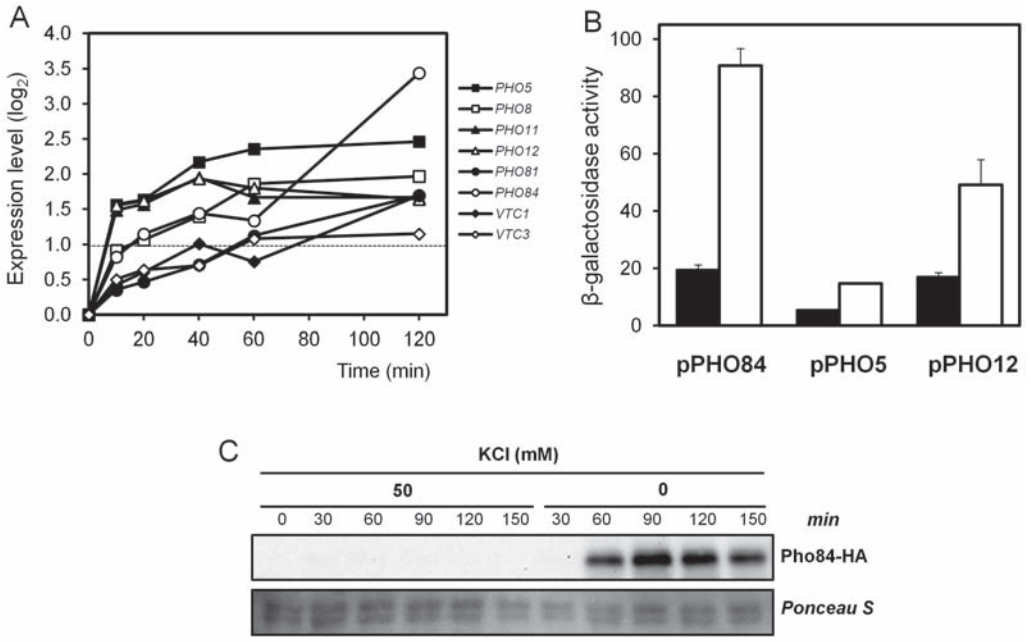

Fig. 2. Potassium starvation triggers induction of genes controlled by the *PHO* regulon.
A. Expression data relative to *PHO*-regulated genes was collected from the analysis of the time-dependent transcriptomic response to potassium deprivation reported in Barreto *et al.* (2012) and is represented as changes in $\log_2$ scale. Values above the discontinuous line indicate changes in mRNA level higher than twofold.
B. The wild type strain BY4741 was transformed with the *lacZ* reporter plasmids for the indicated promoters. Cultures were then transferred to synthetic medium containing no potassium (empty bars) or 50 mM KCl (closed bars) and growth resumed for 90 min. Cells were then collected and processed for β-galactosidase activity measurements. Data are mean ± SEM from nine independent determinations.
C. Wild-type BY4741 cells were grown on synthetic medium in the presence (50 mM) or absence of potassium for the indicated periods. Cells were collected and processed for SDS-electrophoresis (10% polyacrylamide gels) and immunodetection of HA-tagged Pho84 as described in Experimental Procedures section. Ponceau S staining of the membrane is shown for reference.

inactivated, and the Pho85–Pho80 kinase complex becomes active and phosphorylates Pho4, which is excluded from the nucleus and no longer able to induce expression of the *PHO*-regulated genes (Toh-e *et al.*, 1988; Kaffman *et al.*, 1994; Ogawa *et al.*, 2000).

A requirement for potassium for normal phosphate uptake in yeast was reported many years ago (Schmidt *et al.*, 1949; Goodman and Rothstein, 1957). However, these experiments were performed with yeast cultures undefined from a genetic point of view and, more importantly, under non-physiological conditions. Only recently, the effect of phosphate accumulation on metal homeostasis has been investigated in some detail (Rosenfeld *et al.*, 2010), showing that *pho80* mutants, which have lost the ability to downregulate the *PHO* pathway in the presence of abundant phosphate in the medium, also display abnormal intracellular levels of diverse metals, including potassium. In this work we investigate by a combination of biochemical and genetic approaches the reverse effect, that is, how alterations in potassium homeostasis affect phosphate metabolism. Our work demonstrates that the scarcity of extracellular potassium or the perturbation of the normal influx of the cation alters phosphate metabolism and triggers a response that mimics that of phosphate starvation in a way that depends on the integrity of the *PHO* signaling pathway. Therefore, our results bring to light the close relationship between potassium and phosphate homeostatic mechanisms.

Results

Potassium starvation triggers the induction of genes controlled by the PHO regulon

Our recent transcriptomic analysis of the yeast response to acute potassium starvation highlighted a substantial increase in mRNA of several genes known to be induced by phosphate limitation. These included *PHO5* and *PHO12*, encoding repressible acid phosphatases, *PHO84*, encoding the main high-affinity H^+/Pi transporter (but not *PHO89*, coding for a Na^+/Pi transporter active at alkaline pH), and *VTC1* and *VTC3*, involved in vacuolar polyphosphate accumulation (Fig. 2A). To confirm these results and to establish if these changes were due to activation of the gene promoters, we introduced in wild type cells transcriptional reporters based on the translational fusion of the

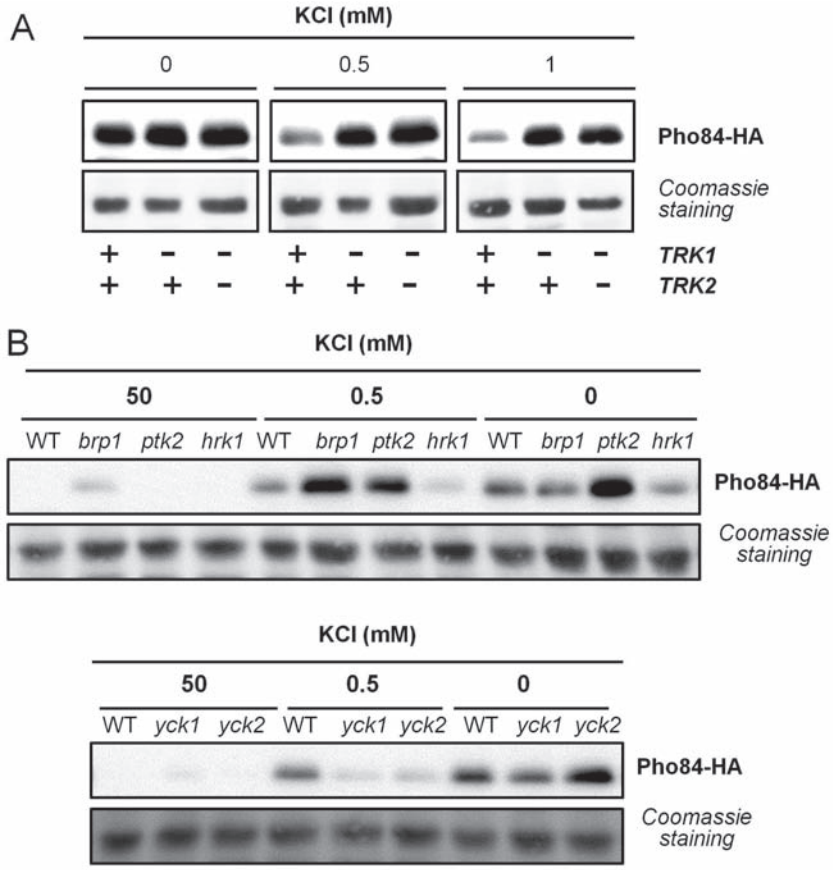

Fig. 3. Mutations that affect potassium homeostasis modify the expression of Pho84. A. Wild-type BY4741, DCS31 (*trk1*) and DCS32 (*trk1 trk2*) were grown in the presence of 50 mM KCl and then transferred to the synthetic medium containing the indicated amounts of KCl. Growth was resumed for 60 min and cells were collected and processed as in Fig. 2C. Membranes were stained with Coomassie Blue R-250.
B. Cultures of the strains shown (WT, wild type) were transferred to synthetic medium containing the indicated amounts of potassium for 60 min and cells were collected and processed for immunoblot as in Fig. 2C. Coomassie staining of the membranes is shown for reference.

PHO84, *PHO12* and *PHO5* promoters to the *lacZ* reporter gene encoding β-galactosidase. As shown in Fig. 2B, in all cases, cells exposed to lack of potassium for 90 min display a significant increase in β-galactosidase activity, indicating that lack of potassium results in activation of these promoters. Since expression of the Pho84 Pi transporter is a major readout of the response to phosphate availability, we generated a functional version of *PHO84* C-terminally tagged with a 3×-HA epitope that was expressed from its own promoter in a centromeric plasmid. As shown in Fig. 2C, when wild-type cells carrying this construct were transferred to a medium lacking potassium, the accumulation of Pho84 could be easily detected by immunoblot 1 h after removal of the cation, confirming that lack of potassium in the medium triggers a phosphate starvation-like response. Pho84 was detected in the particulate fraction when the cell content was separated by centrifugation at 16 000 × g for 30 min, suggesting that the protein could be located at the membrane (not shown).

Expression of Pho84 is affected by mutations that impact on potassium transport

We then sought to investigate how impairing potassium transport could affect Pho84 expression. To this end wild type, as well as *trk1* and *trk1 trk2* cells, lacking the high-affinity potassium transporters, were transformed with the Pho84-3×-HA construct, transferred to medium with different levels of potassium and the expression of Pho84 monitored by immunoblot. When cells were completely deprived of potassium, all three strains expressed Pho84 in similar amounts (Fig. 3A). However, when potassium is present in limiting amounts (0.5–1 mM), which makes the function of the high-affinity potassium transport necessary for a correct potassium supply, expression of Pho84 was clearly stronger in the *trk1* and *trk1 trk2* strains. Deletion of *TRK2*, which has a negligible effect on potassium uptake when *TRK1* is present, resulted in wild-type expression of Pho84 (not shown). Under conditions of potassium abundance (50 mM) none of the strains expressed Pho84 (Fig. 2C and data not shown). These experiments indicate again that perturbing potassium homeostasis impacts on normal phosphate metabolism.

The observation that mutation of *TRK1* affected expression of Pho84 in cells grown under limiting potassium levels prompted us to investigate if other mutations that directly or indirectly could interfere with normal potassium influx would have similar effect. Influx of potassium is largely driven by the electrochemical gradient generated by the *PMA1* proton pump. Thus, mutations decreasing

PMA1 function adversely affect potassium influx. Since *PMA1* is an essential gene, we resorted to the *BRP1* deletion, which affects the *PMA1* promoter function and results in decreased Pma1 activity (Porat *et al*., 2005), to the *ptk2* mutant, lacking a protein kinase that potently activates Pma1 (Goossens *et al*., 2000), and to the *hrk1* deletion strain, deficient in the Hrk1 protein kinase that has also been suggested to activate Pma1, although with much less potency (Goossens *et al*., 2000). As shown in Fig. 3B, expression of Pho84 was stronger in the *brp1* and *ptk2* mutants than in the wild-type strain. The effect of the *brp1* mutation was more evident at limiting external potassium concentrations (0.5 mM), whereas the consequence of the *ptk2* deletion was manifest also in the complete absence of potassium. In contrast, the *hrk1* mutation did not increase the expression of Pho84 compared to the wild-type strain and even yielded somewhat lower levels. Similarly, deletion of the *YCK1* or *YCK2* protein kinases, which are known to inhibit Pma1 function (Estrada *et al*., 1996), decreased Pho84 expression in cells that were grown under limiting (0.5 mM) potassium concentrations (Fig. 3C). As mentioned earlier, decreased *PMA1* function results in decreased potassium influx. However, since low-affinity Pi transport is based on H^+/Pi co-transport (as it is also the case for Pho84), the possibility that a reduced efflux of protons could limit Pi uptake (thus triggering Pho84 expression) was worth considering. To distinguish between this possibility from a limitation of potassium uptake via Trk1, we constructed double *trk1 brp1* and *trk1 ptk2* mutants and tested, in comparison with the single mutants, the expression level of Pho84 under limiting K^+ conditions. The rationale behind this experiment is that if the effect of decreased Pma1 activity is unrelated to that of the *trk1* mutation, then both effects should be additive. However, our results (Supplementary Fig. S1) indicate that this is not the case, since the level of expression of Pho84 in the double mutants is the same than that produced by the *trk1* mutation, thus supporting the notion that the effect of defective Pma1 activity likely occurs through limitation of K^+ uptake.

Influx of potassium through the Trk1 and Trk2 transporters is downregulated (by still unknown mechanisms) by the Ppz1 protein phosphatase. In turn, Ppz1 activity is inhibited by its regulatory subunits Hal3 and Vhs3. Therefore, elimination of Hal3 and Vhs3 activity should increase Ppz1 function and, consequently, impact negatively on potassium influx. As reported some years ago, a double *hal3 vhs3* mutant is not viable because these two proteins have moonlighting activities and, in addition to regulating Ppz1, they have essential functions in the CoA biosynthetic pathway (Ruiz *et al*., 2009; Abrie *et al*., 2012). Therefore, we constructed a conditional mutant by deleting *VHS3* and replacing the *HAL3* promoter by a *tetO* promoter regulatable by doxycycline. Transcriptomic analysis of the conditional strain after 15 h of addition of doxycycline (which leads to substantial blockage of *HAL3* expression, see inset in Fig. 4A) highlighted the induction 48 genes (Supp. Table S1). Interestingly, among the most potently induced genes were diverse members of the *PHO* regulon, such as *PHO84*, *PHO5* or *PHO12*, whereas *PHO89* was not induced (Fig. 4A). To confirm these results, we transformed the *tetO:HAL3 vhs3* conditional mutant with *PHO5*, *PHO12*, *PHO84* and *PHO89* *lacZ* reporters and tested β-galactosidase activity 15 h after the addition of doxycycline. As can be deduced from Fig. 4B, *PHO5*, *PHO12* and *PHO84* promoter activities are enhanced by progressive depletion of Hal3 in the *vhs3* background. In contrast, the *PHO89* promoter remained insensitive, in agreement with the lack of response observed in the microarray experiments. This difference is not surprising on the light of the different response kinetics exhibited by *PHO84* and *PHO89* in response to phosphate starvation and other forms of stress, highlighted in a very recent report (Serra-Cardona *et al*., 2014). Importantly, this effect was fully abolished by the deletion of the *PPZ1* gene, indicating that the observed effect is due to deregulation of Ppz1 (and likely to the consequent impact on potassium homeostasis) and not to the role of Hal3 and Vhs3 in CoA biosynthesis. Also of interest is the observation that deletion of *PHO81* drastically blocked the activation of *PHO5*, *PHO12* and *PHO84* promoters as well.

The relevance of regulation of Ppz1 was also assessed by monitoring expression of HA-tagged Pho84 by immunoblot and by fluorescence microscopy resorting to a Pho84-GFP construct. As shown in Fig. 4C, deletion of *HAL3* alone leads to detection of a faint immunoblot signal for Pho84. The Pho84 signal turns very strong in two different *tetO:HAL3 vhs3* strains (MAR24 and MAR119), differing only in the marker used for the deletion of *VHS3*, but expression of Pho84 is fully blocked by deletion of Ppz1. Attempts to detect GFP-tagged Pho84 in the BY4741 background were not satisfactory, likely due to low levels of the protein. We then monitored by immunoblot the expression level of Pho84 in different wild-type genetic backgrounds available in the laboratory stock. As shown in Supplementary Fig. S2, expression of Pho84 was particularly low in the BY4741 background under potassium deprivation. In contrast, expression levels in the JA100 strain were rather strong and, therefore, we resorted to this genetic background for Pho84 monitoring by fluorescence microscopy. As observed in Fig. 5A, whereas virtually no cells positive for Pho84 signal are visible in the wild-type strain, they occur abundantly in the *tetO:HAL3 vhs3* strain growing on Yeast Extract, Peptone, Dextrose (YPD) after 6 h in the presence of doxycycline. In contrast, Pho84 was almost undetectable when *PPZ1* was deleted in both backgrounds. Interestingly, while

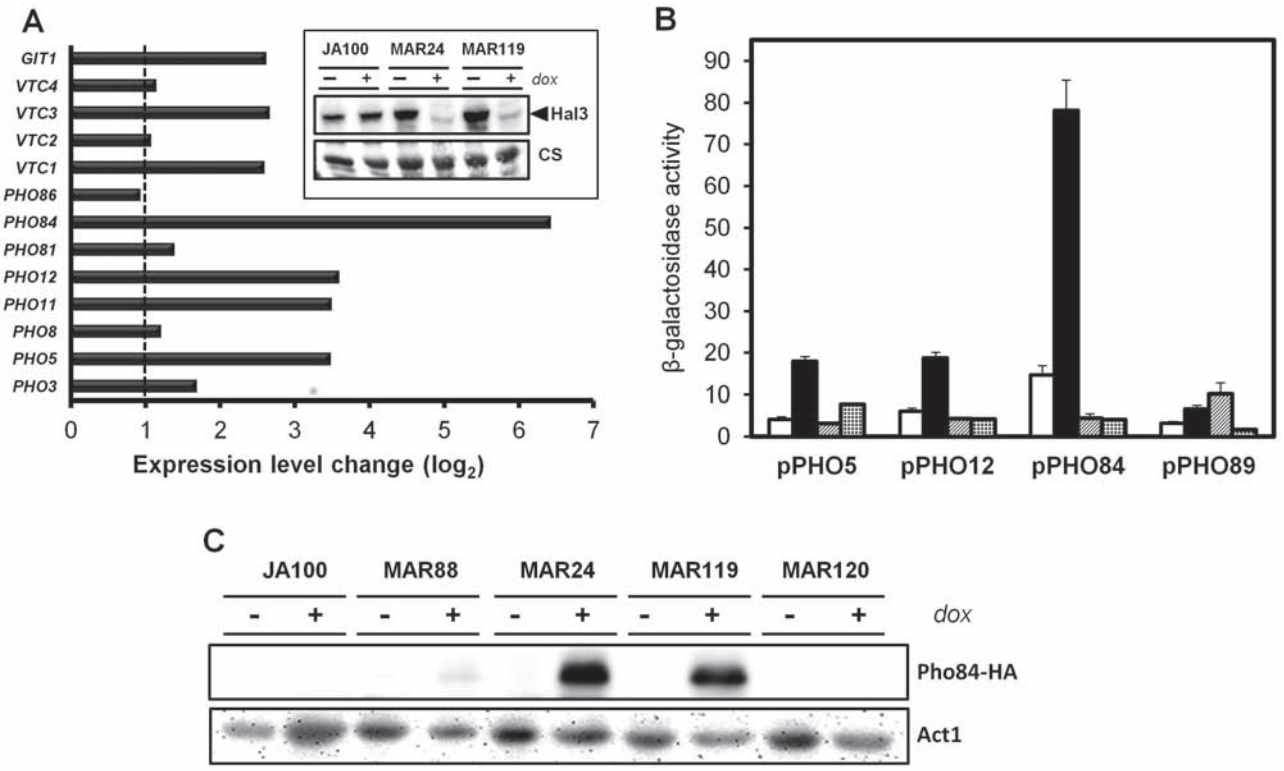

Fig. 4. Modulation of Ppz1 function affects expression of the *PHO*-regulon and Pho84 accumulation.
A. Strain MAR24 (*tetO:HAL3 vhs3::URA3*) was grown in the presence or absence of doxycycline (100 μg ml^{-1}) for 15 h, total RNA was prepared and genome-wide transcriptomic analysis carried out by DNA microarrays. The expression level ratio (minus/plus doxycycline) of diverse *PHO*-regulated genes is shown in $\log_2$ scale. The discontinuous line indicates the twofold change in mRNA level threshold. The immunoblot in inset shows the relative amounts of Hal3 present in wild type (JA100), MAR24 and MAR119 (*tetO:HAL3 vhs3::nat1*) strains with (+) or without (–) doxycycline treatment (100 μg ml^{-1}) for 15 h. Cells were grown in synthetic medium with 50 mM KCl. CS, Coomassie staining.
B. The *lacZ*-reporters for the indicated gene promoters were introduced in strain JA100 (wild type, open bars), MAR119 (*tetO:HAL3 vhs3*, closed bars), AGS11 (*tetO:HAL3 vhs3 ppz1*, stripped bars), and AGS6 (*tetO:HAL3 vhs3 pho81*, crossed bars) and β-galactosidase activity measured after 15 h in the presence of doxycycline. Data are mean ± SEM from 4 to 12 independent determinations.
C. Strains JA100 (wild type), MAR88 (*hal3*), MAR24 and MAR119 (two equivalent *tetO:HAL3 vhs3* strains, differing only in the marker used for deletion of *VHS3*), and MAR120 (*tetO:HAL3 vhs3 ppz1*) were transformed with plasmid pMM17-PHO84 and grown in the presence of doxycycline (100 μg ml^{-1}) as above. Cells were then processed for immumodetection of tagged Pho84 (40 μg protein/lane). Actin (Act1) signal is shown for comparison.

Pho84 was clearly detectable in the wild type and the *tetO:HAL3 vhs3* strains when cells were exposed for 6 h to limiting phosphate concentration in the medium, appearance of the transporter was also blocked by deletion of *PPZ1*, suggesting that the lack of the phosphatase could decrease normal Pho84 expression in response to phosphate scarcity. To confirm this possibility, extracts were prepared and the presence of Pho84 was assessed by immunoblot. As deduced from Fig. 5B, deletion of *PPZ1* has a clear negative impact in the amount of Pho84 produced in response to partial phosphate depletion (0.2 mM). Collectively, these results suggest that changes in potassium transport as a result of modulation of Ppz1 activity may affect phosphate homeostasis. Monitoring of Pho84 levels in yeast cells overexpressing Ppz1 was not feasible due to the very poor growth of these cells (Clotet *et al.*, 1996).

Potassium restriction decreases ATP and ADP levels, depletes polyphosphate reserves and affects growth in phosphate-limiting conditions

To further investigate the effects of potassium deprivation on phosphate homeostasis, we monitored the levels of total and free Pi in cells shifted to a medium lacking potassium. Figure 6A shows that a small but statistically significant increase of free Pi was detected after 90 min of potassium starvation. However, the levels of total Pi did not change during the experiment. We also monitored the effect of potassium starvation in the variation of adenine nucleotide levels. Figure 6B shows that removal of potassium caused a time-dependent depletion of the intracellular concentrations of ATP and ADP, with a concomitant increase in AMP levels. It is worth noting that the total amount of adenine nucleotides also decreased with time,

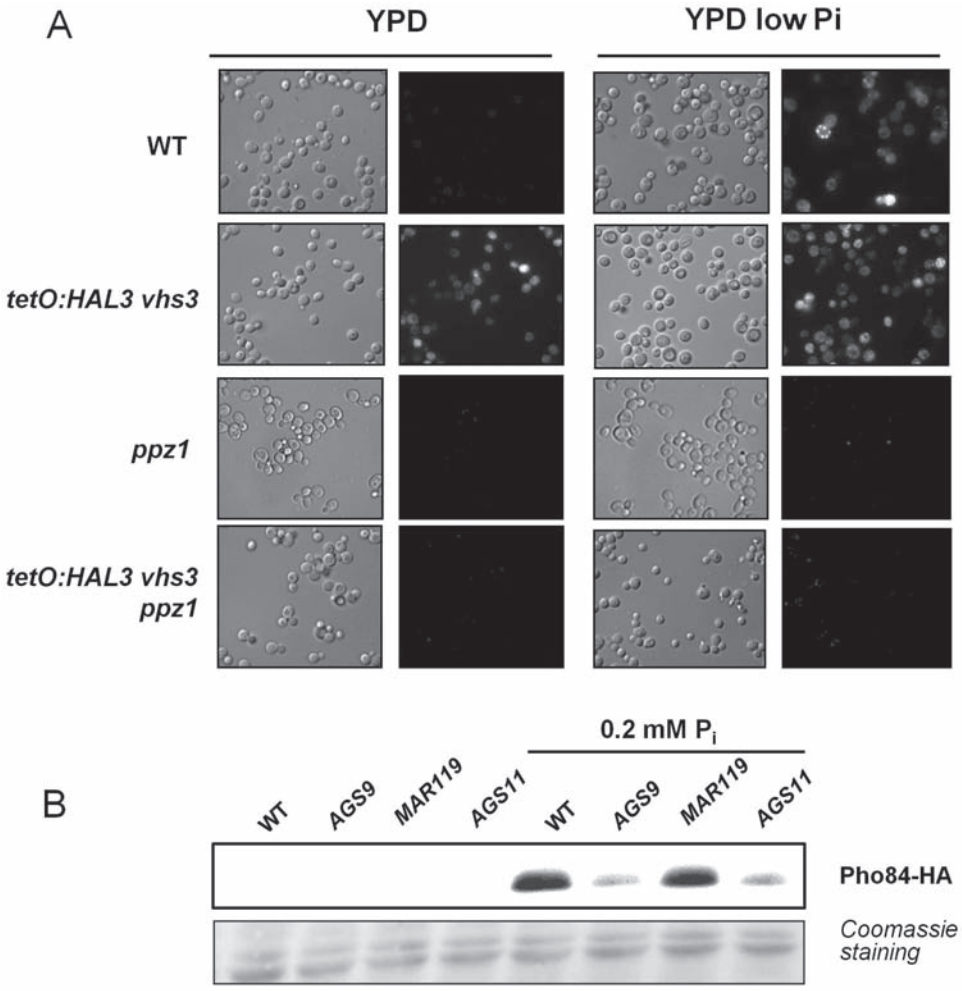

Fig. 5. Ppz1 influences Pho84 expression in phosphate-limiting conditions.
A. The indicated strains (WT, JA100; AGS9, *ppz1*; MAR119, *tetO:HAL3 vhs3*; AGS11, *tetO:HAL3* v*hs3 ppz1*) were transformed with plasmid EB0666, expressing a GFP-tagged version of Pho84. Cultures were incubated in synthetic medium in the presence of doxycycline (100 μg ml^{-1}) for 12 h and then transferred to fresh YPD medium or the same medium previously depleted for phosphate (containing doxycycline), and growth resumed for 6 h before monitoring of expressed Pho84 by fluorescence microscopy.
B. The mentioned strains were transformed with plasmid pMM15-PHO84, and cultures were grown in synthetic medium containing 10 mM phosphate. Cells were then transferred to the same medium containing limiting amounts (0.2 mM) of phosphate and growth was resumed for 3 h. All media contained 100 μg ml^{-1} doxycycline. Protein extracts were prepared and processed for SDS–PAGE and immunoblot. Coomassie staining of the membrane is shown for reference.

reaching around 60% of the initial values after 20 min of potassium depletion and remain stable thereafter (not shown). Polyphosphate levels steadily decreased upon removal of potassium, reaching less than 25% of the initial values after 40 min and becoming almost undetectable after 120 min (Fig. 6C). This profile was similar to that observed when cells were shifted to phosphate-limiting medium (0.1 mM), although in this case, the decrease rate was somewhat faster. Remarkably, if cells starved for potassium for 40 min received 50 mM potassium in the medium, polyphosphate stores rapidly recovered, and normal levels of the polymer were attained 80 min after re-addition of the cation (141.1 ± 17.2 mM). Addition of 50 mM of NaCl, although avoided further depletion of polyphosphate, did not allow recovering normal polyphosphate levels, leading to levels of only 62.4 ± 12.1 mM after 80 min of addition of the salt. Increasing the extracellular concentration of NaCl up to 200 mM further improved PolyP accumulation (105.9 ± 16.7 mM), although not reaching yet the values attained by 50 mM KCl. These differences could be due to the fact that yeast cells take up preferentially potassium over sodium cations. The perturbation of Ppz1 activity also impacts on polyphosphate levels. As observed in Fig. 6D, exposure of MAR24 or MAR119 strains to doxycycline for 16 h results in a substantial decrease in polyphosphate content (below 20% of the initial levels), and this decrease is totally blocked by deletion of *PPZ1* (strain MAR120). Since proper accumu-

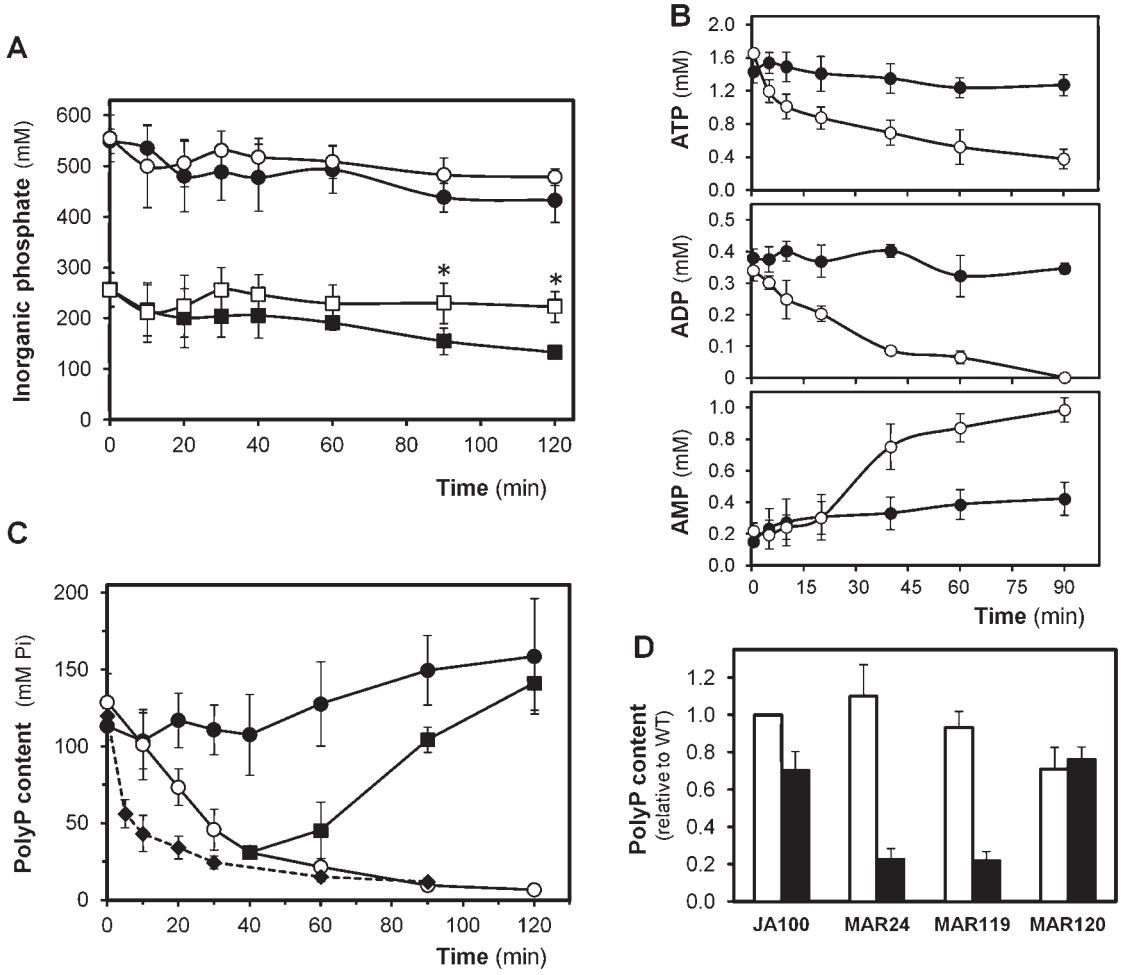

Fig. 6. Perturbation of potassium homeostasis alters normal polyphosphate levels.
A. Wild-type BY4741 cells were grown in synthetic medium in the presence of 50 mM potassium and 10 mM phosphate up to OD_{600} of 0.6 and then transferred to fresh medium (closed symbols) or the same medium lacking potassium (open symbols). Aliquots were collected at the indicated times and processed for total (circles) or free (squares) Pi determination. Data are mean ± SEM from five independent experiments. Asterisks denote significant differences ($P < 0.02$).
B. Cells were treated as described in panel (A) except that samples were rapidly quenched as described (Barreto *et al.*, 2012). Open symbols denote potassium-starved cells. Data are mean ± SD from three independent experiments.
C. Cells cultured as in panel (A) were transferred to fresh medium (●), the same medium lacking potassium (○), or containing only 0.1 mM phosphate (◆, discontinuous line). In some experiments, potassium (50 mM) was re-added to the medium after 40 min of potassium starvation (■). In all cases, aliquots were collected at the indicated times and processed for polyphosphate determination. Values were divided by a factor of 0.215 to account for polyphosphate recovery during the purification procedure. Data are mean ± SEM from three to four independent experiments.
D. Strains JA100 (wild type), MAR24 and MAR119 (both *tetO:HAL3 vhs3*) and MAR120 (*tetO:HAL3 vhs3 ppz1*) were grown for 16 h in the presence of doxycycline (100 μg ml^{-1}, closed bars). Cells were collected and processed for polyphosphate determination as above. Data are relative to the content in the wild-type strain and is expressed as the mean ± SEM from five independent experiments.

lation of polyphosphate is strongly linked to a regular phosphate metabolism (see Persson *et al.*, 2003 and references therein), these results reinforce the notion that alterations in normal potassium availability or transport have an impact on phosphate homeostasis.

This scenario is confirmed when cells deficient in the high-affinity potassium transport system are grown in normal or Pi-depleted YPD medium (YPD LPi). As shown in Fig. 7A, the *trk1 trk2* strain could not grow in YPD LPi medium, but growth was restored by further addition of KCl to the medium or expression of the *TRK1* gene from a centromeric plasmid. The beneficial effect of expression of Trk1 is linked to its ability to transport potassium, since a version of the transporter carrying the M1153R mutation, which abolish transport of potassium (Haro and Rodriguez-Navarro, 2003), did not promote growth at low Pi. This effect was also perceptible in the *trk1* mutant (Fig. 7A), whereas deletion of *TRK2* had no effect on growth at low Pi (not shown), in agreement with the minor role of this transporter in potassium influx. Likewise, when

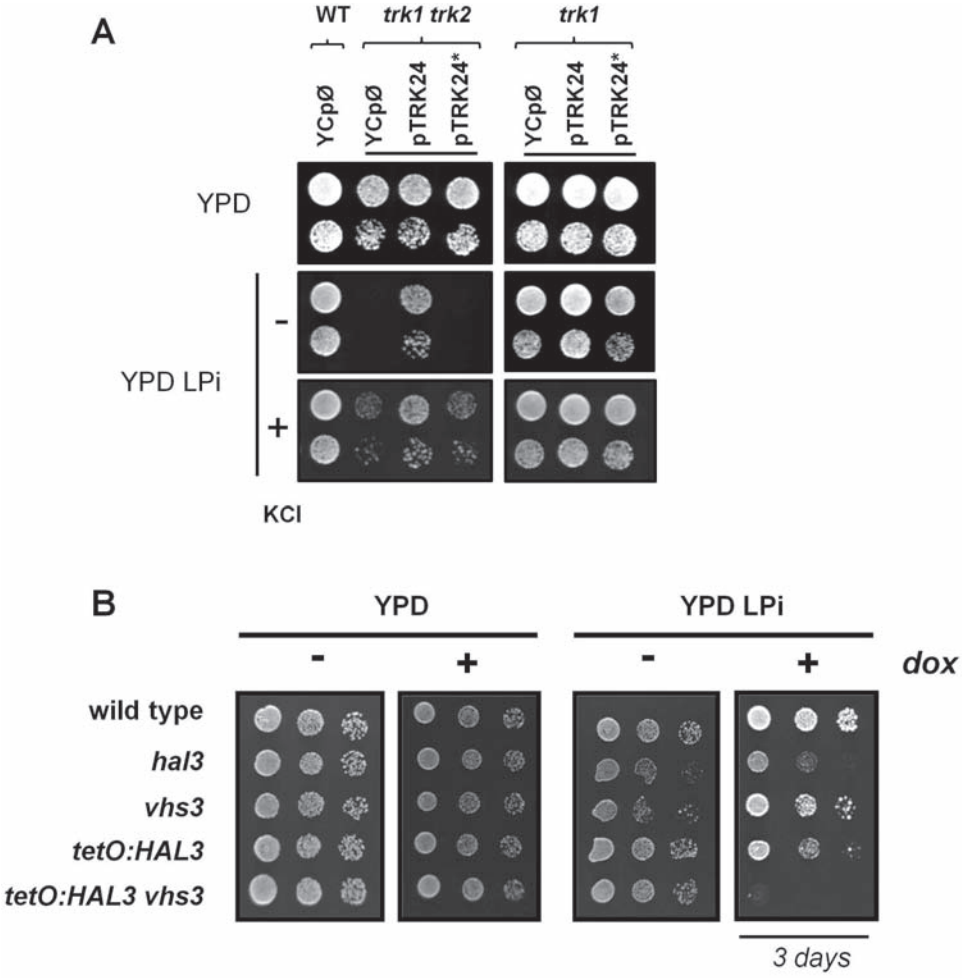

Fig. 7. Potassium high-affinity transport is necessary for growth in low phosphate conditions.
A. All strains (BY4741 background) were transformed with the empty YCp33 plasmid (YCpØ), and *trk1* and *trk1 trk2* strains were transformed also with the centromeric plasmid pTRK24, carrying the wild-type *TRK1* gene or the same plasmid in which the *TRK1* gene contains the mutation M1153R (pTRK24*), which blocks potassium transport capacity. Cells were diluted to OD_{600} 0.05 and 0.005 and grown for 2 days on plates containing YPD or phosphate-depleted YPD (YPD LPi). The sign (–) indicates that the medium contains the standard amount of potassium (~22 mM KCl) and (+) denotes that the medium was supplemented up to 35 mM KCl.
B. Cultures (OD_{600} 0.05) and two dilutions of the indicated strains were spotted in YPD or YPD LPi agar plates in the presence (+) or absence (–) of doxycycline, and growth was recorded after 2 or 3 days.

strains carrying mutations in the Ppz1 regulatory subunits were examined (Fig. 7B), we observed that a *hal3* mutant already showed some growth defect in phosphate-limiting medium (more evident in the plate grown for 3 days), similarly to the *tetO:HAL3* strain grown in the presence of doxycycline. The *vhs3* mutant grows normally, which fits with the less prominent role of Vhs3 in inhibiting Ppz1 function (Ruiz *et al.*, 2004). Remarkably, the *tetO:HAL3 vhs3* strain, which grew well on standard YPD in the presence of doxycycline, or on Pi-depleted YPD in the absence of doxycycline, did not grow at all in the presence of the drug when Pi was scarce. These results indicate that improper phosphate metabolism due to alterations in potassium homeostasis can severely affect cell growth.

Regulation of Pho84 expression by potassium requires the entire PHO signaling pathway

Pho81 represents a key signaling step in response to phosphate starvation. The observation that mutation of *PHO81* was able to abolish the expression of *PHO*-regulated genes in cells depleted for Hal3 and Vhs3 prompted us to investigate the importance of the integrity of the *PHO* signaling pathway in the response to alterations in potassium homeostasis. To this end, we first transformed wild-type and *pho81* cells with *PHO84* and *PHO5 lacZ* reporters and subjected the cells to potassium starvation for 90 and 120 min, respectively. As shown in Fig. 8A, the increase in *PHO84*- and *PHO5*-driven expression was fully

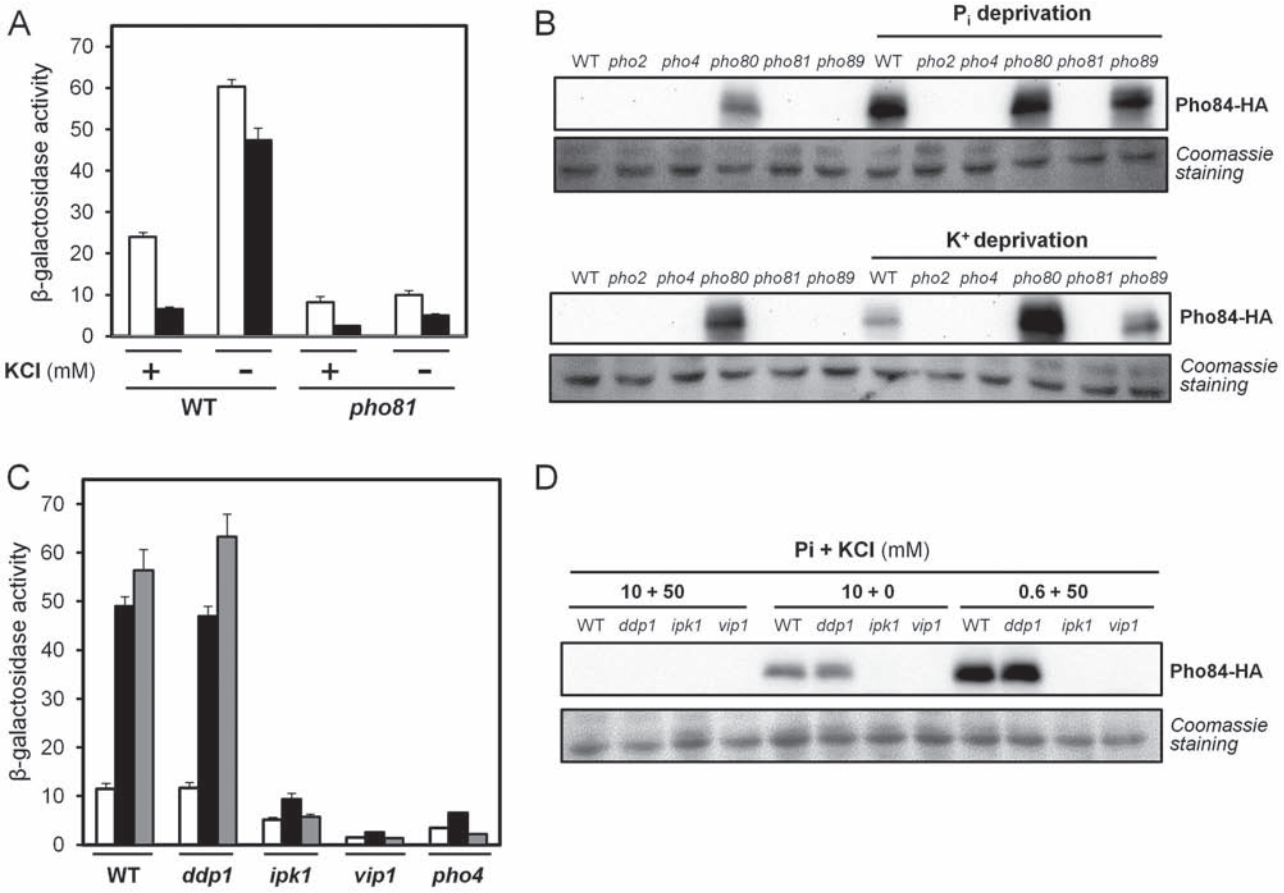

Fig. 8. Disruption of components of the *PHO* pathway blocks induction of *PHO*-regulated genes and Pho84 expression upon potassium deprivation.

A. Wild-type strain BY4741 and its isogenic *pho81* derivative were transformed with the *PHO5* (open bars) or *PHO84* (closed bars) *lacZ* reporters. Cultures growing in the presence of 50 mM KCl were subjected to potassium deprivation (–), and cells were collected after 90 min (pPHO84-lacZ) or 120 min (pPHO5-lacZ) and processed for β-galactosidase activity determination. Data are mean ± SEM from six to nine independent determinations.

B. Cultures of the indicated strains in the BY4741 background (WT) were subjected to potassium or phosphate deprivation for 60 min, and the presence of immunoreactive Pho84 in protein extracts (25 μg) assessed by immunoblotting. Coomassie staining of the membrane is shown for comparison.

C. The indicated strains in the BY4741 background were transformed with plasmid pPHO84-lacZ. Cultures were transferred to synthetic medium containing 40 mM KCl plus 10 mM monopotassium phosphate (open bars), 10 mM ammonium phosphate (closed bars), and 50 mM KCl plus 0.6 mM potassium phosphate (stripped bars) and β-galactosidase activity measured after 90 min. Data are mean ± SEM from 12 independent determinations.

D. The indicated strains, containing plasmid pMM15-PHO84, were grown to exponential phase and then transferred to synthetic medium containing KCl and potassium phosphate in the corresponding amounts. Cells were collected after 60 min and processed for immunoblot for Pho84 as above.

abolished in cells deleted for *PHO81*. These observations prompted us to evaluate up to what extent the entire pathway is required to respond to potassium limitation conditions. To this end, we first compared the kinetics of the appearance of Pho84 under conditions of complete phosphate or potassium removal. As observed in Supplemental Fig. S3A, although the levels of Pho84 expression attained under conditions of potassium starvation are clearly lower than those observed upon removal of phosphate from the medium, the kinetics of the response is virtually identical. This suggests that depletion of extracellular potassium triggers a response qualitatively similar but less potent than that of complete removal of phosphate. In fact, expression of Pho84 in wild-type cells after 60 min of depletion of potassium seems to be roughly equivalent to that observed in cells grown under external phosphate concentrations of 0.6 mM (Supplementary Fig. S3B). This concentration is below the K_m for low-affinity phosphate transport in *S. cerevisiae* (~1 mM) and, therefore, represents a condition of moderate phosphate starvation.

We then grew a number of strains deficient in known components of the middle–late steps of the *PHO*-signaling pathway, either in the absence of phosphate or potassium for 60 min, and monitored the level of Pho84 expression. As shown in Fig. 8B, under normal growth conditions (plenty of potassium and phosphate), only the *pho80* mutant showed constitutive (deregulated) Pho84 expression, as it was expected. Under conditions of complete phosphate depletion, wild-type, *pho80* and *pho89* cells also expressed high levels of Pho84. These same strains displayed increased expression of Pho84 when they were fully deprived of potassium in the medium (Fig. 8B). Deletion of *PHO81* resulted in the absence of expression of Pho84 in potassium-starved cells, and the same effect was observed for *pho2* or *pho4* mutants. In contrast, the potency of the induction of Pho84 was roughly the same in *pho80* cells, when compared with the non-stressed cells, in response to the absence of potassium or phosphate. These results indicate that the effect of potassium limitation on Pho84 induction is exerted through the Pho81–Pho85/Pho80–Pho2/Pho4 signaling module.

In a similar way, we explored the earlier events in the phosphate signaling pathway, leading to the generation of IP_7 (see Fig. 1). As documented in Fig. 8C, the Pho84 promoter was induced in the *ddp1* strain (an IP_7 phosphatase) in the absence of external potassium similarly to that observed for wild-type cells. In contrast, mutation of *VIP1* or *IPK1* (IP_6 and IP_5 kinases, respectively), encoding enzymes required for the synthesis of IP_7, fully blocked the induction of the *PHO84* promoter caused by lack of potassium. This profile was perfectly reproduced when cells were subjected to the equivalent phosphate limitation (0.6 mM) in the presence of plenty of potassium. When the generation of the Pho84 protein was investigated by immunoblot (Fig. 8D), the absence of Pho84 synthesis in potassium- or phosphate-starved *vip1* and *ipk1* mutants could be confirmed. These experiments indicate that the entire *PHO* pathway is necessary for signaling the absence of potassium.

Discussion

A requirement for potassium cations for optimal uptake of phosphate in yeast was noticed long time ago (Goodman and Rothstein, 1957), although the experimental conditions used were far from physiological (i.e. involving long periods of starvation in water), thus making difficult to assess the biological relevance of the finding, which has not been further characterized. We recently observed that depletion of potassium cations in an otherwise standard Yeast Nitrogen Base (YNB)-based medium triggers a strong transcriptional response in the yeast *S. cerevisiae* (Barreto *et al*., 2012) that includes many genes known to be induced by phosphate starvation, thus raising the possibility for a physiological relationship between potassium and phosphate homeostatic mechanisms. We describe here that this phosphate-starvation-like response is observed not only by eliminating potassium from the medium, but it can also occur in the presence of abundant extracellular potassium when cells harbor mutations that directly or indirectly modulate the capacity for potassium uptake. These observations, which support a physiological link between the mechanisms regulating the uptake and accumulation of potassium and phosphate, are in agreement with recent work showing that the increase in intracellular phosphate levels caused by hyperactivation of the *PHO* regulon is accompanied by an increase of about 60% in intracellular potassium content (Rosenfeld *et al*., 2010).

We observe that mutations that directly or indirectly attenuate potassium influx result in higher-than-normal expression of Pho84, a sensitive readout for Pi limitation. For instance, a *trk1* mutant, lacking the major high-affinity potassium transporter, shows abnormally high Pho84 expression when growing under limiting amounts of potassium, but this effect is abolished by supplementing the medium with potassium well above the K_m values for the low-affinity potassium transport. Similarly, *ptk2* and *brp1* are mutations that significantly decrease the activity of the Pma1 H^+-ATPase (Goossens *et al*., 2000; Porat *et al*., 2005; Barreto *et al*., 2011), and result in strong derepression of Pho84 expression (Fig. 3B), whereas lack of *hrk1*, which has a only a modest effect on Pma1 activity and proton extrusion (Goossens *et al*., 2000; Barreto *et al*., 2011) does not result in exacerbated Pho84 expression. These observations fit with an earlier work in which the effect of the decrease of Pma1 activity on phosphate uptake and *PHO5* expression was reported (Lau *et al*., 1998). Inhibition of Pma1 activity is known to negatively affect K^+ uptake, an effect that is reflected in the fact that mutants lacking *PTK2* or *BRP1* display a strong defect in Rb^+ (a K^+ analog) uptake and grow poorly on limiting amounts of potassium, whereas the *hrk1* strain behaves similarly to the wild-type strain (Barreto *et al*., 2011). We show here that the effect of the *ptk2* and *brp1* mutations on Pho84 expression is most likely due to alterations in potassium influx, since additional deletion of *TRK1* does not result in enhanced expression levels. Finally, we also observe that down-regulation of Trk1 activity by the Ppz1 protein phosphatase leads to deregulation of *PHO*-mediated gene expression (Figs. 4 and 5). The interaction between potassium homeostasis and *PHO*-regulated expression can be also detected under conditions in which potassium uptake is improved, as documented by the fact that deletion of *YCK1* or *YCK2*, which code for negative regulators of the H^+ pump, leads to increased Pma1

activity (Estrada *et al.*, 1996), and result in almost negligible expression of Pho84 when these mutants grow at limiting potassium (Fig. 3B). All these results reinforce the notion that alterations in phosphate homeostatic mechanisms can occur as a response to physiological regulation of potassium uptake.

It is known that removal of potassium from the medium causes hyperpolarization of the yeast cells (Navarrete *et al.*, 2010), and that a similar effect can be observed in *trk1 trk2* mutants, devoid of the high-affinity potassium transport system (Madrid *et al.*, 1998; Maresova *et al.*, 2006). This is reminiscent of the previously proposed relationship between Pi and sulfate uptake, and the cell surface potential (Roomans and Borst-Pauwels, 1979a; Roomans *et al.*, 1979b). However, membranes in *ptk2* or *brp1* mutants are not hyperpolarized (Barreto *et al.*, 2011) and still these mutants display a substantial derepression of Pho84 expression. Furthermore, we have tested the expression levels of Pho84 in *vps54* or *tlg2* mutants, which have hyperpolarized membranes and normal requirements for potassium (Barreto *et al.*, 2011), and found that they are similar to wild-type cells (not shown). Therefore, the induction of a phosphate-starvation response in these mutants does not correlate with their membrane potential, but with their ability to effectively transport potassium cations.

We show here that the induction of the expression of Pho84 in response to alteration in potassium homeostasis requires the integrity of the *PHO* regulon, since it is blocked in the absence of either upstream or downstream elements of the pathway, such as Vip1, Pho81 or Pho4 and, in contrast, it is potentiated by lack of negative regulators such as Pho80. As a result of removal of potassium from the medium or interference with normal uptake of the cation, we observe a dramatic decrease in the levels of PolyP, with no detectable effect on total Pi content and a moderate increase in the pool of free Pi (perhaps due to the mobilization of PolyP reserves). This would fit with the proposed role of PolyP as a buffer filtering transient fluctuations in extracellular Pi levels (Thomas and O'Shea, 2005). Although PolyP has been identified in diverse subcellular localizations, the yeast vacuole appears particularly enriched in this polymer (Urech *et al.*, 1978; Kornberg, 1995; Saito *et al.*, 2005). It is suggestive that the vacuole is the only subcellular organelle in which potassium content drastically decreases (four- to fivefold) after 4 h of potassium starvation (Herrera *et al.*, 2013). In fact, potassium vacuolar loss starts as soon as potassium is removed from the medium (J. Ramos, personal communication). The parallel vacuolar depletion of PolyP and potassium would fit with a charge balance effect, in which the positive charge of potassium (the most abundant cation in yeast cells) would counteract negatively charged PolyP chains.

The role of Pi as a signal for the regulation of the *PHO* pathway in *Saccharomyces cerevisiae* was proposed some time ago (Auesukaree *et al.*, 2004), although the authors already suggested the existence of additional signaling molecules. Indeed, our results do not fit with a signaling nature for free or total Pi, providing further support to the notion that additional signaling elements should exist. We observed a marked decline in the levels of ATP and ADP, which are reduced over 50% after 40 min of K^+ starvation (Fig. 6B) and a reduction in the overall level of adenine nucleotides. The decay in the cell energy charge values could be attributed, at least in part, to the increase in activity of the Pma1 ATPase, which is immediately activated after removal of potassium from the medium (Kahm *et al.*, 2012). In fact, hyperactivation of Pma1 could also be observed in *trk1 trk2* mutants even in the presence of 50 mM potassium. Notably, it has been proposed that the level of adenine nucleotides could serve as markers for signaling through the *PHO* pathway (Gauthier *et al.*, 2008). Specifically, these authors show that *PHO84* mRNA is substantially increased in *ado1* and *adk1* cells, lacking the enzymes required for synthesis of AMP from adenosine and phosphorylation of AMP to ADP, respectively. It is worth noting that the expression of *IMD2*, *IMD3* and *IMD4*, encoding the branch that derives IMP, the common AMP and GMP precursor, to the synthesis of GMP is repressed as a result of potassium deprivation or in *trk1 trk2* mutants even in the presence of plenty of potassium (Barreto *et al.*, 2012). This transcriptional response could reflect an attempt of the cellular regulatory mechanisms to derive IMP to increase the nucleotide pool. All together, our data would fit with the notion sustained by Gauthier *et al.* (2008), in that one (or a combination of) adenine nucleotide(s) could be a relevant signal to maintain phosphate homeostasis in yeast.

Our results show that, in addition to changes in potassium availability in the medium, the modulation of potassium uptake can impact on the homeostatic mechanisms regulating phosphate acquisition and utilization, resulting in growth arrest in the presence of limiting Pi availability. This link between potassium and phosphate homeostasis might extend to other nutrients. For instance, we recently observed that induction of expression of the sulfate transporter-encoding genes (*SUL1* and *SUL2*) is not only provoked by lack of sulfate in the medium (Ljungdahl and Daignan-Fornier, 2012), but also triggered in wild-type cells by potassium starvation or by the *trk1 trk2* mutation even in the presence of plenty of potassium (Barreto *et al.*, 2012). The link between potassium homeostasis and proper nutrient uptake and/or utilization could explain certain phenotypes recently reported in potassium-deficient yeast cells, such as an invasive phenotype (Gonzalez *et al.*, 2013), that is characteristic of nutrient deprivation.

Table 1. Yeast strains used in this work.[a]

Name	Relevant genotype	Source/References
JA100	*MATa ura3-52 leu2-3,112 his4 trp1–1 can-1r*	(de Nadal *et al.*, 1998)
MAR79	JA100 *vhs3::URA3*	(Ruiz *et al.*, 2004)
MAR88	JA100 *hal3::kanMX4*	(Ruiz *et al.*, 2004)
AGS9	JA100 *ppz1::LEU2*	This work
JC001	JA100 *tetO:HAL3*	(Ruiz *et al.*, 2004)
MAR24	JA100 *tetO:HAL3 vhs3::URA3*	(Ruiz *et al.*, 2004)
MAR119	JA100 *tetO:HAL3 vhs3::nat1*	(Gonzalez *et al.*, 2013)
MAR120	JA100 *tetO:HAL3 vhs3::nat1 ppz1::URA3*	(Gonzalez *et al.*, 2013)
AGS11	JA100 *tetO:HAL3 vhs3::nat1 ppz1::LEU2*	This work
AGS6	JA100 *tetO:HAL3 vhs3::nat1 pho81::TRP1*	This work
BY4741	*MATa his3Δ1 leu2Δ met15Δ ura3Δ*	EUROSCARF
BYT1	BY4741 *trk1Δ::loxP*	(Navarrete *et al.*, 2010)
BYT12	BY4741 *trk1Δ::loxP trk2Δ::loxP*	(Navarrete *et al.*, 2010)
DCS31	BY4741 *trk1::LEU2*	This work
DCS32	BY4741 *trk2::nat1 trk1::LEU2*	This work
DCS33	BY4741 *brp1::kanMX4*	This work
DCS34	BY4741 *ptk2::kanMX4*	This work
DCS39	BY4741 *trk1::LEU2 brp1::kanMX4*	This work
DCS40	BY4741 *trk1::LEU2 ptk2::kanMX4*	This work
SC001	BY4741 *vip1::kanMX4*	This work

a. All other kanMX4 deletans in the BY4741 background used in this work correspond to the EUROSCARF collection.

Experimental procedures

Yeast strains and DNA recombinant techniques

S. cerevisiae cells were grown at 28°C in YPD medium (10 g/l yeast extract, 20 g l^{-1} peptone and 20 g l^{-1} dextrose) or, when carrying plasmids, in synthetic minimal medium lacking the appropriate selection requirements and supplemented if necessary with 50 mM KCl (Adams *et al.*, 1997). Low phosphate (low Pi) medium was prepared from YNB-based medium without amino acids and phosphate (Formedium Ltd., reference CYN0803, requested to lack also potassium salts), adding 50 mM KCl and indicated amount of potassium phosphate. The equivalent high phosphate (high Pi) medium was made by including 40 mM KCl and 10 mM potassium phosphate. Potassium-free YNB-based medium (Navarrete *et al.*, 2010) was obtained from Formedium Ltd. (Ref. CYN7505). This medium contains only 15 μM of potassium. In some experiments, YPD Low phosphate (YPD LPi) medium was prepared by phosphate precipitation from YPD with $MgSO_4$ and ammonia as previously described (Kaneko *et al.*, 1982). The media were adjusted to pH 5.5 after addition of all components.

Yeast strains AGS9 and AGS11 were constructed by transforming strain JA100 and MAR119, respectively, with a 2.5 kbp NdeI/PstI fragment from plasmid YEp181-ppz1::*LEU2*. This fragment contains the entire *PPZ1* gene in which the XhoI/StuI portion of PPZ1 was replaced with the *LEU2* marker (Ruiz *et al.*, 2004). Strain AGS6 was constructed by transforming strain MAR119 with a 2.16 kbp AvaI fragment from plasmid pDPHO81-Ws. This construct consists in a pUC19 plasmid containing the entire *PHO81* gene that was digested with BglII and the missing portion of *PHO81* was replaced with the 0.84 kbp fragment corresponding to the *TRP1* marker extracted from plasmid YDp-W (Berben *et al.*, 1991). Strain DCS31 (*trk1*) was made by transforming BY4741 with a cassette extracted by digestion with SacI from plasmid pUC19-TRK1::LEU2 (Haro *et al.*, 1999). To generate strain DCS32 (*trk1 trk2*), a *trk2::nat1* strain was constructed by short flanking homology recombination in the BY4741 background as described in Gonzalez *et al.* (2013). Then, the *trk1* deletion was introduced as described earlier. The *BRP1* and *PTK2* genes were disrupted with the kanMX4 marker as described in Barreto *et al.* (2011) in the BY4741 strain, to produce strains DCS33 and DCS34, or in the DCS31 strain, to generate strains DCS39 and DCS40 respectively. In SC001 strain, the replacement of the *VIP1* coding region by the *kanMX4* marker in the BY4741 background was accomplished by the short-flanking recombination strategy. A DNA fragment containing the *kanMX4* marker flanked by *VIP1* genomic sequences corresponding to positions –40/+1 and +3250/+3290 from the ATG codon was amplified by PCR from plasmid pFA6a-KanMX4 (Wach *et al.*, 1994) with the oligonucleotides 5′vip1-nat (CAAAAGCATCTCGTAGCATATTAATATATTGCAGAAGGTC cgtacgctgcaggtcgac) and 3′vip1-nat (GGCATAATGACCCT GGTAAATTTGTTTCTCAATTTCTGTTatcgatgaattcgagctcg). Capital letters denote *VIP1* genomic sequences. Yeast strains used in the present study are described in Table 1.

Escherichia coli DH5α cells were used as plasmid DNA host and were grown at 37°C in LB (Luria–Bertani) broth supplemented, if necessary, with 100 μg ml^{-1} ampicillin. Recombinant DNA techniques and bacterial and yeast cells transformations were performed using standard methods. Construction of plasmid pMM15-PHO84, which express *PHO84* from its native promoter with a 3×-HA C-terminal tag, was described in Serra-Cardona *et al.* (2014). Plasmid pMM17-PHO84 was constructed in a similar way, but using plasmid pMM17 (*LEU2* marker), generously provided by E. Herrero (Universitat de Lleida, Spain) as vector. Plasmids pTRK24 (a centromeric plasmid expressing wild-type *TRK1* gene from its own promoter) and $pTrk1^{M1153R}$, expressing the corresponding mutant versions of the Trk1 transporter that

is virtually unable to transport potassium (Haro and Rodriguez-Navarro, 2003), were a generous gift of A. Rodriguez-Navarro (U. Politécnica de Madrid, Spain).

β-Galactosidase assays

To evaluate the corresponding promoter activities, different strains were transformed with the reporter plasmids pPHO84-lacZ, pPHO89-lacZ and pPHO12-lacZ described in Serrano *et al.* (2002) and pPHO5-lacZ described in Gonzalez *et al.* (2006). To analyze the response to lack of potassium or low phosphate (0.6 mM P_i), yeast cells were grown to saturation in the appropriate dropout medium, then inoculated into high Pi medium supplemented with 50 mM KCl and incubated to reach an OD_{600} of 0.6. Aliquots of 1 ml were centrifuged, washed and resuspended in the same volume of medium with (50 mM) or without KCl, or low phosphate medium. Growth was resumed after 90 min (*PHO84* and *PHO12*), or 90–120 min (*PHO5*). Alternatively, in strains carrying the doxycycline-regulatable *HAL3* gene (*tetO:HAL3*), cultures were grown overnight in selective medium, diluted up to an OD_{600} of 0.005 and then grown for 15 h in YPD adjusted to pH 5.5 in the presence or absence of a semi-permissive concentration of doxycycline (100 μg ml^{-1}). In both cases, cells were collected and processed for β-galactosidase assay as described (Reynolds *et al.*, 1997).

Protein extractions and immunoblot analysis

For evaluation of the presence of the Pho84 protein, different strains were transformed with pMM15-PHO84 or pMM17-PHO84 plasmids carrying *PHO84* gene fused with the 3×-HA epitope. After the appropriate treatment, total protein was extracted following the method described in Horak and Wolf (2001). Briefly, cells were lysed with NaOH and proteins were precipitated for 10 min on ice by 50% trichloroacetic acid. The pellet was resuspended in 50 mM Tris–HCl buffer (pH 6.8) containing 8 M urea, 5% sodium dodecyl sulfate (SDS), 0.1 mM EDTA, and 1.5% dithiothreitol. For detection of Hal3, cultures (10 ml, OD_{600} 0.6) were collected by centrifugation and disrupted with glass beads in the presence of 100 μl of a 100 mM Tris–HCl (pH 7.5), 150 mM NaCl, 10% glycerol, 1 mM EDTA, 1 mM DTT, 0.1% Triton-X100 buffer supplemented with 1 mM PMSF and antiprotease mixture (Complete EDTA-free cocktail, Roche). After centrifugation (10 min at 750 × *g* at 4°C), the supernatant was recovered. Proteins (25–40 μg for Pho84, 60 μg for Hal3) were separated by electrophoresis on a 10% SDS–polyacrylamide gel and electroblotted on PVDF filters (Immobilon-P, Millipore). Pho84 was detected by the use of anti-HA antibody (Covance, Ref. MMS-101P, 1:1000 dilution) followed by anti-mouse immunoglobulin G antibodies (Amersham Biosciences) at a 1:20 000 dilution. Hal3 was visualized by a polyclonal anti-Hal3 antibody (Ferrando *et al.*, 1995) at 1:1000 dilution, followed by anti-rabbit immunoglobulin G antibodies (Amersham Biosciences) at a 1:20 000 dilution. Immunoreactive proteins were visualized using an ECL Western blotting detection kit (GE Healthcare). Total protein staining (Ponceau S or Coomassie Blue R-250) or the specific Act1 signals (I-19 anti-actin antibodies, Santa Cruz Biotechnology, Inc., 1:2000 dilution) were used as loading controls.

Measurements of PolyP, total and free phosphate, and adenine nucleotide levels

PolyP extraction and quantification methods used were as described in Werner *et al.* (2005). Shortly, 1 ml of exponentially growing cells (OD_{600} 0.6) was pelleted by centrifugation (approximately 12 000 × *g*, 1 min), the supernatant was discarded, 50 μl 1 M sulfuric acid was added and the suspension was neutralized with 50 μl of 2 M NaOH. After vortexing, 100 μl of a Tris–HCl buffer solution made of 1 M Tris–HCl, pH 7.5, plus 6% neutral red solution (0.1% neutral red in 70% ethanol) was added. Cell fragments were pelleted by centrifugation (~800 × *g*, 10 min, 4°C) and 200 μl of the supernatant was used for PolyP purification using a NaI 6 M solution and Qiagen PCR purification columns as in Werner *et al.* (2005). Eluted PolyP was enzymatically digested with an excess of recombinant exopolyphosphatase Ppx1 from *S. cerevisiae*, to release free phosphate. Recombinant Ppx1 was obtained from *E. coli* containing a plasmid-borne, His-tagged version of the *PPX1* gene, as described in Ruiz *et al.* (2001), after one-step purification with HisTrap™ HP columns (GE Healthcare). PolyP recovery in this process was estimated to be 20–22%, based on the use of commercial polyphosphate P45 (Sigma-Aldrich S4379) as reference.

For measurement of total and free phosphate, cells were collected by filtration, washed with cold water and resuspended in 100 μl of 1 M H_2SO_4 and split into two identical aliquots. For total phosphate quantification, 150 μl of 1 M H_2SO_4 was added to one 50 μl aliquot and heated to 95°C for 20 min as in Freimoser *et al.* (2006). For free orthophosphate determination, the remaining aliquot was neutralized with 50 μl of a 2 M NaOH solution, followed by 100 μl of 1 M Tris–HCl (pH 7.5) buffer, as described in Rosenfeld *et al.* (2010). In both treatments, cell debris was pelleted by centrifugation (800 × *g*, 10 min, 4°C) and supernatants were used for phosphate measurement. Total and free phosphate, as well as phosphate released from PolyP was quantified with the molybdate and malachite green colorimetric assay (Cogan *et al.*, 1999). The amount of phosphate was expressed as mM Pi. ATP, ADP and AMP intracellular concentrations were measured by HPLC–mass spectrometry as described in Barreto *et al.* (2012). A cellular volume of 49 fl/cell for the BY4741 derivatives, as determined in Navarrete *et al.* (2010) using a Cell Counter Z2 (Beckman-Coulter) and experimentally confirmed in our laboratory with Scepter Cell counter (Millipore), was used for calculations. One OD_{600} of an exponentially growing culture was found to contain 8.8×10^6 cells.

DNA microarray experiments

Wild-type (JA100) and *tetO:HAL3 vhs3* strains were inoculated at an initial OD_{660} of 0.005 in synthetic complete medium and grown for 15 h in the presence of 100 μg ml^{-1} of doxycycline. Total RNA was isolated and microarray experiments were performed using DNA microarrays from our laboratory as described previously (Alberola *et al.*, 2004; Serrano *et al.*, 2006). The fluorescent intensity of the spots was measured and processed using GenePix Pro 6.0 software (Molecular Devices). Data from three microarrays experiments was combined (two biological replicates plus one dye swapping).

Microarray data have been deposited at GEO database with submission number GSE58985.

Microscopy

Detection of Pho84 by fluorescence microcopy was carried out by transforming the indicated strains with plasmid EB0666, which expresses a version of Pho84 fused to GFP (Lau *et al.*, 2000). Transformants were selected and inoculated in 5 ml of synthetic medium lacking uracil up to OD_{600} 0.2 (JA100 and *ppz1*) or 0.3 (*tetO:HAL3 vhs3* and *tetO:HAL3 vhs3 ppz1*) in the presence of 100 μg ml^{-1} doxycycline for 12 h. Cells were then centrifuged, the pellet was resuspended in 5 ml of YPD or YPD low phosphate adjusted to pH 5.8, supplemented with doxycycline and growth was resumed for 6 h. The localization of Pho84 was followed by fluorescence microscopy in a Nikon Eclipse E-800 fluorescence microscope with a FITC filter (magnification ×1.000). Images were captured using an ORCA-ER C4742-80-12AG digital camera (Hamamatsu Photonics) and the Wasabi v.1.5 software.

Acknowledgments

The excellent technical assistance of Montserrat Robledo is acknowledged. We thank Dr. D. Valverde for determination of adenine nucleotide levels, Dr. Roberto Docampo (University of Georgia, Athens, USA) for reagents and generous advice, and E. Herrero (U. de Lleida), R. Haro and A. Rodriguez-Navarro (U. Politécnica de Madrid), and D. Wykoff (Villanova University, Villanova, PA, USA) for relevant plasmids. Work was supported by grants EUI2009-04147 (ERA-NET SysMo2) and BFU2011-30197-C3-01 (MICINN, Spain). J.A. is the recipient of an Ajut 2014SGR-4 and an Institució Catalana de Recerca i Estudis Avançats (ICREA) Academia 2009 Award (Generalitat de Catalunya). D.C. is recipient of a pre-doctoral fellowship from the Spanish Ministry of Education.

References

Abrie, J.A., Gonzalez, A., Strauss, E., and Arino, J. (2012) Functional mapping of the disparate activities of the yeast moonlighting protein Hal3. *Biochem J* **442:** 357–368.

Adams, A., Gottschling, D.E., Kaiser, C.A., and Stearns, T. (1997) *Methods in Yeast Genetics*. Cold Spring Harbor, NY: Cold Spring Harbor Laboratory Press.

Aiking, H., and Tempest, D.W. (1976) Growth and physiology of *Candida utilis* NCYC 321 in potassium-limited chemostat culture. *Arch Microbiol* **108:** 117–124.

Alberola, T.M., Garcia-Martinez, J., Antunez, O., Viladevall, L., Barcelo, A., Arino, J., and Perez-Ortin, J.E. (2004) A new set of DNA macrochips for the yeast *Saccharomyces cerevisiae*: features and uses. *Int Microbiol* **7:** 199–206.

Arino, J., Ramos, J., and Sychrova, H. (2010) Alkali metal cation transport and homeostasis in yeasts. *Microbiol Mol Biol Rev* **74:** 95–120.

Auesukaree, C., Homma, T., Kaneko, Y., and Harashima, S. (2003) Transcriptional regulation of phosphate-responsive genes in low-affinity phosphate-transporter-defective mutants in Saccharomyces cerevisiae. *Biochem Biophys Res Commun* **306:** 843–850.

Auesukaree, C., Homma, T., Tochio, H., Shirakawa, M., Kaneko, Y., and Harashima, S. (2004) Intracellular phosphate serves as a signal for the regulation of the PHO pathway in Saccharomyces cerevisiae. *J Biol Chem* **279:** 17289–17294.

Barreto, L., Canadell, D., Petrezselyova, S., Navarrete, C., Maresova, L., Perez-Valle, J., *et al.* (2011) A genomewide screen for tolerance to cationic drugs reveals genes important for potassium homeostasis in saccharomyces cerevisiae. *Eukaryot Cell* **10:** 1241–1250.

Barreto, L., Canadell, D., Valverde-Saubi, D., Casamayor, A., and Arino, J. (2012) The short-term response of yeast to potassium starvation. *Environ Microbiol* **14:** 3026–3042.

Berben, G., Dumont, J., Gilliquet, V., Bolle, P.A., and Hilger, F. (1991) The YDp plasmids: a uniform set of vectors bearing versatile gene disruption cassettes for Saccharomyces cerevisiae. *Yeast* **7:** 475–477.

Bun-ya, M., Nishimura, M., Harashima, S., and Oshima, Y. (1991) The PHO84 gene of Saccharomyces cerevisiae encodes an inorganic phosphate transporter. *Mol Cell Biol* **11:** 3229–3238.

Bun-ya, M., Shikata, K., Nakade, S., Yompakdee, C., Harashima, S., and Oshima, Y. (1996) Two new genes, PHO86 and PHO87, involved in inorganic phosphate uptake in Saccharomyces cerevisiae. *Curr Genet* **29:** 344–351.

Clotet, J., Posas, F., de Nadal, E., and Arino, J. (1996) The NH2-terminal extension of protein phosphatase PPZ1 has an essential functional role. *J Biol Chem* **271:** 26349–26355.

Cogan, E.B., Birrell, G.B., and Griffith, O.H. (1999) A robotics-based automated assay for inorganic and organic phosphates. *Anal Biochem* **271:** 29–35.

Erez, O., and Kahana, C. (2002) Deletions of SKY1 or PTK2 in the Saccharomyces cerevisiae trk1Deltatrk2Delta mutant cells exert dual effect on ion homeostasis. *Biochem Biophys Res Commun* **295:** 1142–1149.

Estrada, E., Agostinis, P., Vandenheede, J.R., Goris, J., Merlevede, W., Francois, J., *et al.* (1996) Phosphorylation of yeast plasma membrane H+-ATPase by casein kinase I. *J Biol Chem* **271:** 32064–32072.

Ferrando, A., Kron, S.J., Rios, G., Fink, G.R., and Serrano, R. (1995) Regulation of cation transport in *Saccharomyces cerevisiae* by the salt tolerance gene *HAL3*. *Mol Cell Biol* **15:** 5470–5481.

Forment, J., Mulet, J.M., Vicente, O., and Serrano, R. (2002) The yeast SR protein kinase Sky1p modulates salt tolerance, membrane potential and the Trk1,2 potassium transporter. *Biochim Biophys Acta* **1565:** 36–40.

Freimoser, F.M., Hurlimann, H.C., Jakob, C.A., Werner, T.P., and Amrhein, N. (2006) Systematic screening of polyphosphate (poly P) levels in yeast mutant cells reveals strong interdependence with primary metabolism. *Genome Biol* **7:** R109.

Gaber, R.F., Styles, C.A., and Fink, G.R. (1988) TRK1 encodes a plasma membrane protein required for high-affinity potassium transport in Saccharomyces cerevisiae. *Mol Cell Biol* **8:** 2848–2859.

Gauthier, S., Coulpier, F., Jourdren, L., Merle, M., Beck, S., Konrad, M., *et al.* (2008) Co-regulation of yeast purine and

phosphate pathways in response to adenylic nucleotide variations. *Mol Microbiol* **68:** 1583–1594.
Ghillebert, R., Swinnen, E., De, S.P., Smets, B., and Winderickx, J. (2011) Differential roles for the low-affinity phosphate transporters Pho87 and Pho90 in Saccharomyces cerevisiae. *Biochem J* **434:** 243–251.
Gonzalez, A., Ruiz, A., Serrano, R., Arino, J., and Casamayor, A. (2006) Transcriptional profiling of the protein phosphatase 2C family in yeast provides insights into the unique functional roles of Ptc1. *J Biol Chem* **281:** 35057–35069.
Gonzalez, A., Casado, C., Petrezselyova, S., Ruiz, A., and Arino, J. (2013) Molecular analysis of a conditional hal3 vhs3 yeast mutant links potassium homeostasis with flocculation and invasiveness. *Fungal Genet Biol* **53:** 1–9.
Goodman, J., and Rothstein, A. (1957) The active transport of phosphate into the yeast cell. *J Gen Physiol* **40:** 915–923.
Goossens, A., de la Fuente, N., Forment, J., Serrano, R., and Portillo, F. (2000) Regulation of yeast H(+)-ATPase by protein kinases belonging to a family dedicated to activation of plasma membrane transporters. *Mol Cell Biol* **20:** 7654–7661.
Haro, R., and Rodriguez-Navarro, A. (2003) Functional analysis of the M2(D) helix of the TRK1 potassium transporter of Saccharomyces cerevisiae. *Biochim Biophys Acta* **1613:** 1–6.
Haro, R., Sainz, L., Rubio, F., and Rodriguez-Navarro, A. (1999) Cloning of two genes encoding potassium transporters in Neurospora crassa and expression of the corresponding cDNAs in *Saccharomyces cerevisiae*. *Mol Microbiol* **31:** 511–520.
Herrera, R., Alvarez, M.C., Gelis, S., and Ramos, J. (2013) Subcellular potassium and sodium distribution in Saccharomyces cerevisiae wild type and vacuolar mutants. *Biochem J* **454:** 525–532.
Horak, J., and Wolf, D.H. (2001) Glucose-induced monoubiquitination of the Saccharomyces cerevisiae galactose transporter is sufficient to signal its internalization. *J Bacteriol* **183:** 3083–3088.
Kaffman, A., Herskowitz, I., Tjian, R., and O'Shea, E.K. (1994) Phosphorylation of the transcription factor PHO4 by a cyclin-CDK complex, PHO80-PHO85. *Science* **263:** 1153–1156.
Kahm, M., Navarrete, C., Llopis-Torregrosa, V., Herrera, R., Barreto, L., Yenush, L., *et al.* (2012) Potassium starvation in yeast: mechanisms of homeostasis revealed by mathematical modeling. *PLoS Comput Biol* **8:** e1002548.
Kaneko, Y., Toh-e, A., and Oshima, Y. (1982) Identification of the genetic locus for the structural gene and a new regulatory gene for the synthesis of repressible alkaline phosphatase in Saccharomyces cerevisiae. *Mol Cell Biol* **2:** 127–137.
Ko, C.H., and Gaber, R.F. (1991) TRK1 and TRK2 encode structurally related K+ transporters in Saccharomyces cerevisiae. *Mol Cell Biol* **11:** 4266–4273.
Ko, C.H., Buckley, A.M., and Gaber, R.F. (1990) TRK2 is required for low affinity K+ transport in Saccharomyces cerevisiae. *Genetics* **125:** 305–312.
Kornberg, A. (1995) Inorganic polyphosphate: toward making a forgotten polymer unforgettable. *J Bacteriol* **177:** 491–496.
Lau, W.T., Howson, R.W., Malkus, P., Schekman, R., and O'Shea, E.K. (2000) Pho86p, an endoplasmic reticulum (ER) resident protein in Saccharomyces cerevisiae, is required for ER exit of the high-affinity phosphate transporter Pho84p. *Proc Natl Acad Sci U S A* **97:** 1107–1112.
Lau, W.W., Schneider, K.R., and O'Shea, E.K. (1998) A genetic study of signaling processes for repression of PHO5 transcription in Saccharomyces cerevisiae. *Genetics* **150:** 1349–1359.
Lee, Y.S., Mulugu, S., York, J.D., and O'Shea, E.K. (2007) Regulation of a cyclin-CDK-CDK inhibitor complex by inositol pyrophosphates. *Science* **316:** 109–112.
Lee, Y.S., Huang, K., Quiocho, F.A., and O'Shea, E.K. (2008) Molecular basis of cyclin-CDK-CKI regulation by reversible binding of an inositol pyrophosphate. *Nat Chem Biol* **4:** 25–32.
Ljungdahl, P.O., and Daignan-Fornier, B. (2012) Regulation of amino acid, nucleotide, and phosphate metabolism in Saccharomyces cerevisiae. *Genetics* **190:** 885–929.
Lubin, M., and Ennis, H. (1964) On the role of intracellular potassium in protein synthesis. *Biochim Biophys Acta* **80:** 614–631.
Madrid, R., Gomez, M.J., Ramos, J., and Rodriguez-Navarro, A. (1998) Ectopic potassium uptake in trk1 trk2 mutants of Saccharomyces cerevisiae correlates with a highly hyperpolarized membrane potential. *J Biol Chem* **273:** 14838–14844.
Maresova, L., Urbankova, E., Gaskova, D., and Sychrova, H. (2006) Measurements of plasma membrane potential changes in Saccharomyces cerevisiae cells reveal the importance of the Tok1 channel in membrane potential maintenance. *FEMS Yeast Res* **6:** 1039–1046.
Martinez, P., and Persson, B.L. (1998) Identification, cloning and characterization of a derepressible Na+-coupled phosphate transporter in Saccharomyces cerevisiae. *Mol Gen Genet* **258:** 628–638.
Merchan, S., Bernal, D., Serrano, R., and Yenush, L. (2004) Response of the *Saccharomyces cerevisiae* Mpk1 mitogen-activated protein kinase pathway to increases in internal turgor pressure caused by loss of Ppz protein phosphatases. *Eukaryot Cell* **3:** 100–107.
Mulet, J.M., Leube, M.P., Kron, S.J., Rios, G., Fink, G.R., and Serrano, R. (1999) A novel mechanism of ion homeostasis and salt tolerance in yeast: the Hal4 and Hal5 protein kinases modulate the Trk1-Trk2 potassium transporter. *Mol Cell Biol* **19:** 3328–3337.
de Nadal, E., Clotet, J., Posas, F., Serrano, R., Gomez, N., and Arino, J. (1998) The yeast halotolerance determinant Hal3p is an inhibitory subunit of the Ppz1p Ser/Thr protein phosphatase. *Proc Natl Acad Sci U S A* **95:** 7357–7362.
Navarrete, C., Petrezselyova, S., Barreto, L., Martinez, J.L., Zahradka, J., Arino, J., *et al.* (2010) Lack of main K+ uptake systems in Saccharomyces cerevisiae cells affects yeast performance in both potassium-sufficient and potassium-limiting conditions. *FEMS Yeast Res* **10:** 508–517.
Ogawa, N., Saitoh, H., Miura, K., Magbanua, J.P., Bun-ya, M., Harashima, S., and Oshima, Y. (1995) Structure and distribution of specific cis-elements for transcriptional regulation of PHO84 in Saccharomyces cerevisiae. *Mol Gen Genet* **249:** 406–416.

Ogawa, N., DeRisi, J., and Brown, P.O. (2000) New components of a system for phosphate accumulation and polyphosphate metabolism in Saccharomyces cerevisiae revealed by genomic expression analysis. *Mol Biol Cell* **11:** 4309–4321.

Page, M.J., and Di Cera, E. (2006) Role of Na+ and K+ in enzyme function. *Physiol Rev* **86:** 1049–1092.

Pattison-Granberg, J., and Persson, B.L. (2000) Regulation of cation-coupled high-affinity phosphate uptake in the yeast Saccharomyces cerevisiae. *J Bacteriol* **182:** 5017–5019.

Perez-Valle, J., Jenkins, H., Merchan, S., Montiel, V., Ramos, J., Sharma, S., *et al.* (2007) Key role for intracellular K+ and protein kinases Sat4/Hal4 and Hal5 in the plasma membrane stabilization of yeast nutrient transporters. *Mol Cell Biol* **27:** 5725–5736.

Persson, B.L., Petersson, J., Fristedt, U., Weinander, R., Berhe, A., and Pattison, J. (1999) Phosphate permeases of Saccharomyces cerevisiae: structure, function and regulation. *Biochim Biophys Acta* **1422:** 255–272.

Persson, B.L., Lagerstedt, J.O., Pratt, J.R., Pattison-Granberg, J., Lundh, K., Shokrollahzadeh, S., and Lundh, F. (2003) Regulation of phosphate acquisition in Saccharomyces cerevisiae. *Curr Genet* **43:** 225–244.

Porat, Z., Wender, N., Erez, O., and Kahana, C. (2005) Mechanism of polyamine tolerance in yeast: novel regulators and insights. *Cell Mol Life Sci* **62:** 3106–3116.

Posas, F., Casamayor, A., Morral, N., and Arino, J. (1992) Molecular cloning and analysis of a yeast protein phosphatase with an unusual amino-terminal region. *J Biol Chem* **267:** 11734–11740.

Posas, F., Camps, M., and Arino, J. (1995) The PPZ protein phosphatases are important determinants of salt tolerance in yeast cells. *J Biol Chem* **270:** 13036–13041.

Reynolds, A., Lundblad, V., Dorris, D., and Keaveney, M. (1997) Yeast vectors and assays for expression of cloned genes. In *Current Protocols in Molecular Biology*. Ausubel, F.M., Brent, R., Kingston, R.E., Moore, D.D., Seidman, J.G., Smith, J.A., and Struhl, K. (eds). John Wiley & Sons, pp. 13.6.1–13.6.6.

Rodriguez-Navarro, A. (2000) Potassium transport in fungi and plants. *Biochim Biophys Acta* **1469:** 1–30.

Roomans, G.M., and Borst-Pauwels, G.W. (1979a) Interaction of cations with phosphate uptake by Saccharomyces cerevisiae. Effects of surface potential. *Biochem J* **178:** 521–527.

Roomans, G.M., Kuypers, G.A., Theuvenet, A.P., and Borst-Pauwels, G.W. (1979b) Kinetics of sulfate uptake by yeast. *Biochim Biophys Acta* **551:** 197–206.

Rosenfeld, L., Reddi, A.R., Leung, E., Aranda, K., Jensen, L.T., and Culotta, V.C. (2010) The effect of phosphate accumulation on metal ion homeostasis in Saccharomyces cerevisiae. *J Biol Inorg Chem* **15:** 1051–1062.

Ruiz, A., Munoz, I., Serrano, R., Gonzalez, A., Simon, E., and Arino, J. (2004) Functional characterization of the *Saccharomyces cerevisiae* VHS3 gene: a regulatory subunit of the Ppz1 protein phosphatase with novel, phosphatase-unrelated functions. *J Biol Chem* **279:** 34421–34430.

Ruiz, A., Gonzalez, A., Munoz, I., Serrano, R., Abrie, J.A., Strauss, E., and Arino, J. (2009) Moonlighting proteins Hal3 and Vhs3 form a heteromeric PPCDC with Ykl088w in yeast CoA biosynthesis. *Nat Chem Biol* **5:** 920–928.

Ruiz, F.A., Rodrigues, C.O., and Docampo, R. (2001) Rapid changes in polyphosphate content within acidocalcisomes in response to cell growth, differentiation, and environmental stress in Trypanosoma cruzi. *J Biol Chem* **276:** 26114–26121.

Saito, K., Ohtomo, R., Kuga-Uetake, Y., Aono, T., and Saito, M. (2005) Direct labeling of polyphosphate at the ultrastructural level in Saccharomyces cerevisiae by using the affinity of the polyphosphate binding domain of Escherichia coli exopolyphosphatase. *Appl Environ Microbiol* **71:** 5692–5701.

Schmidt, G., Hecht, L., and Thannhauser, S. (1949) The effect of potassium ions on the absorption of orthophosphate and the formation of metaphosphate by bakers' yeast. *J Biol Chem* **178:** 733–742.

Serra-Cardona, A., Petrezselyova, S., Canadell, D., Ramos, J., and Arino, J. (2014) Co-regulated expression of Na+/phosphate Pho89 transporter and Ena1 Na+-ATPase allows their functional coupling under high pH stress. *Mol Cell Biol* **34:** 4420–4435.

Serrano, R., Ruiz, A., Bernal, D., Chambers, J.R., and Arino, J. (2002) The transcriptional response to alkaline pH in *Saccharomyces cerevisiae*: evidence for calcium-mediated signalling. *Mol Microbiol* **46:** 1319–1333.

Serrano, R., Martin, H., Casamayor, A., and Arino, J. (2006) Signaling alkaline pH stress in the yeast Saccharomyces cerevisiae through the Wsc1 cell surface sensor and the Slt2 MAPK pathway. *J Biol Chem* **281:** 39785–39795.

Thomas, M.R., and O'Shea, E.K. (2005) An intracellular phosphate buffer filters transient fluctuations in extracellular phosphate levels. *Proc Natl Acad Sci U S A* **102:** 9565–9570.

Toh-e, A., Tanaka, K., Uesono, Y., and Wickner, R.B. (1988) PHO85, a negative regulator of the PHO system, is a homolog of the protein kinase gene, CDC28, of Saccharomyces cerevisiae. *Mol Gen Genet* **214:** 162–164.

Urech, K., Durr, M., Boller, T., Wiemken, A., and Schwencke, J. (1978) Localization of polyphosphate in vacuoles of Saccharomyces cerevisiae. *Arch Microbiol* **116:** 275–278.

Wach, A., Brachat, A., Pohlmann, R., and Philippsen, P. (1994) New heterologous modules for classical or PCR-based gene disruptions in Saccharomyces cerevisiae. *Yeast* **10:** 1793–1808.

Werner, T.P., Amrhein, N., and Freimoser, F.M. (2005) Novel method for the quantification of inorganic polyphosphate (iPoP) in Saccharomyces cerevisiae shows dependence of iPoP content on the growth phase. *Arch Microbiol* **184:** 129–136.

Wykoff, D.D., and O'Shea, E.K. (2001) Phosphate transport and sensing in Saccharomyces cerevisiae. *Genetics* **159:** 1491–1499.

Yenush, L., Mulet, J.M., Arino, J., and Serrano, R. (2002) The Ppz protein phosphatases are key regulators of K+ and pH homeostasis: implications for salt tolerance, cell wall integrity and cell cycle progression. *EMBO J* **21:** 920–929.

Yenush, L., Merchan, S., Holmes, J., and Serrano, R. (2005) pH-Responsive, posttranslational regulation of the Trk1 potassium transporter by the type 1-related Ppz1 phosphatase. *Mol Cell Biol* **25:** 8683–8692.

Zvyagilskaya, R.A., Lundh, F., Samyn, D., Pattison-Granberg, J., Mouillon, J.M., Popova, Y., *et al.* (2008) Characterization of the Pho89 phosphate transporter by functional hyperexpression in Saccharomyces cerevisiae. *FEMS Yeast Res* **8:** 685–696.

Supporting information

Additional supporting information may be found in the online version of this article at the publisher's web-site.

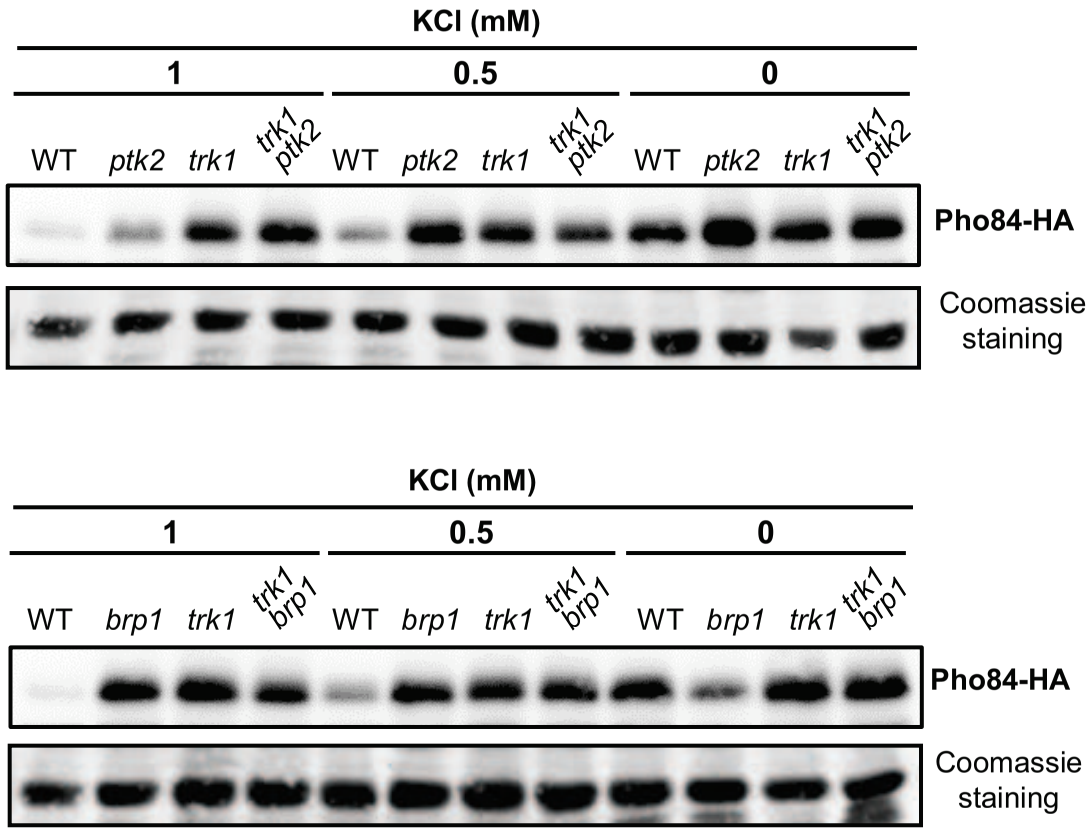

Supplementary Figure 1. The indicated strains were grown on synthetic medium and then transferred for 1 h to the same medium containing the indicated amounts of KCl. Samples were taken, protein extracts prepared as described in Experimental Procedures and subjected to SDS-PAGE (25 µg of protein). HA-tagged Pho84 was revealed by immunoblot. Blue Coomassie staining of the membrane is shown for lane to lane comparison.

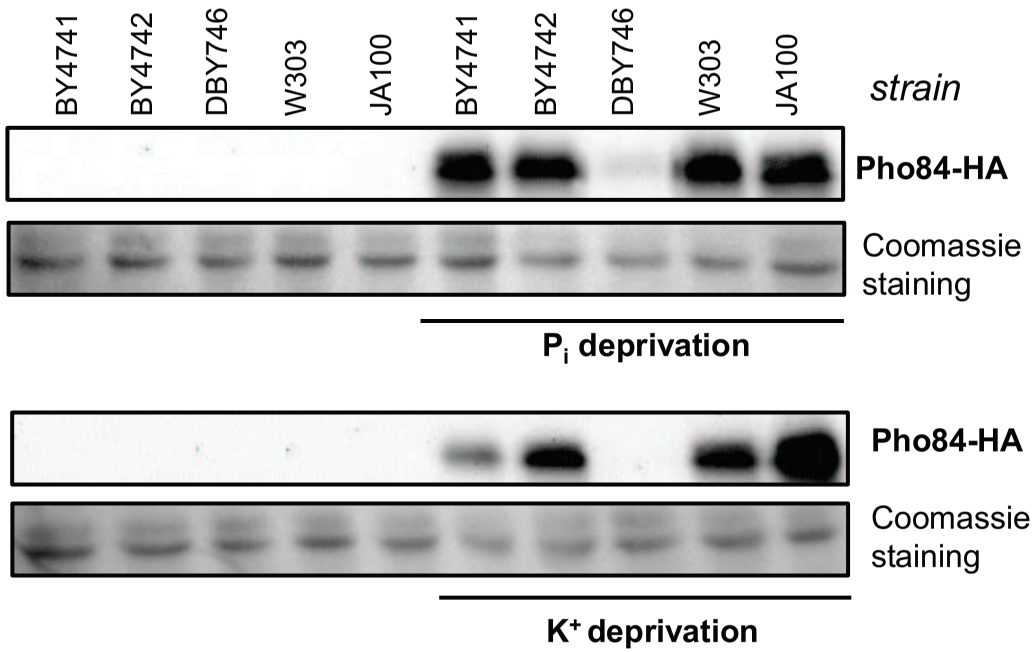

Supplementary Figure 2.- The indicated wild type strains were grown on synthetic medium and then subjected to potassium or phosphate starvation for one h. Samples were taken, protein extracts prepared as described in Experimental Procedures and subjected to SDS-PAGE (25 µg of protein). HA-tagged Pho84 was revealed by immunoblot. Blue Coomassie staining of the membrane is shown for lane to lane comparison.

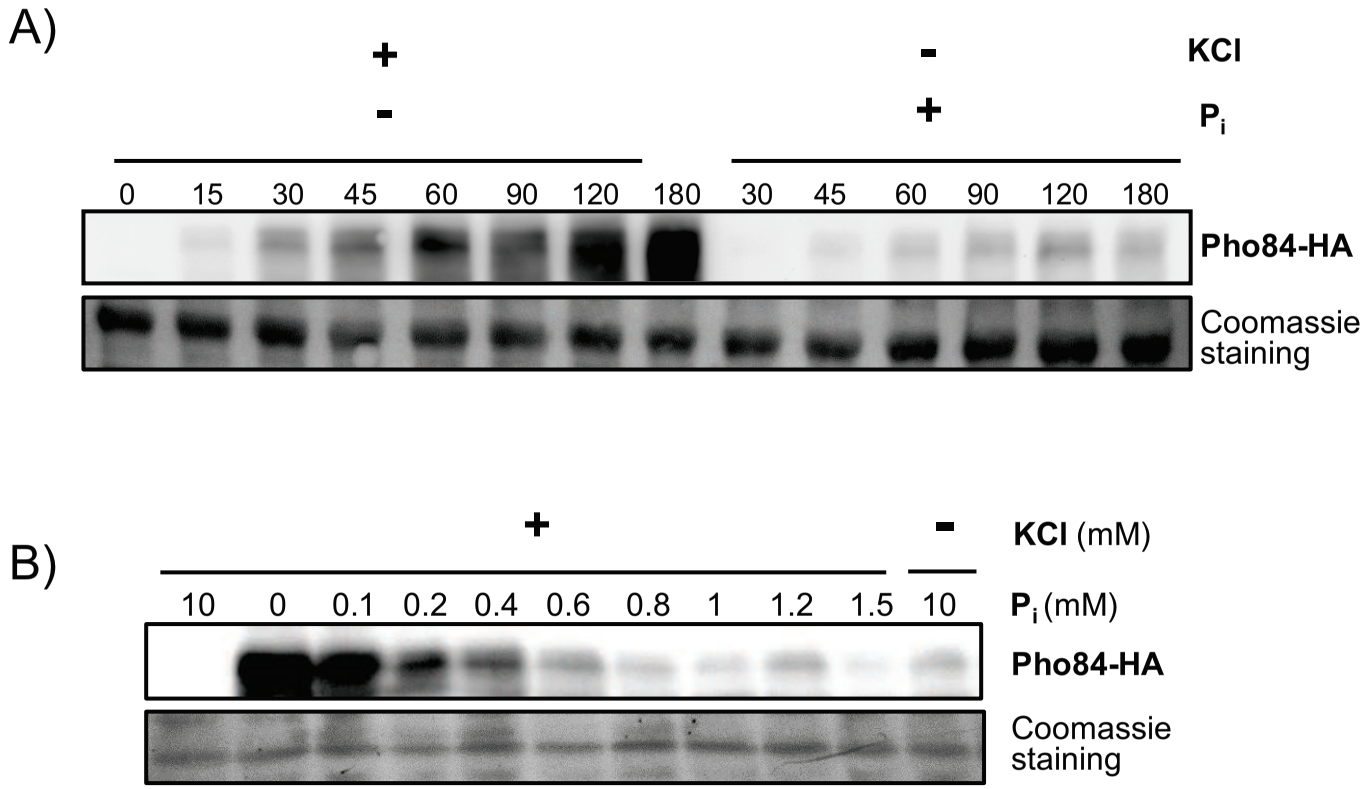

Supplementary Figure 3.- A) Wild type strain BY4741 was grown on synthetic medium and then subjected to potassium or phosphate starvation for the indicated periods. B) Cultures were grown as above, transferred to synthetic medium containing the indicated concentrations of Pi in the presence (+) of 50 mM KCl or the absence (-) of the salt, and growth resumed for one h. In all cases samples were taken, protein extracts prepared as described in Experimental Procedures and subjected to SDS-PAGE (25 µg of protein). HA-tagged Pho84 was revealed by immunoblot. Blue Coomassie staining of the membrane is shown for lane to lane comparison.

Supplemental Table 2. Genes induced by depletion of Hal3 and Vhs3 function.

Gene ID	Name	Change (log2)	Description
YML123C	*PHO84*	6.42	High-affinity inorganic phosphate (Pi) transporter; also low-affinity manganese transporter; regulated by Pho4p and Spt7p; mutation confers resistance to arsenate; exit from the ER during maturation requires Pho86p; cells overexpressing Pho84p accumulate
YIR019C	*FLO11*	3.81	GPI-anchored cell surface glycoprotein (flocculin); required for pseudohyphal formation, invasive growth, flocculation, and biofilms; transcriptionally regulated by the MAPK pathway (via Ste12p and Tec1p) and the cAMP pathway (via Flo8p); required for for
YHR215W	*PHO12*	3.59	One of three repressible acid phosphatases; glycoprotein that is transported to the cell surface by the secretory pathway; pregulated by phosphate starvation; PHO12 has a paralog, PHO11, that arose from a segmental duplication
YAR071W	*PHO11*	3.48	One of three repressible acid phosphatases; glycoprotein that is transported to the cell surface by the secretory pathway; induced by phosphate starvation and coordinately regulated by PHO4 and PHO2; PHO11 has a paralog, PHO12, that arose from a segmental
YBR093C	*PHO5*	3.48	Repressible acid phosphatase; 1 of 3 repressible acid phosphatases that also mediates extracellular nucleotide-derived phosphate hydrolysis; secretory pathway derived cell surface glycoprotein; induced by phosphate starvation and coordinately regulated by
YCL048W	*SPS22*	2.84	Protein of unknown function; SPS22 has a paralog, SPS2, that arose from the whole genome duplication; redundant with Sps2p for the organization of the beta-glucan layer of the spore wall
YPL019C	*VTC3*	2.66	Subunit of vacuolar transporter chaperone (VTC) complex; involved in membrane trafficking, vacuolar polyphosphate accumulation, microautophagy and non-autophagic vacuolar fusion; VTC3 has a paralog, VTC2, that arose from the whole genome duplication
YCR098C	*GIT1*	2.60	Plasma membrane permease; mediates uptake of glycerophosphoinositol and glycerophosphocholine as sources of the nutrients inositol and phosphate; expression and transport rate are regulated by phosphate and inositol availability
YER072W	*VTC1*	2.59	Subunit of the vacuolar transporter chaperone (VTC) complex; VTC complex is involved in membrane trafficking, vacuolar polyphosphate accumulation, microautophagy and non-autophagic vacuolar fusion; also has mRNA binding activity; protein abundance increas
YKR093W	*PTR2*	2.08	Integral membrane peptide transporter; mediates transport of di- and tri-peptides; conserved protein that contains 12 transmembrane domains; PTR2 expression is regulated by the N-end rule pathway via repression by Cup9p
YLR411W	*CTR3*	1.79	High-affinity copper transporter of the plasma membrane; acts as a trimer; gene is disrupted by a Ty2 transposon insertion in many laboratory strains of S. cerevisiae
YCLX01W		1.69	
YBR092C	*PHO3*	1.66	Constitutively expressed acid phosphatase similar to Pho5p; brought to the cell surface by transport vesicles; hydrolyzes thiamin phosphates in the periplasmic space, increasing cellular thiamin uptake; expression is repressed by thiamin
YER115C	*SPR6*	1.62	Protein of unknown function; expressed during sporulation; not required for sporulation, but gene exhibits genetic interactions with other genes required for sporulation
YFR055W	*IRC7*	1.56	Beta-lyase involved in the production of thiols; null mutant displays increased levels of spontaneous Rad52p foci; expression induced by nitrogen limitation in a GLN3, GAT1-dependent manner and by copper levels in a Mac1-dependent manner
YJR148W	*BAT2*	1.46	Cytosolic branched-chain amino acid (BCAA) aminotransferase; preferentially involved in BCAA catabolism; homolog of murine ECA39; highly expressed during stationary phase and repressed during logarithmic phase; BAT2 has a paralog, BAT1, that arose from th
YOL101C	*IZH4*	1.45	Membrane protein involved in zinc ion homeostasis; member of the four-protein IZH family; expression induced by fatty acids and altered zinc levels; deletion reduces sensitivity to excess zinc; possible role in sterol metabolism; protein increases in abun
YGR160W		1.43	Dubious open reading frame; unlikely to encode a functional protein, based on available experimental and comparative sequence data
YBL100C		1.38	Dubious open reading frame; unlikely to encode a functional protein, based on available experimental and comparative sequence data; almost completely overlaps the 5' end of ATP1
YGR233C	*PHO81*	1.35	Cyclin-dependent kinase (CDK) inhibitor; regulates Pho80p-Pho85p and Pcl7p-Pho85p cyclin-CDK complexes in response to phosphate levels; inhibitory activity for Pho80p-Pho85p requires myo-D-inositol heptakisphosphate (IP7) generated by Vip1p; relative dist
YJL122W	*ALB1*	1.35	Shuttling pre-60S factor; involved in the biogenesis of ribosomal large subunit; interacts directly with Arx1p; responsible for Tif6p recycling defects in absence of Rei1p
YDR399W	*HPT1*	1.30	Dimeric hypoxanthine-guanine phosphoribosyltransferase; catalyzes the transfer of the phosphoribosyl portion of 5-phosphoribosyl-alpha-1-pyrophosphate to a purine base (either guanine or hypoxanthine) to form pyrophosphate and a purine nucleotide (either
YOR287C	*RRP36*	1.28	Component of 90S preribosomes; involved in early cleavages of the 35S pre-rRNA and in production of the 40S ribosomal subunit
YDL181W	*INH1*	1.23	Protein that inhibits ATP hydrolysis by the F1F0-ATP synthase; inhibitory function is enhanced by stabilizing proteins Stf1p and Stf2p; has a calmodulin-binding motif and binds calmodulin in vitro; INH1 has a paralog, STF1, that arose from the whole genom
YLR214W	*FRE1*	1.22	Ferric reductase and cupric reductase; reduces siderophore-bound iron and oxidized copper prior to uptake by transporters; expression induced by low copper and iron levels
YOL124C	*TRM11*	1.22	Catalytic subunit of adoMet-dependent tRNA methyltransferase complex; required for the methylation of the guanosine nucleotide at position 10 (m2G10) in tRNAs; contains a THUMP domain and a methyltransferase domain; another complex member is Trm112p
YOR146W		1.20	Dubious open reading frame; unlikely to encode a functional protein, based on available experimental and comparative sequence data; open reading frame overlaps the verified gene PNO1/YOR145C
YDR481C	*PHO8*	1.18	Repressible vacuolar alkaline phosphatase; regulated by levels of Pi and by Pho4p, Pho9p, Pho80p, Pho81p and Pho85p; dephosphorylates phosphotyrosyl peptides; contributes to NAD+ metabolism by producing nicotinamide riboside from NMN
YCL036W	*GFD2*	1.17	Protein of unknown function; identified as a high-copy suppressor of a dbp5 mutation; GFD2 has a paralog, YDR514C, that arose from the whole genome duplication
YOR078W	*BUD21*	1.15	Component of small ribosomal subunit (SSU) processosome; this complex contains U3 snoRNA; required at post-transcriptional step for efficient retrotransposition; absence results in decreased Ty1 Gag:GFP protein levels; originally isolated as bud-site sele
YHR136C	*SPL2*	1.14	Protein with similarity to cyclin-dependent kinase inhibitors; downregulates low-affinity phosphate transport during phosphate limitation by targeting Pho87p to the vacuole; upstream region harbors putative hypoxia response element (HRE) cluster; overprod
YOR385W		1.13	Putative protein of unknown function; green fluorescent protein (GFP)-fusion protein localizes to the cytoplasm; YOR385W is not an essential gene
YAR068W		1.12	Fungal-specific protein of unknown function; induced in respiratory-deficient cells; YAR068W has a paralog, YHR214W-A, that arose from a segmental duplication
YGL029W	*CGR1*	1.11	Protein involved in nucleolar integrity and processing of pre-rRNA; has a role in processing rRNA for the 60S ribosome subunit; transcript is induced in response to cytotoxic stress but not genotoxic stress; relocalizes from nucleus to nucleolus upon DNA
YFL040W		1.10	Putative transporter; member of the sugar porter family; YFL040W is not an essential gene
YMR006C	*PLB2*	1.09	Phospholipase B (lysophospholipase) involved in lipid metabolism; displays transacylase activity in vitro; overproduction confers resistance to lysophosphatidylcholine
YNL182C	*IPI3*	1.08	Component of the Rix1 complex and pre-replicative complexes (pre-RCs); required for processing of ITS2 sequences from 35S pre-rRNA; component of the pre-60S ribosomal particle with the dynein-related AAA-type ATPase Mdn1p; required for pre-RC formation an
YJL012C	*VTC4*	1.07	Vacuolar membrane polyphosphate polymerase; subunit of the vacuolar transporter chaperone (VTC) complex involved in synthesis and transfer of polyP to the vacuole; regulates membrane trafficking; role in non-autophagic vacuolar fusion; protein abundance i
YLR438W	*CAR2*	1.06	L-ornithine transaminase (OTAse); catalyzes the second step of arginine degradation, expression is dually-regulated by allophanate induction and a specific arginine induction process; not nitrogen catabolite repression sensitive; protein abundance increas
YNL289W	*PCL1*	1.05	Cyclin, interacts with cyclin-dependent kinase Pho85p; member of the Pcl1,2-like subfamily, involved in the regulation of polarized growth and morphogenesis and progression through the cell cycle; is ubiquitinated by Dma1p; phosphorylation by Pho85p targe
YFL004W	*VTC2*	1.04	Subunit of vacuolar transporter chaperone (VTC) complex; involved in membrane trafficking, vacuolar polyphosphate accumulation, microautophagy and non-autophagic vacuolar fusion; VTC2 has a paralog, VTC3, that arose from the whole genome duplication
YDR492W	*IZH1*	1.03	Membrane protein involved in zinc ion homeostasis; member of the four-protein IZH family; transcription is regulated directly by Zap1p, expression induced by zinc deficiency and fatty acids; deletion increases sensitivity to elevated zinc; IZH1 has a para
YCR007C		1.03	Putative integral membrane protein; member of DUP240 gene family; YCR007C is not an essential gene
YDR396W		1.03	Dubious open reading frame unlikely to encode a functional protein; extensively overlaps essential NCB2 gene encoding the beta subunit of the NC2 dimeric histone-fold complex
YBL054W	*TOD6*	1.02	PAC motif binding protein involved in rRNA and ribosome biogenesis; subunit of the RPD3L histone deacetylase complex; Myb-like HTH transcription factor; hypophosphorylated by rapamycin treatment in a Sch9p-dependent manner; TOD6 has a paralog, DOT6, that
YOR145C	*PNO1*	1.01	Essential nucleolar protein required for pre-18S rRNA processing; interacts with Dim1p, an 18S rRNA dimethyltransferase, and also with Nob1p, which is involved in proteasome biogenesis; contains a KH domain
YER147C-a		1.01	Dubious open reading frame; unlikely to encode a functional protein, based on available experimental and comparative sequence data; overlaps ORF SPT15/YER148W
YBL028C		1.01	Protein of unknown function that may interact with ribosomes; green fluorescent protein (GFP)-fusion protein localizes to the nucleolus; predicted to be involved in ribosome biogenesis